PREPARATION AND CHARACTERISATION OF MgO; A HETEROGENEOUS BASIC CATALYST FOR LIQUID PHASE REACTIONS

By Chunli Xu

Thesis submitted to Cardiff University for degree of

Doctor of Philosophy

August 2006

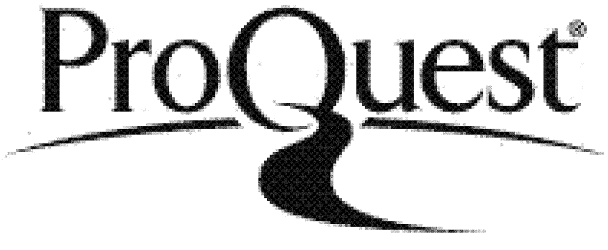

ProQuest LLC
789 East Eisenhower Parkway
P.O. Box 1346
Ann Arbor, MI 48106-1346

ACKNOWLEDGEMENTS

There are many people to whom I owe a debt of ingratitude for their help towards this thesis. Firstly thanks go to my academic supervisors Graham Hutchings, Jonathan K. Bartley, Dan I. Enache and David W. Knight and my industrial supervisor Matthew Lunn and Martin Lok whose support has been greatly appreciated.

Thanks to all at Cardiff University, in particular Rob Jenkins for continually going out of his way to help and to Alun Davies for fixing everything that went wrong. I am also grateful to every member of my group for their help and friendliness. Thanks to the people I have been lucky enough to call my friends over the past few years.

Finally my husband and daughter, whose continual love and support over the past three years has been incredible. They have always been a great tower of strength for me.

Abstract

We systematically studied the preparation method of magnesium oxide as cheap heterogeneous basic catalysts, and found a very simple method to obtain MgO with high surface area and high catalytic activity. Furthermore, the structure of MgO was characterized using many techniques, such as BET, TGA, XRD and SEM. The relationship of catalytic activity and structure of MgO has been investigated in detail. At last, the obtained MgO was used in the liquid phase reactions, including Meerwein-Pondorf-Verley reaction, Michael addition, Knoevenagel condensation, transesterification of vegetable oil to biodiesel and synthesis of β-Keto 1,3-dithianes.

The prepared magnesium oxide catalyst was used in the liquid phase Meerwein-Pondorf-Verley reaction of benzaldehyde with alcohol. Effect of preparation method on the catalytic activity and structure of MgO has been investigated in detail. The experimental result showed that the optimal calcination temperature was 450 °C. Lithium supported magnesium oxide was also studied.

Magnesium oxide obtained using a novel but simple procedure was systematically investigated as a heterogeneous base catalyst for the Michael addition and Knoevenagel condensation. The activity of MgO was studied in detail, together with the effects of solvent and of substrate on the catalytic activity for each type of reaction. A key finding is that the formation of enols affected the activity of MgO. The preparation method and activity of MgO was determined and compared with CaO.

MgO was used for the first time as a heterogeneous basic catalyst to synthesis β-keto-1,3-dithianes from conjugated ynones and ynoates. It was found that MgO is an active catalyst with activity better than or comparable with previously identified homogeneous or heterogeneous catalysts for this reaction. The effect of preparation methods on the activity of MgO is described.

Transesterification of vegetable oil to biodiesel with MgO as catalyst was studied at 60 °C and 200 °C, respectively. Effect of methanol-to-oil molar ratio, catalyst loading, reaction temperature and calcination temperature was investigated. 90% yield can be obtained at 60 °C for 3h, and 80% at 200 °C for 15min. The results showed that the prepared MgO was active for the synthesis of biodiesel.

CONTENTS

Chapter 1: Introduction

			PAGE
1.1	**Introduction**		**1**
1.2	**Different types of heterogeneous basic catalysts**		**5**
	1.2.1	Single component metal oxides	5
	1.2.2	Systems constituted by more than a metal oxide or mixed oxides	5
	1.2.3	Supported alkali or alkaline earth metals and alkali metal salts	5
	1.2.4	Single hydroxides	6
	1.2.5	Metal phosphates	6
	1.2.6	Metal carbonates	6
	1.2.7	Carbons/alkaline carbons	7
	1.2.8	Anion-exchange resin catalysts	7
	1.2.9	Clay minerals	7
		1.2.9.1 Base sepiolites	7
		1.2.9.2 Oxynitride systems	8
		1.2.9.3 LDH's and related compounds (e.g. calcined hydrotalcites)	8
	1.2.10	Zeolite zeotropes	8
	1.2.11	Nitrides and carbides	9
1.3	**Characterization of Basic Sites**		**10**
1.4	**Reaction catalyzed by solid bases**		**13**
	1.4.1	Transesterification	13
	1.4.2	Michael addition	14
	1.4.3	Knoevenagel condensation	17
	1.4.4	Meerwein-Ponndorf-Verley (MPV) reduction	19
	1.4.5	Aldol condensation	22
	1.4.6	Cyanoethylation of alcohols	24
	1.4.7	Tishchenko reaction	25
	1.4.8	Nitroaldol reaction	25
	1.4.9	Alkene and alkyne isomerization	27
	1.4.10	Alkylation of toluene with methanol and formaldehyde	29
	1.4.11	Some other reactions	30
1.5	**Aims of this thesis**		**32**
References			**33**

Chapter 2: Experimental

2.1	**Preparation of heterogeneous base catalysts**		**52**
	2.1.1	Preparation of MgO	52
	2.1.2	Preparation of lithium doped magnesium oxides	54
	2.1.3	Preparation of CaO	54
	2.1.4	Preparation of Hydrotalcites	55
2.2	**Reactors used in the current study**		**55**
	2.2.1	Glass batch reactor	55

2.2.2 Stirred tank reactor 57
2.3 Catalyst characterisation **57**
2.3.1 Surface area and Pore Analysis 57
2.3.2 Thermal Gravimetric Analysis 58
2.3.3 Powder X-Ray Diffraction (XRD) 59
2.3.4 Scanning Electron Microscope (SEM) 61
2.4 Product Analysis **62**
2.4.1 Gas chromatography (GC) 64
2.4.2 Gas chromatography - Mass spectrometry (GC-MS) 64
2.4.3 High Performance Liquid Chromatography (HPLC) 66
2.4.4 Principle of NMR 66
2.5 Leaching analysis of MgO **67**
2.5.1 Atomic absorption (AA) 67
References **69**

Chapter 3: Preparation of high surface area MgO and its application in Meerwein-Ponndorf-Verley reduction of benzaldehyde

3.1 Introduction **70**
3.2 Experimental **71**
3.2.1 Catalyst preparation 71
3.2.2 Catalyst testing 71
3.3 Results and discussion **71**
3.4 Conclusions **94**
References **94**

Chapter 4: High surface area MgO as a highly effective heterogeneous base catalyst for Michael addition and Knoevenagel condensation reactions

4.1 Introduction **95**
4.2 Experimental **97**
4.2.1 Michael addition 97
4.2.2 Knoevenagel condensation 98
4.3 Results and discussion **98**
4.3.1 Results obtained for the Michael addition reaction 98
4.3.2 Results obtained for the Knoevenagel condensation reaction 109
4.4 Activity of CaO **116**
4.5 Conclusions **120**
References **120**

Chapter 5: Synthesis of β-Keto-1,3-Dithianes in the Presence of MgO

5.1 Introduction **123**
5.2 Experimental **125**
5.3 Results and discussion **126**
5.4 Conclusions **131**
References **132**

Chapter 6: Transesterification of vegetable oil to biodiesel with MgO as catalyst

6.1 Introduction **134**
6.2 Experimental **138**
6.2.1 Catalyst preparation 138
6.2.2 Transesterification reaction 139
6.2.2.1 Reaction performed at about 60 °C 139
6.2.2.2 Reaction performed at 200 °C in Johnson Matthey 140
6.2.2.3 Reaction performed at 200 °C in Cardiff University 140
6.2.3 Analytical monitoring of biodiesel production 141
6.2.3.1 ^{1}H NMR analysis 141
6.2.3.2 High performance liquid chromatography analysis 146
6.3 Results and Discussion **147**
6.3.1 Reaction performed at 60 °C 147
6.3.2 Reaction performed at 200 °C 153
6.3.2.1 Results obtained at Cardiff University 153
6.3.2.2 Results obtained at Johnson Matthey 157
6.4 Reuse of MgO **162**
6.5 Conclusions **164**
References **165**

Chapter 7: Conclusions and future work

7.1 Structure of MgO **168**
7.2 Model reactions **170**
7.2.1 MPV reactions 170
7.2.2 Michael additions and Knoevenagel condensation 172
7.2.3 Synthesis of β-Keto-1,3-Dithianes 172
7.2.4 Transesterification of vegetable oil to biodiesel 173
7.3 Future work **174**

Appendix One Product analysis and characterisation **176**
Appendix Two HPLC results for biodiesel synthesis **206**
Appendix Three Publication list **214**

Chapter 1

Introduction: Heterogeneous basic catalysis

1.1 Introduction

Catalysts can be divided into two main types - heterogeneous catalyst and homogeneous catalyst. In a heterogeneous reaction, the catalyst is in a different phase from the reactants. In a homogeneous reaction, the catalyst is in the same phase as the reactants.

Among chemical reactions, which are promoted by catalysts, are the acid-catalyzed and base-catalyzed reactions, which are initiated by acid-base interactions between reactants and catalysts followed by catalytic cycles. In acid-catalyzed reactions, the catalysts act as an acid toward the reactants, whereas in base-catalyzed reactions, the catalysts act as a base toward the reactants.[1] The materials may be called base catalysts only if acting as a base toward the reactants by abstraction of a proton (Brønsted base) or by donation of an electron pair (Lewis base) to form anionic intermediates that undergo catalytic cycles. When the heterogeneous catalyst works as a base toward the reactants, it is referred to as heterogeneous base catalysts or solid base catalysts.

Compared with conventional homogeneous catalysts (NaOH, KOH), heterogeneous basic catalysts have a number of advantages (such as no corrosion of reaction vessels or reactors, easier separation from the products, consequently possibility of reuse and less environmental problems).[2-4] In homogeneous systems, a huge number of acid-catalyzed reactions and base-catalyzed reactions are well known. In heterogeneous systems, a limited number of reactions are recognized as acid- or base-catalyzed reactions.

The first study of heterogeneous basic catalysts, the discovery that sodium metal dispersed on alumina acted as an efficient catalyst for double bond migration of alkenes, was published in 1955 by Pines *et al.* [5] Sodium metal dispersed on alumina can act as a solid base catalyst because of the strong tendency of sodium to donate electrons. The breakthrough in heterogeneous basic catalysis was the recognition that many materials act as solid base catalysts if properly pretreated.[6] Before the 1970s, catalysts were pretreated normally at low temperatures of around 723K, at which the surfaces of basic materials are covered with carbon dioxide, water, oxygen, etc., and show no activities for base-catalyzed reactions. Removal of the carbon dioxide, water, oxygen, etc. from the surfaces by pre-treatment at high temperature allowed the surfaces to exhibit basic properties and promoted base-catalyzed reactions.

Table 1.1 Number of solid acid, base and acid-base bifunctional catalysts in industrial processes.[7]

Catalyst	Number
Solid acid catalysts	103
Solid base catalysts	10
Solid acid-base bifunctional catalysts	14
Total	127

In the 1970s, studies of solid base catalysts became more popular. A number of single component metal oxides were found to act as solid base catalysts in the absence of alkali metals. In addition to the single component metal oxides, alkali ion-exchanged X and Y type zeolites were found to be catalysts for base-catalyzed reactions. Following these findings, a wide variety of solid base catalysts have been identified. The types of solid base catalysts will be discussed in Section 2.

Table 1.2 Industrial processes using solid base catalysts.[6-7]

Type of process/Entry No.	Reaction	Catalyst	Year[a]
Alkylation			
1	Alkylation of phenol with methanol	MgO	1970,1985
2	Alkenylation of o-xylene with butadiene	Na/K_2CO_3	1995
3	Alkylation of cumene with ethylene	$Na/KOH/Al_2O_3$	1988
Isomerization			
4	Isomerization of safrole to isosafrole	$Na/NaOH/Al_2O_3$	1988
5	Isomerization of 2,3-dimethyl-1-butene	$Na/NaOH/Al_2O_3$	1988
6	Isomerization of 3,5-vinylbicyclo[2.2.1]heptene	$Na/NaOH/Al_2O_3$	1988
7	Isomerization of 1,2-propadiene to propyne	K_2O/ Al_2O_3	1996
Dehydration/Condensation			
8	Dehydration of 1-hexylethanol	ZrO_2	1986
9	Dehydration of propylamine-2-ol	ZrO_2-KOH	1992
10	Isobutyraldehyde to isobutylisobutyrate	ZrO_2	1974
11	Dehydrotrimerization of isobutyraldehyde	BaO-CaO	1998
Esterification			
12	Esterification of ethylene oxide with alcohol	Hydrotalcite	1994
Miscellaneous			
13	Reduction of carboxylic acid to aldehyde	ZrO_2-Cr_2O_3	1988
14	Thiols from alcohols with hydrogen sulfide	$Alkali/Al_2O_3$	1988
15	Cyclization of imine with sulfur dioxide	Cs-zeolite	1995

[a] Year in which details were disclosed in a paper or process operation was confirmed.

Some of the solid base catalysts have been used in industrial processes. Tanabe and Hoelderich reviewed industrial applications of solid base catalysts as well as solid acid catalysts.[7] Among 127 processes, 10 processes use solid base catalysts and 14 processes

use acid-base bifunctional catalysts according to their classification (Table 1.1). Table 1.2 lists the industrial processes in which solid base catalysts are used in the present classification. Most processes were developed within the last 20 years. The studies of solid base catalysts starting in the 1970s have been crystallized into industrial processes in the last 20 years.

Heterogeneous acid catalysis attracted more attention primarily because heterogeneous acidic catalysts could act as catalysts in petroleum refinery and are known as a main catalyst in the cracking process, which is the largest process among the industrial chemical processes. Extensive studies of heterogeneous cracking catalysts undertaken in the 1950s revealed that the essential nature of cracking catalysts is acidic, and generation of acidic sites on solids was extensively studied.

There is increasing interest in the study of heterogeneous base catalysts for the fine chemical industry. The fine-chemicals industry, although more slowly than petroleum refining and bulk-chemical industries, seemed to have embraced the benefits of heterogeneous catalysis. If we consider the E-factor (defined as the mass ratio of waste to desired product),[8] fine chemical processes are "the dirtier ones", with E-factors of the order of 5-50 kg waste per kg.[9] Consequently, especially in the case of fine chemistry, there seems to be room for the design of more efficient and selective base processes and base catalysts achieving the dual goal of environmental protection and economic benefit involved in Sustainable/Green Chem. concept.[10]

There have been several review articles on heterogeneous basic catalysis.[1,6-7, 11-15] In the present chapter, the type of heterogeneous base catalysts, characterization of basic surfaces, application of heterogeneous base catalysts for organic synthesis and aims of this thesis are presented.

1.2 Different types of heterogeneous basic catalysts

1.2.1 Single component metal oxides

Single component metal oxides, such as alkaline earth oxides, alkali metal oxides, rare earth oxides and some other oxides, can work as heterogeneous basic catalysts in organic reactions.

a) Alkaline earth oxides: the most extensively used catalyst, within this group, is probably MgO.[16-32] In some cases its catalytic performance is compared to some other members of the series.[33-38]

b) Alkali metal oxides.[39]

c) Rare earth oxides, such as La_2O_3, [33, 38,40-42] CeO_2 [33, 42-43] or Nb_2O_3. [41]

d) Some other oxides, such as ZrO_2,[33,38,43] ZnO,[33,38,40,42] Al_2O_3.[38,40]

1.2.2 Systems constituted by more than a metal oxide or mixed oxides.

Some examples are CaO-TiO_2,[44] MgO-La_2O_3,[45] MgO-ZrO_2 and MgO-TiO_2 systems, [46-48] MgO-Al_2O_3,[49-51] LiO/MgO,[52-53] MgO/CaO.[54] Recently, Flego *et al.* described the synthesis of three-element mixed oxides of formula $(IA)_x(IIA)_yAlO_2$, where IA and IIA denote an alkali and an alkaline-earth metal, respectively. [55]

1.2.3 Supported alkali or alkaline earth metals and alkali metal salts

Heterogeneous basic catalysts were prepared by doping alkali or alkaline earth metals and alkali metal salts on support.

a) MgO can be promoted with alkali[56-62] or alkaline earth metals[57,63] in order to

increase its base strength. Some other examples of oxides promoted by alkali metals are ZrO_2,[64,65] SiO_2,[62,66] Al_2O_3[62,67-69] ZnO.[70] More recently, Alkali metal ions doped on platinum catalysts has been reported.[71]

b) Potassium fluoride has extensively been supported on Al_2O_3[13,37,53,72-80] and phosphates.[81-84] Campelo *et al.*[73] and Bautista *et al.*[85] supported KF on a wide range of systems such as ZnO, SnO_2, sepiolite, AlPO4-Al_2O_3 or $AlPO_4$-ZnO. Finally, there are also examples of KF supported on NaY zeolite.[86] Three more examples of potassium salts supported on different materials are KNO_3,[87-89] K_2CO_3[88] and KNH_2.[13, 90-91]

1.2.4 Single hydroxides

The most extensively used are alkaline earth hydroxides [$Ba(OH)_2$ mainly] [72,92-111] though alkali metal ones are also described in the literature.[33]

1.2.5 Metal phosphates

Here we can cite natural phosphate and modified natural phosphate,[112-113] $Na_2CaP_2O_7$,[114] magnesium phosphates[115-118] or magnesium-sodium mixed phosphates.[119-121] On some occasions, phosphates are modified by the addition of carbonates,[122-125] MgO[24] or ZnO.[73] Further examples of modification of phosphates are $AlPO_4$-Al_2O_3[126-127] and CsO-$AlPO_4$ systems.[128]

1.2.6 Metal carbonates

The activity of alkali carbonate has been reported, such as K_2CO_3, Rb_2CO_3, Cs_2CO_3 and Li_2CO_3.[129-130]

1.2.7 Carbons/alkaline carbons

Montes-Moran *et al.* have made a review on the nature of basic sites on carbon surfaces. [131] In this review the authors discussed on the two theories on the origin of such basicity: presence of basic-oxygen containing groups or delocalized π-electrons of the basal planes. Moreover, the incorporation to the carbons of alkaline metals[132-134] or some other elements such as Mg or Zr[135] in order to get base materials is described in the literature.

1.2.8 Anion-exchange resin catalysts

Ion exchange resins are classified as strong or weak acid resin (cation exchangers), which have positively charged mobile ions available for exchange, and strong or weak base resin (anion exchangers), whose exchangeable ions are negatively charged. Both anion and cation resins are produced from the same basic organic polymers. They differ in the ionizable group attached to the hydrocarbon network. It is this functional group that determines the chemical behaviour of the resin. Strong or weak base resins are so named because their chemical behaviour is similar to that of a base. These anion-exchange resins can work as heterogeneous basic catalysts for organic reactions.[136-137]

1.2.9 Clay minerals

1.2.9.1 Base sepiolites

Sepiolite is an abundant fibrous talc-like mineral of $Si_{12}Mg_8(OH)_4O_{30}\cdot 8H_2O$ formula whose structure is formed by an array of parallel channels, consisting of a double layer SiO_4 tetrahedra sandwiching an internal octahedral MgO_6 layer. Alkali-substituted sepiolites are described in the literature as base materials.[138-140]

1.2.9.2 Oxynitride systems

Here we can cite aluminovanadate oxynitrides (VALON),[141] nitrided phosphates ZrPON[142-143] and AlPON[144-149] and mixed nitrided galloaluminophosphates (AlGaPON).[141]

1.2.9.3 LDH's and related compounds (e.g. calcined hydrotalcites)

There are several reviews available about the structure and application of layered double hydroxides (LDHs).[15,150-152] LDHs consist of positively charged metal hydroxide layers separated each other by anions and water molecules. These compounds possess a general formula $[M(II)_{1-x}M(III)_x(OH)_2]^{x+}A^{n-}_{x/n} \cdot mH_2O$, where M(III) partially substitutes M(II) metal cations in brucite-like octahedral layers. A wide variety of LDHs containing various divalent and trivalent cations [M(II)=Mg, Ca,[153-159] Cu,[155,157] Co,[155]..., M (III)=Al, Ga,[153,160-163] In,[153,160] Cr,[155] Fe[155] in combination is Mg/Al hydrotalcite.[78,153,163-172]

Calcination of LDHs results in a porous mixed oxide. On some occasions, calcined LDHs are rehydrated, yielding catalysts with free hydroxyl groups.[14]

1.2.10 Zeolites zeotypes

Alkali and alkaline-earth exchanged zeolites or zeotypes (e.g. MCM-41)[13, 37, 139,173-187] have been extensively used as base catalysts. However, they are weak bases. Alternatively, either alkali metal or alkali and alkaline-metal oxides can be occluded into zeolites and zeotypes in order to increase their basicity.[188,68,186,189-194] This is usually referred to as the introduction of a basic guest into a zeolite host. Moreover, the loading

of Yterbium or Europium metal on zeolites, thus yielding strong bases, has been reported.[12]

Functionalisation of zeolites and zeotypes by anchoring organic bases constitutes a different approach.[195,196-201]

Finally, organic bases can be invorporated into the zeolite pores through the ship-in-the-bottle method.[202]

1.2.11 Nitrides and carbides

Some examples within this group are rare-earth nitrides,[203] silicon nitride[204] or molybdenum nitride and carbide.[205,206]

The materials listed above do not necessarily function as a base in all cases. Some materials above may act as an acid if the reactants are strongly basic. The terms, acid and base, should be used according to the function. The materials have been recognized as solid base catalysts for the reason listed below.[6]

a) Characterizations of the surfaces by various methods such as colour change of acid-base indicators, adsorption of acidic molecules, and several spectroscopic methods indicate that basic sites exist on the surface.
b) Catalytic activities correlated with the amount of basic sites or strength of basic sites. In addition, the active sites are poisoned by acidic molecules such as HCl, CO_2, and H_2O.
c) Reactions proceeding over the materials are similar to the "base-catalyzed reactions" well-known in homogeneous systems.
d) Mechanistic studies of the reactions and spectroscopic observations of the surface

species indicate that anionic intermediates are involved in the reactions.

1.3 Characterization of Basic Sites

The surface properties of solid base catalysts have been studied by various methods.[1,6,14] Different characterization methods give different information about the surface properties. All the properties of basic sites cannot be measured by any single method. Similar to the case of solid acid catalysts, the existence of basic sites was first realized by the indicator method. Until now, the most widely applied technique for the investigation of basic sites on solid catalysts is the application of molecular probes and their study by temperature-programmed desorption experiments (TPD), FTIR spectroscopy, X-ray photoelectron spectroscopy (XPS) and NMR spectroscopy.

Acid-base indicators change colour according to the strength of the surface sites and pK_{BH} values of the indicators. The strength of the surface basic sites is expressed by an acidity function (H_-) proposed by Paul and Long.[207] The H_- function , also called Hammett constants, is defined by the following equation:

$$H_- = pK_{BH} + \log([B^-]/[BH])$$

Where [BH] and [B^-] are the concentration of the indicator and its conjugated base, respectively, and pK_{BH} is the logarithm of the dissociation constant of BH. The reaction of the indicator BH with the basic site $\underline{B}$ is:

$$BH + \underline{B} = B^- + \underline{B}H^+$$

The amount of basic sites of different strength can be measured by titration with benzoic acid. The benzoic acid titer is a measure of the amount of basic sites with a basic strength

corresponding to the pK_{BH} value of the indicator used. Using this method, the exposure of basic sites on CaO and MgO by pre-treatment above 400 °C was revealed.[208]

The indicator method, however, has disadvantages. Although the colour change is assumed to be the result of an acid-base reaction, and indicator may change colour by reactions different from the acid-base reaction. In addition, a long time is required for benzoic acid to reach adsorption equilibrium during titration carried out in a solution. In some cases, the surface of solid base catalysts may dissolve into the titration solution. If this occurs, the number of basic sites will be overestimated.[6] For this reason, the ratio [B^-]/[BH] is usually measured by spectroscopy methods (normally UV-Vis spectroscopy).The H_- values of different solid bases are shown in Figure 1.1.[11] The higher the H_- values, the higher the basic strength is.

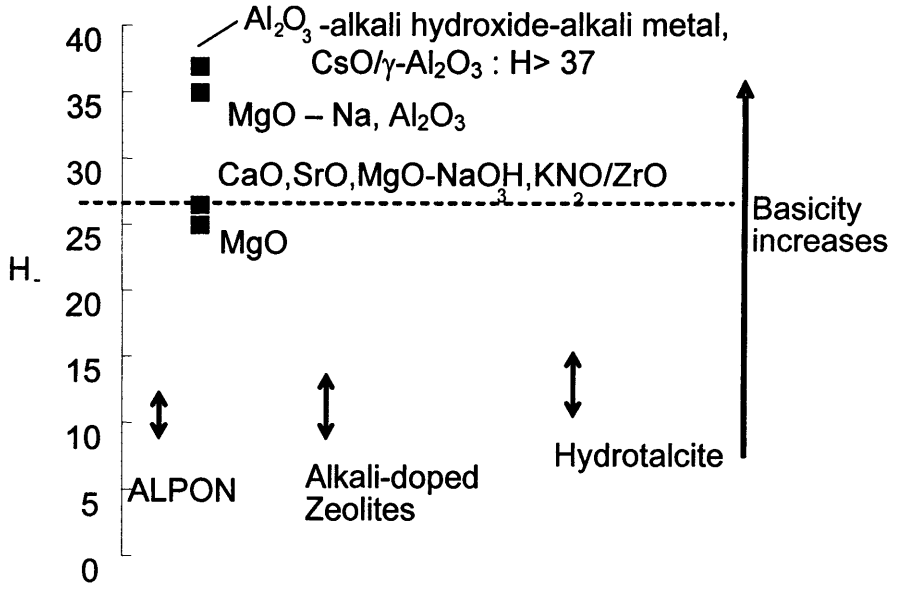

Figure 1.1 Basic strength (in terms of Hammett constants, H_-) for different solids.

Several other methods are available to measure basic sites. TPD of carbon dioxide is frequently used to characterize basic sites. The strength and amount of basic sites are reflected in the desorption temperature and the peak area, respectively, in a TPD plot.[209] CO_2 is a good probe molecule not only for TPD but also for infrared spectroscopy (IR). IR of CO_2 gives information about the adsorbed state of CO_2 on the basic sites, which reflects the structure of basic sites.[210]

Knözinger and Huber reviewed the application of pyrrole, acetylenes and deuterated chloroform as FTIR probes for the investigation of basic solids.[211] The spectra obtained with these probes tended to be less complicated than those observed with CO_2, but the occurrence of different adsorption structures may again render the interpretation difficult.

Sánchez- Sánchez *et al.* applied pyrrole and chloroform as NMR probes for basic zeolites.[212, 213] The ^{1}H NMR shift of the hydrogen atoms at the ring nitrogens indicates the different base strengths of zeolite oxygen atoms contributing to the H-bonding with pyrrole molecules. Applying ^{13}C MAS NMR spectroscopy, Bosacek *et al.* found a correlation between the ^{13}C NMR shift of methoxy groups and the base strength of the framework oxygen atoms.[214] ^{133}Cs NMR can distinguish the Cs located inside the cavity form the Cs located on the outer surface of zeolite and ion-exchanged Cs.[215] ^{19}F NMR also provide information about certain aspects of basic sites.[216]

The XPS binding energy (BE) for oxygen reflects the basic strength of the oxygen. As the O_{1s} BE decreases, electron pair donation becomes stronger. Okamoto *et al.* studied the effects of zeolite composition and the type of cation on the BE of the constituent

elements for X- and Y- zeolites with a series of alkali cations as well as H-forms of A, X, Y, and mordenite.[217]

A very popular technique for characterizing basic solids is the application of catalytic test reactions, such as alkylation of toluene, alkene and alkyne isomerization and aldol reaction, which will be described in the next section.

1.4 Reaction catalyzed by solid bases

1.4.1 Transesterification

Transesterification of vegetable oil with methanol (Figure 1.2) is an important process to synthesise methyl esters of fatty acid, known as biodiesel, which can replace the conventional diesel fuel. Over the past couple of decades alternative fuels for diesel engines are becoming increasingly important due to the limited resources of fossil fuel, increasing prices of crude oil and environmental concerns.[218] The energy content, octane number and viscosity of biodiesel are similar to those of petroleum-based fuel.[219-221] Moreover, the biodiesel is free of sulphur and aromatics, and, as it is obtained from renewable sources, it reduces the lifecycle of carbon dioxide emissions by almost 70% compared to conventional diesel fuel.[222]

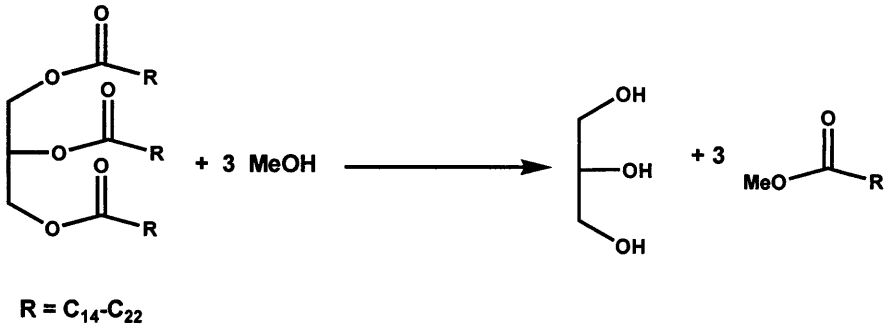

Figure 1.2 Transesterification of vegetable oil with methanol.

The conventional catalysts to produce biodiesel are usually homogeneous basic catalysts such as alkaline or alkaline earth hydroxides or alkoxides. However, removal of these catalysts is technically difficult and a large amount of waste water is produced to separate and clean the catalyst and product.[223-225] Many different heterogeneous base catalysts have been developed to catalyze the tranesterification of vegetable oils to prepare biodiesel, such as hydrotalcite,[226-228] MgO,[226,229] zeolites,[230,231] mixed oxide of zinc and aluminium,[222] Na/NaOH/γ-Al_2O_3[232] and KF/ZnO.[233]

Transesterification of ethyl acetate with alcohols (Figure 1.3) also can be conducted over heterogeneous base catalysts at room temperature.[234] The rate varied with the type of alcohol and the type of solid base catalyst. The strength of basic sites is the decisive factor to control the activity of the catalyst.

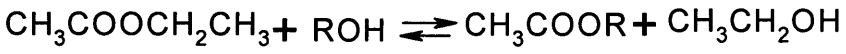

Figure 1.3 Transesterification of ethyl acetate with alcohols.

1.4.2 Michael addition

Michael addition is conjugate additions of carbanions to α,β-unsaturated carbonyl compounds, which is one of the important reactions to form C-C bond (general equation, Figure 1.4a). In heterogeneous system, the basic sites are responsible for forming the carbanions by abstraction of an H^+ from the donor molecule having an α-hydrogen.

Michael addition of ethyl acrylate and acetone (Figure 1.3b) on basic zeolites and superbases, leads to the formation of 5-oxohexanic acid ethyl ester which, once ring transformed and dehydrogenated yields resorcines, valuable compounds for production of rubber materials.[235] Matin Aranda *et al.* performed Michael addition between

imadazoles and ethyl acrylate (Figure 1.4c) using Li^+ and Cs^+ montmorillonites.[236] N-substituted imidazoles and their derivatives are of interest in the pharmaceutical industry.

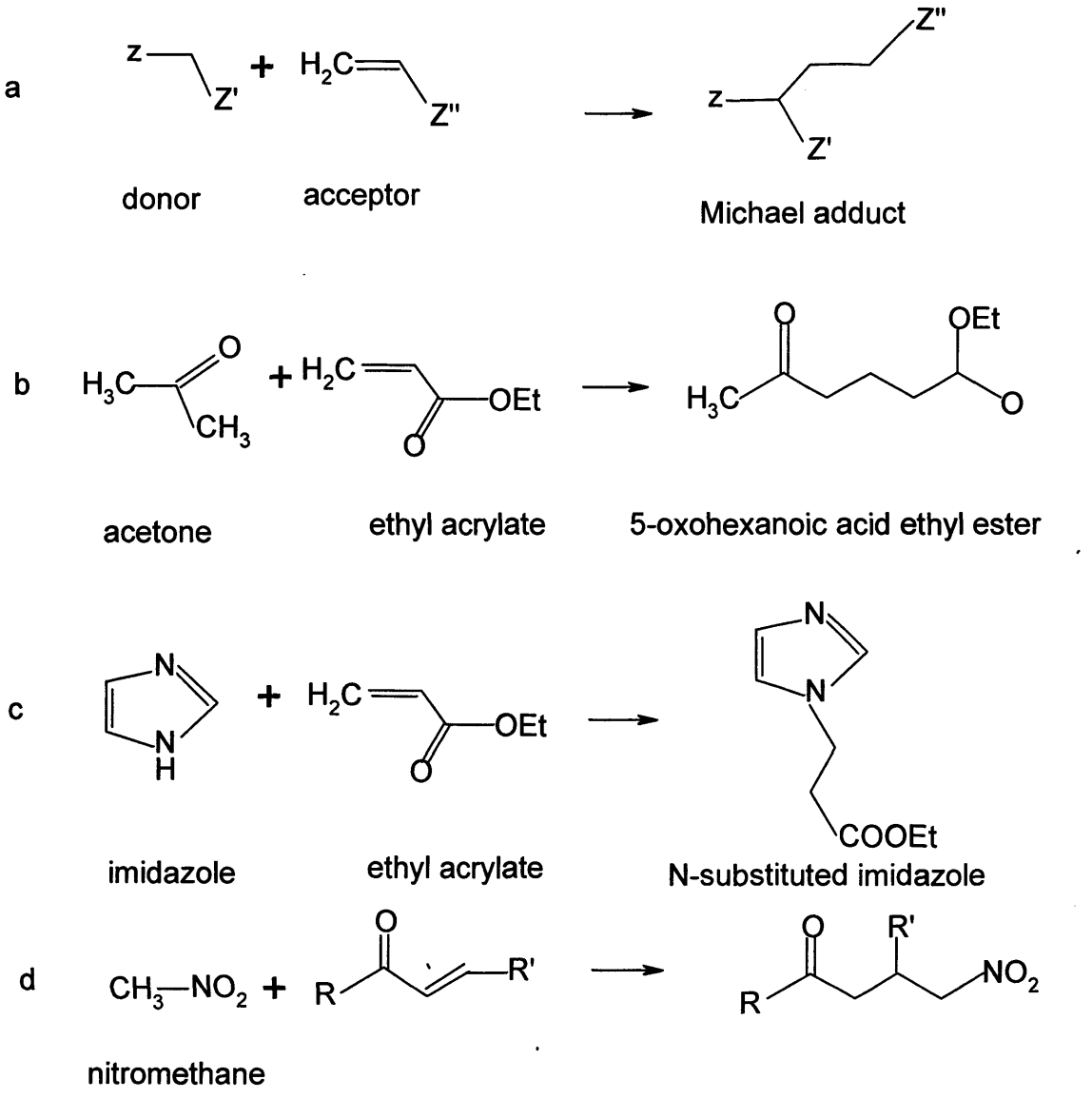

Figure 1.4 Michael additions on base catalysts.

Kabashima *et al.* carried out Michael addition of nitromethane to methyl crotonate, 3-buten-2-one, 2-cyclohexen-1-one and crotonaldehyde (Figure 1.4d).[37] KF/alumina and KOH/alumina exhibited high activities, while MgO and CaO exhibited no activity for methyl crotonate and 3-buten-2-one, but low activities for 2-cyclohexen-1-one and crotonaldehyde. SrO, BaO and La_2O_3 exhibited practically no activities for all Michael additions examined.

Further examples of Michael additions are reported using malonitrile, diethyl malonate, ethyl cyanacetate, cyanoacetamide or thiols as acceptors and methyl vinyl ketone, methyl acrylate and simple and substituted chalcones as acceptors on a variety of heterogeneous base catalysts, which include $Ba(OH)_2$,[95,237] hydrotalcite and modified hydrotalcite,[238,239] Mg-La mixed metal oxide[45] and phosphate.[113]

There are also examples of enantioselective Michael reactions on MCM-41 heterogenized chiral amines (cinchonidine and cinchonine) (Figure 1.5).[199]

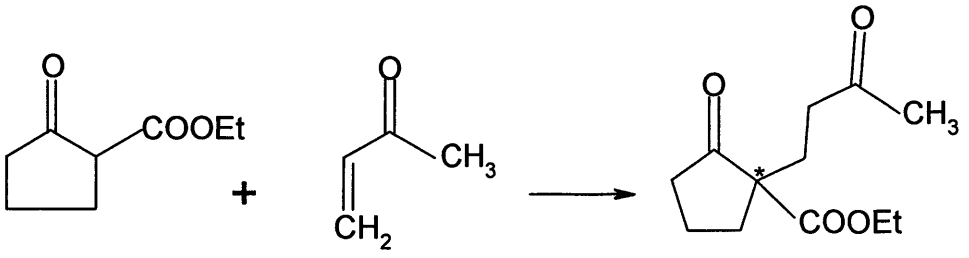

Figure 1.5 Enantioselective Michael reactions on MCM-41 heterogenized chiral amines.

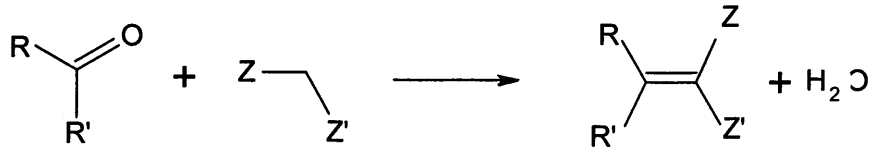

Figure 1.6 Knoevenagel condensations.

1.4.3 Knoevenagel condensation

Knoevenagel condensation involves the condensation of a carbonyl component with active methylene compounds, which is one of the most popular methods of synthesizing functionalized alkenes (Figure 1.6).

The typical Knoevenagel condensation of various aldehyde with malonitrile, diethyl malonate or cyanoacetate were performed on a variety of heterogeneous base catalysts, such as MgO,[239,240] hydrotacite and modified hydrotalcite,[239,241-245] Zeolite,[246] KF/Al_2O_3,[247] Aminosilica,[248] $AlPO_4/Al_2O_3$,[249] $Na_2Ca_2P_2O_7$,[250] Xenotlite,[251] and MCM-41.[239]

The condensation of salicylaldehyde derivative with diethyl 2-pentenedicarboxylate (diethylglutaconate) under Knoevenagel conditions leads to coumarin-3-acrylates and chromene derivatives (Figure 1.7).[197] Chromenes (2H-1-benzopyran derivatives) and coumarins (2H-1-benzopyran-2-one derivatives) are widely used as aromas in the perfume industry, as blood coagulants in anticoagulant therapy and as optical brighteners and fluorescent dyes because of the intense fluorescence of the coumarin based compounds. These syntheses have been performed over different solid base catalysts such as functionalized MCM-41[197] and hydrotalcites.[252]

The two-step synthesis of dicyanomethylene derivative dyes was performed using different solid bases (Figure 1.8).[149] The first step is the Knoevenagel condensation of acetophenone and malonitrile to give the corresponding α-methylbenzyl-idenemalononitrile. Subsequent condensation of α-methylbenzyl-idenemalononitrile with benzaldehyde gives the 1,1-dicyano-1,3-butadiene dye.

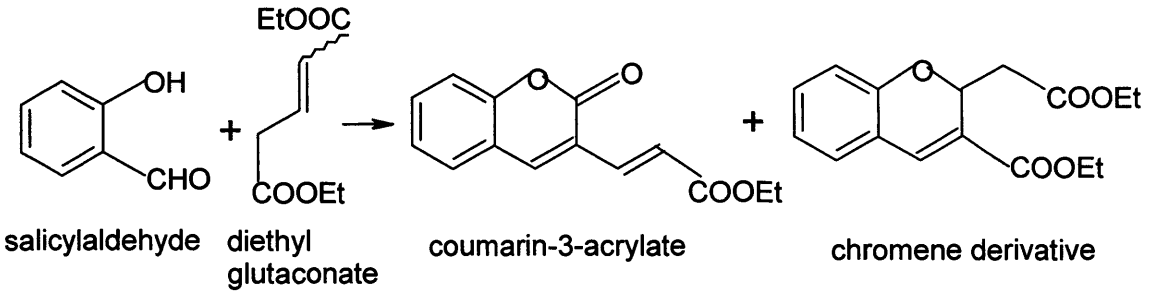

Figure 1.7 Synthesis of chromene and coumarin derivatives over base catalysts

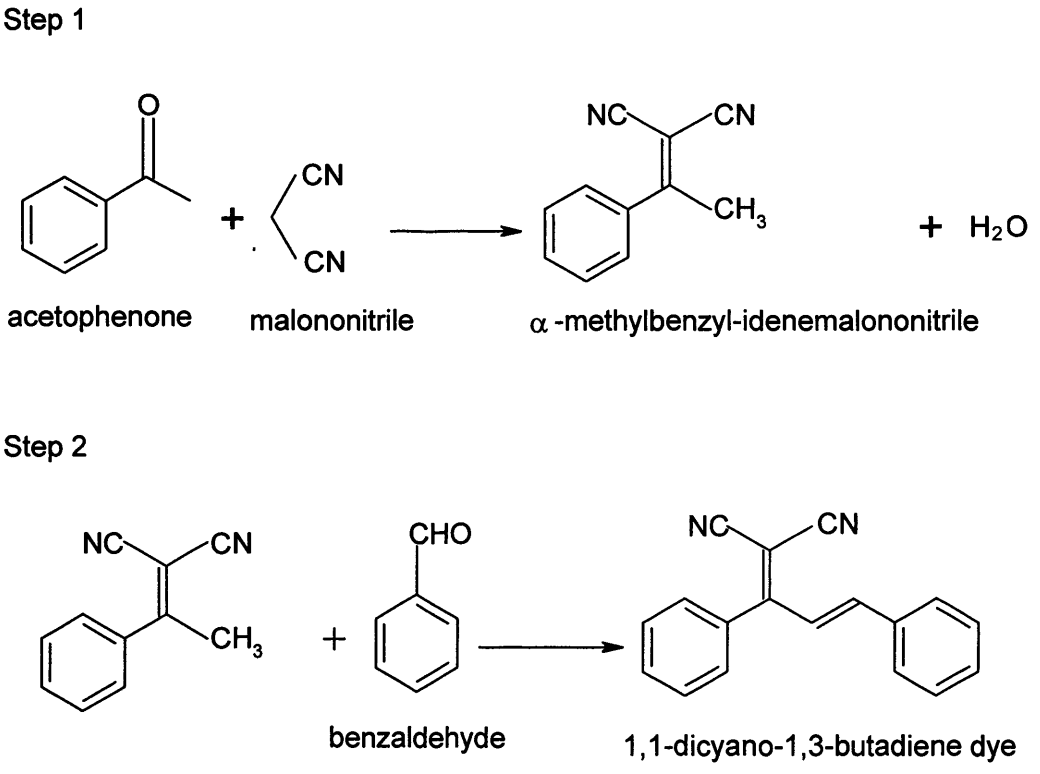

Figure 1.8 Two-step synthesis of dicyanomethylene derivative dyes via Knoevenagel condensation.

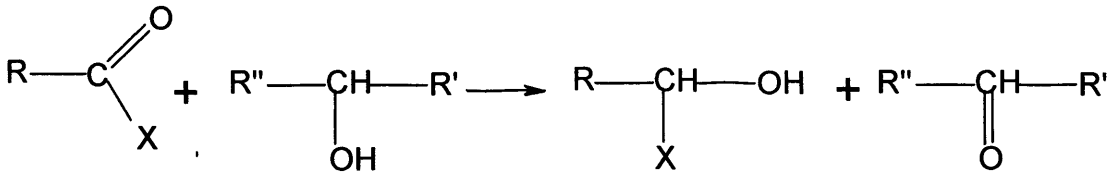

Figure 1.9 General equation of MPV reduction.

1.4.4 Meerwein-Ponndorf-Verley (MPV) reduction

The hydrogenation of unsaturated aldehydes leads to saturated aldehydes or unsaturated alcohols as primary products, which can be over-hydrogenated to saturated alcohols. The most important product from an industrial point of view, and unfortunately the most difficult to obtain, is the unsaturated alcohol. This reaction can be performed with hydrogen. If the hydrogen donor used is an alcohol, the hydrogen transfer process is known as the Meerwein-Ponndorf-Verley (MPV) reduction. The MPV process allows the highly selective reduction of aldehydes and ketones under mild reaction conditions because it avoids the use of hydrogen at high pressures. This reduction reaction is so highly selective that it leaves C=C double bonds untouched (Figure 1.9).[15,253] The reaction can be performed with acid or base catalysts.[254] One of the drawbacks of an acid catalysed process in the possible dehydration of the alcohol with formation of ethers and olefins.

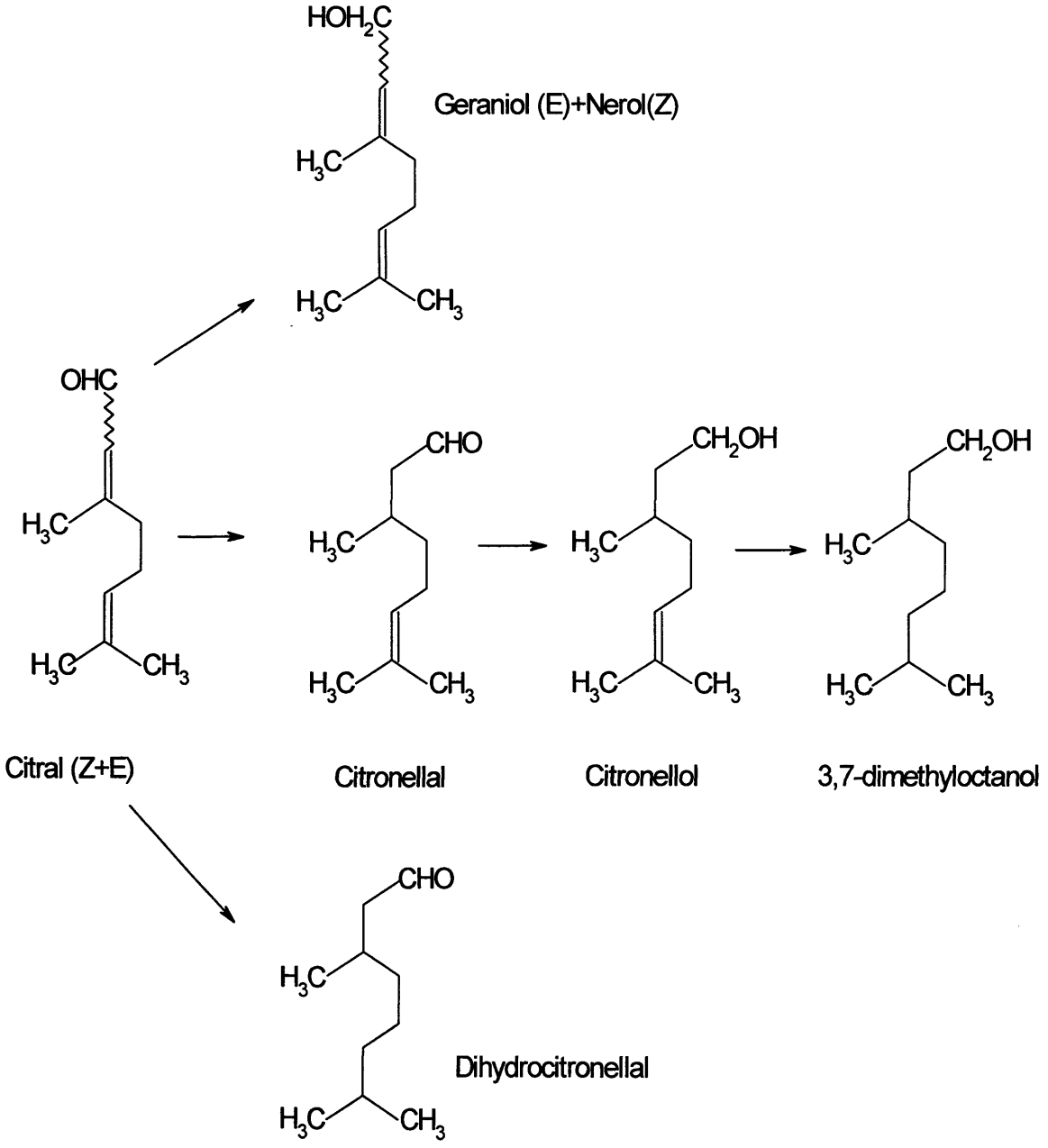

Figure 1.10 Different products obtained on hydrogenation of citral.

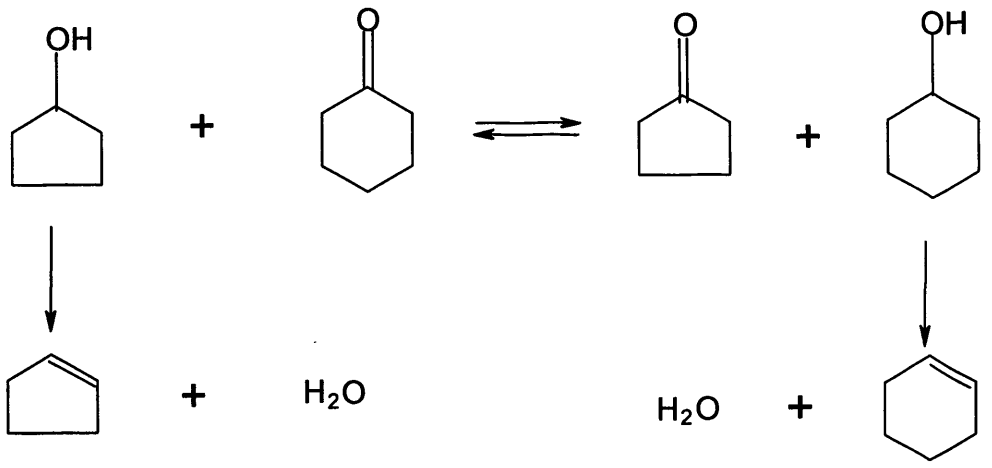

Figure 1.11 Transformation of the cyclopentanol/cyclohexanone mixture as suggested by Berkani *et al.*[258]

One of the most extensively studied reactions is citral (3,7-dimethyl-2,6-octadieanl) hydrogenation (Figure 1.10).[22,153,255] The reaction has been performed without a metal phase, using base catalysts such as MgO or hydrotalcites and 2-propanol, mainly, as the hydrogen donor. Some other examples of carbonyl compounds reduced by hydrogen transfer from alcohols are benzaldehyde on MgO or hydrotalcite;[34] heterocyclic carboxaldehydes on hydrotalcite;[256] cyclohexanone over MgO or hydrotalcite;[23,257] as well as 4-tert-butylcyclohexanone over hydrotalcite, zeolites or KF/Al_2O_3.[80]

MPV reaction can be used as test reaction to characterize the basicity of solid base catalysts.[258] Berkani *et al.* proposed the transformation of an alcohol (cyclopentanol) in the presence of a ketone (cycleohexane) as a model reaction to characterize the acidity and the basicity of oxide catalysts (Figure 1.11). The authors found a good correlation between basicity of NaCsX zeolites or K-impregnated alumina and their activities for

hydrogen transfer (monitored by cyclohexanol or cyclohexene production). On the other hand, the more acidic the catalyst is, the higher the dehydration extent.

1.4.5 Aldol condensation

An Aldol condensation is an organic reaction where an enolate ion reacts with a carbonyl compound to form a β-hydroxyaldehyde or β-hydroxyketone followed by dehydration to a conjugated enone. The first part of this reaction is an aldol reaction, the second part elimination. Adolization is widely used in organic synthesis for C-C bonds creation. It is commonly used to manufacture of perfumes and pharmaceuticals (Chalcones and more generally α,β-unsaturated ketones) and platicizers.[15]

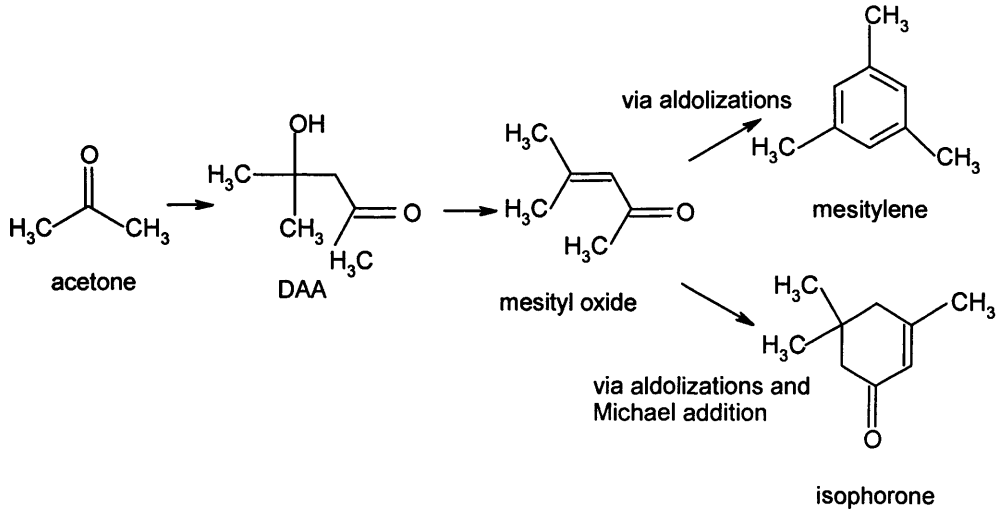

Figure 1.12 Different products coming from acetone aldol addition/condensation.

Acetone addition and condensation have been extensively studied (Figure 1.11), over a variety of solid bases, such as alkaline earth oxides, La_2O_3, ZrO_2, $Ba(OH)_2$, hydrotalcite, $CsOH/SiO_2$ and alkali-modified vanadium phosphate. [1,6,159,171,259-263] Aldol addition of

acetone is an important reaction in industry, since acetone can undergo addition to form diacetone alcohol (DAA) which can be dehydrated to produce mesityl oxide, used in the synthesis of methyl isobutyl ketone (MIBK). MIBK is one of the most widely used alphatic ketones, used in paints, protective coatings and as intermediates in the production of various plastics and resins.[263] Moreover, the reaction is a useful way to reveal information about the basicity of the tested solids.[48,264]

Cross aldol condensation of acetone with citral (Figure 1.13),[265] in the presence of hydrotalcite bearing OH^-, gives selectively the product of pseudoionone, which is an intermediate in the commercial production of vitamin A.

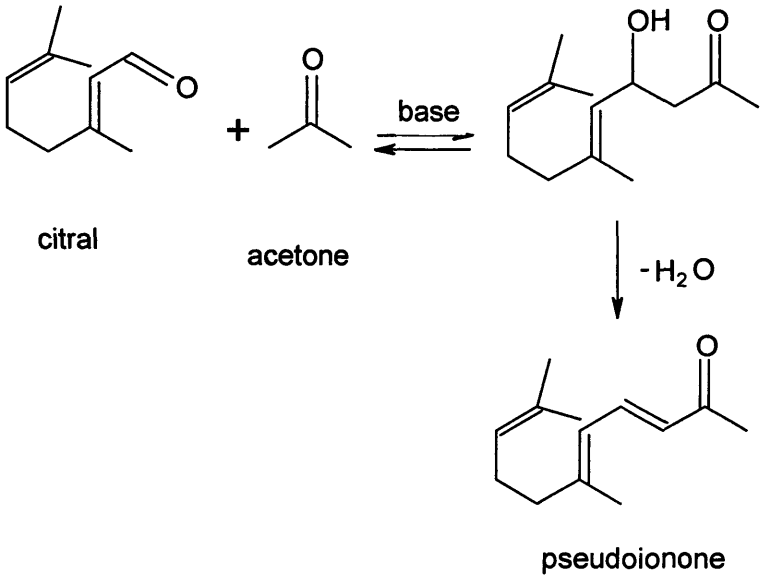

Figure 1.13 Aldol condensation of citral with acetone.

Aldol condensations between a ketone acting as methylene compound and an aldehyde are termed Claisen-Schmidt condensations.[14] Therefore, Claisen-Schmidt condensations between acetophenone and benzaldehyde derivatives allow the synthesis of α,β-unsaturated ketones known as chalcones (Figure 1.14).[80,166,266-268] Chalcones are

flavonoids of numerous applications as pesticides, photoprotector in plastics, solar creams, food additives and many biological activities (anti-malarial, anti-inflamatory, anticancer...). Vesidryl (2',4',4-trimethoxy chalcone) constitutes an example of pharmaceutical interesting chalcones, due to its diuretic and choleretic properties.[14]

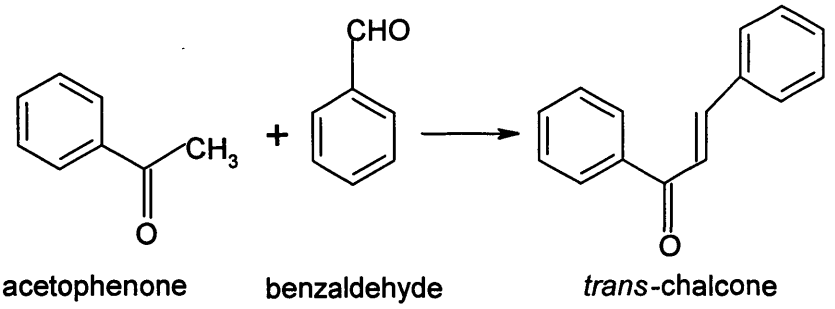

Figure 1.14 Obtention of chalcone by Claisen-Schmidt condensation between acetophenone and benzaldehyde.

1.4.6 Cyanoethylation of alcohols

Cyanoethylation of alcohols (Figure 1.15) is an important reaction, as it gives an entry into preparation of alkoxypropionitriles/propanamines/propionic acids, which are important for the syntheses of drug intermediates and fine chemicals.[269] The reaction has been studied over a variety of heterogeneous base catalysts, such as hydrotalcite, aqueous agar gel-entrapped NaOH catalyst, alkaline earth oxides and hydroxides, KF/Al_2O_3, and KOH/Al_2O_3.[270-274]

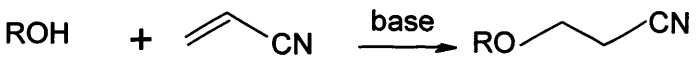

Figure 1.15 Cyanoethylation of alcohols.

1.4.7 Tishchenko reaction

The classical Tishchenko reaction is a dimerization of aldehydes to the corresponding esters by base catalysts, in which one molecule is oxidized and another reduced (Figure 1.16 a). Some base solids can catalyse the process. Handa *et al.* performed self condensation of benzaldehyde to benzyl benzoate on KF-loaded alumina.[235] Seki *et al.* carried out the intramolecular Tishchenko reaction of o-phthaldehyde to phthalide with alkaline earth oxides (Figure 1.16 b).[74] There are also examples of mixed Tischenko reaction over solid base catalysts, such as alkaline earth oxides, La_2O_3, ZrO_2, ZnO, γ-Al_2O_3, hydrotalcite, KF/alumina and KOH/alumina.[33]

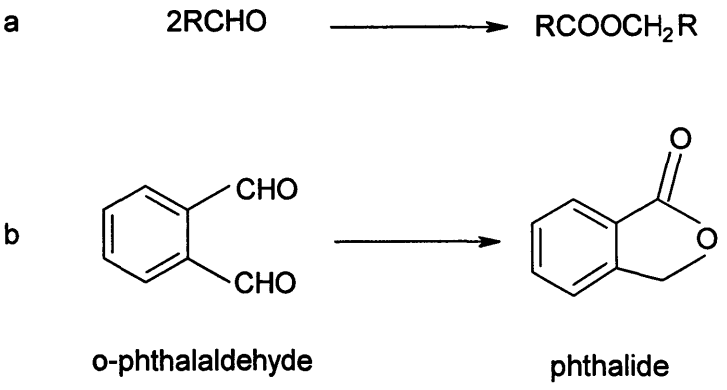

Figure 1.16 Tischenko reaction: a) general scheme and b) example of intramolecular Tischenko reaction taken from the literature.[74]

1.4.8 Nitroaldol reaction

Nitrodaldol reaction is the reaction of a nitro compound with a carbonyl compound to form a nitroalcohol under basic conditions. The reactions often proceed further to afford nitroalkenes (Figure 1.17).[183,276,277] Unsaturated nitrocompounds are important precursors of a large variety of target molecules and possess biological activity representative of insecticides, fungicides and pharmacologically active substances. They are powerful

dienophiles in the Diels-Alder reaction and readily undergo of the nitro group into a variety of diverse functionalities, nitroalkenes are quite versatile compounds in synthetic organic chemistry.[183]

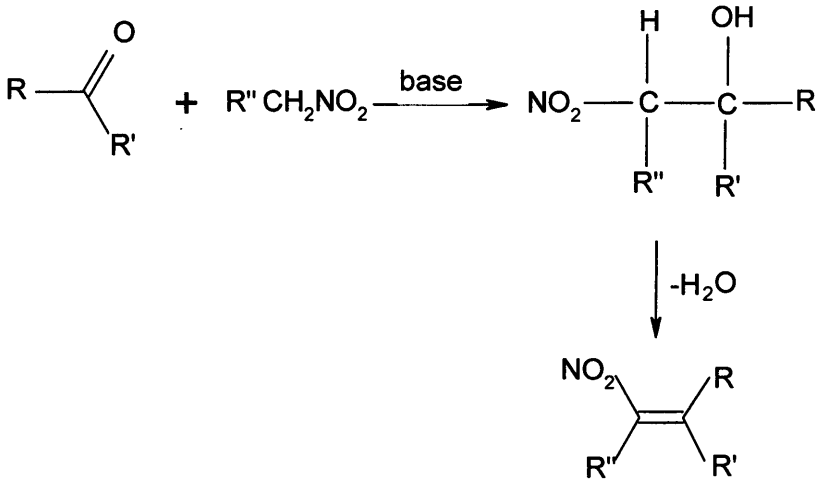

Figure 1.17 Nitroaldol condensation.

MgO, CaO, $Ba(OH)_2$, KOH/Al_2O_3, KF/Al_2O_3, $Sr(OH)_2$, hydrotalcite, and $MgCO_3$ all exhibit high activity for the nitroaldol reaction of nitromethane with propionaldehyde. Moderate activities were observed with $Mg(OH)_2$, γ-Al_2O_3, SrO, $Ca(OH)_2$, $BaCO_3$, $SrCO_3$, BaO and La_2O_3.[278] Mg-Al mixed oxides prepared by calcinations of hydrotalcite catalyze the nitroaldol condensation to nitroalcohols. The reaction is diastereoselective.[279]

Some examples of heterogeneous base catalysts used in this process were alkaline ion-exchanged zeolites,[183] N,N-diethylpropylamine supported on amorphous silica n,[280] amberlyst A-21,[281] or incorporation of La^{3+} in an organic network.[282]

1.4.9 Alkene and alkyne isomerization

Isomerization of alkenes, also called double bond migration, proceeds through anion intermediates formed by abstraction of an allylic proton from alkene molecules by solid bases.[12] Isomerization of alkene as carried out over the first solid base catalyst, Na dispersed on Al_2O_3.[5]

Strong solid bases are active for the isomerization of 2,3-dimethylbut-1-ene.[12] Among the studied solid base catalyst, alkali amides supported on Al_2O_3 and alkaline earth metal oxides show very high activity for isomerization. 1-N-pyrroli-dino-2-propene isomerises to 1-N-pyrroridino-1propene in 100% selectivity over alkaline earth oxides.[1]

Regarding characterization of strong basic catalysts, it was suggested that alkene isomerization can be used as the test reaction to characterize the solid base catalyst since alkenes have high pKa values.[1,12] Within this group of reactions, 1-butene,[64,156,190,191,215,283] 2,3-dimethyl-1-butene,[61,175] cis-2-butene,[87,88,177,188,192] 1-pentene,[284] 1-hexene,[284] β-isophorone,[155,285] 3-carene,[286] β-pinene,[287] or 3-phenyl-1-propene (allylbenzene, Figure 1.18)[47,48] can be cited as the probe molecules.[11]

The Isomerization of 1-butene is a good test reaction to investigate the active sites and the function of the catalyst (Figure 1.19).[288] The reaction is initiated by abstraction of an allylic H^+ by a basic site to form the *cis* and *trans* forms of the allyl anion. A high *cis/trans* ratio is characteristic of base-catalyzed double bond migration, in contrast to a value close to unity for acid-catalyzed double bond migration. The *cis/trans* ratio in 2-butenes produced can be used to judge whether the reaction is a base-catalyzed or acid-catalyzed. Many catalysts have been recognized as solid base catalysts by their catalytic behaviour in double bond migration of 1-butene, such as CaO[289] BaO[289] ThO_2[290]and TiO_2.[291]

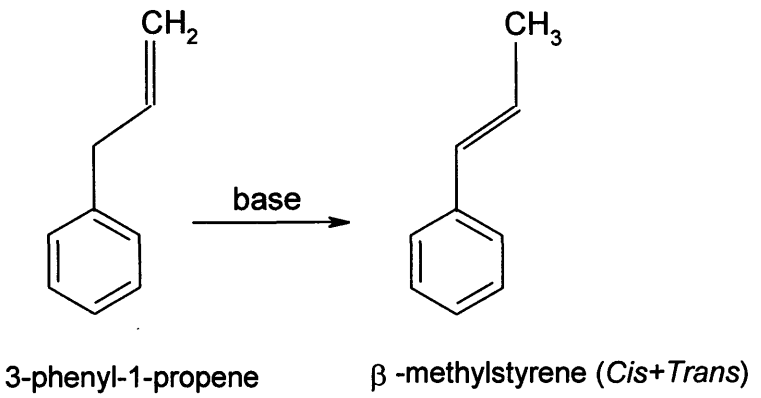

Figure 1.18 3-phenyl-1-propene transformation on basic sites.

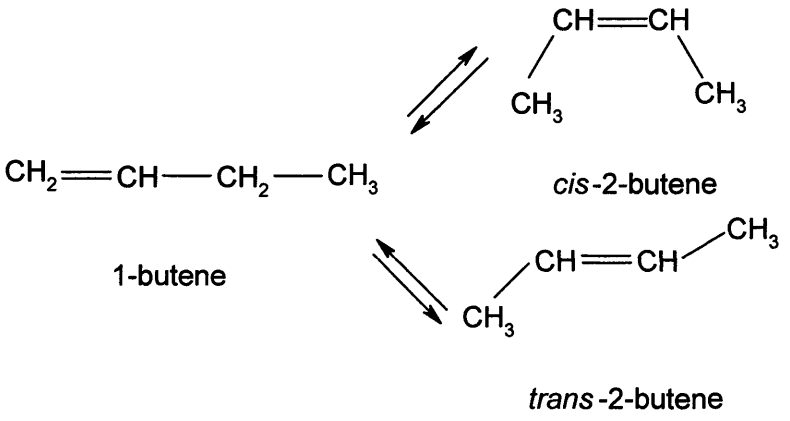

Figure 1.19 Double migration of 1-butene.

1.4.10 Alkylation of toluene with methanol and formaldehyde

Base catalysts lead to side-chain alkalation, while acid catalysts bring about ring alkylation (Figure 1.20),[292,293] therefore, this reaction can supply some information on the basicity of the test solids. The reaction is also interesting from the industrial point of

view, since alkylation of benzene with ethylene on basic sites followed by dehydrogenation of ethylbenzene yields styrene, used in the production of plastics and rubbers.[55,184,294] The reaction has being applied to some substrates (ethylbenzene, cumene, xylenes, phenol, aniline...) and reactants (ethane, pronene, 1,2-diphenylethylene).[61,125,157,295-297] A variety of heterogeneous base catalysts have been tested for the alkylation of toluene, such as zeolite,[292] three-element mixed oxides,[55] $Mg_3(PO_4)_2$ [125] and hydrotalcite.[157,296]

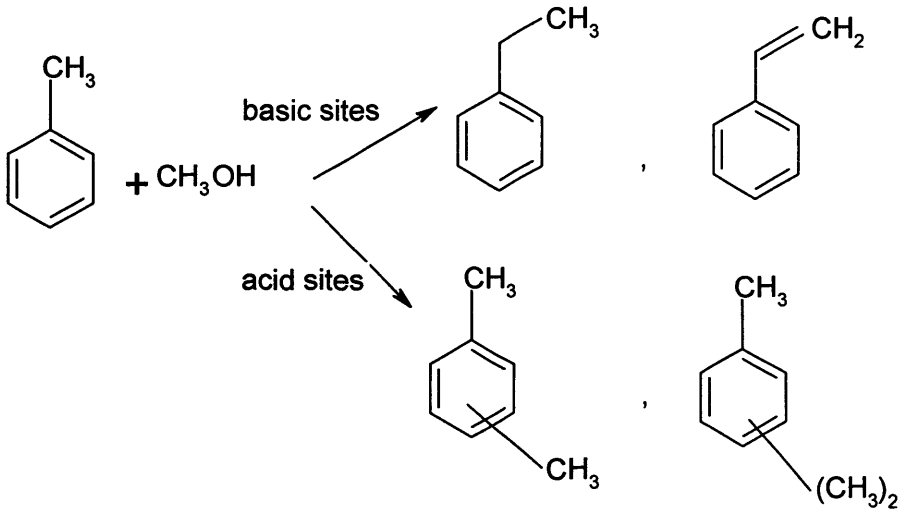

Figure 1.20 Alkylation of toluene with methanol on acid and basic sites.

1.4.11 Some other reactions

a) Si-C bond formation

Nucleophilic substitution occurs when an anion attacks silicon.[12]

$$Nu^- + R_3SiL \longrightarrow NuSiR_3 + L^-$$

Here, L^- is a leaving group from the Si atom.

The reaction of trimethylsilyacetylene over KNH_2/Al_2O_3 or KF/Al_2O_3 leads to the metathesis of the alkyne, with the products being bis(trimethylsily)acetylene and acetylene.[298]

$$Me_3SiC{\equiv}CH \longrightarrow Me_3SiC{\equiv}CSiMe_3 + HC{\equiv}CH$$

b) Pudovik reaction (P-C bond formation)

The Pudovik reaction involves the addition of compounds containing a labile P-H bond to unsaturated systems and is one of the most versatile pathways for the formation of carbon-phosphorus bonds.[12]

Semenzin *et al.* reported that KOH/Al_2O_3 is a very efficient catalyst for some Pudovik reactions.[299] The reaction of diethyl phosphonate with benzalacetone in the presence of KOH/Al_2O_3 instantly gave the 1,2 adduct in a 100% yield at 293K, while the 1,4 adduct was quantitatively obtained at 373K (Figure 1.21).

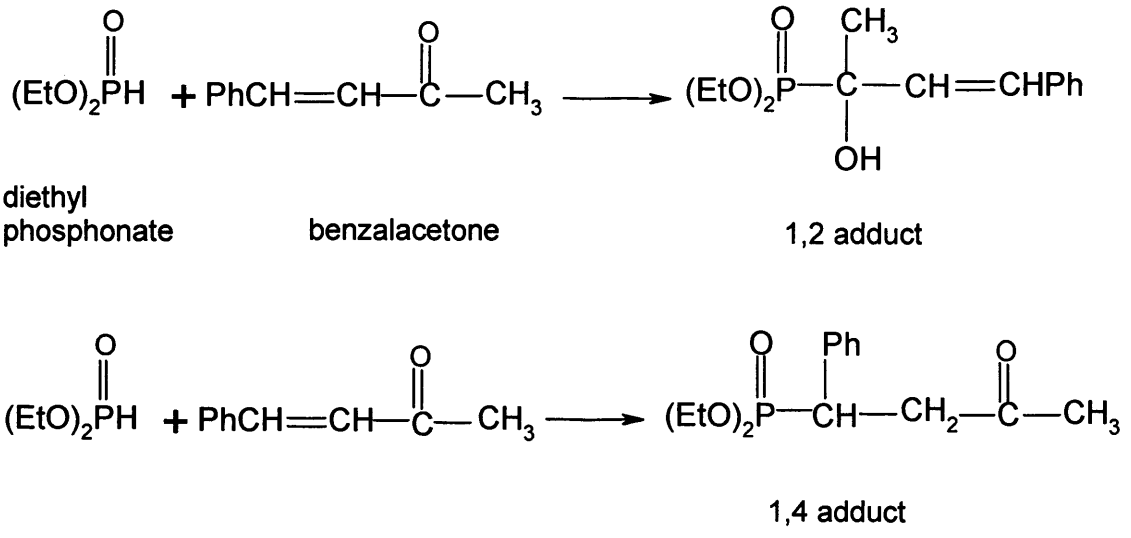

Figure 1.21 Pudovik reaction of diethyl phosphonate with benzalacetone.

c) Synthesis of heterocycles

The reactions of primary amines with carbon disulfide afford N,N'-disubstituted thioureas in high yields over a Zn-Al mixed oxide prepared from the hydrotalcite like material.[300] The thiocarbamic acid, RNH-C(=S)SH, which is formed by nucleophilic attack of the amine to CS_2, is suggested to be the intermediate. When the amine has an additional nucleophilic group, the intermediate is quickly converted into heterocyclic thiones. (Figure 1.22)

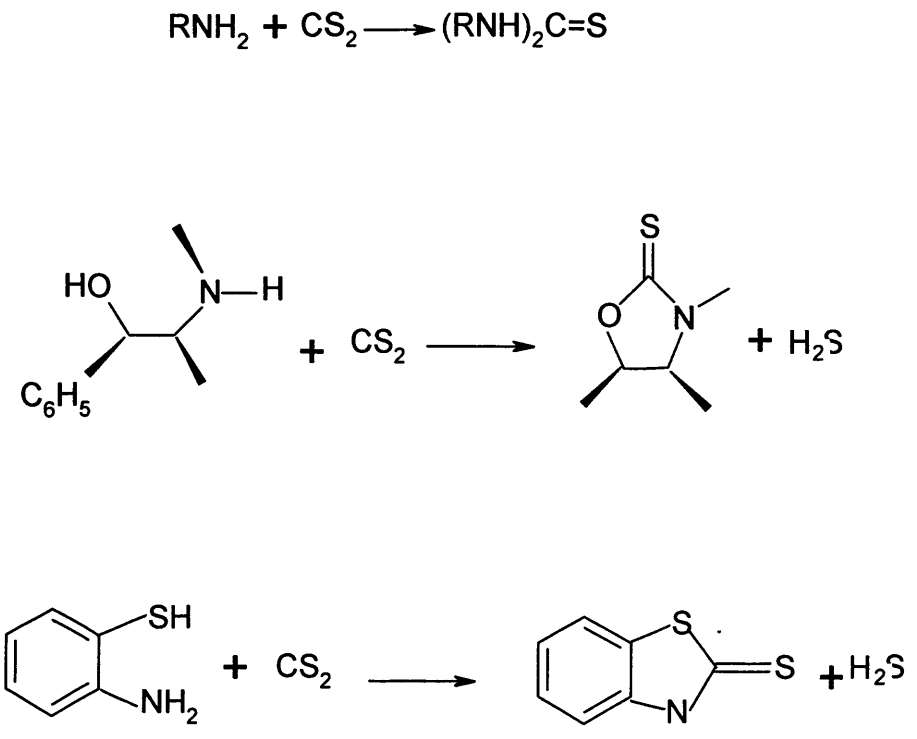

Figure 1.22 Synthesis of heterocycles.

1.5 Aims of this thesis

Solid base catalysts have potential use numerous applications in fine and bulk chemical synthesis but are only utilised in a small number of reactions. The solid base catalysts reported have been introduced (Section 1.2). Magnesium oxide (MgO) is a typical basic oxide (Hammett constant, $H_- = +26.0$)[301] and has the lowest solubility among the alkaline earth oxides. In view of this, we consider that MgO has the potential to be a reusable catalyst, as it may not be lost by leaching into the reaction mixture. Furthermore, MgO is inexpensive and easily obtained and as a result it can be readily applied in large scale manufacture. These characteristics suggest that MgO has potential use in numerous applications in fine and bulk chemical synthesis, but at the present time, it is used only in a small number of reactions, primarily because the structure and activity of MgO are affected by the preparation method,[1, 15, 23,302-3.3] and the commercial sample of MgO that are currently available shows low surface area (typically < 20 $m^2 g^{-1}$)[304] and hence, low activity. Consequently, as activity is linked to surface area, many preparative methodologies for the synthesis of high surface area MgO have been developed,[23,303-308] such as chemical vapour deposition,[305] sol-gel procedures[306] and aerogel syntheses.[304-307] However, these methods are relatively complex. As the cost of fabricating a catalyst can be a critical factor in its industrial applications, few commercial materials have been synthesized in this way. Consequently, we consider that simpler and more economic preparation method of MgO is still desirable.

This main aim of this thesis is to investigate the effect of preparation route on the structure and catalytic activity of the common solid base MgO and the relationship between the structure and catalytic activity. A number of preparative routes are investigated as well as the effect of factors such as the calcination temperature. This is complemented by testing the catalysts in a range of liquid phase reactions from small-

scale organic transformations, such as MPV reaction, Michael additions and Knoevenagel reactions, to bulk transformations such as biodiesel synthesis. The other aim of this thesis to find new reactions that can be catalyzed by MgO.

References

1. H. Hattori, *Chem. Rev.*, 1995, **95**, 537.
2. F. King and G. J. Kelly, *Catal. Today*, 2002, **73**, 75.
3. W. F. Hoelderich, *Catal. Today*, 2000, **62**, 115.
4. A. Corma, S. Iborra, I. Rodriguez and F. Sanchez, *J. of Catal.*, 2002, **211**, 208.
5. H. Pines, J. A. Veseley and V. N. IPatieff, *J. Am. Chem. Soc.*, 1955, **77**, 6314.
6. H. Hattori, *J. Jpn. Pet. Inst.*, 2004, **47**, 67.
7. K. Tanabe and W. F. Hoelderich, *Appl. Catal. A: General*, 1999, **181**, 399.
8. R. A. Sheldon, *Comptes Rendus del'Academie des Sciences, Serie Iic: Chimie*, 2000, **3**, 541.
9. R. A. Sheldon and R. S. Downing, *Appl. Catal. A: General*, 1999, **189**, 163.
10. P. T. Anastas, M. M. Kirchhoff and T. C. Williamson, *Appl. Catal. A: General*, 2001, **221**, 3.
11. A. Marinas, J. M. Marinas, M. A. Aramendia and F. J. Urbano, *New Developments in Catalysis Research*, 2005, 85.
12. Y. Ono, *J. Catal.*, 2003, **216**, 406.
13. Y. Ono and T. Baba, *Catal. Today*, 1997, **38**, 321.
14. J. Weitkamp, M. Hunger and U. Rymsa, *Micropor. Mesopor. Mat.*, 2001, **48**, 255.
15. F. Figueras, *Topics in Catalysis*, 2004, **29**, 189.
16. C. Xu, J. K. Bartley, D. I. Enache, D. W. Knight and G. J. Hutchings, *Synthesis*, 2005, **19**, 3468.
17. M. Drexler and M. Amiridis, *J. Catal.*, 2003, **214**, 136.
18. S. Kus, M. Otremba, A. Torz and M. Taniewski, *Appl. Catal. A: General*, 2002,

230, 263.

19. M. Bailly, C. Chizallet, G. Costentin, H. Lauron-Pernot, J. Krafft, P. Bazin, J. Saussey and M. Che, *Proceedings of the 13th ICC 2004, Paris (France)*, 2004, Reference: O1-044.
20. M. Aramendia, V. Borau, C. Jimenez, J. Marinas, A. Porras and F. Urbano, *J. Mater. Chem.*, 1996, **6**, 1943.
21. M. Aramendia, V. Borau, C. Jimenez, J. Marinas, A. Porras and F. Urbano, *J. Catal.*, 1996, **161**, 829.
22. M. Aramendia, V. Borau, C. Jimenez, J. Marinas, A. Porras and F. Urbano, *Appl. Catal. A: General,* 1998, **172**, 31.
23. M. Aramendia, V. Borau, C. Jimenez, J. Marinas, J. Ruiz and F. Urbano, *Appl. Catal. A: General*, 2003, **244**, 207.
24. M. Aramendia, V. Borau, C. Jimenez, J. Marinas and F. Romero, *J. Catal.,* 1999, **183**, 119.
25. A. Corma, S. Iborra, S. Miquel and J. Primo, *J. Catal.*, 1998, 173, 315.
26. E. Garrone, D. Bartalini, S. Coluccia, G. Martra, D. Tichit and F. Figueras, *Stud. Surf. Sci. Catal.*, 1994, **90**, 183.
27. M. Glinski and P. Radomski, *Pol. J. Chem.*, 1999, **73**, 1233.
28. R. Martin-Aranda, M. Rojas-Cervantes, A. Lopez-Peinado and J. Lopez-Gonzalez, *Catal. Lett.*, 1994, **25**, 385.
29. G. Szollosi and M. Bartok, *J. Mol. Catal. A: Chem.*, 1999, **148**, 265
30. G. Szollosi and M. Bartok, *Catal. Lett.*, 1999, **59**, 179.
31. O. Woo, N. Ayala and L. Broadbelt, *Catal. Today*, 2000, **55**, 161.
32. S. Ardizzone, C. Bianchi and B. Vercelli, *Appl. Surf. Sci.*, 1998, **126**, 169.
33. T. Seki, H. Kabashima, K. Akutsu, H. Tachikawa and H. Hattori, *J. Catal.,* 2001, **204**, 393.

34. M. Aramendia, V. Borau, C. Jimenez, J. Marinas, J. Ruiz and F. Urbano, *J. Colloid Interf. Sci.*, 2001, **238**, 385

35. T. Wei, W. Wei, M. Wang, Y. Sun and B. Zhong, *Proceedings of the 13th ICC, Paris (France),* 2004, Reference: O4-005.

36. A. Ndou, N. Plint and N. Coville, *Appl. Catal. A: General*, 2003, 251, 337.

37. H. Kabashima, H. Tsuji and H. Hattori, *Appl. Catal. A: General*, 1997, **165**, 319.

38. Q. Li, W. Zhang, N. Zhao, W. Wei and Y. Sun, *Catal. Today*, 2006, **115**, 111.

39. M. Ai, *B. Chem. Soc. Jpn.*, 1991, **64**, 1342.

40. B. Bhanage, S. Fujita, Y. Ikushima and M. Arai, *Appl. Catal. A: General*, 2001, **219**, 259.

41. S. Kus, M. Otremba and M. Taniewske, *Fuel*, 2003, **82**, 1331.

42. S. Bancquart, C. Vanhove, Y. Pouilloux and J. Barrault, *Appl. Catal. A: General*, 2001, **218**, 1.

43. M. Watanabe, M. Osada, H. Inomata, K. Arai and A. Kruse, *Appli. Catal. A: General*, 2003, **245**, 333.

44. B. Reddy, K. Ratnam and P. Saikia, *J. Mol. Catal. A: Chem.*, 2006, **252**, 238.

45. B. Veldurthy, J. Clacens and F. Figueras, *Adv. Synth. Catal*, 2005, **347**, 767.

46. Q. Su, X. Chen, B. Liu and L. Wang, *Faming Zhuanli Shenqing Gongkai Shuomingshu*, CODEN: CNXXEV CN 1762578 A 20060426, 2006.

47. M. Aramendia, V. Borau, C. Jimenez, A. Marinas, J. Marinas and F. Urbano, *J. Catal.*, 2002, **211**, 556.

48. M. Aramendia, V. Borau, C. Jimenez, A. Marinas, J. Marinas, J. Ruiz and F. Urbano, *J. Mol. Catal. A: Chem.*, 2004, **218**, 81.

49. D. Jiang, B. Zhao, X. Huang, H. Huang, G. Pan, G. Ran and E. Min, *228th ACS National Meeting, Philadelphia, PA, United States*, 2004.

50. M. Aramendia, V. Borau, C. Jimenez, J. Marinas, J. Ruiz and F. Urbano, *J. Chem.*

Soc. Perk. T. 2, 2002, **6**, 1122.

51. D. Jiang, B. Zhao, Y. Xie, G. Pan, G. Ran and E. Min, *Appl. Catal. A: General*, 2001, **219**, 69.
52. K. Parida and S. Rao, *React. Kinet. Catal. Lett.*1991, **44**, 95.
53. J. Palomeque, J. Lopez and F. Figueras, *J. Catal.*, 2002, **211**, 150.
54. R. Philipp, K. Ometa, A. Aoki and K. Fujimoto, *J. Catal.*, 1992, **134**, 422.
55. C. Flego, G. Cosentino and M. Tagliabue, *Appl. Catal. A: General*, 2004, **270**, 113.
56. S. Malinowski and J. Kkienski, *J. Catal.*, 1981, **4**, 130.
57. J. Di Cosimo, V. Diez and C. Apesteguia, *Appl. Catal. A: General*, 1996, **137**, 149
58. V. Diez, M. Capitanich, C. Apesteguia and J. Di Cosimo, *Proceedings of the 13th ICC, Paris (France)*, 2004, Reference: P5-133.
59. W. Ignaczak, W. Jozwiak, D. Gebauer and T. Paryjczak, *Pol. J. Chem.*, 1997, **71**, 962.
60. H. Matsuhashi and K. Arata, *J. Phys. Chem.*, 1995, **99**, 11178.
61. N. Sun and K. Klabunde, *J. Catal.*, 1999, **185**, 506.
62. E. Doskocil, S. Bordawekar and R. Davis, *J. Catal.*, 1997, **169**, 327.
63. P. Thomasson, O. Tyagi and H. Knözinger, *Appl. Catal. A: General*, 1999, **181**, 181.
64. Z. Li, H. Prescott, J. Deutsch, A. Trunschke, H. Lieske and E. Kemnitz, *Catal. Lett.*, 2004, **92**, 175.
65. M. Cutrufello, I. Ferino, R. Monaci, E. Rombi and V. Solinas, *Stud. Surf. Sci. Catal.*, 2001, **140**, 175.
66. C. Hamilton, S. Jackson and G. Kelly, *Appl. Catal. A: General*, 2004, **263**, 63.
67. M. Climent, A. Corma, S. Hamid, S. Iborra and M. Mifsud, *Green Chem.*, 2006, **8**, 524.
68. M. Tu and R. Davis, *J. Catal.*, 2001, **199**, 85.

69. S. Bordawekar, E. Doskocil and R. Davis, *Catal. Lett.*, 1997, **44**, 193.

70. P. Winiarek and J. Kijenski, *J. Chem. Soc. Faraday T.*, 1998, **94**, 167.

71. M. Telkar, C. Rode, V. Rane and R. Chaudhari, *Catal. Commun.*, 2005, **6**, 725.

72. H. Kabashima, T. Katou and H. Hattori, *Appl. Catal. A: General*, 2001, **214**, 121.

73. J. Campelo, M. Climent and J. Marinas, *React. Kinet. Catal. Lett.*1992, **47**, 7.

74. T. Seki and H. Hattori, *Chem. Commun.*, 2001, 2510.

75. H. Kochkar, J. Clacens and F. Figueras, *Catal. Lett.*, 2002, **78**, 91.

76. T. Baba, Y. Kawanami, H. Yuasa and S. Yoshida, *Catal. Lett.*, 2003, **91**, 31.

77. J. Clacens, D. Genuit, L. Delmotte, A. Garcia-Ruiz, G. Bergeret, R. Montiel, J. Lopez and F. Figueras, *J. Catal.*, 2004, **221**, 483.

78. J. Fraile, J. Garcia, D. Marco, J. Mayoral, E. Sanchez, A. Monzon and E. Romeo, *Stud. Surf. Sci. Catal.*, 2000, **130B**, 1673.

79. J. Zhu, H. Tsuji, H. Kabashima, H. Hattori and H. Kita, *Chinese Chemical Letters*, 1995, 6, 811.

80. J. Lopez, J. Valente, J. Clacens and F. Figueras, *J. Catal.*, 2002, **208**, 30.

81. A. Smahi, A. Solhy, H. El Badaoui, A. Amoukal, A. Tikad, M. Maizi and S. Sebti, *Appl. Catal. A: General*, 2003, **250**, 151.

82. M. Zahouily, B. Bahlaouan, M. Aadil, A. Rayadh and S. Sebti, *Org. Process Res. Dev.*, 2004, **8**, 275.

83. M. Zahouily, M. Salah, B. Bahlaouan, A. Rayadh, A. Houmam, E. Hamed and S. Sebti, *Tetrahedron*, 2004, **60**, 1631.

84. Y. Abrouki, M. Zahouily, A. Rayadh, B. Bahlaouan and S. Sebti, *Tetrahedron Lett.*, 2002, **43**, 8951.

85. F. Bautista, J. Campelo, A. Garcia, D. Luna, J. Marinas and A. Romero, *J. Chem. Soc. Perk. T. 2*, 2002, **2**, 227.

86. J. Zhu, Y. Chun, Y. Qin and Q. Xu, *Micropor. Mesopor. Mat.*, 1998, **24**, 19.

87. J. Zhu, Y. Chun, Y. Wang and Q. Xu, *Mater. Lett.*, 1997, **33**, 207.

88. T. Yamaguchi, J. Zhu, Y. Wang, M. Komatsu and M. Ookawa, *Chem. Lett.*, 1997, 989.

89. J. Zhu, Y. Wang, Y. Chun and X. Wang, *J. Chem. Soc. Faraday T.*, 1998, **94**, 1163.

90. H. Handa, T. Baba and Y. Ono, *J. Chem. Soc. Faraday T.*, 1998, **94**, 451.

91. T. Baba, H. Kizuka, H. Handa and Y. Ono, *Appl. Catal. A: General*, 2000, **194**, 203.

92. A. Aguilera, A. Alcantara, J. Marinas and J. Sinisterra, *Can. J. Chem.*, 1987, **65**, 1165.

93. A. Alcantara, J. Marinas and J. Sinisterra, *React. Kinet. Catal. Lett.*1986, 32, 377.

94. A. Alcantara, J. Marinas and J. Sinisterra, *Tetrahedron Lett.*, 1987, **28**, 1515.

95. J. Barrios, J. Marinas, C. Martinez and J. Sinisterra, *J. Mater. Sci. Lett.*, 1986, **5**, 840.

96. J. Barrios, J. Marinas and J. Sinisterra, *Bulletin des Societes Chimiques Belges*, 1986, **95**, 107.

97. J. Barrios, J. Sinisterra, C. Mertinez-Dalmau and J. Marinas, *J. Colloid Interf. Sci.*, 1987, **120**, 195.

98. M. Climent, J. Marinas and J. Sinisterra, *React. Kinet. Catal. Lett.*, 1987, **34**, 201.

99. M. Climent, J. Marinas, Z. Mouloungui, Y. Le Bigot, M. Delmas, A. Gaset and J. Sinisterra, *J. Org. Chem.*, 1989, **54**, 3695.

100. A. Fuentes, J. Marinas and J. Sinisterra, *Tetrahedron Lett.*, 1987, **28**, 4541.

101. A. Fuentes, J. Marinas and J. Sinisterra, *Tetrahedron Lett.*, 1987, **28**, 2951.

102. A. Garcia-Raso, J. Sinisterra and J. Marinas, *Pol. J. Chem.*, 1982, **56**, 1435.

103. A. Garcia-Raso, J. Sinisterra and J. Marinas, *React. Kinet. Catal. Lett.*1981, **18**, 33.

104. A. Garcia-Raso, J. Sinisterra and J. Marinas, *Revue Roumaine de Chimie*, 1982, **27**,

1047

105. A. Garcia-Raso, J. Sinisterra and J. Marinas, *React. Kinet. Catal. Lett.*1982, **19**, 145.

106. M. Iglesias, J. Marinas and J. Sinisterra, Tetrahedron, 1987, 43, 2335.

107. J. Sinisterra, F. Garcia-Blanco, M. Iglesias and J. Marinas, *React. Kinet. Catal. Lett.*, 1984, **25**, 277.

108. J. Sinisterra, F. Garcia-Blanco, M. Iglesias and J. Marinas, *React. Kinet. Catal. Lett.*, 1985, **27**, 263.

109. J. Sinisterra and J. Marinas, *Tetrahedron Lett.*, 1986, **27**, 4971.

110. J. Sinisterra and J. Marinas, *Bulletin des Societes Chimiques Belges*, 1987, **96**, 293.

111. J. Sinisterra, M. Jimenez, M. Iglesias and J. Marinas, *React. Kinet. Catal. Lett.*, 1988, **37**, 23.

112. M. Zahouily, B. Bahlaouan, A. Rayadh and S. Sebti, *Tetrahedron Lett.*, 2004, **45**, 4135.

113. M. Zahouily, H. Charki, Y. Abrouki, B. Mounir, B. Bahlaouan, A. Rayadh, and S. Sebti, *Letters in Organic Chemistry*, 2005, **2**, 354.

114. M. Zahouily, A. Elmakssoudi, A. Mezdar, A. Rayadh, S. Sebti, H. Lazrek, *Letters in Organic Chemistry*, 2005, **2**, 428.

115. M. Aramendia, J. Barrios, V. Borau, C. Jimenez, J. Marinas, F. Romero, J. Ruiz and F. Urbano, *Stud. Surf. Sci. Catal.*, 1994, **82**, 769.

116. M. Aramendia, V. Borau, C. Jimenez, J. Marinas and F. Romero, *React. Kinet. Catal. Lett.*, 2000, **69**, 311.

117. M. Aramendia, V. Borau, C. Jimenez, J. Marinas, F. Romero and F. Urbano, *J. Mol. Catal. A: Chem.*, 2002, **182**, 25.

118. M. Aramendia, V. Borau, C. Jimenez, J. Marinas and F. Romero, *Catal. Lett.*, 1999, **58**, 53.

119. M. Aramendia, V. Borau, C. Jimenez, J. Marinas, R. Roldan and F. Romero, *Stud. Surf. Sci. Catal.*, 2002, **143**, 899.

120. M. Aramendia, V. Borau, C. Jimenez, J. Marinas and F. Romero, *React. Kinet. Catal. Lett.*, 1996, **58**, 183.

121. M. Aramendia, V. Borau, C. Jimenez, J. Marinas and F. Romero, *J. Colloid Interf. Sci.*, 1999, **217**, 288.

122. M. Aramendia, V. Borau, C. Jimenez, J. Marinas, F. Romero, J. Navio and J. Barrios, *J. Catal.*, 1995, **157**, 97.

123. M. Aramendia, V. Borau, C. Jimenez, J. Marinas and F. Romero, *J. Catal.*, 1995, **151**, 44.

124. M. Aramendia, V. Borau, C. Jimenez, J. Marinas, M. Ortega, F. Romero, J. Ruiz and F. Urbano, *Stud. Surf. Sci. Catal.*, 2000, **130C**, 2141.

125. M. Aramendia, V. Borau, C. Jimenez, J. Marinas and F. Romero, *Colloid Surface A*, 2000, **170**, 51.

126. F. Bautista, M. Climent and J. Marinas, *Catal. Lett.*, 1993, **19**, 137.

127. J. Campelo, A. Garcia, D. Luna and J. Marinas, *Can. J. Chem.*, 1984, **62**, 638.

128. F. Bautista, J. Campelo, A. Garcia, R. Leon, D. Luna, J. Marinas, A. Romero, J. Navio and M. Macias, *React. Kinet. Catal. Lett.*, 1998, **65**, 245.

129. M. Aramendia, V. Borau, C. Jimenez, J. Marinas and F. Romero, *Chem. Lett.*, 2000, 574.

130. M. Renz and A. Corma, *European J. Org. Chem.*, 2004, 2036.

131. M. Montes-Moran, D. Suarez, J. Menendez and E. Fuente, *Carbon*, 2004, **42**, 1219.

132. R. Martin-Aranda, M. Rojas Cervantes, A. Lopez-Peinado and J. Lopez-Gonzalez, *J. Mol. Catal.*, 1993, **85**, 253.

133. J. de Lopez-Gonzalez, A. Lopez-Peinado, R. Martin-Aranda, M. Rojas-Cervantes, *Carbon*, 1993, **31**, 1231.

134. J. Lopez-Pestana, J. Diaz-Teran, M. Avila-Rey, M. Rojas-Cervantes, R. Martin-Aranda, *Micropor. Mesopor. Mat.*, 2004, **67**, 87.

135. M. Rojas-Cervantes, L. Alonso, J. Diaz-Teran, A. Lopez-Peinado, R. Martin-Aranda and V. Gomez-Serrano, *Carbon*, 2004, **42**, 1575.

136. V. Serra-Holm, T. Salmi, J. Multamaki, J. Reinik, P. Maki-Arvela, R. Sioholm and L. Lindfors, *Appl. Catal. A: General*, 2000, **198**, 207.

137. V. Serra-Holm, T. Salmi, P. Maeki-Arvela, E. Paatero and L. Lindfors, *Org. Process Res. Dev.*, 2001, **5**, 368.

138. A. Corma and R. Martin-Aranda, *J. Catal.*, 1991, **130**, 130.

139. A. Corma and R. Martin-Aranda, *Appl. Catal. A: General*, 1993, **105**, 271.

140. A. Corma and D. Kumar, *Stud. Surf. Sci. Catal.*, 1998, **117**, 201.

141. S. Delsarte, F. Mauge, J. Lavalley and P. Grange, *Catal. Lett.*, 2000, **68**, 79.

142. N. Fripiat, R. Conanec, A. Auroux, Y. Laurent and P. Grange, *J. Catal.*, 1997, **167**, 543.

143. N. Fripiat, V. Parvelescu and P. Grange, *Appl. Catal. A: General,* 1999, **181**, 331.

144. M. Climent, A. Corma, V. Fornes, A. Frau, R. Guil-Lopez, S. Iborra and J. Primo, *J. Catal.*, 1996, **163**, 392.

145. L. Gandia, R. Malm, R. Marchand, R. Conanec, Y. Larrent and M. Montes, *Appl. Catal. A: General*, 1994, **114**, L1.

146. J. Benitez, J. Odriozola, R. Marchand, Y. Laurent and P. Grange, *J. Chem. Soc. Faraday T.*, 1995, **91**, 4477.

147. P. Grange, P. Bastians, R. Conanec, R. Marchand and Y. Laurent, *Appl. Catal. A: General*, 1994, **114**, L191.

148. A. Massinon, J. Odriozola, P. Bastians, R. Conanec, R. Marchand, Y. Laurent and P. Grange, *Appl. Catal. A: General*, 1996, **137**, 9.

149. M. Climent, A. Corma, R. Guil-Lopez and S. Iborra, *Catal. Lett.*, 2001, **74**, 161.

150. D. Evans and X. Duan, *Chem. Commun.*, 2006, 485.

151. F. Basile and A. Vaccari, *Layered Double Hydroxides*, 2001, 285.

152. B. Sels, D. Vos and P. Jacobs, *Catal. Rev.*, 2001, 43, 443.

153. M. Aramendia, V. Borau, C. Jimenez, J. Marinas, J. Ruiz and F. Urbano, *Appl. Catal. A: General*, 2001, **206**, 95.

154. A. Corma, S. Iborra, J. Primo and F. Rey, *Appl. Catal. A: General*, 1994, **114**, 215.

155. J. Valente, F. Figueras, M. Gravelle, P. Kumbhar, J. Lopez and J. Besse, *J. Catal.*, 2000, **189**, 370.

156. A. Beres, I. Palinko, I. Kiricsi, J. Nagy, Y. Kiyozumi and F. Mizukami, *Appl. Catal. A: General*, 1999, **182**, 237.

157. S. Velu and C. Swamy, *Catal. Lett.*, 1996, **40**, 265.

158. V. Rives and S. Kannan, *J. Mater. Chem.*, 2000, **10**, 489.

159. D. Tichit and B. Coq, *CATTECH*, 2003, **7**, 206.

160. M. Aramendia, Y. Aviles, V. Borau, J. Luque, J. Marinas, J. Ruiz and F. Urbano, *J. Mater. Chem.*, 1999, **9**, 1603.

161. I. Rousselot, C. Taviot-Gueho and J. Besse, *Int. J. Inorg. Mater.*, 1999, **1**, 165.

162. R. Prihod'ko, M. Sychev, I. Kolomitsyn, P. Stobbelaar, E. Hensen and R. Santen, *Micropor. Mesopor. Mat.*, 2002, **56**, 241.

163. M. Aramendia, V. Borau, C. Jimenez, J. Marinas, J. Ruiz and F. Urbano, *Appl. Catal. A: General*, 2003, **249**, 1.

164. M. Aramendia, V. Borau, C. Jimenez, J. Luque, J. Marinas, J. Ruiz and F. Urbano, *Appl. Catal. A: General*, 2001, **216**, 257.

165. M. Climent, A. Corma, S. Iborra and A. Velty, *Green Chem.*, 2002, **4**, 474.

166. M. Climent, A. Corma, S. Iborra and A. Velty, *J. Catal.*, 2004, **221**, 474.

167. M. Di Serio, R. Tesser, A. Ferrara and E. Santacesaria, *J. Mol. Catal. A: Chem.*, 2004, **212**, 251.

168. T. Raja, T. Jyothi, K. Sreekumar, M. Talawar, J. Santhanalakshmi and B. Rao, *B. Chem. Soc. Jpn.*, 1999, **72**, 2117.

169. K. Rao, M. Gravelle, J. Valente and F. Figueras, *J. Catal.*, 1998, **173**, 115.

170. C. Veloso, C. Henriques, E. Santos and J. Monteiro, *Proceedings of the 13th ICC, Paris (France)*, 2004, Reference: P5-062.

171. M. Bennani, D. Tichit, F. Figueras and S. Abouarnadasse, *Journal de Chimie Physique et de Physico-Chimie Biologique*, 1999, **96**, 498.

172. P. Kumbhar, J. Sanchez-Valente, J. Lopez and F. Figueras, *Chem. Commun.*, 1998, 535.

173. M. Camblor, A. Corma, R. Martin-Aranda and J. Perez-Pariente, *Proceedings of the International Zeolite Conference 9th*, 1993, **2**, 647.

174. M. Climent, A. Corma, S. Iborra and J. Primo, *J. Catal.*, 1995, **151**, 60.

175. A. Corma, R. Martin-Aranda and F. Sanchez, *J. Catal.*, 1990, **126**, 192.

176. A. Corma, R. Martin-Aranda and F. Sanchez, *Stud. Surf. Sci. Catal.*, 1991, **59**, 503.

177. H. Handa, Y. Fu, T. Baba and Y. Ono, *Catal. Lett.*, 1999, **59**, 195.

178. M. Huang, A. Adnot and S. Kaliaguine, *J. Catal.*, 1992, **137**, 322.

179. J. Lavalley, J. Lamotte, A. Travert, J. Czyzniewska and M. Ziolek, *J. Chem. Soc. Faraday T.*, 1998, **94**, 331.

180. G. Madhavi, S. Kulkarni, K. Murthy, V. Viswanathan and K. Raghavan, *Appl. Catal. A: General*, 2003, **246**, 265.

181. G. Martra, R. Ocule, L. Marchese, G. Centi and S. Coluccia, *Catal. Today*, 2002, **73**, 83.

182. S. Lai, C. Ng, R. Martin-Aranda and K. Yeung, *Micropor. Mesopor. Mat.*, 2003, **66**, 239.

183. R. Ballini, F. Bigi, E. Gogni, R. Maggi and G. Sartori, *J. Catal.*, 2000, **191**, 348.

184. A. Palomares, G. Eder-Mirth and J. Lercher, *J. Catal.*, 1997, **168**, 442.

185. A. Palomares, G. Eder-Mirth, M. Rep and J. Lercher, *J. Catal.*, 1998, **180**, 56.

186. K. Kloetstra and H. Bekkum, *Journal of the Chemical Society Chem. Commun.*, 1995, 1005.

187. B. Bonelli, M. Ribeiro, A. Antunes, S. Valange, Z. Gabelica and E. Garrone, *Micropor. Mesopor. Mat.*, 2002, **54**, 305.

188. J. Zhu, Y. Chun, Y. Wang and Q. Xu, *Catal. Today*, 1999, **51**, 103.

189. E. Doskocil and P. Mankidy, *Appl. Catal. A: General*, 2003, **252**, 119.

190. S. Bordawekar and R. Davis, *J. Catal.*, 2000, **189**, 79.

191. H. Tsuji, F. Yagi and H. Hattori, *Chem. Lett.*, 1991, 1881.

192. Y. Wang, J. Zhu, J. Cao, C. Yuan and Q. Xu, *Micropor. Mesopor. Mat.*, 1998, **26**, 175.

193. J. Zhu, Y. Wang, Y. Chun, Z. Xing and Q. Xu, *Mater. Lett.*, 1998, **35**, 177.

194. J. Yu, S. Shiau and A. Ko, *Catal. Lett.*, 2001, **77**, 165.

195. A. Corma, S. Iborra, I. Rodriguez and F. Sanchez, *J. of Catal.*, 2002, **211**, 208.

196. I. Rodriguez, S. Iborra, A. Corma, F. Rey and J. Jorda, *Chem. Commun.*. 1999, 593.

197. I. Rodriguez, S. Iborra, F. Rey and A. Corma, *Appl. Catal. A: General*, 2000, **194-195**, 241.

198. B. Choudary, M. Kantam, P. Sreekanth, T. Bandopadhyay, F. Figueras and A. Tuel, *J. Mol. Catal. A: Chem.*, 1999, **142**, 361.

199. A. Corma, S. Iborra, I. Rodriguez, M. Iglesias and F. Sanchez, *Catal. Lett.*, 2002, **82**, 237.

200. X. Zhang, E. Lai, R. Martin-Aranda and K. Yeung, *Appl. Catal. A: General*, 2004, **261**, 109.

201. A. Blanc, C. Vargas, F. Quignard, D. Macquarrie and D. Brunel, Proceedings of the 13th ICC, Paris (France), 2004, Reference: P1-261.

202. R. Sercheli, A. Ferreira, M. Guerreiro, R. Vargas, R. Sheldon and U. Schuchardt, *Tetrahedron Lett.*, 1997, **38**, 1325.

203. H. Imamura, T. Nuruyu, T. Kawasaki, T. Teranishi and Y. Sakata, *Catal. Lett.*, 2004, **96**, 185.

204. S. Kaskel and K. Schlichte, *J. Catal.*, 2001, **201**, 270.

205. S, Bej and L. Thompson, *Appl. Catal. A: General*, 2004, **264**, 141.

206. R. McGee, S. Bej and L. Thompson, *Proceedings of the 13th ICC, Paris (France)*, 2004, Reference: P1-453.

207. M. Paul and F. Long, *Chem. Rev.*, 1957, **57**, 1.

208. T. Lizuka, H. Hattori, Y. Ohno, J. Sohma andK. Tanabe, *J. Catal.*, 1971, **22**, 130.

209. G. Zhang, H. Hattori and K. Tanabe, *Appl. Catal.*, 1988, **36**, 189.

210. H. Tsuji, A. Okamura-Yoshida, T. Shishido and H. Hattori, *Langmuir*, 2003, **19**, 8793.

211. H. Knözinger and S. Huber, *J. Chem. Faraday Trans.*, 1998, **94**, 2047.

212. M. Sánchez- Sánchez and T. Blasco, *Chem. Commun.*, 2000, 491.

213. M. Sánchez- Sánchez, T. Blasco and F. Rey, *Phys. Chem. Chem. Phys.*, 1999, **1**, 4529.

214. V. Bosacek, R. Klik, F. Genoni G. Spano, F. Rivetti and F. Figueras, *Magn. Reson. Chem.*, 1999, 37, S135.

215. F. Yagi, K. Kanuka, H. Tsuji, S. Nakata, H. Kita and H. Hattori, *Microporous Mater.*, 1997, **9**, 229.

216. H. Kabashima, H. Tsuji, S. Nakata, Y. Tanaka and H. Hattori, *Appl. Catal. A: General*, 2000, **194**, 227.

217. Y. Okamoto, M. Ogawa, A. Maezawa and T. Imanaka, *J. Catal.*, 1988, **112**, 427.

218. F. Ma and M. A. Hanna, *Biores. Technol.*, 1999, **70**, 1.

219. W. Xie and X. Huang, *Catal. Lett.*, 2006, **107**, 53.

220. A. Ramadhas, *Fuel*, 2005, **84**, 335.

221. S. Karmee, *Biores. Technol.* 2005, **96**, 1425.

222. L. Bournay, D. Casanave, B. Delfort, G. Hillion and J. Chodorge,. *Catal. Today*, 2005, **106**, 190.

223. U. Kreutzer, *J. Am. Oil. Chem. Soc.*, 1984, **61**, 343.

224. J. Encinar, *Energy Fuel*, 2002, **16**, 443.

225. S. Dmytryshyn, *Biores. Technol*, 2004, **92**, 55.

226. M. Serio, M. Ledda, M. Cozzolino, G. Minutillo, R. Tesser and E. Santacesaria, *Industrial & Engineering Chemistry Research*, 2006, **45**, 3009.

227. W. Xie, H. Peng and L. Chen, *J. Mol. Catal. A: Chem.*, 2006, 246, 24.

228. D. Cantrell, L. Gillie, A. Lee and K. Wilson, *Appli. Catal. A: General*, 2005, **287**, 183.

229. T. Dossin, M. Reyniers and G. Marin, *Applied Catalysis B: Environmental*, 2006, **61**, 35.

230. J. Jitputti, B. Kitiyanan, P. Rangsunvigit, K. Bunyakiat, L. Attanatho, P. Jenvanitpanjakul, *Chemical Engineering Journal*, 2006, **116**, 61.

231. G. Suppes, M. Dasari, E. Doskocil, P. Mankidy and M. Goff, *Appli. Catal. A: General*, 2004, **257**, 213.

232. H. Kim, B. kang, M. Kim, Y. M. Park, D. Kim, J. Lee and K. Lee, *Catal. Today*, 2004, **93-95**, 315.

233. W. Xie and X. Huang, *Catal. Today*, 2006, **107**, 53.

234. H. Hattori, M. Shima and H. Kabashima, *Stud. Surf. Sci. Catal.*, 2000, **130**, 3507.

235. U. Meyer, H. Gorzawski and W. Hölderich, *Catal. Lett.*, 1999, **59**, 201.

236. R. Martin-Aranda, E. Ortega-Cantero, M. Rojas-Cervantes, M. Vicente-Rodriguez and M. Bañares-Munoz, *Catal. Lett.*, 2002, **84**, 201.

237. García-Raso, A.; García-Raso, J.; Campaner, B.; Mestres, R.; Sinisterra, J. V., Synthesis, 1982, 1037.

238. B. Choudary, M. Kantam, M.; C. Reddy, K. Rao and F. Figueras, *J. Mol. Catal. A: Chem.*, 1999, **146**, 279.

239. M. Climent, A. Corma, S. Iborra and A. Velty, *J. Mol. Catal. A: Chem.*, 2002, **182-183**, 327.

240. H. Moison, F. Texier-Boullet and A. Foucaud, *Tetrahedron*, 1987, **43**, 537.

241. E. Angelescu, O. Pavel, R. Birjega, R.. Zavoianu, G. Costentin and M. Che, *Appli. Catal. A: General*, 2006, **308**, 13.

242. B. Choudary, M. Kantam, B. Kavita, C. Reddy and F. Figueras, *Tetrahedron*, 2000, **56**, 9357.

243. B. Choudary, M. Kantam, V. Neeraja, K. Rao , F. Figueras and L. Delmotte, *Green Chem.*, 2001, **3**, 257.

244. T. Reddy and R. Varma, *Tetrahedron Lett.*, 1997, **38**, 1721.

245. U. Costantino, M. Curini, F. Montanari, M. Nocchetti and O. Rosati, *J. Mol. Catal. A*, 2003, **195**, 245.

246. S. Saravanamurugan, M. Palanichamy, M. Hartmann, V. Murugesan, *Appli. Catal. A: General,* 2006, **298**, 8.

247. T. Saito, H. Gato, K. Honda and T. Fujii, *Tetrahedron Lett.*, 1992, **33**, 7535.

248. P. Rao and R. Venkataratnan, *Tetrahedron Lett.*, 1991, **32**, 5821.

249. D. Macquarrie, J. Clark, A. Lambert, J. Mdoe and A. Priest, *React. Funct. Polym.*, 1997, **35**, 153.

250. J. Bennazha, M. Zahouily, S. Sebti, A. Boukhari and E.M. Holt, *Catal. Commun.*, 2001, **2**, 101.

251. S. Chalais, P. Laszlo and A. Mathy, *Tetrahedron Lett.*, 1985, **26**, 4453.

252. A. Ramani, B. Chanda, S. Velu and S. Sivasanker, *Green Chem.*, 1999, **1**, 163.

253. R. Johnstone, A. Wilby and I. Entwistle, *Chem. Rev.*, 1985, **85**, 129.

254. V. Ivanov, J. Bachelier, F. Audry and J. Lavalley, *J. Mol. Catal.*, 1994, **91**, 45.

255. D. Tomczak and J. Allen, J. Catal., 1994, 146, 155.

256. C. Jimenez-Sanchidrian, J. Hidalgo and J. Ruiz, *Appli. Catal. A: General*, 2006, **303**, 23.

257. M. Aramendia, V. Borau, C. Jimenez, J. Marinas, J. Ruiz, F. Urbano, *Appl. Catal. A: General*, 2003, **255**, 301.

258. M. Berkani, J. Lemberton and M. Marczewski, *Catal. Lett.*, 1995, **31**, 405.

259. H. Hattori, *Appl. Catal. A: General*, 2001, **222**, 247.

260. L. Thomas, R. Tanner, P. Gill, R. Wells, J. Bailie, G. Kelly, S. Jackson and G. Hutchings, *Phys. Chem. Chem. Phys.*, 2002, **4**, 4555.

261. G. Zhang, H. Hattori and K. Tanabe, *Appli. Catal.*, 1988, **40**, 183.

262. G. Zhang, H. Hattori and K. Tanabe, *Appli. Catal.*, 1988, **36**, 189.

263. A. Canning, S. Jackson, E. McLeod and E. Vass, *Appli. Catal. A: General*, 2005, **289**, 59.

264. J. Di Cosimo and C. Apesteguia, *J. Mol. Catal. A: Chem.*, 1998, **130**, 177.

265. J. Roelofs, A. Dillen and K. Jong, *Catal. Lett.*, 2001, **74**, 91.

266. M. Climent, H. Garcia, J. Primo and A. Corma, *Catal. Lett.*, 1990, **4**, 85.

267. S. Sebti, A. Solhy, R. Tahir, S. Abdelatif, S. Boulaajaj, J. Mayoral, J. Garcia, J. Fraile, A. Kossir and H. Oumimoun, *J. Catal.*, 2003, **213**, 1.

268. S. Sebti, A. Solhy, R. Tahir and A. Smahi, *Appl. Catal. A: General*, 2002, **235**, 273.

269. J. Macgregor and C. Pugh, *J. Chem. Soc.*, 1945, 535.

270. P. Kumbhar, J. Sanchez-Valente and F. Figueras, *Chem. Commun.*, 1998, 1091.

271. B. Choudary, M. Kantam and B. Kavita, *Green Chem.*, 1999, **1**, 289.

272. E. Angelescu, O. Pavel, M. Che, R. Birjega and G. Constentin, *Catal. Commun.*, 2004, **5**, 647.

273. S. Chaphekar and S. Samant, *Appl. Catal. A: General*, 2003, **242**, 11.

274. H. Kabashima and H. Hattori, *Catal. Today*, 1998, **44**, 277.

275. H. Handa, T. Baba and H. Sugisawa, *J. Mol. Catal. A: Chem.*, 1998, **134**, 171.

276. F. Luzzio, *Tetrahedron*, 2001, **57**, 915.

277. H. Sasai, T. Suzuki, N. Itoh, K. Tanaka, T. Date, K. Okamura and M. Shibasaki, *J. Am. Chem. Soc.*, 1993, **115**, 10372.

278. K. Akutu, H. Kabashima, T. Seki and H. Hattori, *Appl. Catal. A: General*, 2003, **247**, 65.

279. V. J. Bulbulbe, V. H. Deshpande, S. Velu, A. Sudalai, S. Shivasankar and V. T. Sathe, *Tetrahedron*, 1999, **55**, 9325.

280. R. Ballini, G. Bosica, D. Livi, A. Palmieri, R. Maggi, G. Sartori, *Tetrahedron Lett.*, 2003, 44, 2271.

281. R. Ballini, G. Sosica and P. Forconi, *Tetrahedron*, 1996, **52**, 1677.

282. T. Saiki and Y. Aoyama, *Chem. Lett.*, 1999, 797. CHEM LETT

283. F. Yagi, H. Tsuji and H. Hattori, *Microporous Materials*, 1997, **9**, 237.

284. J. Kijenski and R. Hombek, *J. Catal.*, 1997, **167**, 503.

285. F. Figueras, J. Lopez, J. Sanchez-Valente, T. Vu, J. Clacens and J. Palomeque, *J. Catal.*, 2002, **211**, 144.

286. U. Meyer and W. Hoelderich, *J. Mol. Catal. A: Chem.*, 1999, **142**, 213.

287. H. Gorzawski and W. Hoelderich, Hoelderich, *J. Mol. Catal. A: Chem.*, 1999, **144**, 181.

288. H. Hattori, N. Yoshii and K. Tanabe, *Proc. 5th Intern. Congr. Catal., Miami Beach,* 1972, 233.

289. H. Hattori and A. Satoh, *J. Catal.*, 1976, **45**, 32.

290. Y. Imizu, T. Yamaguchi, H. Hattori and K. Tanabe, *Bull. Chem. Soc. Jpn.*, 1977, **50**, 1040.

291. H. Hattori, M. Itoh and K. Tanabe, *J. Catal.*, 1976, **41**, 46.

292. T. Yashima, K. Sato, T. Hayasaka and N. Hara, *J. Catal.*, 1972, **26**, 303.

293. C. B. Dartt and M. E. Davis, *Catal. Today*, 1994, **19**, 151.

294. J.M. Serra, A. Corma, D. Farrusseng, L. Baumes, C. Mirodateos, F. Flego and C. Perego, *Catal. Today*, 2003, **81**, 425.

295. M.A. Aramendia, V. Borau, C. Jimenez, J. M. Marinas and F. J. Romero, *J. Colloid Interf. Sci.*, 1999, **219**, 201.

296. S. Velu and C. S. Swamy, *Appl. Catal. A: General*, 1994, **119**, 241.

297. J. Kijenski, P. Radomski and E. Fedorynska, *J. Catal.*, 2001, **203**, 407.

298. T. Baba, A. Kato, H. Takahashi, F. Toriyama, H.Handa, Y. Ono and Y. Sugisawa, *J. Catal.*, 1998, **176**, 488.

299. D. Semenzin, G. Etemad-Moghadam, G. Albouy, O. Diallo and M. Koenig, *J. Org. Chem.*, 1997, **62**, 2414.

300. M. Ballabeni, R. Ballini, F. Bigi, R. Maggi, M. Parrini, G. Predieri and G. Sartori, *J. Org. Chem.*, 1999, **64**, 1029.

301. A. Gervasini and A. Auroux, *J. Catal.*, 1991, **131**, 190.

302. C. Perego and P. Villa, *Catal. Today*, 1997, **34**, 281.

303. E. Ruckenstein and Y. H. Hu, *Appl. Catal. A: General*, 1997, **154**, 185.

304. V. V. Chesnokov, A. F. Bedilo, D. S. Heroux, I. V. Mishakov and K. J. Klabunde, *J. Catal.*, 2003, **218**, 438.

305. E. Knozinger, O. Diwald and M. Sterrer, *J .Mol. Catal., A: Chem.*, 2000, **162**, 83.

306. J. A. Wang, X. Bokhimi, O. Novaro, T. López and R. Gómez, *J. Mol. Catal., A: Chem.*, 1999, **145**, 291.

307. P. K. Stoimenov, V. Zaikovski and K. J. Klabunde, *J. Am. Chem. Soc.*, 2003, **125**, 12907.

308. P. Putanov, E. Kis and G. Boskovic, *Appl. Catal.*, 1991, **73**, 17.

Chapter 2

Experimental

2.1 Preparation of heterogeneous base catalysts

2.1.1 Preparation of MgO

MgO was prepared by a number of different routes.

Commercially available magnesium hydroxide (Fluka, 99%), basic magnesium carbonate ($(MgCO_3)_4Mg(OH)_2$, ≥40% MgO; Fluka) and magnesium carbonate ($MgCO_3$, Acros Organics, 40~45% MgO) were calcined in static air. The materials were designated as MgO-COH, MgO-CBC and MgO-CC respectively.

Rehydrated $(MgCO_3)_4Mg(OH)_2$ was obtained from the commercially available basic magnesium carbonate ($(MgCO_3)_4Mg(OH)_2$; 25 g), which was suspended in distilled water (750 ml), stirred at 70-90 °C for 30 min., filtered, dried (90 °C; 24 h) and then recalcined. This material was designated as MgO-RBC.

Commercially available magnesium hydroxide (Fluka, 99%; 21.8 g) was calcined at 600 °C for 2 h. The magnesium oxide obtained (10 g) was rehydrated by refluxing in distilled water (125 ml) for 3 h. The resultant solid, denoted as rehydrated $Mg(OH)_2$, was dried and then calcined. This material was designated as MgO-ROH.

Freshly prepared magnesium hydroxide, was obtained by precipitating $MgSO_4$ solution (250 ml; 1.0 M) with KOH solution (250 ml; 1.0 M). The resulting mixture was aged at room temperature for 3 h, filtered, washed five times with distilled water, dried (90 °C; 24 h) and then calcined. This material was designated as MgO-FOH.

MgO was also obtained by calcination of magnesium oxalate (MgC_2O_4). MgC_2O_4 was prepared following the method described by Putanov *et al.*[1] Magnesium oxalate (MgC_2O_4) as the magnesium oxide precursor was precipitated from saturated aqueous solutions of $Mg(CH_3COO)_2{\cdot}4H_2O$ using aqueous solution of $H_2C_2O_4{\cdot}2H_2O$. The saturated aqueous solutions of $Mg(CH_3COO)_2{\cdot}4H_2O$ was made by adding $Mg(CH_3COO)_2{\cdot}4H_2O$ (53.6 g) to distilled H_2O (50 ml). The aqueous solution of $H_2C_2O_4{\cdot}2H_2O$ was prepared by diluting $H_2C_2O_4{\cdot}2H_2O$ (31.5 g) with distilled H_2O (200 ml). The magnesium oxalate was precipitated from moderately heated magnesium acetate solutions at 40 °C and immediately filtered. The precipitate was dried at 90 °C for 24 h. The resulting material was calcined at various temperatures in static air. This material was designated as MgO-OX.

All calcination was conducted in two ways. One method involved calcination in the temperature range of 200~800 °C for 2 h in static air at the ramp of 10 °C min^{-1}. After calcining, the temperature was cooled down to 280 °C and the sample moved to a vial which was sealed and placed in a dessicator previous to use. The alternative method was calcination in a N_2 flow in the temperature range of 200~800 °C for 2 h at the ramp of 10 °C min^{-1}. The MgO obtained was cooled down to room temperature in flowing N_2 and kept under N_2 atmosphere (JM) or in a dessicator (Cardiff) previous to use.

2.1.2 Preparation of lithium doped magnesium oxides

2 wt % Li/MgO was synthesized by adding MgO (10 g) obtained from the above MgO precursors after calcination at 450 °C for 2 h and $LiCO_3$ (1.1 g, Aldrich, 99%) or $LiOH{\cdot}H_2O$ (1.2 g, Aldrich, 98+ %) to deionised water (80 ml). The suspension was kept at 78 °C under vigorous stirring until the water had evaporated. The resultant paste was dried at 90 °C for 24 h and then calcined in static air at 450 °C for 2 h. The temperature was raised from ambient temperature at a rate of 10 °C min^{-1}.

2.1.3 Preparation of CaO

CaO was prepared as depicted in Figure 2.1. Commercially available $Ca(OH)_2$ (10 g) was calcined at 600 °C for 3 h. Distilled H_2O (50 ml) was slowly added to the CaO. The resulting mixture was stirred for 2 h to make sure that CaO completely reacted with H_2O, then filtered, dried in oven, finally calcined at different temperature (200 °C ~ 800 °C) in static air for 2 h at the ramp of 10 °C min^{-1}.

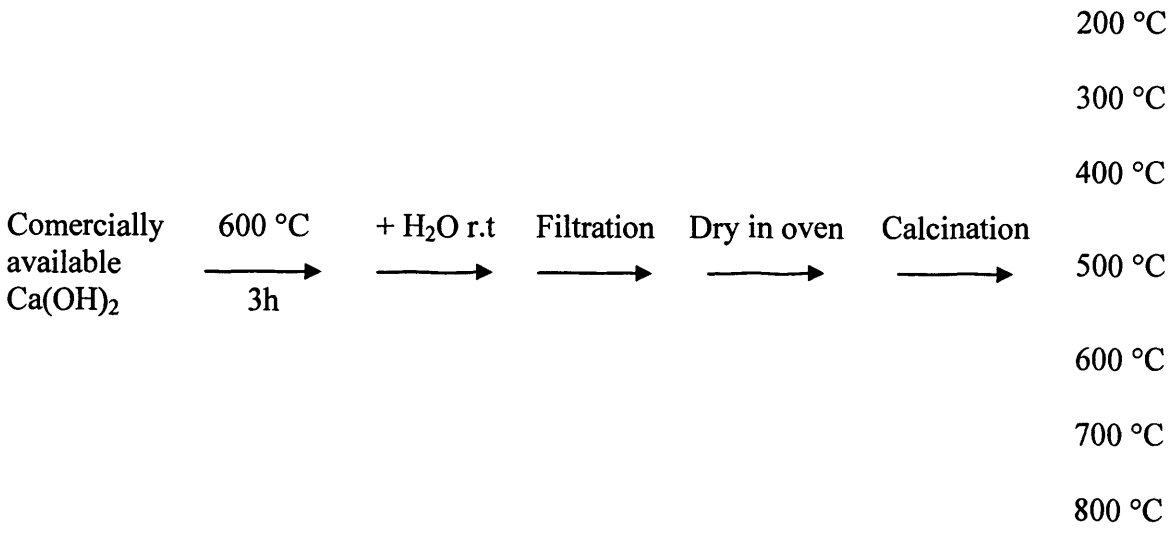

Figure 2.1 Procedure to prepare CaO.

2.1.4 Preparation of Hydrotalcites

Hydrotalcites with different Al^{3+}:Mg^{2+} atomic ratios (1:3; 1:4 and 1:2) were prepared using a standard aqueous co-precipitation method at constant pH and temperature. An aqueous solution (166 ml) of the metal nitrates in a desired Al^{3+}:Mg^{2+} molar ratio with a total concentration of 1.5 M was mixed slowly with continuous stirring with an alkaline solution of $NaCO_3$/NaOH. The molar amount of $NaCO_3$ was twice that of Al^{3+}. The pH of the mixture was kept constant, typically at values between 9 and 10, by adjusting the flow rate of the alkaline solution. The temperature was maintained at 60 °C. Following this addition, which resulted in the formation of heavy slurry, the mixture was aged at 60 °C for 18 h with stirring, to facilitate the selective growth of the precipitated hydrotalcite phase. The slurry was then cooled to 25 °C, filtered, and washed with water and dried at 90 °C for 12 h. The resulting material was calcined at 450 °C for 2 h in static air. The temperature was raised from ambient temperature at a rate of about 10 °C min^{-1}.

The activity of commercially available hydrotalcite (Aldrich) has been tested and compared with that of the laboratory made hydrotalcite.

2.2 Reactors used in the current study

2.2.1 Glass batch reactor

The reactions were carried out in a standard round bottom two-neck glass flask equipped with a vertical condenser at specified temperature under vigorous stirring. In order to follow the progress of the reaction, samples (about 0.5 ml) were withdrawn from the reactor at specified times by one syringe. Then the needle connected to the

syringe was removed and substituted by one syringe driven filter. Catalyst was separated from the sample by pushing the solution through the syringe driven filter. The solution obtained was stored in one vial for further analysis.

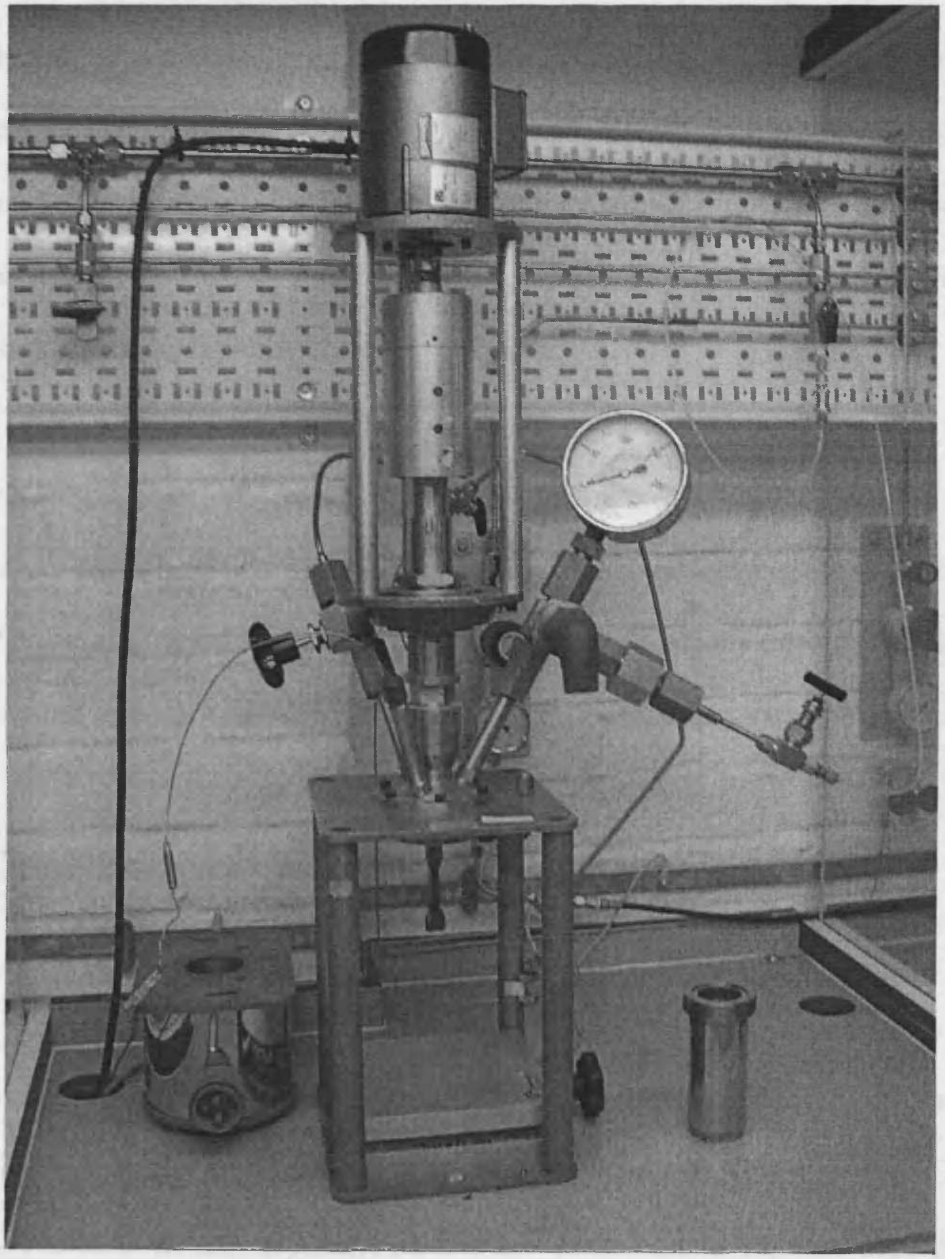

Figure 2.2 Digital picture of the Baskerville high pressure autoclave

2.2.2 Stirred tank reactor

Biodiesel synthesis was carried out in a high pressure stainless steel Baskerville autoclave (100 ml) (Figure 2.2). Reactions took place within a glass liner (volume 80 ml) which was placed within the stainless steel jacket. The jacket was screwed into the body of the unit. To ensure the unit would maintain pressure a Teflon ring was placed between the jacket and the mount compressed to form a seal. A Teflon gas entrainment impeller was connected to a sealed magnetic drive unit, which was rotated by a Parvalux DC shunt motor, located above the reactor. Agitation of the reactor contents was controlled by a variable resistance dial with the capability of up to 1400 rpm. The reaction mixture was typically stirred at 1000 rpm.

Reaction temperature was monitored with a thermocouple connected to a digital temperature indicator. This indicator controlled an electric heating unit, which fitted around the reactor jacket when required. Reactions were normally carried out at 200 °C. The reactions running in Johnson Matthey were conducted using Parr 4843 autoclave.

2.3 Catalyst characterisation[6]

2.3.1 Surface area and Pore Analysis

The surface area and pore character of the catalysts was carried out using a Micromeritics Gemini 2360 Surface Area Analyser. The sample was degassed at 150 °C for 30 minutes in helium prior to surface area measurement. Physical adsorption of N_2 at low temperatures can be used to determine the surface area of porous materials. Nitrogen tends to form monolayer of closely packed molecules on the surface area of

the material at cryogenic temperatures. The surface area of that material is then deduced from the BET isotherm derived by Brunauer, Emmett, and Teller[7]:

$$\frac{P}{V(P_o - P)} = \frac{1}{V_m \cdot C} + \frac{(C-1)}{V_m \cdot C} \cdot \frac{P}{P_o}$$

Where V is the volume adsorbed at pressure P, V_m is the volume of gas required to form an adsorbed monolayer, P_0 is the saturated vapour pressure of the gas at -196 °C and C is a constant.

V_m is calculated from the isotherm, and the surface area is determined by assuming each molecule of adsorbed nitrogen occupies 0.165 nm^2.

Information was also obtained on the pore characteristics of the samples. Pore volume and pore area distributions were conducted by the BJH (Barrett, Joyner, and Halenda) method using a variety of thickness equations including a user-defined, standard isotherm (2380 model)

2.3.2 Thermal Gravimetric Analysis

Thermal gravimetric analysis (TGA) measures the change in weight of a material as it decomposed when heated. TGA experiments were carried out using TA Instruments LTD SDT Q600 thermal analysis machine under a flow of nitrogen. The sample weight used was about 10 milligrams, and the temperature ranged from 30 °C to 800 °C with a ramping rate of 20 °C min^{-1}.

2.3.3 Powder X-Ray Diffraction (XRD)

X-rays are electromagnetic radiation of wavelength about 1 Å (10^{-10} m), which is about the same size as an atom. They occur in that portion of the electromagnetic spectrum between gamma-rays and the ultraviolet. The discovery of X-rays in 1895 enabled scientists to probe crystalline structure at the atomic level. X-ray diffraction has been in use in two main areas, for the fingerprint characterization of crystalline materials and the determination of their structure.

Bragg's Law refers to the simple equation:

$$n\lambda = 2d\sin\theta$$

derived by the English physicists Sir W.H. Bragg and his son Sir W.L. Bragg in 1913 to explain why the cleavage faces of crystals appear to reflect X-ray beams at certain angles of incidence (theta, θ). The variable *d* is the distance between the crystal planes and the λ is the wavelength of the incident X-ray beam; n is an integer.

With a powder sample some of the crystallites will always be orientated so as to satisfy the Bragg equation and diffraction will occur. This is the basis for powder X-ray diffraction. The X-ray diffraction experiment requires an X-ray source, the sample under investigation and a detector to pick up the diffracted X-rays. Figure 2.3 is a schematic diagram of a powder X-ray diffractometer.

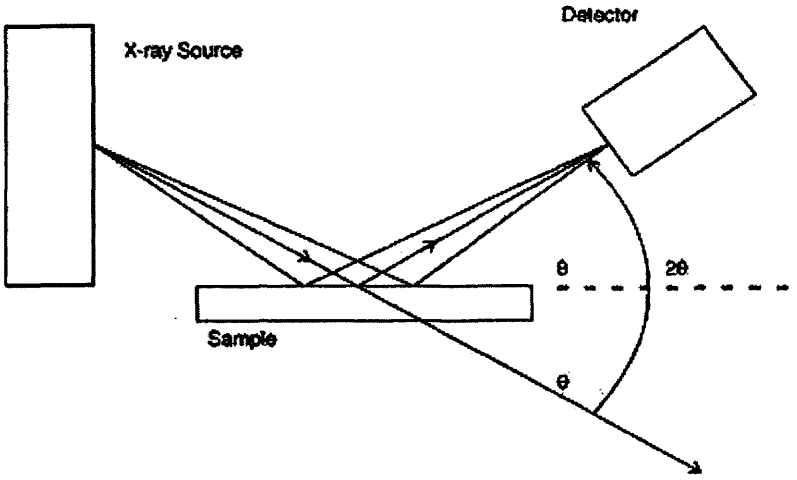

Figure 2.3 Schematic diagram of an X-ray powder diffractometer.

Powder X-ray diffraction was performed using an ENRAF Nonius FR 590 X-ray powder diffractometer, using a Cu-K_α source fitted with an Inel CPS 120 hemispherical detector.

Crystallite size from XRD line broadening is calculated using the method developed by Scherrer in 1918, which uses the Scherrer equation[8]:

$$d = K\lambda / (\beta \cos\theta)$$

where d = Crystallite size, K = Scherrer constant (8.9), λ = wavelength of radiation, which is 1.540562 Å for K_α line of Cu used in our experiment, β is the difference between measured FWHM (full width at half maximum) and the unbroadened FWHM of single crystal which was assumed as 0° in this study. This approach does, however, neglect the effect that strain can have on crystallite size.

2.3.4 Scanning Electron Microscope (SEM)

The Scanning Electron Microscope is a microscope that uses electrons rather than light to form an image. There are many advantages to using the SEM instead of a light microscope.

The image resolution of a microscope is inversely proportional to the wavelength of electromagnetic radiation illuminating the sample. Optical microscopes using visible light (λ = 400 to 800 nm) have a maximum magnification of 1000 to 3000x. An electron microscope uses a monochromatic beam of electrons, which can give a much higher magnification.

The SEM has a large depth of field, which allows a large amount of the sample to be in focus at one time. The SEM also produces images of high resolution, which means that closely spaced features can be examined at a high magnification. Preparation of the samples is relatively easy since most SEM only require the sample to be conductive. The combination of higher magnification, larger depth of focus, greater resolution, and ease of sample observation makes the SEM one of the most heavily used instruments in research areas today. SEM micrographs were performed using FEI XL30 ESEM FEG in the Earth Science Department at Cardiff University.

2.4 Product Analysis[9]

2.4.1 Gas chromatography (GC)

Gas chromatography is a chromatographic technique that can be used to separate volatile organic compounds. The schematic diagram of a gas chromatograph is shown in Figure 2.4.

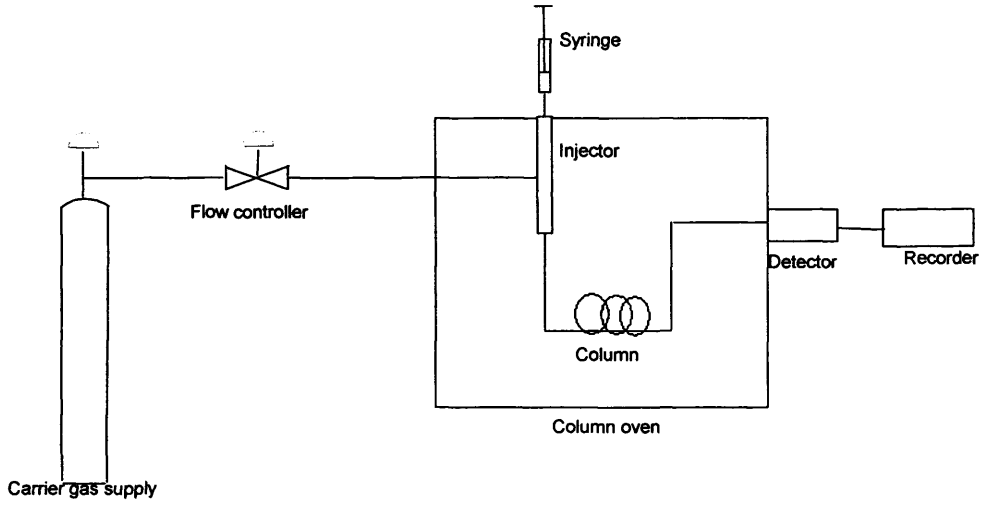

Figure 2.4 Schematic diagram of a gas chromatograph

A gas chromatograph consists of a flowing mobile phase, an injection port, a separation column containing the stationary phase, and a detector. The organic compounds are separated due to differences in their partitioning behaviour between the mobile gas phase and the stationary phase in the column.

The carrier gas must be chemically inert. Commonly used gases include hydrogen, nitrogen, helium, argon, and carbon dioxide. The choice of carrier gas is often dependant upon the type of detector which is used. The carrier gas system also contains a molecular sieve to remove water and other impurities. The injection port consists of a rubber septum through which a syringe needle is inserted to inject the sample. The

injection port is maintained at a higher temperature than the boiling point of the least volatile component in the sample mixture. Since the partitioning behaviour is dependant on temperature, the separation column is usually contained in a thermostat-controlled oven. Separating components with a wide range of boiling points is accomplished by starting at a low oven temperature and increasing the temperature over time to elute the high-boiling point components. Most columns contain a liquid stationary phase on a solid support. Separation of low-molecular weight gases is accomplished with solid adsorbents.

After the components of a mixture are separated using gas chromatography they must be detected as they exit the GC column. There are many detectors which can be used in gas chromatography. Different detectors will give different types of selectivity. The thermal-conductivity (TCD) and flame-ionization (FID) detectors are the two most common detectors on commercial gas chromatographs. The requirement of a GC detector depends on the separation application. For example, one analysis might require a detector that is selective for chlorine-containing molecules; another analysis might require a detector that is non-destructive so that the analyte can be recovered for further spectroscopic analysis. In this work, FID was used. The FID detector employs hydrogen as the combustion gas which is mixed with the column effluent (Helium and air). Gas chromatography was performed on a Varian Star 3400 CX GC equipped with a DB-4 capillary column and an FID detector.

2.4.2 Gas chromatography - Mass spectrometry (GC-MS)

Mass spectrometry is a technique for analysis of materials that relies on conversion of a sample into a gaseous ionic form, followed by separation of the ions according to their mass-to-charge ratios. The relative amounts of different ions formed in a mass spectrometer under specified conditions produce a "mass spectrum" when they are plotted against the mass-to-charge (m/e) ratio. Spectra are reproducible and contain much specific information; hence computerized data retrieval and comparison of large numbers of spectra make rapid identification possible.[10]

Figure 2.5 Schematic diagram of a mass spectrometer

As Figure 2.5 shows, there are several parts in a typical mass spectrometer. In the ion source, the sample is admitted in the gaseous state or converted to a gas by heating and ionized. In the mass analyzer, the ions produced in the source are sorted into beams of ions of the same m/e ratio. In the detection system, the mass analyzed ions are detected.

The Gas Chromatography/Mass Spectrometry instrument separates chemical mixtures (the GC component) and identifies the components at a molecular level (the MS component). It is one of the most accurate tools for analyzing organic samples. The GC works on the principle that a mixture will separate into individual substances when heated. The heated gases are carried through a column with an inert gas (such as helium). The stream of separated compounds is fed on-line into the ion source, a metallic filament to which voltage is applied. This filament emits electrons which ionize the compounds. The ions can then further fragment, yielding predictable

patterns. Intact ions and fragments pass into the mass spectrometer's analyser and are eventually detected. Mass spectrometry identifies compounds by the mass of the analyte molecule. A "library" of known mass spectra, covering several thousand compounds, is stored on a computer. Mass spectrometry is considered the only definitive analytical detector. GC-MS (Perkin Elmer Autosystem XL), equipped with a DB-1 column was employed in the study.

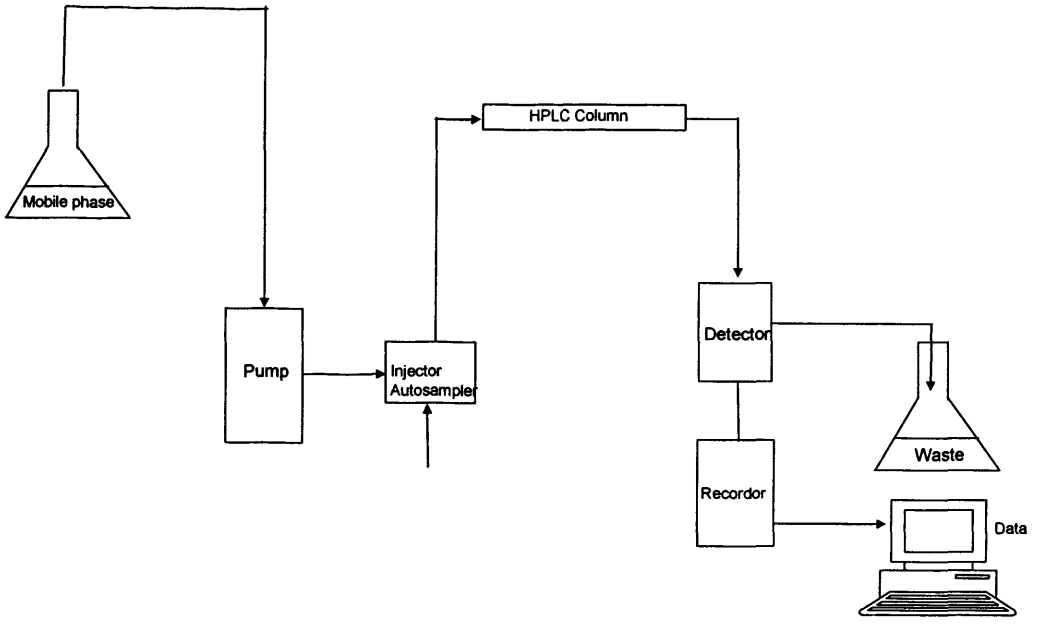

Figure 2.6 Schematic diagram of an HPLC instrument

2.4.3 High Performance Liquid Chromatography (HPLC)

High Performance Liquid Chromatography, also known as High Pressure Liquid Chromatography, is a form of liquid chromatography to separate compounds that are dissolved in solution. HPLC instruments consist of a reservoir of mobile phase, a high pressure pump, an injector, a separation column, and a detector. Schematic diagram of an HPLC instrument was shown below. Waters 2690 Separations Module was employed in this study.

2.4.4 Principle of NMR

The principle behind NMR is that the nuclei of many elemental isotopes have a characteristic spin (**I**). Some nuclei have integral spins (e.g. I = 1, 2, 3 ....), some have fractional spins (e.g. I = 1/2, 3/2, 5/2 ....), and a few have no spin, I = 0 (e.g. ^{12}C, ^{16}O, ^{32}S, ...).

The spin state will determine whether a spinning nucleii will be able to generate an NMR signal. The most common isotope of the first element hydrogen does possess a nuclear spin state that is capable of generating an NMR signal. However, Deuterium does not have a nuclear spin state, and therefore, will not generate an NMR signal. Carbon-12 does not have a favourable spin state, but Carbon-13 does have a spin state that will generate an NMR signal. Isotopes of particular interest and use to organic chemists are ^{1}H, ^{13}C, ^{19}F and ^{31}P, all of which have I = 1/2.

All nuclei are electrically charged. If an external magnetic field is applied, an energy transfer is possible between the base energy to a higher energy level (generally a single

energy gap). The energy transfer takes place at a wavelength that corresponds to radio frequencies and when the spin returns to its base level, energy is emitted at the same frequency. The signal that matches this transfer is measured in many ways and processed in order to yield an NMR spectrum for the nucleus concerned.

Nuclear Magnetic Resonance (NMR) spectroscopy is an analytical chemistry technique used for determining the content and purity of a sample as well as its molecular structure.

^{1}H-NMR spectra were recorded on a Bruker 400MHz instrument, ^{13}C-NMR on one Bruker 500MHz instrument with tetramethylsilane (TMS) as an internal standard. All samples were run in deuterochloroform unless otherwise stated.

2.5 Leaching analysis of MgO

2.5.1 Atomic absorption (AA)

A solid heated to incandescence emits a more or less continuous spectrum of light over a wide range of wavelengths. However, when a gas or vapour is heated, the emitted light consists of a series of lines, complicated in structure, having wavelengths characteristic of the elements present.

Spectroscopic determination of atomic species can only be performed on a gaseous medium in which the individual atoms are well separated from one another. Consequently, the first step in all atomic spectroscopic procedures is atomization, a process in which the sample is volatilized and decomposed in such a way as to produce an atomic gas. The efficiency and reproducibility of the atomization step in large measure determine the method's sensitivity, precision, and accuracy; that is, atomization is by far the most critical step in atomic spectroscopy. Several methods are

available to atomize samples for atomic spectroscopic studies, among them are flame and inductively coupled argon plasma.

An atomic spectrometer that analyses the emitted light in order to identify the elements present is called an atomic emission spectrometer. The complement to the atomic emission spectrometer is the atomic absorption spectrometer. The eluted sample from the column is usually burnt in a flame (either directly or by use of a spray) and light characteristic of the element being examined is passed through the flame and allowed to fall on a photoelectric cell or diode array. When the element is present in the flame its characteristic light is adsorbed and the output from the photo cell is reduced proportionally.

The analyte concentration is determined from the amount of absorption, based on the Beer-Lambert law. The Beer-Lambert law (or Beer's law) is the linear relationship between absorbance and concentration of an absorbing species. The general Beer-Lambert law is usually written as:

$$A = \lambda * b * c$$

where A is the measured absorbance, λ is a wavelength-dependent absorptivity coefficient, b is the path length, and c is the analyte concentration.

Applying the directly Beer-Lambert law in AA spectroscopy is difficult due to variations in the atomization efficiency from the sample matrix, and nonuniformity of concentration and path length of analyte atoms. Concentration measurements are usually determined from a working curve after calibrating the instrument with standards

of known concentration. Varian 55B Flame Atomic Absorption Spectrometer was employed in analyzing MgO leaching in the solution.

References

1. P. Putanov, E. Kis and G. Boskovic, *Appl. Catal.*, 1991, **73**, 17.
2. H. Meerwein and R. Schmidt, *Justus Liebigs Ann. Chem.*, 1925, **39**, 221.
3. W. Pordorf, *Angew. Chem.*, 1926, **39**, 138.
4. M. Verley, *Bull. Soc. Chim. Fr.*, 1925, **37**, 871.
5. A. Srivastava and R. Prasad, *Renewable & Sustainable Energy Reviews*, 2000, **4**, 111.
6. P. Atkins, *Physical Chemistry*, Oxford University Press, 1998.
7. S. Brunauer, P. H. Emmett and E. Teller, *J. Am. Chem. Soc.*, 1938, **60**, 309.
8. B. D. Cullity, *Elements of X-ray Diffraction*, Addison-Wesley Publishing Company, 1978, 102.
9. D. Skoog, D. West and F. Holler, *Fundamentals of Analytical Chemistry*, Saunders College Press, 1996.
10. H. Strobel, *Chemical Instrumentation*, Addison-Wesley Press, 1973, 822-823.

Chapter 3
Preparation of high surface area MgO and its application in Meerwein-Ponndorf-Verley reduction of benzaldehyde

3.1 Introduction

In the present work, we systematically studied non-complex methods to synthesise MgO, and observe that the preparation method has a marked effect on both the morphology and surface properties of the final product. The Meerwein-Ponndorf-Verley (MPV) reduction (Scheme 3.1) was chosen as a model reaction. The results show that using a relatively simple calcination method, high surface area MgO can be obtained that exhibits excellent catalytic activity in MPV reactions and provides a stable reusable base catalyst.

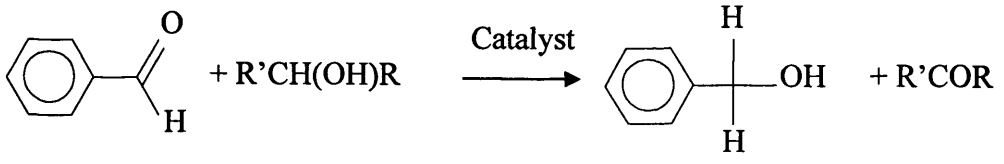

Scheme 3.1

3.2 Experimental

3.2.1 Catalyst preparation

MgO was prepared by calcining a number of different precursors (see Chapter 2 and Table 3.1 for details). 2wt% Li/MgO was synthesized in this study (see Chapter 2 for details).

All calcinations were conducted in the range of 200~800 °C for 2 h in static air at a ramp of 10 °C min^{-1}. After calcination, the temperature of the furnace was permitted to decrease to 280 °C (except if specifically stated) and the sample was recovered and stored in a sealed vial in a desiccator. Freshly prepared samples of MgO and Li/MgO were used in this study for all catalyst evaluations.

3.2.2 Catalyst testing

Benzaldehyde (0.006 mol, Aldrich), alcohol (0.12 mol) and the catalyst (0.5 g) were placed in a two-neck flask and heated under reflux. Samples were taken at specified times, after reaching the reaction temperature and were analysed using GC-MS (Perkin Elmer Autosystem XL), equipped with a DB-1 column.

3.3 Results and discussion

To determine the influence of the calcination temperature on the catalytic activity of the MgO samples, commercially available $(MgCO_3)_4Mg(OH)_2$ was calcined at different temperatures between 350 °C and 800 °C and then tested as a catalyst for the reaction of benzaldehyde with 2-butanol. Figure 3.1 shows the conversion after 5 min reaction as a function of the calcination temperature. These results show that MgO calcined at 450 °C

was the most active catalyst. When the calcination temperature was 400-475 °C, conversion > 70% was achieved after five minutes reaction, whereas, a low level of activity was observed when the calcination temperature was either < 350 °C and or > 600 °C.

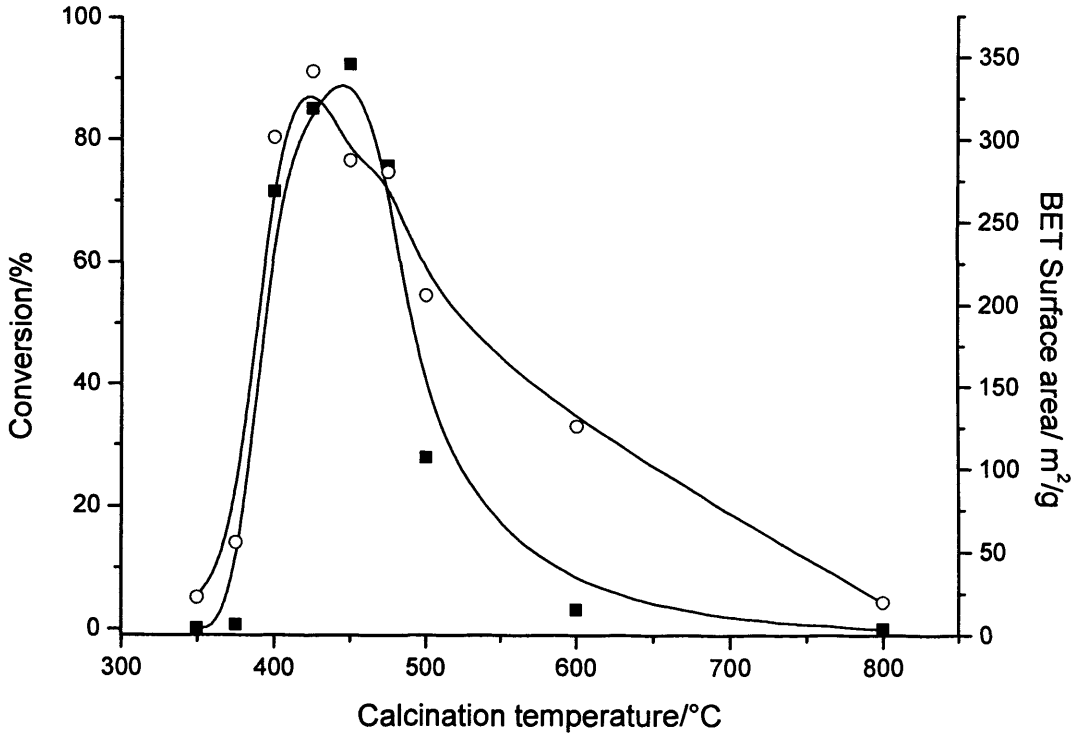

Figure 3.1 Activity for the MPV reaction of benzaldehyde and 2-butanol after 5 minutes over MgO catalysts derived from commercially available $MgCO_3Mg(OH)_2$ and their BET surface area as a function of calcination temperature; (■) Conversion, (O) BET Surface area.

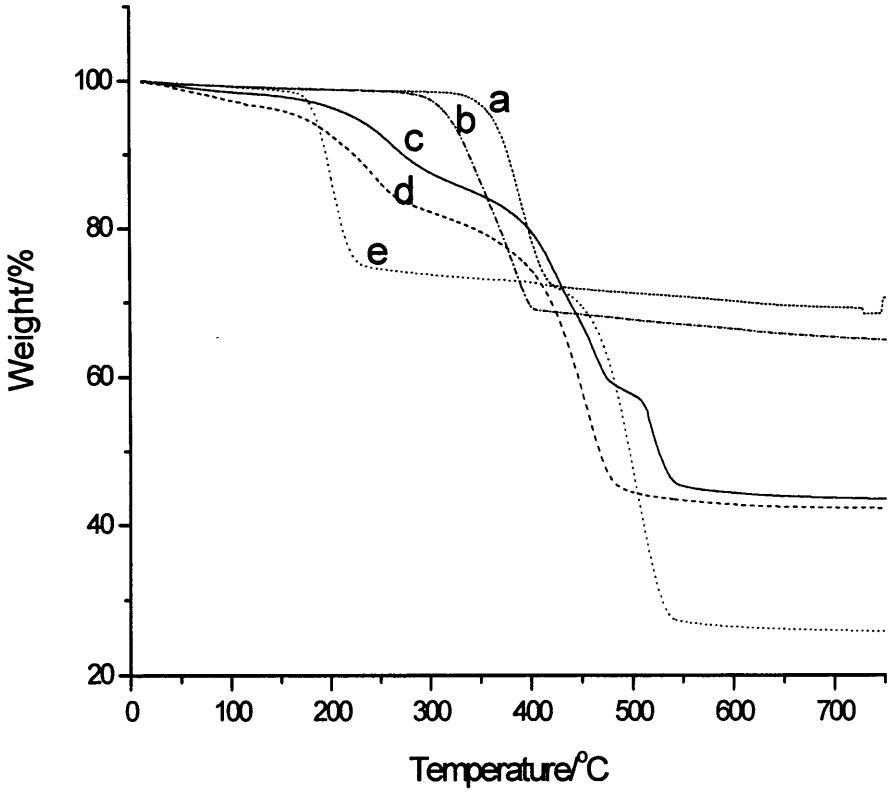

Figure 3.2 TGA curves of MgO precursors: (a) Rehydrated $Mg(OH)_2$, (b) Commercial $Mg(OH)_2$, (c) $((MgCO_3)_4Mg(OH)_2$, (d) $MgCO_3$, (e) MgC_2O_4.

TGA shows the temperatures at which the MgO precursors decompose when heated in a controlled environment (Figure 3.2). Water is removed from the precursors between 250 ~ 400 °C, whereas carbon dioxide is lost between 325 ~ 550 °C. The thermal pre-treatment resulted in a change in the XRD pattern, caused by the removal of CO_2 and H_2O from the starting material (Figure 3.3). The diffraction patterns of the samples heated at temperatures < 375 °C were different from that of MgO, while samples activated at temperatures > 400 °C displayed diffraction reflections characteristic of MgO, which became, as expected, more crystalline with increasing calcination temperature. Figure 3.4a shows that after calcinations at 450 °C for 2 h contain MgO as

the major phase and $MgCO_3$ as a minor phase. MgO as a single phase is observed after calcination at > 600 °C for 2 h (Figure 3.4b).

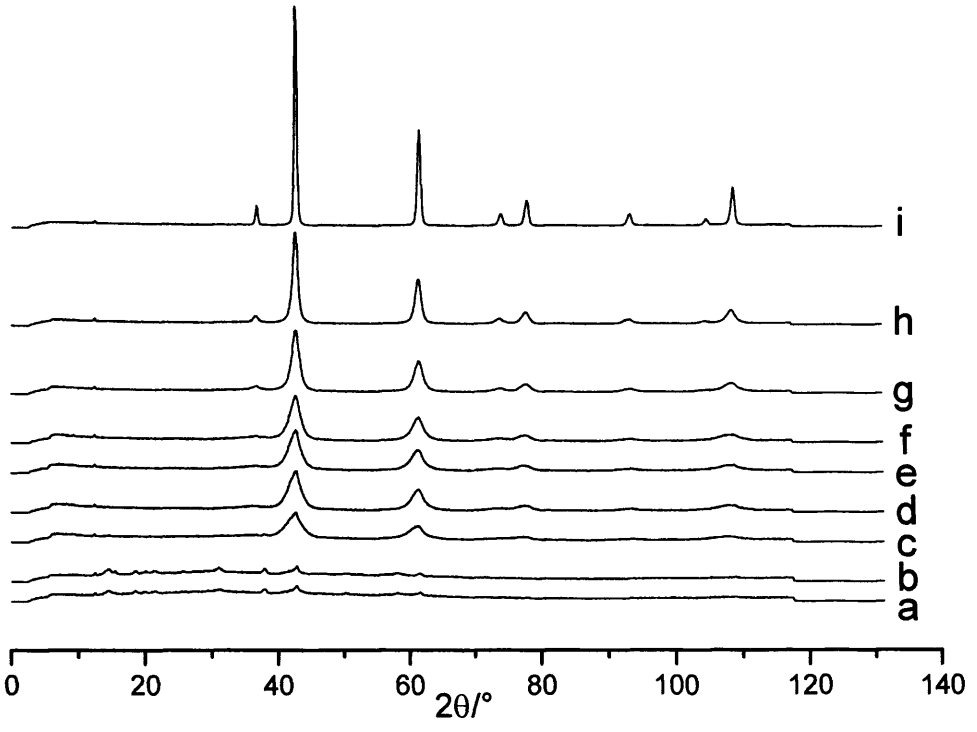

Figure 3.3 XRD patterns from the materials obtained by calcining commercially available $(MgCO_3)_4Mg(OH)_2$ at different temperatures; (a) 350 °C, (b) 375 °C, (c) 400 °C, (d) 425 °C, (e) 450 °C, (f) 475 °C, (g) 500 °C, (h) 600 °C, (i) 800 °C.

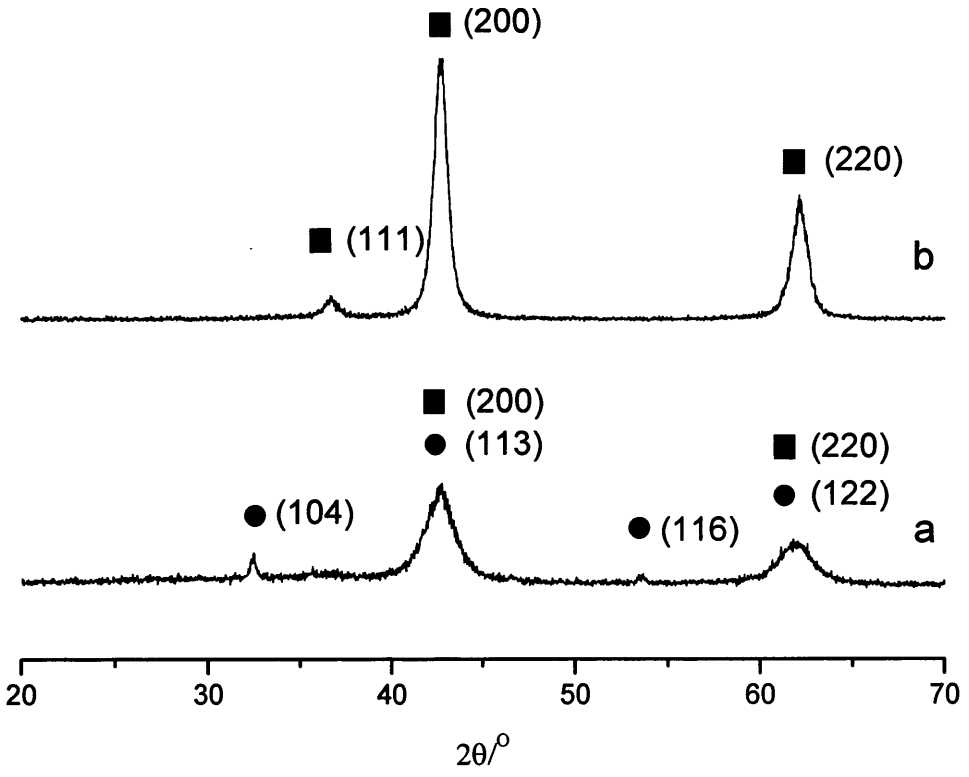

Figure 3.4 XRD patterns from the materials derived by calcining commercially available $(MgCO_3)_4Mg(OH)_2$ {with (■) MgO, (●) $MgCO_3$ phases} at different temperatures (a) 450 °C, (b) 600 °C.

The changes observed in the XRD patterns (Figures 3.3 and 3.4) coincided with a change in the catalytic activity (Figure 3.1). Calcinations at 375 °C did not lead to the formation of MgO, and, consequently, the catalytic activity was very low. The best catalytic performance was obtained for calcination temperatures between 400 and 475 °C, when the XRD patterns showed a poorly crystalline MgO that had a high surface area (Figure 3.3 and 3.4 and Table 3.1).

Table 3.1 BET surface area and crystal size of MgO materials prepared by different methods.

Catalyst	Precursor	Calcination conditions	Crystallite size(nm)	S_{BET} ($m^2 g^{-1}$)
MgO-CBC	Commercial $(MgCO_3)_4Mg(OH)_2$ (Fluka)	800 °C, 2h	17	20
		700 °C, 2h	17	59
		600 °C, 12h	13	79
		600 °C, 2h	8.6	126
		500 °C, 2h	5.8	206
		475 °C, 2h	4.5	281
		450 °C, 2h	3.9	288
		425 °C, 2h	3.7	342
		400 °C, 2h	2.9	302
		375 °C, 2h	~	56
		350 °C, 2h	~	23
		No calcination	~	14
MgO-RBC	Rehydrated $(MgCO_3)_4Mg(OH)_2$	450 °C, 2h	4.4	296
MgO-CC	Commercial $MgCO_3$ (Acros Organics)	450 °C, 2h	4.2	229
MgO-COH	Commercial $Mg(OH)_2$ (Fluka)	450 °C, 2h	22	58
MgO-ROH	Rehydrated $Mg(OH)_2$	450 °C, 2h	7.0	287
MgOFOH	Freshly-prepared $Mg(OH)_2$ ($MgSO_4$+KOH)	450 °C, 2h	5.0	245
MgO-OX	MgC_2O_4	450 °C, 2h	4.8	312

Table 3.2 BET surface area and crystal size of MgO materials prepared by different methods.

Catalyst	Precursor	Calcination conditions	Crystallite size(nm)	S_{BET} ($m^2 g^{-1}$)
MgO-RBC	Rehydrated $(MgCO_3)_4Mg(OH)_2$	800 °C, 24h	30	12
		600 °C, 24h	14	88
		600 °C, 2h	8.6	142
		450 °C, 24h	9.5	131
		450 °C, 4h	5.5	205
		450 °C, 2h	4.4	**296**
		450 °C, 1h		258
		350 °C, 2h	~	19
		None	~	12
MgO-CC	Commercial $MgCO_3$	800 °C,2h	17	41
		700 °C, 2h	14	69
		600 °C, 2h	7.7	90
		450 °C, 2h	4.2	**229**
		350 °C, 2h	~	77
MgO-COH	Commercial $Mg(OH)_2$	800 °C, 24h	30	21
		700 °C, 2h	20	65
		600 °C, 2h	21	51
		500 °C, 2h	21	86
		450 °C, 12h	25	65
		450 °C, 4h	21	68
		450 °C, 2h	22	**58**
		None	29	6
MgO-ROH	Rehydrated $Mg(OH)_2$	800 °C, 2h	19	63
		700 °C, 2h	12	98
		600 °C, 2h	8.8	181
		500 °C, 2h	7.5	277
		450 °C, 2h	7.0	**287**
		400 °C, 2h	7.0	268
		350 °C, 2h	22	40
		300 °C, 2h	20	24
		200 °C, 2h	19	22
MgO-FOH	Freshly-prepared $Mg(OH)_2$ ($MgSO_4$+KOH)	800 °C, 2h	18	43
		600 °C, 24h	17	60
		600 °C, 2h	11	112
		450 °C, 2h	5.0	**245**
		None	~	105
MgO-OX	MgC_2O_4	800 °C, 2h	23	66
		700 °C, 2h	18	73
		600 °C, 2h	8.7	177
		450 °C, 2h	4.8	**312**
		350 °C, 2h	~	59

The increase in calcination temperature led to a decrease in catalyst activity as the MgO became more crystalline and the BET surface area decreased. It is clear that the crystallite size, and hence surface area, plays a key role in determining the catalytic activity, as the highest activity of the catalyst was obtained when the surface area of the catalyst was at a maximum.

MgO was prepared using a range of precursors with calcinations at 450 °C (Table 3.1). All the samples, except that derived from commercial $Mg(OH)_2$, were found to have a high surface area and small crystal size. The crystallite size was calculated by Scherrer equation (Chapter 2). The surface area decreased with increasing calcination temperature, which was accompanied by a corresponding increase in crystallite size (Table 3.2).

The morphology of MgO-ROH and MgO-COH was different. The precursors of both materials consist of hexagonal discs (Figure 3.5e and 3.5g). After calcination of the precursors to form MgO, MgO-ROH (Figure 3.5h) remains aggregated in a spongy morphology reminiscent of the hydroxide precursor. In contrast, there was a distinct difference between the morphology of MgO-COH (Figure 3.5f) and its precursor. It has been reported that the morphology of MgO is dependent upon the starting material and the thermal pre-treatment conditions.[1] In this study, MgO-ROH and MgO-COH were prepared by calcining their corresponding precursors under the same conditions. Therefore, the morphological difference between the MgO-ROH and MgO-COH may be attributed to the use of different precursors. The SEM images show that the hexagonal plates of MgO-COH precursor are thicker than that of MgO-ROH precursor. The other difference may be that of the purity of the precursors. Schwank *et al.* found that impurities have a significant influence on the morphology of MgO which was produced by dehydration of $Mg(OH)_2$.[2] It is possible that the difference observed in the activity of

the two materials is due to an impurity in the commercial sample which is removed during the water reflux step.

Typical SEM images of the other MgO materials and precursors are also presented in Figure 3.5. They reveal that the size and morphology of the catalysts produced are very strongly influenced by the morphology of the catalyst precursor, which is retained during the calcination procedure.

To study the effect of the precursor on the catalyst activity, the MgO materials obtained using calcination at 450 °C, were tested as catalysts for the MPV reduction of benzaldehyde with 2-butanol. The results are shown in Figure 3.6 (conversion) and Figure 3.7 (selectivity). All of the MgO materials were found to be very active (>90% conversion after 1 h), apart from MgO-COH (<1% conversion after 3 h). For all catalysts the selectivity was found to be high. For the MgO-OX material the selectivity was approximately 86% after 2 h, MgO-FOH was found to be 92% selective, while the other materials showed selectivities of >97%. The main by-product arose from an aldol condensation between benzaldehyde and butanone and the catalysts with lower selectivities showed a considerable drop in selectivity with time due to this secondary reaction.

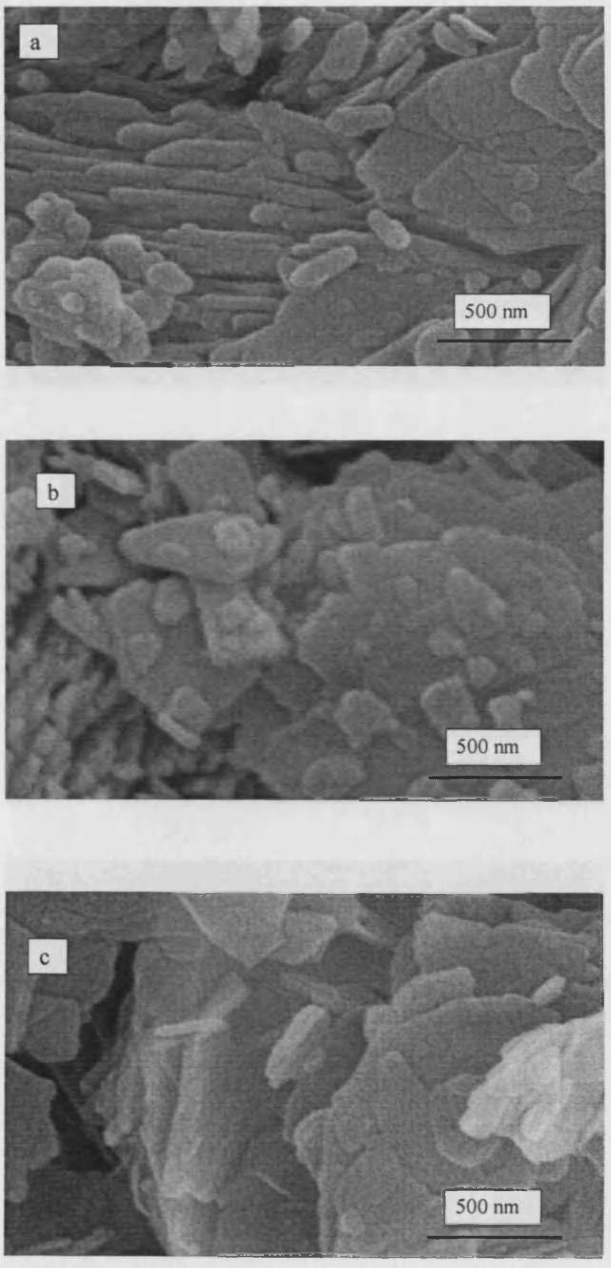

Figure 3.5 SEM images of MgO and its corresponding precursor. All the MgO are prepared by calcining its corresponding precursor at 450 °C; (a) $(MgCO_3)_4Mg(OH)_2$, (b) MgO-CBC, (c) $MgCO_3$

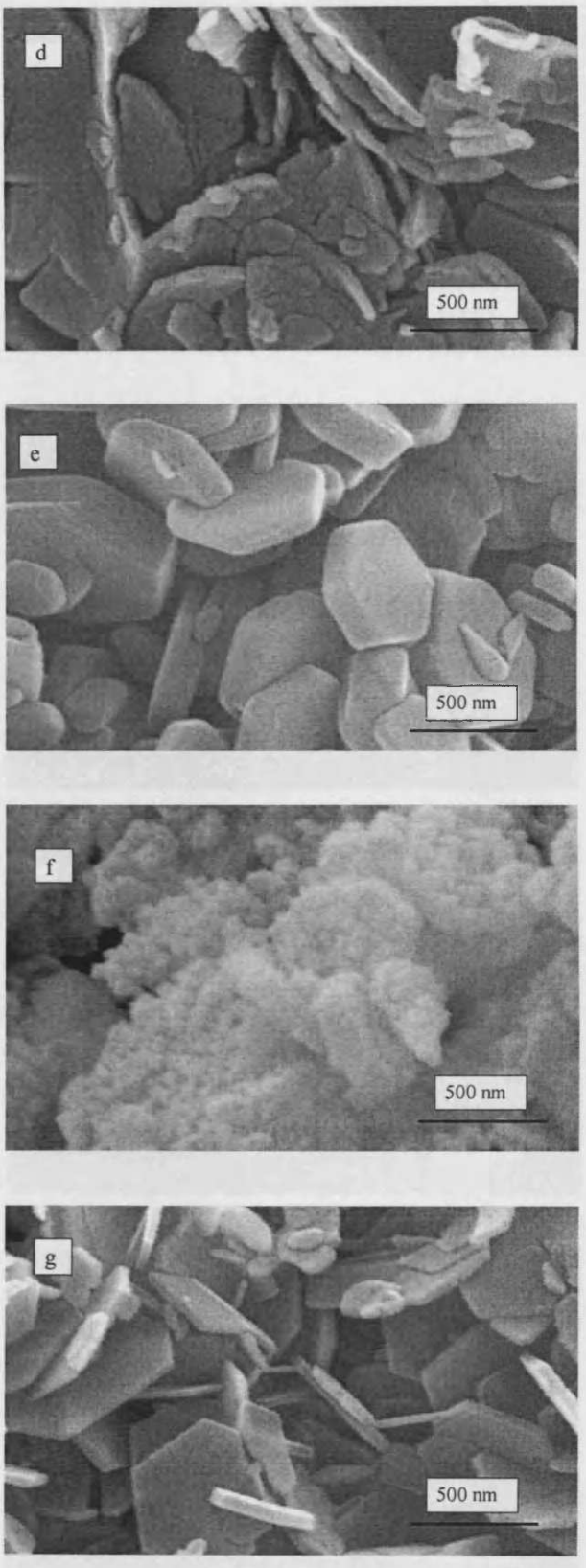

Figure 3.5 (d) MgO-CC, (e) Commercially available $Mg(OH)_2$, (f) MgO-COH, (g) Rehydrated $Mg(OH)_2$

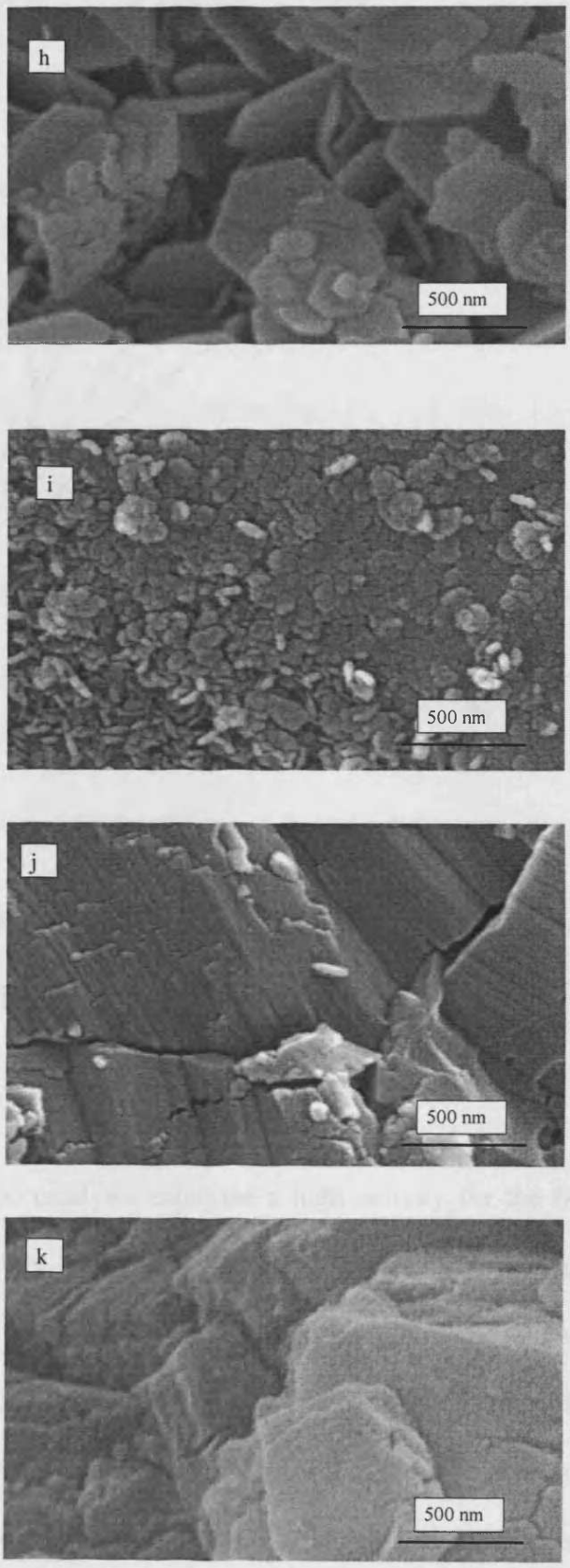

Figure 3.5 (h) MgO-ROH, (i) MgO-FOH, (J) MgC_2O_4, (k) MgO-OX.

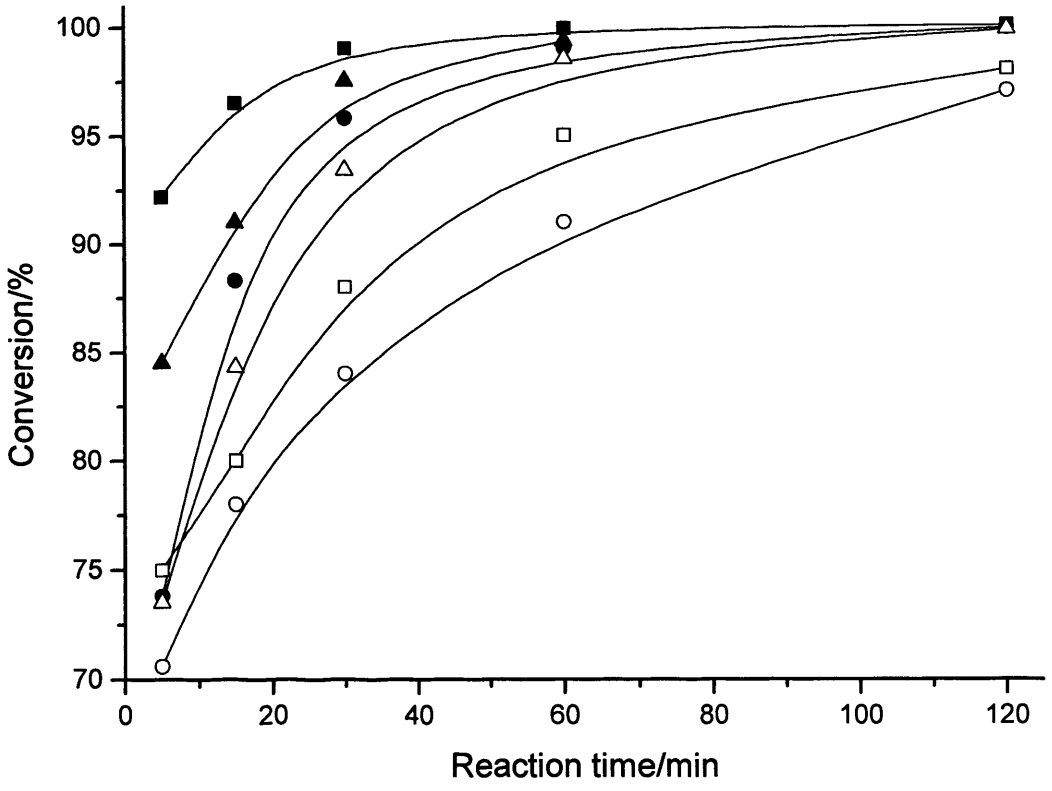

Figure 3.6 Activity for the MPV reaction of benzaldehyde with 2-butanol over MgO; (■) MgO-CBC, (●) MgO-RBC, (○) MgO-CC, (▲) MgO-ROH, (□) MgO-FOH, (△) MgOOX.

Although most of the catalysts exhibited a high activity for the MPV reaction, MgO-COH had a low activity, which is consistent with its low surface area and large crystal size. MgO-COH and MgO-ROH were prepared from the same parent $Mg(OH)_2$ but using a different procedure. MgO-COH was obtained from the direct calcination of commercially available $Mg(OH)_2$, while MgO-ROH was obtained from the calcination of rehydrated $Mg(OH)_2$ (commercial $Mg(OH)_2$ which had been refluxed in water). The preparation procedure has a direct influence on the surface area of MgO-COH and MgO-ROH (MgO-ROH = 287 $m^2 g^{-1}$, MgO-COH = 58 $m^2 g^{-1}$) and consequently the activity of the catalysts. However, when the conversion per unit area of catalyst is calculated MgO-

ROH is still more active. This indicates that the surface area is not the only factor responsible for the activity, and the water reflux step has additional benefits.

Figure 3.8 showed the results obtained from the reaction of benzaldehyde with different alcohols over MgO-CBC. With the exception of 2-methyl-2-propanol, all other substrates yielded a high reaction rate and selectivity. Although the selectivity of the reaction with 2-methy-2-propanol was high the conversion was only 2%. These catalytic activity results can be explained in the light of a mechanism similar to that proposed previously (Scheme 3.2),[3] where the hydrogen transfer is a concerted process that takes place via a six-member intermediate formed between alcohol and benzaldehyde. The rate-determining step of the process is considered to be related to the interaction of the alcohol with basic sites, which causes dissociation to the corresponding alkoxide. In the proposed scheme, the surface-adsorbed alkoxide, forms from the alcohol, transfers a hydride ion that attacks the carbonyl group. For 2-methyl-2-propanol, no hydrogen is available to form a six-member intermediate, which explains the low conversion (Scheme 3.3). 2-butanol had a higher selectivity than 1-butanol, which is in agreement with the finding of Figueras[4]: *i.e.* the best hydrogen donors are secondary alcohols with primary alcohols yielding aldehydes which are more prone to undergo cross-aldol condensations and Tishchenko reactions with the substrate.

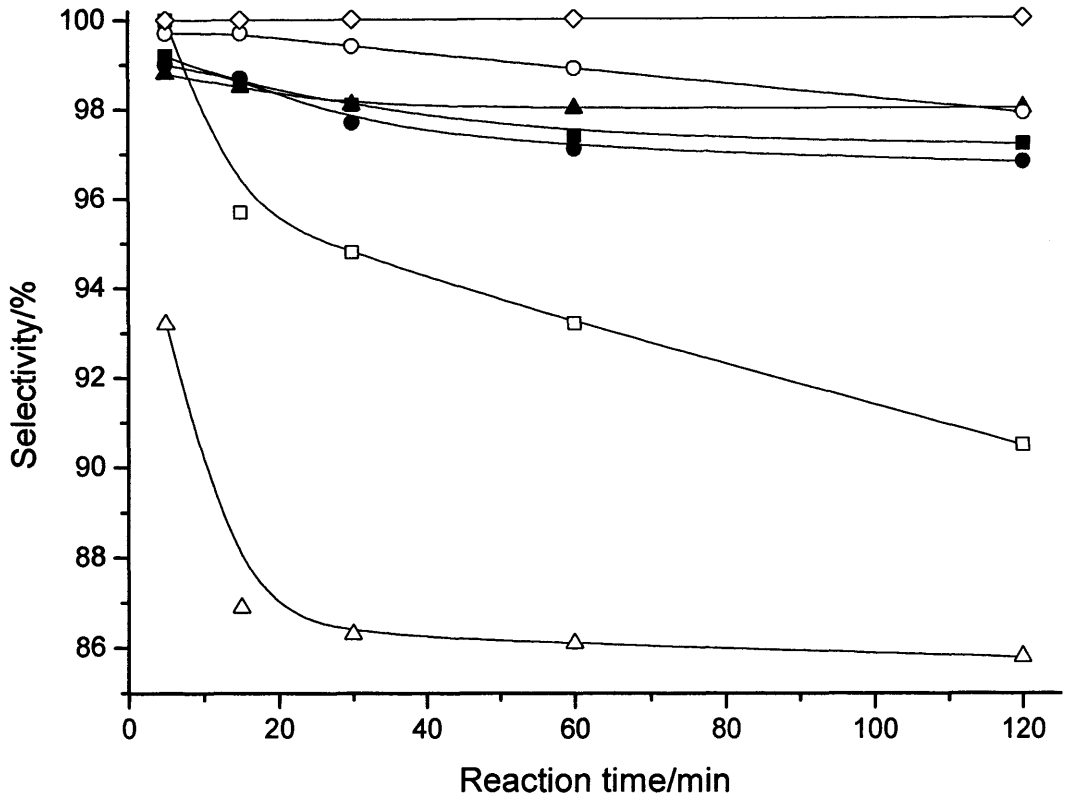

Figure 3.7 Selectivity for the MPV reaction of benzaldehyde with 2-butanol over MgO; (■) MgO-CBC, (●) MgO-RBC, (○) MgO-CC, (◇) MgO-COH, (▲) MgO-ROH, (□) MgO-FOH, (△) MgO-OX.

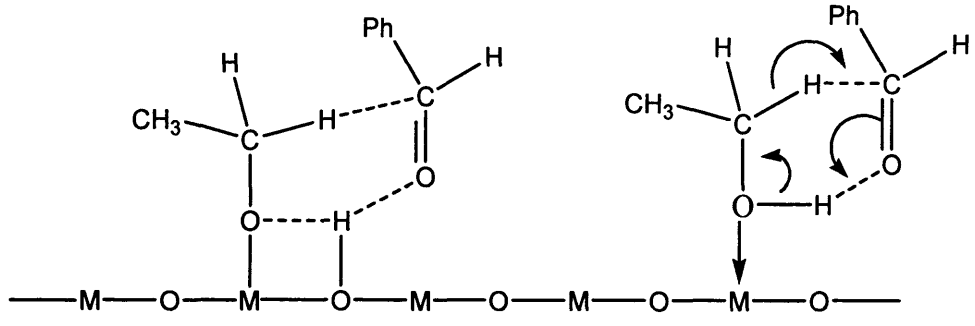

Scheme 3.2 Mechanism of the MPV reaction studied

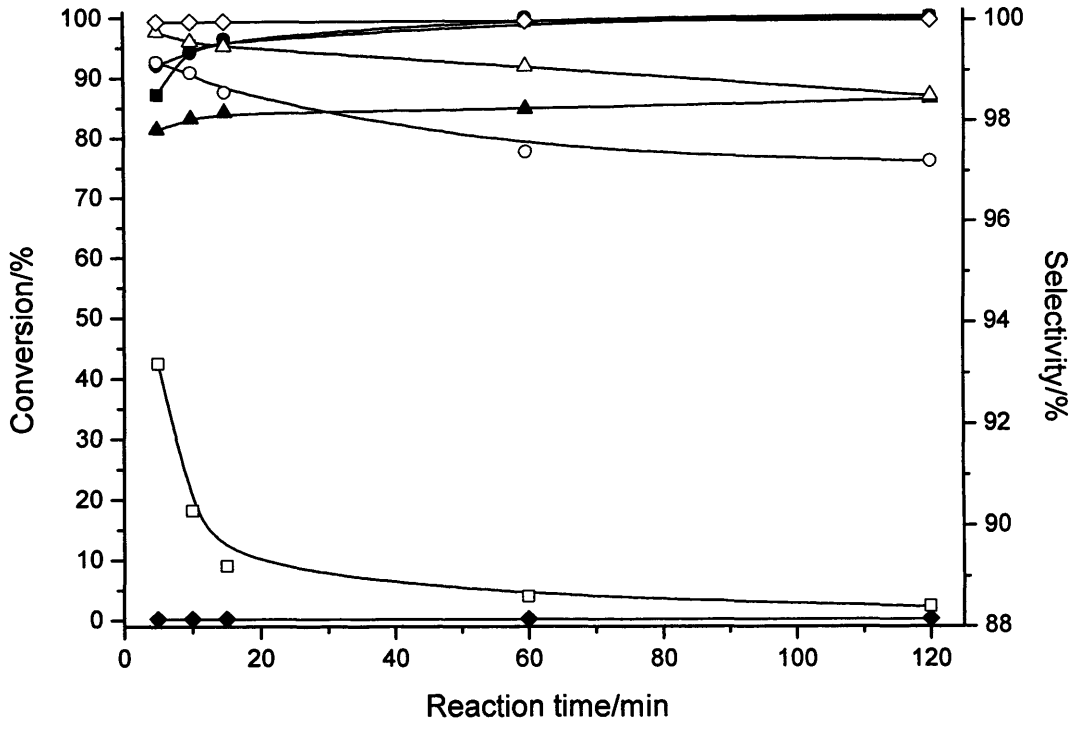

Figure 3.8 Conversion and selectivity data for the MPV reaction of benzaldehyde with different alcohols over MgO-CBC; (■) 1-butanol, (●) 2-butanol, (▲) 2-methyl-1-propanol, (◆) 2-methyl-2-propanol; Solid symbols refer to conversion, open symbols refer to selectivity.

The reusability of the MgO-CBC was investigated by recovering the catalyst after running a reaction of benzaldehyde with 2-butanol for 5min. The conversion and selectivity for the first use of MgO-CBC was presented in entry 1of table 3.3. The catalyst was washed with acetone (10 ml) for three times, refluxed in water (10 ml) for 3 h, dried in oven (24 h) and finally calcined at 450 °C for 2 h. The surface area of the material (287 m^2 g^{-1}) was found to be the same after the reactivation procedure as it was before the initial run (Table 3.1). When the reactivated MgO was used as a catalyst for the same reaction, the activity was the same as that seen for the first reaction (conversion: 88.0%; selectivity: 98.7%).

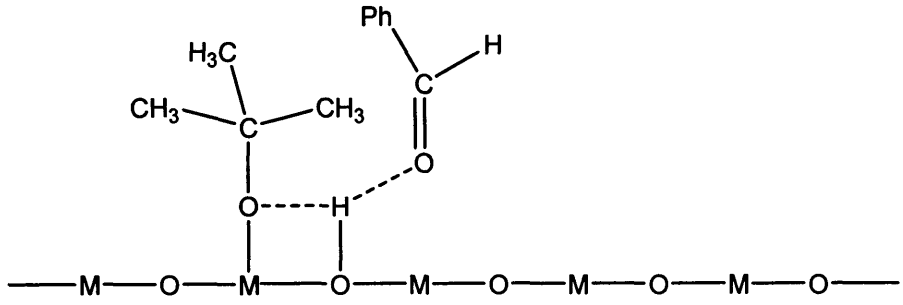

Scheme 3.3 Intermediate for the reaction with 2-methyl-2-propanol

Table 3.3 Catalytic activity and selectivity of MgO-CBC compared to literature data.[5]

Entry	Alcohol	Reaction time	Conversion	Selectivity
1	2-butanol	5 min	92.2%	99.2%
2	2-butanol	1 h	99.9%	97.4%
3	2-butanol[a]	10 h	98.7%	90.3%
4	1-butanol	5 min	87.2%	93.2%
5	1-butanol	1 h	99.3%	88.6%
6	1-butanol[a]	10 h	75.2%	58.6%

[a] Reference,[5] reaction conditions: 0.003 mol benzaldehyde; 0.06 mol alcohol; Reflux temperature; 1 g CaO.

The performance of MgO-CBC was compared with previously reported literature studies (Table 3.3).[5] CaO has been proved to be the most active catalyst among the five heterogeneous base catalysts, including MgO prepared from commercially available $Mg(OH)_2$, CaO/Al_2O_3, MgO/Al_2O_3 and Mg/Ga_2O_3 from the corresponding hydrotalcite precursors. From the comparative data presented in Table 3.3, it is clear that MgO prepared by the methodology describe here gives a superior catalytic performance for the MPV reaction. Under the reaction conditions, 10h was needed to reach high conversion

in the presence of CaO, while 1h for MgO prepared in this study. Furthermore, the amount of CaO was four times that of MgO.

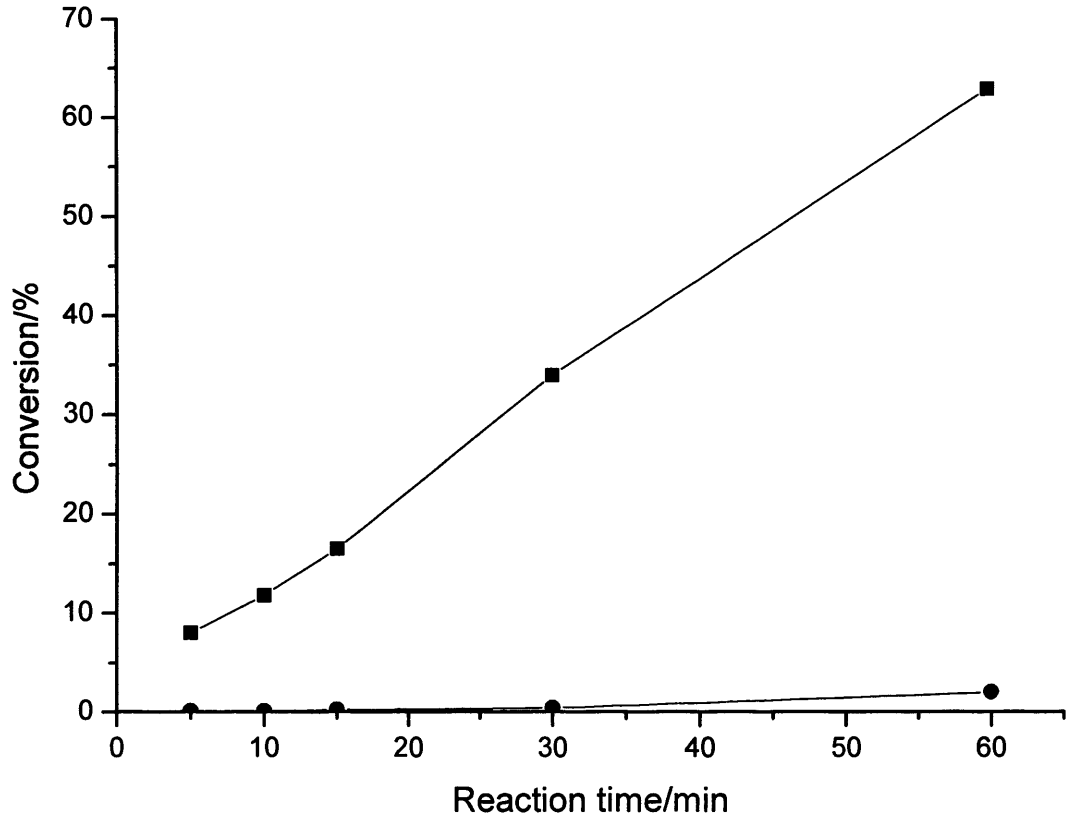

Figure 3.9 The effect of air on the activity of MgO for the MPV reaction of benzaldehyde with 2-butanol; (■) freshly calcined, (●) open to air for 5 h.

It was observed that MgO catalysts rapidly deactivate if they are left exposed to the atmosphere. Figure 3.9 shows the catalytic results for freshly calcined MgO (cooled down to r.t in furnace) and the same sample used after having been left in contact with the atmosphere for additional 5 h. The activity of the former MgO sample is higher than the latter and less than the one cooled down to 280 °C (Figure 3.6, MgO-CBC). In order to study the effect of CO_2 and H_2O on activity of MgO, TGA and DTG curves of MgO cooled down under different conditions were conducted (Figure 3.10).

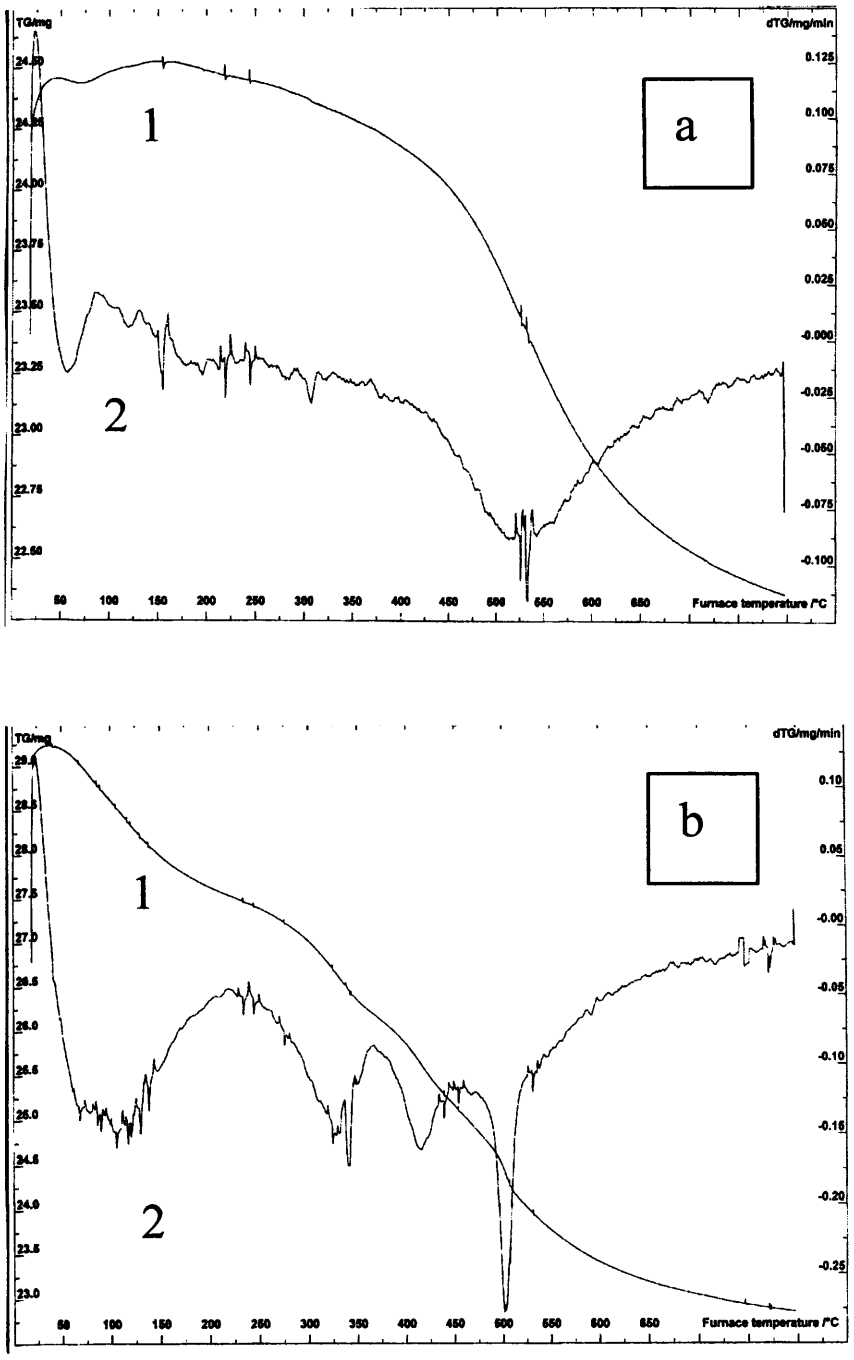

Figure 3.10 TGA (1) and DTG (2) curves of MgO cooled under different conditions; (a) Fresh MgO cooled down to 280 °C in furnace, (b) sample a cooled to room temperature in static air.

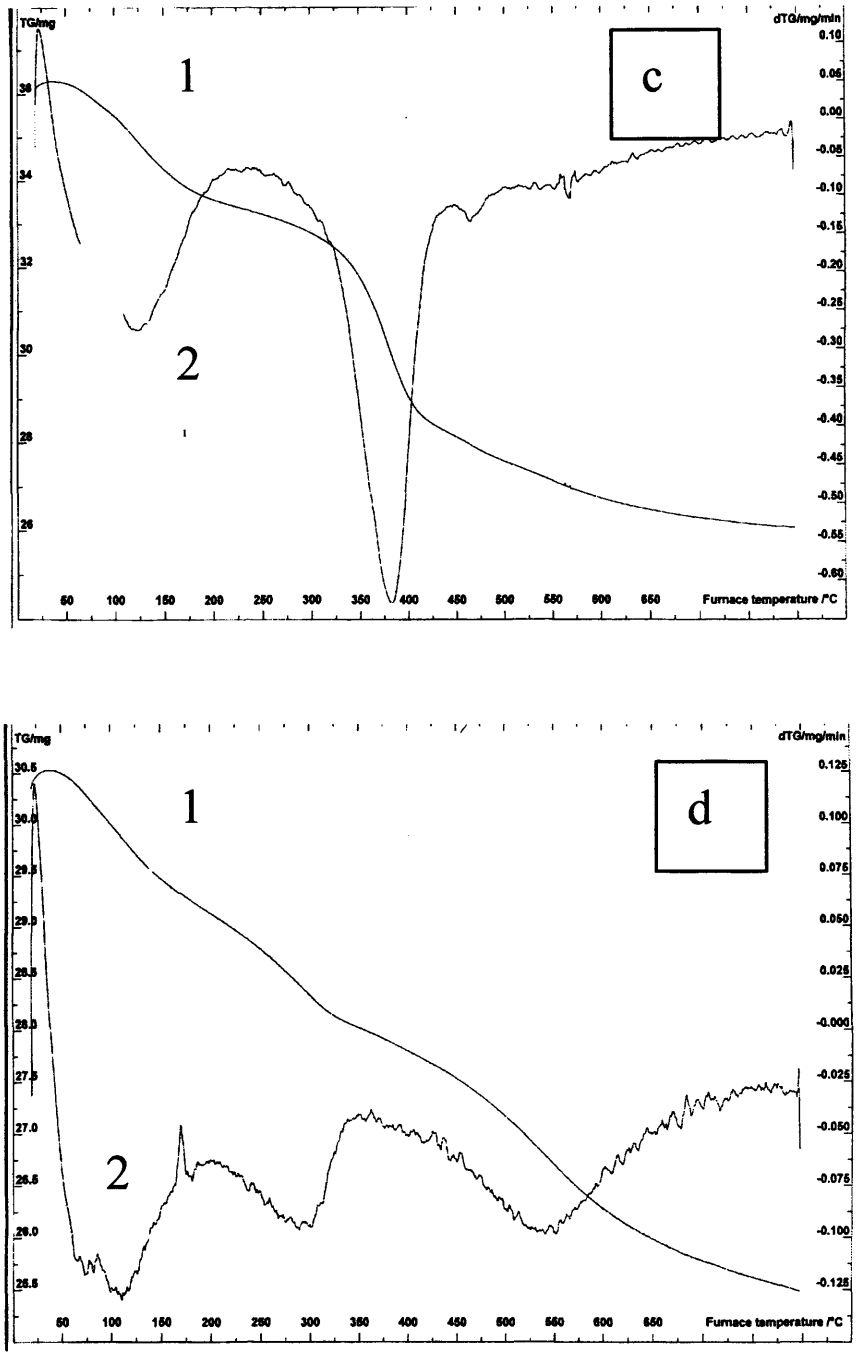

Figure 3.10 (c) sample a cooled to room temperature in CO_2 and H_2O vapour, (d) sample a cooled to room temperature in N_2 and H_2O vapour.

MgO cooled down to 280 °C (Figure3.10, a) lost weight at about 520 °C at which the little $MgCO_3$ left decomposed. However, all of the other three samples lose weight below 520 °C. This infers that the sample, cooled down to 280 °C, adsorbed far less CO_2 or H_2O than the other three samples. Both MgO cooled to room temperature in air (Figure

3.10, b) and in CO_2 and H_2O (Figure 3.10, c) lose weight at similar temperature, which is different from that in N_2 and H_2O (Figure 3.10, d). The results show that both CO_2 and H_2O deactivate the activity of MgO and in order to achieve a good catalyst performance the MgO samples must be freshly calcined before use, or kept in a sealed environment, away from the atmospheric moisture and CO_2.[6]

To determine whether increasing the base strength of the catalyst improved performance, lithium was doped on the prepared various MgO. The addition of lithium to MgO caused a loss of surface area (Table 3.4) compared with the unmodified MgO. For example, the surface area of Li/MgO-CBC is 164 $m^2 g^{-1}$, whereas that of the parent MgO-CBC is 288 $m^2 g^{-1}$; Li/MgO-CC is 186 $m^2 g^{-1}$, but that of the parent MgO-CC is 229 $m^2 g^{-1}$.

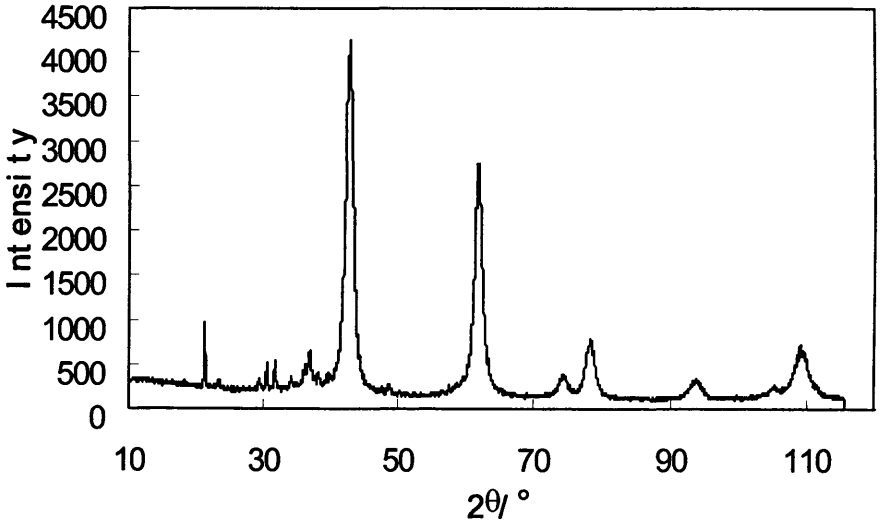

Figure 3.11 XRD patterns of Li/MgO.

The XRD diffraction pattern of Li/MgO (Figure 3.11) shows that the major phase is that of parent MgO (Figure 3.3 and 3.4). However, in the former diffraction pattern, low intensity diffraction peaks occur at the low 2θ value (21°, 29° and 30°), which do not appear in the diffraction pattern of the parent MgO. The XRD structure shows that the

mainly structure of Li/MgO is that of parent MgO. However, the surface is changed a little by the addition of lithium because the diffraction peaks occur in the low 2θ value.

The activity of Li/MgO is tested and compared with that of parent of MgO (Figure 3.12). Both of the conversion and selectivity in the presence of Li/MgO are lower than that of parent MgO. Doping with lithium, Li/MgO-CC decrease the conversion from 98.9% to 55.6% in 2 h and the selectivity from 97.9% to 80.2% compared to the undoped MgO-CC. Using an alternative preparation method gave similar results with the conversion decreasing from 99.9% to 85.2% and selectivity from 98.0% to 83.4%, when MgO-CBC is doped with Li (Li/MgO-CBC).The decrease in conversion can be ascribed to the decrease of the surface area when the lithium is added to the catalyst. The decrease in selectivity is resulted from the increase in the basic strength. The higher basic strength of Li/MgO increases the conversion of by-product, an aldol condensation between benzaldehyde and butanone. For this reason, the selectivity to the MPV product decreased. When the yield was calculated in terms of the number of moles of product m^{-2} h^{-1}, the addition of lithium did not improve the performance of the MgO. This indicates that the basic strength of the catalyst does not improve this reaction and that having a high surface area material is much more important.

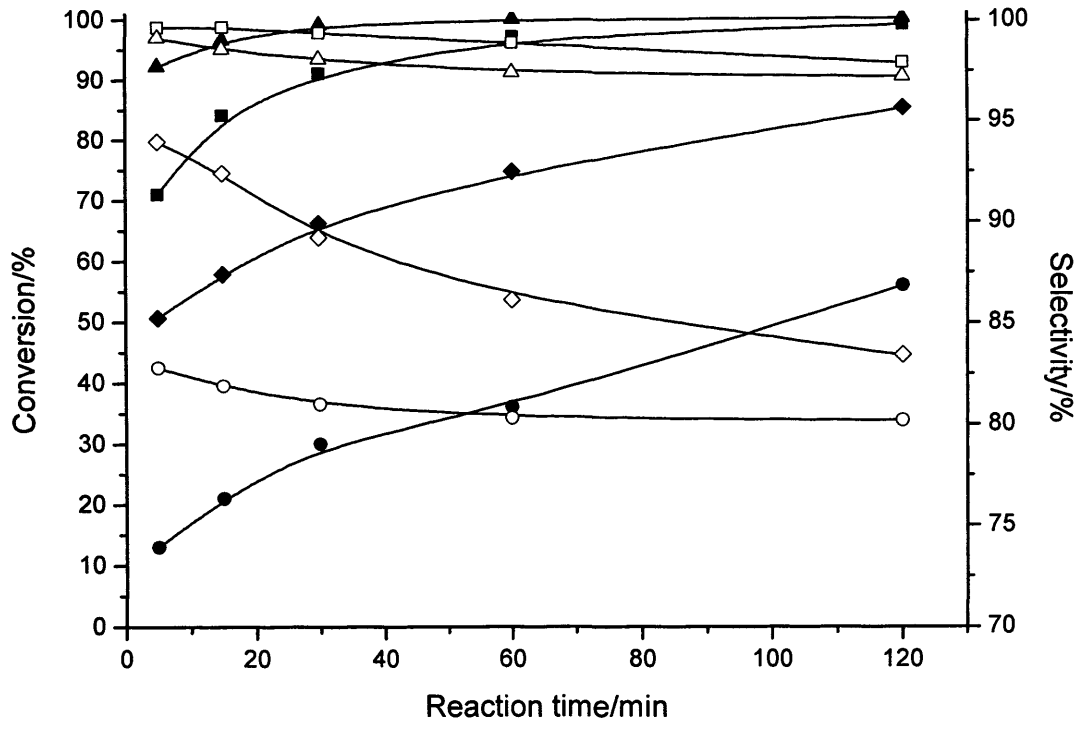

Figure 3.12 Comparison of the conversion and selectivity for the MPV reaction over MgO-CBC and MgO-CC, compared with their Li-doped counterparts; (▲) MgO-CBC, (◆) Li/MgO-CBC, (■) MgO-CC, (●) Li/MgO-CC; Solid symbols refer to conversion, open symbols refer to selectivity.

Table 3.4 BET surface area of 2 wt % Li/MgO.

Catalyst	Support	S_{BET} (m^2 g^{-1})
Li/MgO-CBC	MgO-CBC	164
Li/MgO-CC	MgO-CC	186
Li/MgO-OX	MgO-OX	158
Li/MgO-COH	MgO-COH	174

3.4 Conclusions

Magnesium oxide with high surface area (229~312 m^2 g^{-1}) was prepared by the thermal decomposition of various precursors including $(MgCO_3)_4Mg(OH)_2$, $Mg(OH)_2$, $MgCO_3$ and MgC_2O_4. The high area MgO displayed exceptionally high catalytic activity for the liquid phase Meerwein-Ponndorf-Verley (MPV) reaction of benzaldehyde with different alcohols. The effect of the calcination temperature and precursor source on the catalytic activity and morphology of MgO has been investigated in detail. It was found that the optimum calcination temperature was 450 °C leading to the highest surface area material which is the key controlling parameter for the catalytic activity of MgO for the MPV reaction. Lithium doped magnesium oxide was also studied, but resulted in lower conversion and selectivity than pure MgO, caused by a decrease in the surface area of the doped material. The high area MgO catalyst could be reused without loss of catalyst activity.

References

1. A. G. Shastri, H. B. Chae, M. Bretz and J. Schwank, *J. Phys. Chem.*, 1985, **89**, 3761.
2. G. Leofanti, M. Solari, G. R. Tauszik, F. Garbassi, S. Galvagno and J. Schwank, *Appl. Catal.*, 1982, **3**, 131.
3. V. A. Ivanov, J. Bachelier, F. Audry and J. C. Lavalley, *J. Mol. Catal.*, 1994, **91**, 45.
4. F. Figueras, *Topics Catal.*, 2004, **29**, 189.
5. M. A. Aramendía, V. Borau, C. Jiménez, J. M. Marinas, J. R. Ruiz and F. J. Urbano, *J. Colloid Interf. Sci.*, 2001, **238**, 385.
6. C. Xu, J. K. Bartley, D. I. Enache, D. W. Knight and G. J. Hutchings, *Synthesis*, 2005, **19**, 3468.

Chapter 4

High surface area MgO as a highly effective heterogeneous base catalyst for Michael addition and Knoevenagel condensation reactions

4.1 Introduction

We have found that magnesium oxide with a high surface area can be produced (Chapter 3) and in this chapter, MgO was systematically investigated as a solid base catalyst for Michael additions and Knoevenagel condensations, reactions which are commonly used for the manufacture of fine chemicals.

The particular versions of the Michael addition studied was the addition of active methylene compounds, alcohols and thiols to α,β-unsaturated carbonyl compounds, a useful strategy for the construction of carbon-carbon bonds (Scheme 4.1). The mechanism for such Michael additions involves the formation of an anion from the active methylene compound, conjugate addition of this to the α,β-unsaturated carbonyl compound and finally, product protonation.[1] The Knoevenagel condensation (Scheme 4.2) of active methlyene compounds and aldehydes is one of the most popular methods of synthesizing functionalized alkenes. Basic catalysts can generate significant amounts of carbanions from the active methylene compounds, which can then attack a carbonyl group to give a condensed product.[2]

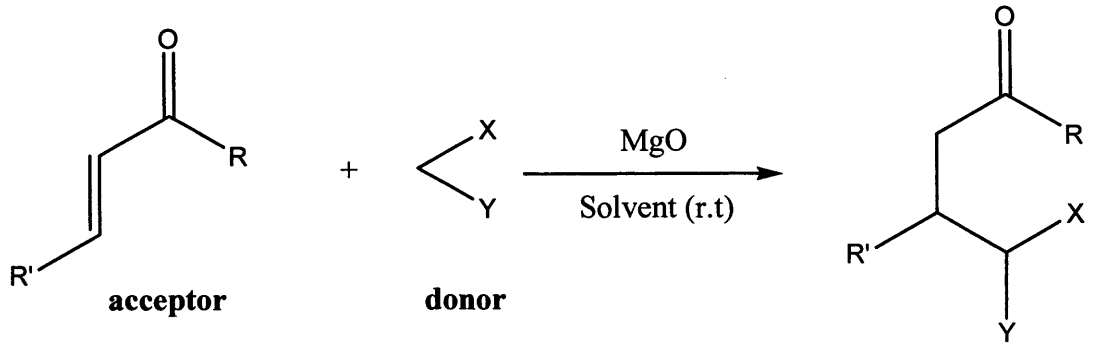

Scheme 4.1

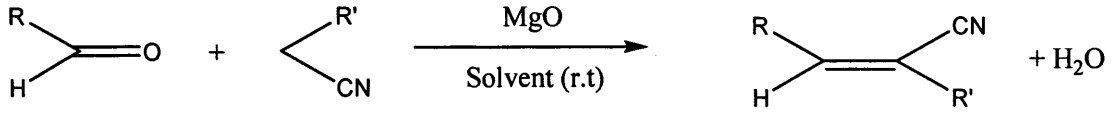

Scheme 4.2

Base-catalyzed Michael additions and Knoevenagel condensations have been extensively studied in homogeneous systems,[3,4] but very few studies have employed heterogeneous catalysts.[5] To date the heterogeneous catalysts studied have shown either low activity or have been prepared in a complex way[6,7] and to the best of our knowledge, there are no reported studies, systematically dealing with the activity of MgO in such Michael additions, especially which examine facts such as: the catalyst preparation method, the reaction condition and, most important, the interaction between MgO and the substrate. In homogeneous base-catalyzed systems, the reaction rate increase with the pKa value (acid value) of the substrate and the basic strength of the catalyst. In the heterogeneous base-catalyzed system, there have been no studies which have systematically investigated the relationship between the acid value of the substrate and the activity of MgO. This will be critical for preparing a successful solid basic catalyst.

In this chapter we investigate a high area form of magnesium oxide as a catalyst for a number of different Michael additions and Knoevenagel condensations and it was found to be very active and reusable. It was found that the activity of MgO, to a large extent, depended upon the solvent and the structure of substrate. The effect of substrate acidity in the heterogeneous system over MgO is different from homogeneous base-catalyzed systems. This discovery may be very helpful for future studies of other metal oxide catalysts. Furthermore, we propose mechanisms for these reactions, over the magnesium oxide catalyst. The activity of CaO was also investigated.

4.2 Experimental

The MgO catalysts used in this study were obtained by calcination of the precursors commercially available $(MgCO_3)_4Mg(OH)_2$, or rehydrated $Mg(OH)_2$ at 450 °C for 2 hours. The heating ramp used in all cases was 10 °C/min.

CaO was prepared as follows. Commercially available $Ca(OH)_2$ (10 g) was calcined at 600 °C for 3 h. Distilled H_2O (50 ml) was slowly added to the CaO. The resulting mixture was stirred for 2 h to make sure that CaO completely reacted with H_2O, then filtered, dried in oven, finally calcined at different temperature (200 °C ~ 800 °C) in static air for 2 h at the ramp of 10 °C min^{-1}.

4.2.1 Michael addition

The reactions were carried out in a standard round bottom glass flask equipped with a vertical condenser at room temperature under vigorous stirring. Reactions were

performed with 2 mmol of acceptor and 2 mmol of donor using 0.2 g of catalyst in 2 ml toluene or 5 ml acetonitrile at room temperature for the specified time.

4.2.2 Knoevenagel condensation

The reactions were carried out in a standard round bottom glass flask equipped with a vertical condenser at room temperature under N_2 atmosphere and vigorous stirring. Reactions were performed with 2 mmol of acceptor and 2 mmol of donor using 0.05 g of MgO catalyst in 2 ml DMF or 5 ml methanol at room temperature for the specified time.

Samples were taken periodically and injected off-line into a GC equipped with a DB-5 capillary column and an FID detector. The yield of product was compared with ^{1}H-NMR. The identification of the products was carried out using a Perkin-Elmer Turbomass GC-MS and ^{1}H-NMR.

4.3 Results and discussion

4.3.1 Results obtained for the Michael addition reaction

Figure 4.1 presents the variation of the conversion of the chalcone and diethyl malonate after 30 minutes of reaction, as a function of the calcination temperature. Calcination of the catalyst below 400 °C, leads to very low conversion. For calcination temperatures between 400-500 °C, the conversion reached maximum values. When the catalyst was calcined above 500 °C, the activity of MgO decreased with increasing calcination temperatures. For the MgO-ROH prepared from rehydrated $Mg(OH)_2$, the results are

consistent with changes in the surface area of the catalyst, which varies with calcination temperature, following a similar trend to the conversion (Figure 4.1). For the MgO-CBC prepared from $(MgCO_3)_4Mg(OH)_2$, the results are also consistent with changes in the surface area of the catalyst, except when the calcination temperature is 500 °C. The surface area of MgO-CBC at 500 °C is 206 $m^2 \cdot g^{-1}$, and 288 $m^2 \cdot g^{-1}$ at 450 °C. Although the surface area is different for the two calcination temperatures, the activity is similar. This implies that the surface area may not be the only factor which determines the activity of MgO-CBC. The calcination temperature may affect the activity of the number of active base sites and the strength of the basic sites, which requires further study of the structure of MgO-CBC.

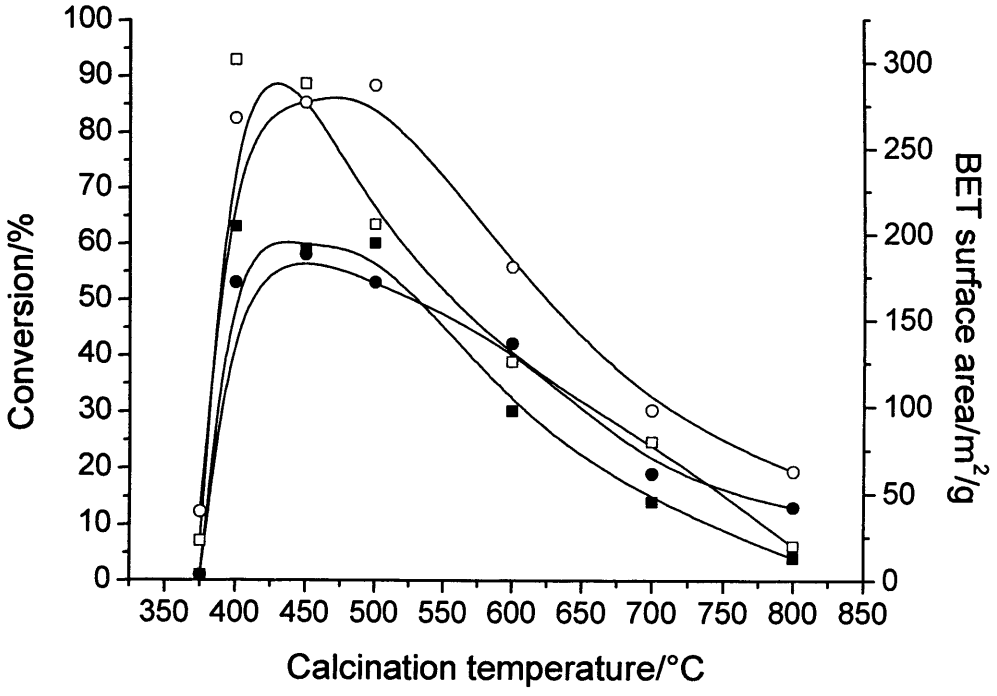

Figure 4.1 The effect of the calcination temperature on the activity of MgO for the Michael addition between chalcone and diethyl malonate, (■) $(MgCO_3)_4Mg(OH)_2$, (●) Rehydrated $Mg(OH)_2$; full symbols – conversion, open symbols – BET surface area.

Table 4.1 Michael additions catalysed by MgO catalyst

Entry	Acceptor	Donor	Solvent	Time (h)	Yields (%)
1	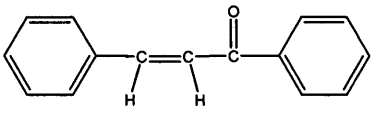	Diethyl malonate	Toluene	2	93
				2[a]	95
				2[b]	95
				48[c]	75
				6[d]	96
				8[e]	95
2	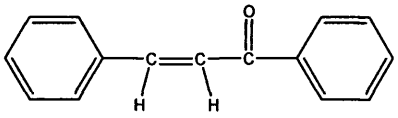	Ethyl cyanoacetate	Toluene	0.5	88
				~[e]	Complex mixtures
3	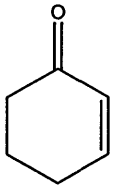	Dimethyl malonate	Toluene	1	93
				1[b]	90
4	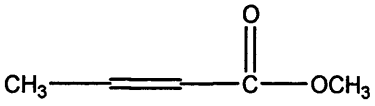	p-toluenethiol	Toluene	0.5	100
5	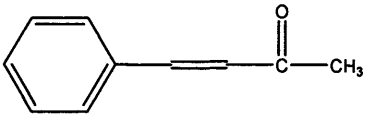	Malononitrile	Toluene	1	13
6	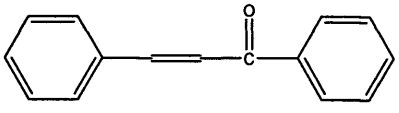	Malononitrile	Acetonitrile	1.5	88
				2[d]	88

[a] HDT-F[8], [b] HDT-^{t}BuO[6], [c] Using potassium tert-butoxide on xonotlite as catalyst[7], [d] HDT-OH[9], [e] $Ba(OH)_2 \cdot 1\text{-}1.5H_2O$[10].

Results of the Michael addition reactions are presented in Table 4.1. The conversion was calculated by the decrease in the amount of the α,β-unsaturated carbonyl compound. The MgO was found to be an efficient and selective catalyst for 1,4-addition to chalcone. The MgO was found to be more active compared with other catalysts reported in the literature such as HDT-F, HDT-^{t}BuO, HDT-OH, barium hydroxide and xonotlite, or in examples of similar activity, it was prepared using a much simpler procedure.

Table 4.2 Effect of the donor using chalcone as the acceptor

Entry	Donor	pKa[a]	Solvent	Time (h)	Yields (%)
1	p-toluenethiol	10.3	Toluene	0.5	17
2	2,4-pentanedione	13.3	Toluene	0.5 (36)	0 (0)
3	5,5-dimethyl-1,3-cyclohexanedione	11.2	DMSO	0.5 (21)	7 (90)
4	Ethyl acetoacetate	14.3	Toluene	0.5 (21)	0 (7)
5	Nitromethane	17.2	Toluene	0.5	7
6	Malononitrile	11.1	Acetonitrile	0.5	80
7	Ethyl cyanoacetate	13.1	Toluene	0.5	88
8	Diethyl malonate	16.4	Toluene	0.5	69

[a] in DMSO

The activity of the catalyst was obtained for a number of different donor species (Table 4.2). The results show that the Michael additions were not affected by the pKa value of the nucleophile. Theoretically, the lower the pKa value of the donor, the easier to abstract the proton and, therefore, form the carbanion and perhaps the Michael adduct.

Several structurally diverse nucleophiles such as malononitrile (Table 4.2, entry 5, pKa = 11.1), ethyl cyanoacetate (Table 4.2, entry 6, pKa = 13.1) and diethyl malonate (Table 4.2, entry 7, pKa = 16.4) underwent clean and remarkably fast Michael additions to chalcone by this procedure (Scheme 4.1). However, 2,4-pentanedione (Table 4.2, entry 2, pKa = 13.3) and ethyl acetoacetate (Table 4.2, entry 3, pKa = 14.3), which are more acidic than diethyl malonate did not undergo fast Michael addition. In the case of 2,4-pentanedione, no conversion was obtained after the reaction had been running for 36 h. This low activity can be ascribed to the formation of a *cis*-enol **2b** (Scheme 4.4).

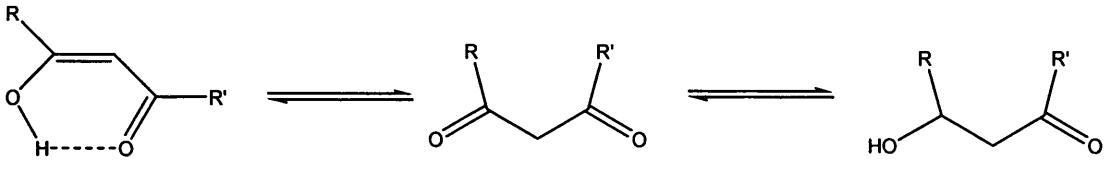

1b **1a** **1c**

Scheme 4.3

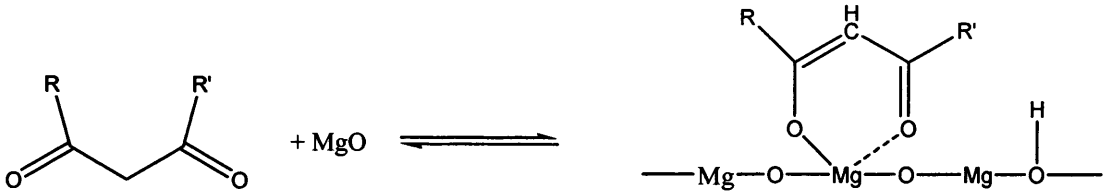

2a **2b**

Scheme 4.4

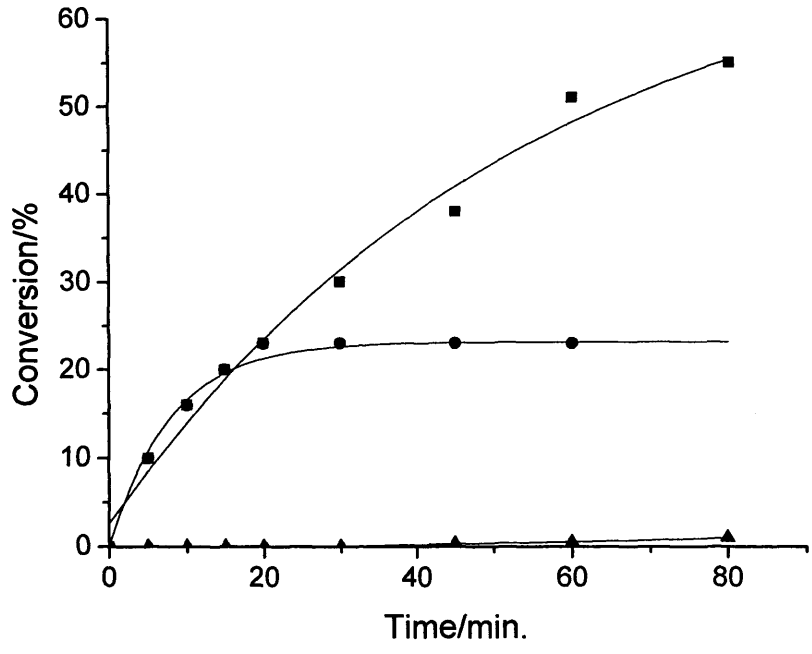

Figure 4.2 The effect of 2,4-pentanedione on the Michael addition between chalcone and Diethyl malonate. (■) no 2,4-pentanedione, (●) 2,4-pentanedione were added 10 minutes after running, (▲) 2,4-pentanedione were added 10 minutes before the addition of Diethyl malonate.

In general, 1,3-dicarbonyl compounds, which include β-diketones and β-keto-esters, may exist in three tautomeric forms: the diketo form **1a**, the *cis*-enolic form **1b**, and the *trans*-enolic form **1c** (Scheme 4.3).[11] Open-chain 1,3-dicarbonyl compounds are observed in the *trans*-enolic form only in rare cases. In solution, such compounds enolize practically exclusively to the *cis*-enolic form **1b**, which is stabilized by intra-molecular hydrogen bonding.

When MgO was added to the solution of 2,4-pentanedione, the new *cis*-enol **2b**, which is stabilized by the intra-molecular Mg-O bond, was presumably formed (Scheme 4.4).[12] This *cis*-enol is so strongly adsorbed onto the catalyst surface that the active site

is blocked and the activity stops. To confirm this, three reactions between diethyl malonate and chalcone were conducted as shown in Figure 4.2. For the reaction conducted without 2,4-pentanedione, the conversion increased steadily with time, however, when 2,4-pentanedione was added after running for 10min, the conversion stopped and if the 2,4-pentanedione was added before the reaction began, the reaction rate decreased dramatically.

In contrast, cyclic 1,3-dicarbonyl compounds, *e.g.* 5,5-dimethyl-1,3-cyclohexanedione **3a** (Scheme 4.5), can only exist as *trans*-enols **3b** (Scheme 4.5) and intra-molecular hydrogen bonding is not possible. When MgO was added in the solution of 5,5-dimethyl-1,3-cyclohexanedione, the *cis*-enol with an intra-molecular Mg-O bond is therefore impossible. As predicted, it was found that the product of Michael addition with 5,5-dimethyl-1,3-cyclohexanedione (Table 4.2, entry 3) can be obtained with high conversion. The activity of nitromethane can be ascribed to the nitro ⇔ *aci-* nitro tautomerism[13] and low pKa value (Table 4.2, entry 5).

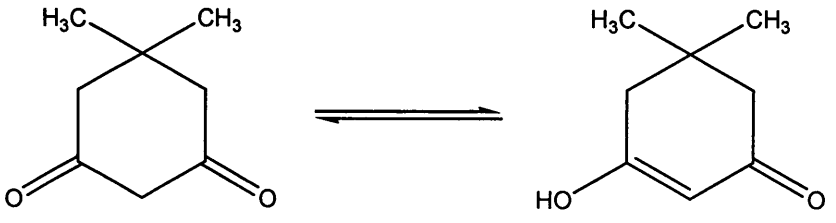

3a **3b**

Scheme 4.5

When methyl crotonate was used as acceptor, high conversion was obtained only with *p*-toluenethiol (Table 4.3). Compared with chalcone, the charge of methyl crotonate at the β-postion is less positive. Since the same MgO catalyst and reaction conditions were used for these reactions, the proton-abstracting ability of the MgO did not change.

Therefore, it can be proposed that proton abstraction is not the crucial step, hence, the lower electrophilicity of the acceptor crotonate is probably the key factor preventing reaction.

Table 4.3 Effect of the donor with methyl crotonate as the acceptor[a]

Entry	Donor	pKa[b]	Time (h)	Yields (%)
1	p-toluenethiol	10.3	0.5	44
2	2,4-pentanedione	13.3	0.5	0
3	Ethyl acetoacetate	14.2	0.5	0
4	Nitromethane	17.2	0.5	0
5	Malononitrile	11.1	0.5	0
6	Ethyl cyanoacetate	13.1	0.5	0
7	Dimethyl malonate	16.4	0.5	0
8	Methanol	29	0.5	0

[a] Reactions were performed in 10 ml of solvent.

[b] in DMSO

One of the most important parameters for the success of the planned reaction is the selection of a suitable solvent (Table 4.4). When chloroform or methanol was used as solvent, the MgO was inactive but high conversion could be obtained using hexane as solvent. Chloroform is an aprotic and acidic solvent with high electrophilicity. It tends to coordinate strongly with anions, and consequently the attack of an anion onto α,β-unsaturated carbonyl compounds was blocked. Methanol is an acid and protic solvent, which stabilizes both anions and cations. Hexane is non-polar, essentially non-solvating, does not undergo auto-ionization and plays a minimal role in the reaction. However, the solubility of the product in hexane is low, which may enhance the reaction rate.

Table 4.4 Solvent effects for the Michael addition[a]

Acceptor	Donor	Solvent	pKa	Polarity	Time (h)	Yields (%)
Chalcone	Diethyl malonate	Chloroform		4.1	2	no
		Methanol	16	5.1	2	low
		Ethyl acetate	25	4.4	2	50
		Acetonitrile	25	5.8	2	50
		Toluene	40	2.4	2	66
		Hexane	48	0	2	80
		DMSO	30	7.2	2	8

[a] Reactions were performed in 10 ml of solvent.

Ethyl acetate, acetonitrile and toluene are aprotic and basic solvents, which tend to coordinate strongly with cations. This should result in an increased basicity of the solid base, MgO. In the case of toluene high conversions can be obtained and although the highest conversions were obtained with hexane, toluene was selected as the solvent for the Michael additions because of the toxicity of hexane.

In addition, the volume of the solvent used in the reaction affected the activity of the MgO. For the Michael additions between chalcone and diethyl malonate, 1 ml toluene per mmol of reactant gave rise to 93% conversion in 2 h, while 66% conversion was obtained for 5 ml toluene per mmol of reactant. This may point to the reaction rate being affected by the reactant concentration.

We also attempted to reuse the catalyst by a variety of methods (Table 4.5). Direct reuse of the catalyst (Table 4.5, entry 2) led to a greater than 50% decrease in activity

while the treatments indicated also resulted in lower conversions (Table 4.5, entry 3,4). This phenomenon probably arose because the reactant and product were not completely

desorbed from the MgO and therefore, the active sites were blocked. However, we found that by washing MgO with toluene and then refluxing in water before calcinations, the catalyst could be recovered and reactivated (Table 4.5, entry 5). The activity and surface area for the freshly prepared and the reused catalyst are almost the same. It should be noted that the catalytic activity also decreased when the calcined catalyst was allowed to stand in air for a few hours before use, but such a loss of activity was not observed when the catalyst was stored in a dessicator over molecular sieves for one month.

Table 4.5 Michael addition between chalcone and diethyl malonate using fresh MgO and reused MgO

Entry	Catalyst	S_{BET} (m^2/g)	Time (min)	Yields (%)
1	MgO (1st use)	288	30	54
2	MgO[a] (2nd use)	~	30	25
3	MgO[b] (2nd use)	239	30	34
4	MgO[c] (2nd use)	165	30	32
5	MgO[d] (2nd use)	287	30	50

[a] MgO was washed 3 times with toluene. The MgO was separated from toluene by centrifugation.

[b] MgO was washed with toluene before calcination.

[c] MgO was refluxed in toluene, filtered, washed with toluene and dried at 110°C. The MgO was then refluxed in water before calcination.

[d] MgO was washed with toluene, then refluxed in water before calcination.

In order to study the effect of water in the solvent, three reactions were carried out. One reaction was carried out in a dry solvent (CH_3CN) and the other two in a solvent with 2% H_2O and 2% D_2O added respectively. Figure 4.3 shows that the effect of both H_2O and D_2O had on the reaction causing the rate to decrease initially; however, neither influence the overall yield of the reaction. Considering that the content of water in common solvents is less than 0.3%, for these reactions with MgO as catalyst solvents can be used directly without drying.

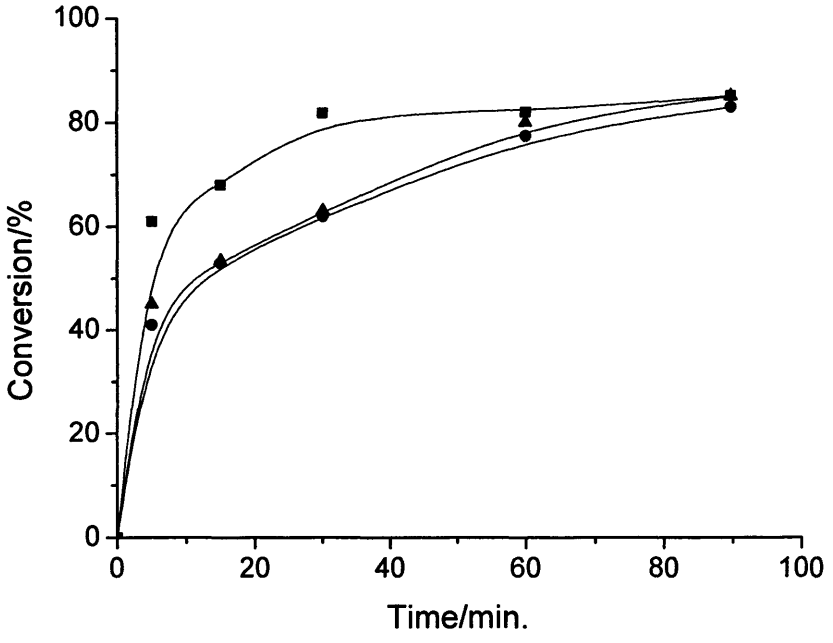

Figure 4.3 The effect of H_2O on the reaction between chalcone and malononitrile. (■) dry conditions, (▲) 0.2 ml H_2O added to the reaction mixture, (●) 0.2 ml D_2O added to the reaction mixture.

NMR and MS showed that D_2O did not exchange proton with malononitrile, but did so with the reactant chalcone and product. It can be deduced that the Michael addition is an irreversible process, otherwise some of the malononitrile protons would have exchanged with the deuterium from D_2O.

Since hydrogen of H_2O is replaceed by its isotope deuterium, the kinetic isotope effect deserved to be considered. The kinetic isotope effect is a variation in the reaction rate of a chemical reaction when an atom in one of the reactants is replaced by one of its isotopes. An isotopic substitution will greatly modify the reaction rate when the isotopic replacement is in a chemical bond that is broken or formed. In such a case, the rate change is termed a primary isotope effect. When the substitution is not involved in the bond that is breaking or forming, one may still observe a smaller rate change, termed a secondary isotope effect. In this study, the substitution of hydrogen for deuterium does not change reaction rate (Figure 4.3). The conversion in the presence of H_2O is similar to that in D_2O. The main reason may be that H_2O is not the reactant of the Michael addition.

4.3.2 Results obtained for the Knoevenagel condensation reaction

Knoevenagel condensations involving aromatic carbonyl compounds with (a) malononitrile and (b) ethyl cyanoacetate (Scheme 4.2) as the active methylene compound were carried out at room temperature with MgO as catalyst and the results are reported in Table 4.6. The aromatic aldehydes readily condensed with malononitrile, while with ethyl cyanoacetate, the reaction was slightly slower. This may be attributed to the fact that abstraction of a proton from the active methylene group of ethyl cyanoacetate was relatively more difficult due to its lower acidity. As can be seen from Table 4.6, all reactions proceeded selectively to the dehydrated products without

any side reactions. The rate of reaction is high and was generally equal or better than those reported in the literature (Table 4.7).

Table 4.6 The Knoevenagel condensation of aldehydes with ethyl cyanoacetate and malononitrile.

Entry	R 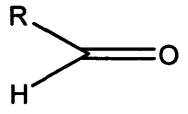	R' 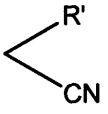	Solvent	Time (min)	Conversions (%)	Selectivity (%)
1	Ph	CN	methanol	30 5	100 94	100
2	Ph	CO_2Et	DMF	30	97	100
3	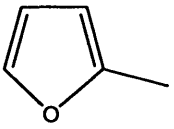	CN	DMF	30	100	100
4	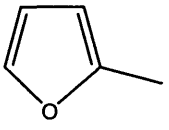	CO_2Et	DMF	30	99.9	100
5	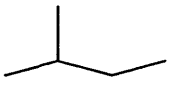	CN	DMF	60	99	100
6	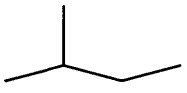	CO_2Et	DMF	60	80	100
7		CN	DMF	30	88	100
8	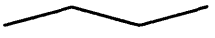	CO_2Et	DMF	30	76	100
9	$-cC_5H_{10}-$	CN	DMF	60	97	100
10	$-cC_5H_{10}-$	CO_2Et	DMF	60	23	100
11	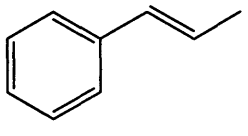	CN	DMF	120	50	57
12	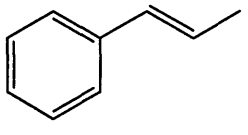	CO_2Et	DMF	60	50	57

Table 4.7 Comparison yields of MgO with different heterogeneous catalysts for the Knoevenagel condensation between benzaldehyde and malononitrile.

Catalyst	Catalyst amount (g)	Reaction condition	Time (min)	Conversions (%)	Yields (%)
MgO (this work)	**0.05**	**r.t., 2mmol, 1.5ml methanol**	**5 30**	**94 100**	
MgO[a] [14]	4	r.t., 10mmol	5		94
HDT[b] [15]	5 wt%	60°C	60	54	
MgO[b] [15]	5 wt%	60°C	60	62	
NiAl HTc[b] [16]	0.05	60°C	30		97
HDT-OH [17]	0.05	r.t., 2mmol, 10ml toluene	60		100
HDT-^{t}Bu [6]	0.05	r.t., 2mmol, 10ml DMF	10		99
HDT-F [8]	0.035	r.t., 1mmol, 5ml DMF	15		100
Zeolite [17]	50 wt%	r.t., 1:1.3, MeCN	720		78
Resin [18]	0.1	r.t., 10mmol, 5ml benzene	300		92
KF/Al_2O_3 [19]			150		80
FAP/BTEAC/water [b 20]	1.25	r.t., 1.5 mmol:2 mmol	4		98
$ZnCl_2$ [b 21]	0.136	100°C, 10mmol	10		91
Aminosilica [22]	0.25	r.t., 20mmol, 25ml solvent	240		99
$AlPO_4/Al_2O_3$ [b 23]	1.5	r.t., 10mmol	15		80
$Na_2Ca_2P_2O_7$ [24]	0.04	r.t., 1.5mmol, 1.6ml CH_3OH	7		94
Xenotlite[b] [7]	0.1	r.t., 10mmol	1440		81

[a] Commercially available MgO.

[b] Reaction carried out in the absence of solvent.

An attempt was made to check the reusability of the catalyst in the following manner. The reaction was performed as usual for 30 minutes, then the stirring was stopped and the reaction mixture was put in a centrifuge for 10 minutes. After the supernatant was separated from the catalyst, DMF was added and the mixture stirred, centrifuged, and separated a second time. Fresh reactants and solvent were added to the residual catalyst and the reaction performed under identical conditions as before. As can be seen in Table 4.8, the activity and selectivity of the catalyst was found to be almost the same. The washing and relocation may result in some loss of catalyst, which probably explains why the conversion using the recovered MgO was slightly lower than in the case of fresh MgO.

The Knoevenagel condensation produces a large amount of water as a by-product. When one molar reactant reacted, one molar of water will be produced. However the reaction rate is very quick in the presence of MgO (Table 4.6). Furthermore, MgO catalyst can be reused. Therefore, water does not appear to affect the activity of the prepared MgO catalysts during the studied Knoevenagel condensation.

Table 4.8 The Knoevenagel condensation between benzaldehyde and ethyl cyanoacetate with fresh MgO and reused MgO

Catalyst	Time (min)	Conversions (%)	Selectivity (%)
MgO (1st use)	30	94	100
MgO (2nd use)	30	90	100

Methanol is a good solvent for the reaction between benzaldehyde and malononitrile (Table 4.9, entry 1). However, for the reaction between benzaldehyde and with ethyl

cyanoacetate, MgO show no activity when methanol is the solvent; in contrast DMF is found to be a good solvent with a high yield obtained after only 30 minutes.

Table 4.9 The effect of solvent on the Knoevenagel condensation reaction

Entry	R	R'	Solvent	Catalyst amount	Time (min)	Conversion (%)	Selectivity (%)
1	Ph	CN	Methanol (1.6ml)	0.05g	30	100	100
2	Ph	CO_2Et	DMF (1.6ml)	0.05g,	30	94	100
			DMF (5ml)	0.05	30	77	100
				0	30	30	66
			DMF (10ml)	0.05	30	69	100
			Toluene (1.6ml)	0.05g	30	17	100
				0.2g	30	60	
			Toluene (10ml)	0.05	30	0	
			Methanol (1.6ml)	0.05	30	0	

Solvent volumes again affected the activity of MgO. When 0.8 ml of toluene per mmol of reactant was used, it gave 17% conversion in 30 minutes, while no conversion was observed when 5 ml of toluene per mmol of reactant was employed. Similar results were obtained when DMF was used as solvent, with 0.8 ml of DMF per mmol of reactant resulting in higher conversion than when 5 ml of DMF per mmol of reactant was used. We can conclude that the higher the concentration of substrate, the higher the reaction rate. It should also be noted that the selectivity to the adduct of the

Knoevenagel condensation (Table 4.9, entry 2) was almost 100% in the presence of MgO, but only 66% in the absence of MgO.

Table 4.10 The effect of the donor on the Knoevenagel condensation with benzaldehyde

Entry	Donor	pKa[a]	Time (h)	Conversions (%)
1	2,4-pentanedione	13.3	0.5	0
2	Ethyl acetoacetate	14.2	0.5	0
3	Nitromethane	17.2	0.5	0
4	Malononitrile	11.1	0.5	100
5	Ethyl cyanoacetate	13.1	0.5	97
6	Dimethyl malonate	16.4	0.5	0

[a] in DMSO

Of the seven substrates tested, only malononitrile and ethyl cyanoacetate resulted in high conversion (Table 4.10) and the other substrates gave rise to no Knoevenagel condensation product. The formation of enol forms can explain the lack of reactivity of 2,4-pentanedione and ethyl acetoacetate, whereas the activity of nitromethane can be ascribed to nitro ⇔ *aci*-nitro tautomerism[13] and its low pKa value.

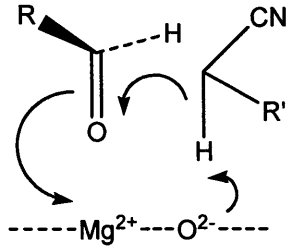

Knoevenagel condensation

Scheme 4.6

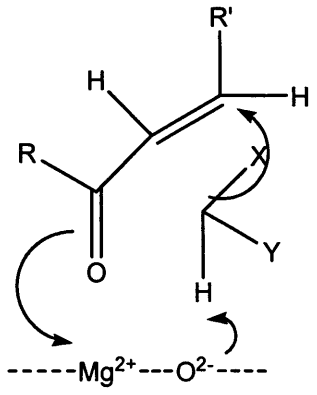

Michael addition

Scheme 4.7

The effect of the donor on the reaction may be used to determine the reaction mechanism. Scheme 4.6 has been proposed by Moison[14] as the mechanism for the Knoevenagel condensation. The mechanism for the Michael addition (Scheme 4.7) based on what that generally accepted. The intermediate (Scheme 4.6 and 4.7) can be confirmed by the effect of the enol form. The formation of the intermediate needs the interaction between acid sites (Mg^{2+}) and acceptor, the conjugated basic sites and anion formed from methylene compounds. The formation of *cis*-enols between the open-chain 1,3-dicarbonyl compounds and the Mg^{2+} active site stops the attack of acceptor on the Mg^{2+} active site, thus formation of intermediate.

4.4 Activity of CaO

To determine the influence of the calcination temperature on the catalytic activity of the CaO samples, $Ca(OH)_2$ was calcined at different temperatures between 100 °C and 600 °C and then tested as a catalyst for the reaction of chalcone and diethyl malonate. Figure 4.4 shows the conversion after 30 min reaction as a function of the calcination temperature. These results show that CaO calcined at 400 °C was the most active catalyst. When the calcination temperature was >400 °C, conversion decreased with increasing the calcinations temeperature.

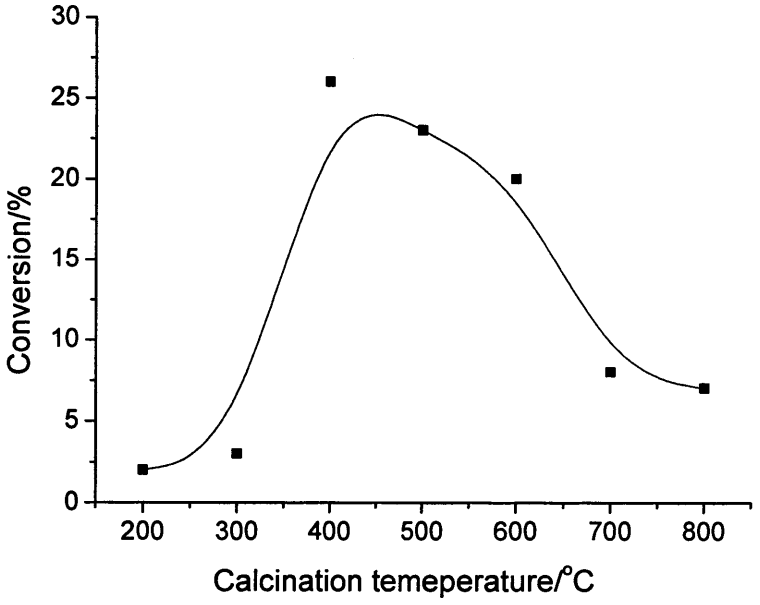

Figure 4.4 Effect of the calcination temperature on the activity of catalyst CaO for the Michael addition between chalcone and dimethyl malonate; ruuning time: 30min.

TGA shows the temperatures at which the $Ca(OH)_2$ precursors decompose when heated in a controlled environment (Figure 4.5). Water is removed from the precursors between 350 ~ 460 °C. The thermal pre-treatment resulted in a change in the XRD pattern, caused by the removal of H_2O from the starting material (Figure 4.6). The

diffraction patterns of the samples heated at temperatures < 400 °C were different from that of CaO, while samples activated at temperature > 400 °C displayed diffraction reflections characteristic of CaO, which became, as expected, more crystalline with increasing calcination temperature.

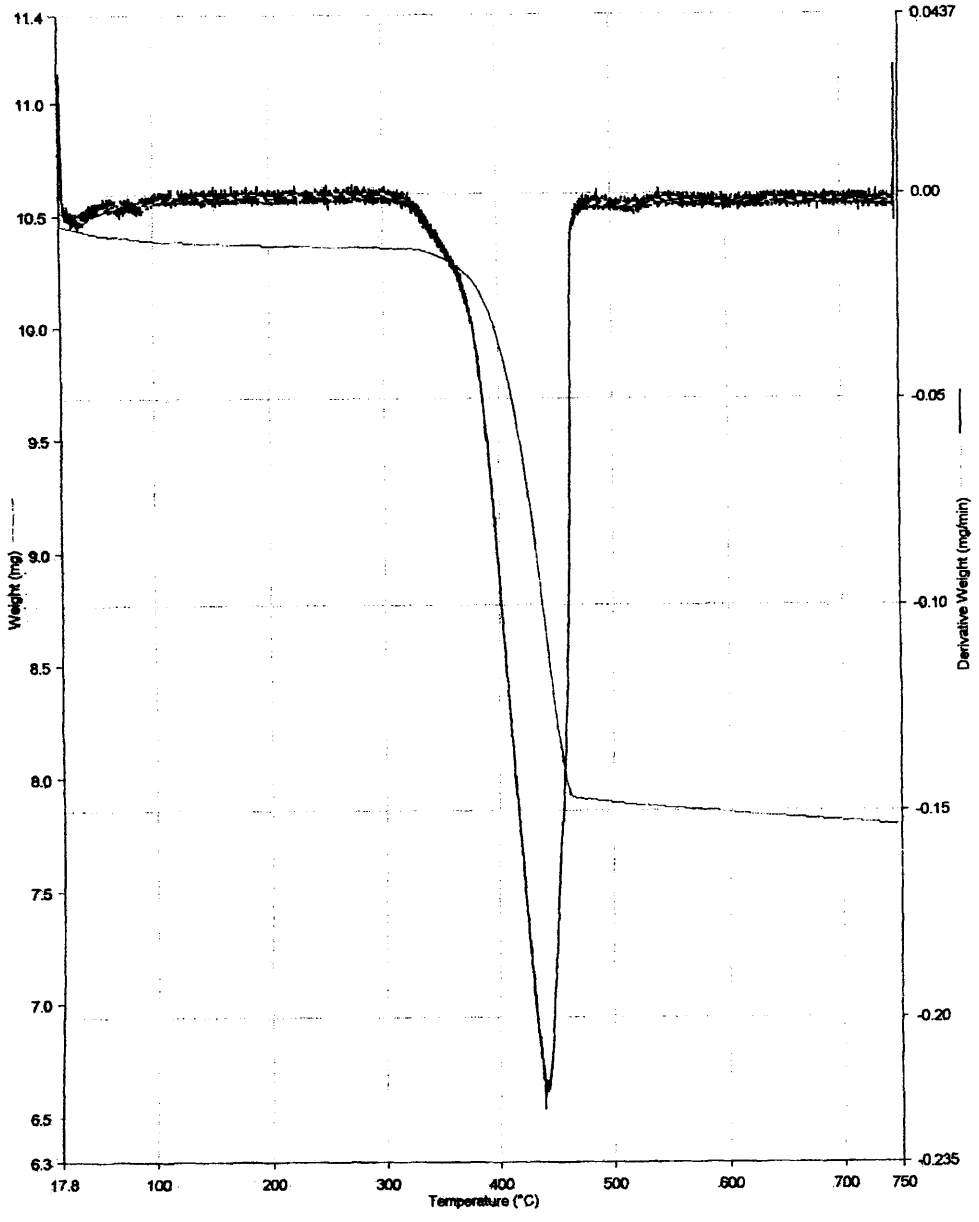

Figure 4.5 TGA and DTG curves of $Ca(OH)_2$.

The changes observed in the XRD patterns (Figures 4.6) coincided with a change in the catalytic activity (Figure 4.4). Calcinations < 400 °C did not lead to the formation of CaO, and, consequently, the catalytic activity was very low. The best catalytic performance was obtained for calcination temperatures at 400 °C, when the XRD patterns showed a poorly crystalline CaO together with a little higher surface area and pore radius than CaO materials calcined at higher temperature (Figure 4.4 and 4.6 and Table 4.11). The increase in calcination temperature led to a decrease in catalyst activity as the CaO became more crystalline and the BET surface area and pore radius decreased. It is clear that the crystallite size, surface area and pore radius, plays a key role in determining the catalytic activity, as the highest activity of the catalyst was obtained when the surface area of the catalyst and pore radius was at a maximum.

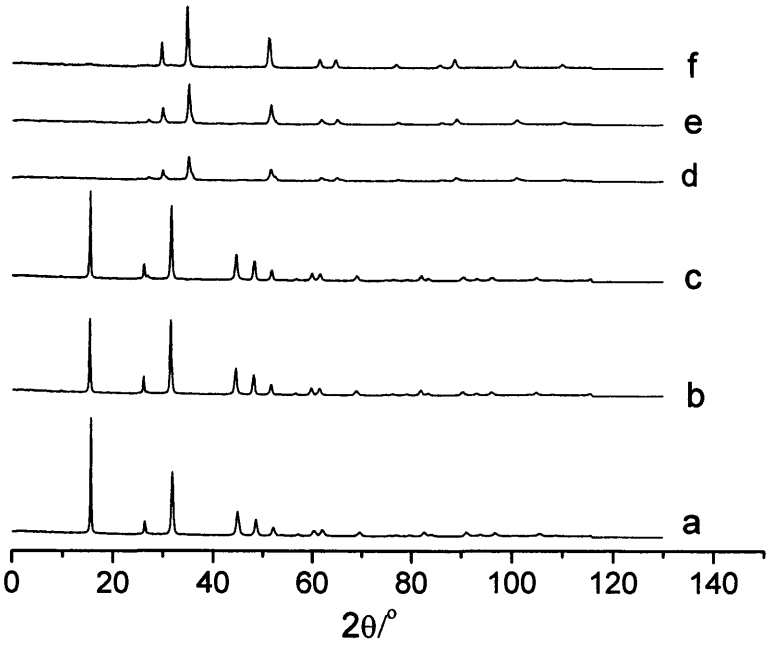

Figure 4.6 The powder X-ray diffraction patterns of materials obtained by calcinning $Ca(OH)_2$ at different temperatures; (a) 100 °C, (b) 200 °C, (c) 300 °C, (d) 400 °C, (e) 500 °C, (f) 600 °C.

Table 4.11 Textural properties of the CaO prepared from rehydration $Ca(OH)_2$

Calcination temperature	S_{BET} (m^2/g)	V_a (cm^3/g)[a]	r_p (Å)[b]
300 °C	24	0.0429	52
400 °C	45	0.0955	52
500 °C	34	0.073	52
600 °C	35	0.0661	52
700 °C	26	0.0411	52
800 °C	21	0.0303	12

[a] Pore volume, [b] Mean pore radius

The activity of CaO was compared with MgO for the Michael addition between chalcone and diethyl malonate (Table 4.12). The conversion of reaction in the presence of CaO was half of that MgO when same weight of catalyst (0.2 g) was used. With the consideration of CaO which has lower surface area and larger molar molecular weight than MgO, the activity of same surface area (0.28 g) and molar CaO (0.67 g) was determined. When the catalyst amount of CaO increased from 0.2 g to 0.67g, the conversion did not improved. This implies that the reaction rate was under diffusion control when the catalyst amount was above 0.2 g. Since the activity of same surface area (0.28 g) and molar CaO (0.67 g) to MgO is less than that of MgO, MgO was more active than CaO.

Table 4.12 Comparison of activity between MgO and CaO for the Michael addition of Chalcone and Diethyl malonate

Catalyst	Amount(g)	S_{BET} (m^2/g)	Conversion (%)
MgO	0.2	288	50
	0.2	45	26
CaO	0.28[a]		
	0.67[b]		

[a] Same mole with MgO, [b] Same surface area with MgO

4.5 Conclusions

A simple preparation method for MgO producing a catalyst that exhibits a high activity for base catalysed reactions is described. The experimental results showed that an optimal calcination temperature in the range 400~500 °C gives poorly crystalline, high surface area MgO that can be regenerated by washing and then reused. The catalytic activity of the MgO for both Michael additions and Knoevenagel condensation was found to compare favorably with previous studies using more complicated and expensive catalysts. Indeed, the simplicity of the preparation and the ease of reactivation after use may offer sufficient compensation to make MgO the base catalyst of choice even if slightly better yields can be obtained with alternative catalysts. It was found that the activity of MgO did not increase with the acidity of all the substrates, in contrast to many homogeneous systems. The enol formation and solvent affect the activity of MgO. The activity of MgO was compared with CaO. It was found that MgO show higher activity than CaO.

References

1. H. Hattori, *J. Jpn. Pet. Inst.*, 2004, **47**, 67.
2. G. Jones, *Org. React.*, Vol. 15; Wiley: New York, 1967.
3. E.D. Bergman, D. Ginsburg, R. Pappo, In: R. Adams, A.H. Blatt, V. Boekelheide, A.C. Cope, D.Y. Curtis, F.C. Mcgrew, C. Niemann (Eds.), *Org. React.*, Vol. 10, Wiley: New York, 1959, 179.
4. H. Pines, M. Stalick, *Base-Catalyzed Reactions of Hydrocarbons and Related Compounds*, Academic Press: New York, 1977, 234.
5. F. Figueras, *Topics Catal.*, 2004, **29**, 189.
6. B.M. Choudary, M.L. Kantam, B. Kavita, Ch.V. Reddy, and F. Figueras,

Tetrahedron, 2000, **56**, 9357.

7. S. Chalais, P. Laszlo, and A. Mathy, *Tetrahedron Lett.*, 1985, **26**, 4453.
8. B.M. Choudary, M.L. Kantam, V. Neeraja, K.K. Rao, F. Figueras, and L. Delmotte, *Green Chem.*, 2001, **3**, 257.
9. B.M. Choudary, M.L. Kantam, Ch.V. Reddy, K.K. Rao, and F. Figueras, *J. Mol. Catal. A* , 1999, **146**, 279.
10. A. Gacia-Raso, J. Garcia-Raso, B. Campaner, R. Mestres, and J.V. Sinisterra, *Synthesis*, 1982, 1037.
11. C. Reichardt, *Solvent Effects in Organic Chemistry*; Verlag Chemie: Weinheim, New York, 1979, 61.
12. M.D. Brown, W.J. Nelson, R.J. Turner, and D.G. Walmsley, *J. Chem. Soc., Faraday Trans. 2*, 1981, **77**, 337.
13. K. Lammertsma, and B. V. Prasad, *J. Am. Chem. Soc.*, 1993, **115**, 2348.
14. H. Moison, F. Texier-Boullet, and A. Foucaud, *Tetrahedron*, 1987, **43**, 537.
15. M.J. Climent, A. Corma, S. Iborra, A. Velty, *J. Mol. Catal. A*, 2002, **182-183**, 327.
16. U. Costantino, M. Curini, F. Montanari, M. Nocchetti, O. Rosati, *J. Mol. Catal. A*, 2003, **195**, 245.
17. T. I. Reddy, R.S. Varma, *Tetrahedron Lett.*, 1997, **38**, 1721.
18. T. I. Reddy, R.S. Varma, *Tetrahedron Lett.*, 1997, **38**, 1721.
19. T. Saito, H. Gato, K. Honda, T. Fujii, *Tetrahedron Lett.*, 1992, **33**, 7535.
20. J. Yamawaki, T. Kawate, T. Ando, T. Hanafusa, *Bull. Chem. Soc. Jpn.*, 1983, **56**, 1885.
21. S. Sebti, R. Nazih, T. Tahir, L. Salhi, A. Saber, *Appl. Catal. A: General*, 2000, **197**, L187.

22. P.S. Rao, R.V. Venkataratnan, *Tetrahedron Lett.*, 1991, **32**, 5821.

23. D.J. Macquarrie, JH. Clark, A. Lambert, J.E.G. Mdoe, A. Priest, *React. Funct. Polym.*, 1997, **35**, 153.

24. J. Bennazha, M. Zahouily, S. Sebti, A. Boukhari, E.M. Holt, *Catal. Commun.*, 2001, **2**, 101

Chapter 5

Synthesis of β-keto-1,3-dithianes in the Presence of MgO

5.1 Introduction

β-keto-1,3-dithianes **2** are highly functionalized three-carbon units which are of much importance as potentially useful synthetic intermediates.[1] For example, the 1,3-dithiane substituent may, if desired, be hydrolyzed to a carbonyl group or converted into a methylene group by reductive desulfurization.[2] Alkylation with this three-carbon unit has also been utilized in several syntheses.[3]

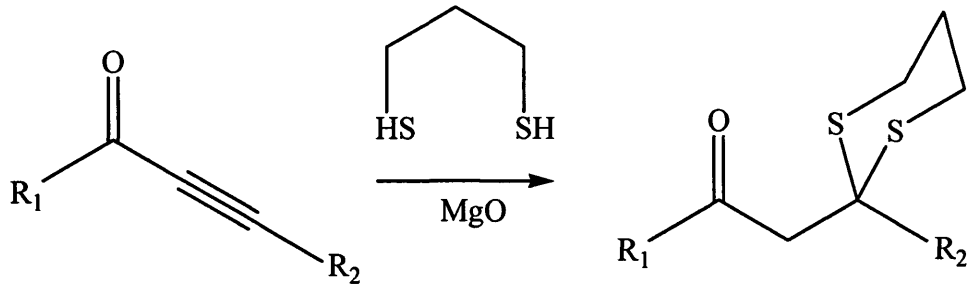

1 **2**

a) R_1 = Me; R_2 = Ph
b) R_1 = Ph; R_2 = Ph
c) R_1 = H; R_2 = C_5H_{11}
d) R_1 = Me; R_2 = $SiMe_3$
e) R_1 = Me; R_2 = H
f) R_1 = EtO; R_2 = H
g) R_1 = MeO; R_2 = H
h) R_1 = EtO; R_2 = Me
i) R_1 = MeO; R_2 = Ph

Scheme 5.1

There are a number of methods available for the generation of β-keto-1,3-dithianes **2**. Procedures reported for the preparation of these compounds include α-alkylation of carbonyl compounds with 1,3-dithiane or its derivatives,[2,4] nucleophilic addition of 1,3-dithiane to epoxides followed by oxidation,[3] conjugate reduction of α-oxo ketene dithio

acetals,[5] and double Michael addition of 1,3-propanedithiol to α, β-acetylenic ketones **1** (Scheme 5.1).[6] However, their synthesis is homogeneous and in most cases complicated; certainly, most of the existing procedures are not especially environmentally friendly.

In recent years, there has been increasing emphasis on the use and design of environmentally friendly solid acid and base catalysts to reduce the amount of toxic waste and by-products arising from chemical processes prompted by stringent environmental protection laws.[7] Hence, reusable heterogeneous catalysts will have a distinct advantage if they can match the performance of homogeneous catalysts.

However, to date, there is only one report about synthesising β-keto-1,3-dithianes **2** by Michael additions through the use of heterogeneous catalysts,[8] in which alumina was used as a solid basic catalyst. The alumina was readily reused; however, a large amount of alumina (7 equivalents) was used. There has been no other report of using a heterogeneous basic catalyst to synthesis β-keto-1,3-dithianes **2**. Magnesium oxide (MgO) is a typical basic oxide (Hammet constant $H_- = +26.0$)[9] and has the lowest solubility among the alkaline earth oxides (MgO, BaO, CaO and SrO) and so can potentially be reused as it will not be lost due to leaching into the reaction mixture. Furthermore, MgO is inexpensive and easily obtained so that it could be applied in large scale manufacture. In view of our success in using MgO as a basic catalyst in both Knoevenagel and especially Michael additions, it appeared that this catalyst might be useful for triggering the "double" Michael addition of 1,3-dithianes to propargylic carbonyl systems to give β-keto-1,3-dithianes **2**. In this chapter, the synthesis of β-keto-

1,3-dithianes **2** was studied with this inexpensive and easily obtained heterogeneous base catalyst (Scheme 5.1).

5.2 Experimental section

The catalysts used in this study were obtained by calcination of the precursors at 450 °C in static air for 2 hours (see Table 5.3 for precursor details), except MgO-AD and MgO-RIB. MgO-AD was the commercially available MgO from Aldrich. MgO-RIB was obtained by igniting Mg ribbon in air. The heating ramp used in all cases was 10 °C/min.

MgO (2.5 equiv. or 1.0 equiv.) was added in one portion to a stirred solution of a propargylic carbonyl compound (1 mmol) and propane-1,3-dithiol (1 mmol) in THF (2 ml) at 0 °C (ice-water was used for cooling to avoid a rise in temperature). The cooling bath was then removed and the mixture stirred at ambient temperature. In order to follow the progress of the reaction, samples (about 0.5 ml) were withdrawn from the reactor at specified times by syringe. Then the needle connected to the syringe was removed and substituted by a syringe- driven filter. The catalyst was separated from the sample by pushing the solution through the syringe driven filter. The filtrate was divided into two parts. One part was directly injected into GC or GC-MS. The other part was evaporated and the residue analysed by ^{1}H-NMR and ^{13}C-NMR using $CDCl_3$ as solvent. The conversion and selectivity were determined by this combination of GC and ^{1}H-NMR data. In this chapter, the GC program used was: column temperature was from 60 °C holding 2 min. to 250 °C holding 10 min with ramp (10 °C/min) and 1ml/min flow rate of carrier gas. Injection temperature was at 250 °C.

5.3 Results and Discussion

A series of substrates have been tested using MgO as the catalyst. After reaction, the solution was filtered to remove the catalyst and solvent was evaporated. No further purification was performed. The results (Table 5.1) showed that MgO is a very active catalyst for the synthesis of β-keto-1,3-dithianes. Substrates (**1a-g**) underwent clean additions with propane-1,3-dithiol by this procedure to give the corresponding β-keto-1,3-dithiane derivatives. The experimental procedure is very simple. The reactions are fast, and the conversions and selectivities are good.

Ley *et al.* proposed the mechanism for the double conjugate addition of dithiols to propargylic carbonyl systems to generate β-keto-1,3-dithianes **2** in the presence of NaOMe. Based on the reference and our result, one mechanism was suggested for this reaction in the presence of MgO (Scheme 5.2). Addition of a dithiol into the ynone initially involves mono-deprotonation followed by addition to the ynone **1** (Scheme 5.1). After proton transfer occurs, both *cis* and *trans* isomers **4** of the α,β-unsaturated carbonyl intermediate are formed from the allenic-enolate intermediate **3**. The α,β-unsaturated carbonyl **4** are themselves substrates for a second conjugate addition, now an intramolecular reaction, which gives the desired β-keto-1,3-dithianes **2** (path a). However, this second addition competes with the reaction of substrate **5** with another molecules of ynone to give dimeric side products **8** (path b), which are observed in some cases.

Very little amount of α,β-unsaturated carbonyl **4** was found in the ^{1}H NMR spectrum of **2f** and **2g** (Figure A5.16 and A5.20), which support the mechanism proposed (Scheme 5.2). However, the reactions with **1a-e** as substrates were so completed that no

α,β-unsaturated carbonyl **4** was found. This suggested that esters **1f** ethyl propiolate and **1g** methyl propiolate were less active than carbonyls **1a-e**.

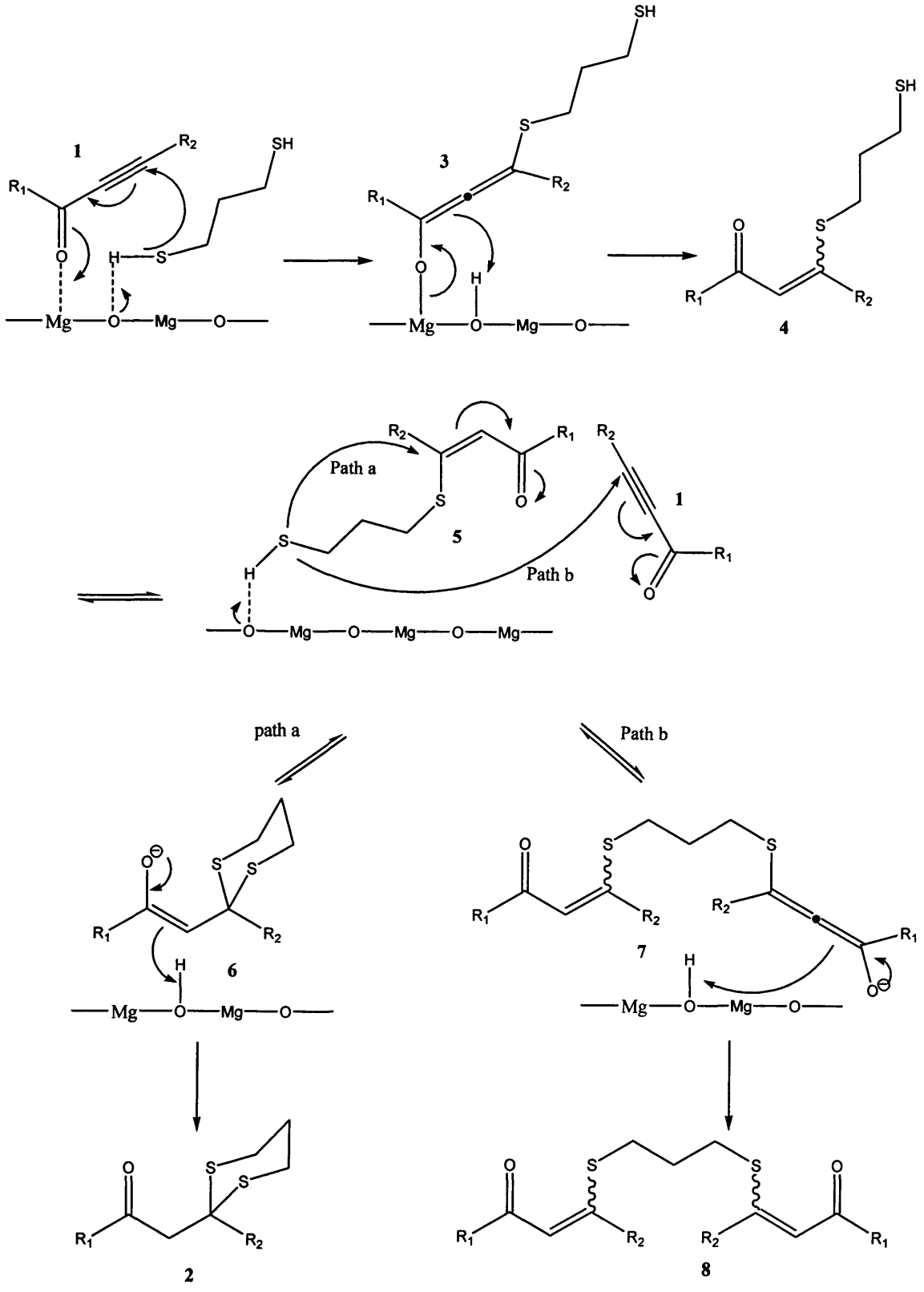

Scheme 5.2 Proposed mechanism for the formation of β-keto-1,3-dithianes.

Table 5.1 Synthesis of β-Keto-1,3-dithianes **2** in the presence of MgO-CBC

Entry	Substrate	Time (h)	Catalyst	Product	Yield (%)
1	**1a** 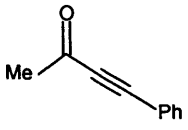	0.5 *24*	MgO (1.0 equiv.) *NaOMe (1.3 equiv)*	**2a** 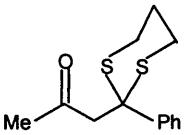 Ref. 6,10	98 *82* [a]
2	**1b** 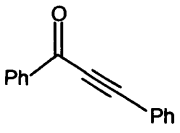	1	MgO	**2b** 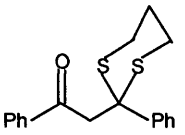 Ref. 11	90[b]
3	**1c** 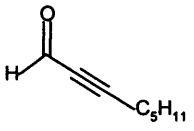	3	MgO	**2c** 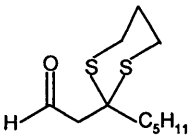 Ref. 12	98
4	**1d** 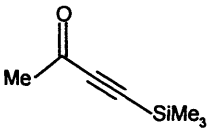	1	MgO	**2d** 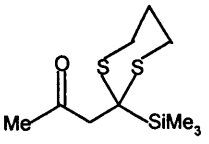	95
5	**1e** 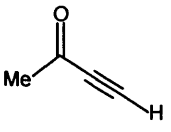	16		**2e** 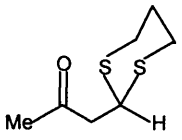 Ref. 4a	90[b]
6	**1f** 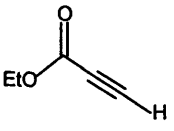	4 *4*	MgO *NaOMe (1.3 equiv)*	**2f** 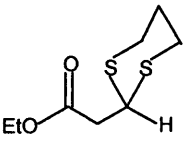 Ref. 6,10	95 *84* [a]
7	**1g** 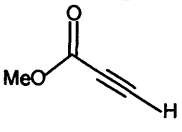	2	MgO	**2g** 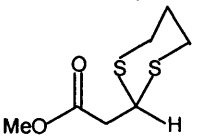 Ref. 13	85

"Ref" refers to papers in which are recorded full characterisation data for this compound, all of which matches those found in the present work.

[a] *Reference 6;*

[b] *base on ^1H NMR data and weight.*

Both substrates **1f** ethyl propiolate and **1g** methyl propiolate have the group RO connected to C=O and **1a-e** do not. Two other substrates **1h** ethyl-2-butynoate and **1i** methyl phenylpropiolate, with the group RO, were tested and resulted in low yields (Table 5.2). Yields of 60~70% were obtained with **1h** ethyl-2-butynoate as substrate, and 30% yield for **1i** methyl phenylpropiolate. The by-products for these two substrates were the dimeric side products **8**.[10] An increased production of side products can be explained by the structural differences of the substrates. The major structure difference of **1h** ethyl-2-butynoate and **1i** methyl phenylpropiolate from **1f** ethyl propiolate and **1g** methyl propiolate is that R^2 was Me or Ph for **1h** and**1i**, H for both **1f** and **1g**. Me or Ph results in more steric hindrance than H, which makes it difficult for the α,β-unsaturated carbonyl **5** to undergo an intra-molecular reaction. This gives the desired β-keto-1,3-dithianes **2** (Scheme 5.2, path a); However, for the substrate **5** to react with another molecule of ynoate to give dimeric side products **8** (Scheme 5.2, path b) is more favourable.

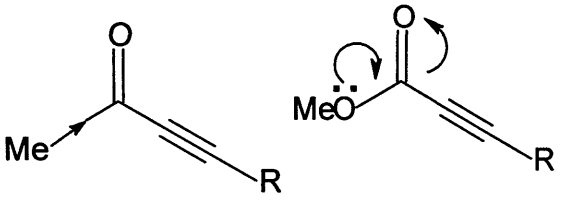

Scheme 5.3

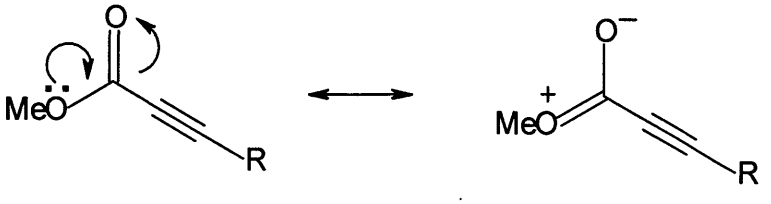

Scheme 5.4

In summary, it is clear that the ynones are more reactive than the corresponding esters, the ynoates. Me has a slight positive inductive effect, which slightly reduces the electron withdrawing power of carbonyl (Scheme 5.3). In the case of MeO, stronger resonance (+ve mesomeric) can occur, which causes a much greater reduction in electron withdrawal by the C=O. Therefore, the reaction rate is slower and there is therefore, more opportunity for other reactions to occur (Scheme 5.4).

Table 5.2 Dithiol additions to **1h** and **1i** in the presence of MgO-CBC

Entry	Substrate	Time (h)	Catalyst	Product	Yield [a] (%)
1	**1h** 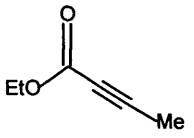	4	MgO	**2h** 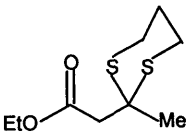 Ref. 14~16	60~70
2	**1i** 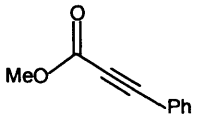	4	MgO	**2i** 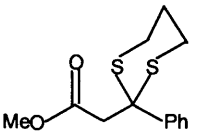 Ref. 17	30

"Ref" refers to papers in which are recorded full characterisation data for this compound, all of which matches those found in the present work.
[a] base on ^1H NMR data and weight.

Table 5.3 Dithiol additions to 4-phenyl-3-butyn-2-one **1a** in the presence of MgO (1.0 equiv.) for 1h

Entry	Precursors	S_{BET} (m^2 g^{-1})	Yield (%)
MgO-RIB	Mg ribbon	10	20
MgO-AD	MgO (Aldrich)	25	0
MgO-CAD	MgO (Aldrich)	25	66
MgO-COH	$Mg(OH)_2$ (Fluka)	65	98
MgO-ROH	$Mg(OH)_2$ (Fluka) calcined at 600 °C for 2h, reflux in H_2O for 3h, then dried in oven.	277	98
MgO-CBC	$(MgCO_3)_4Mg(OH)_2$ (Fluka)	288	98
MgO-OX	MgC_2O_4	312	98
MgO-CC	$MgCO_3$ (Acros Organics)	229	98

The activity of MgO is higher or comparable with that of the previously published homogeneous base catalyst NaOMe (Table 5.1, entry 1).[6] When **1a** was tested as substrate and MgO as the catalyst, 98% yield was reached in 0.5 h, while for the homogeneous base catalyst NaOMe, 24 h were needed to obtain these high yields

although this time may not have been optimised. Furthermore, as far as the catalyst amount is concerned, MgO catalyst amount (1.0 equiv.) is less than that of the homogeneous base catalyst NaOMe (2.5 equiv.). For **1f** as substrate (Table 5.1, entry 6), the reaction rate was quicker when MgO was used as catalyst than the homogeneous base catalyst NaOMe.

However, a stoichiometric equivalent amount of MgO was used for the studied reactions. The amount of MgO is so high that we can not formally assign the term catalyst. Therefore, the amount of MgO needs to be optimized to ensure that the reaction can proceed catalytically.

The effect of the MgO preparation method was also investigated (Table 5.3). MgO-COH, MgO-ROH, MgO-CBC, MgO-OX and MgO-CC were active in the reaction studied. When 2.5 equivalents of MgO were used, all the types of MgO, except MgO-RIB and MgO-AD, can catalyze the reaction to 98% yield within 1h. When 1.0 equivalent MgO was used, MgO-RIB, MgO-AD and MgO-CAD were less active than the others. The low activity of MgO-RIB and MgO-AD may be attributed to the fact that these two catalysts were not degassed before testing. The conversion increased from 0 to 66% when MgO-AD was transformed to MgO-CAD.

5.4 Conclusions

This is the first report of synthesising β-keto-1,3-dithianes **2** by Michael additions through the use of heterogeneous basic catalyst MgO. It was proved that the activity of MgO is higher than the previously published homogeneous catalyst NaOMe in some reactions.

References

1. (a) R.D. Norcross and I. Paterson, *Chem. Rev.*, 1995, **95**, 2041; (b) E.J. Corey and D. Seebach, *Angew. Chem. Int. Ed. Engl.*, 1965, **4**, 1075.
2. I. Paterson and L.G. Price, *Tetrahedron Lett.*, 1981, **22**, 2829.
3. D. Stossel and T.H. Chan, *J. Org. Chem.*, 1988, **53**, 4901.
4. (a) E.C. Taylor and J.L. LaMattina, *Tetrahedron Lett.*, 1977, 2077; (b) K. Hatanaka, S. Tanimoto, T. Sugimoto and M. Okano, *Tetrahedron Lett.*, 1981, **22**, 3243.
5. (a) R. B. Gammill, D. M. Sobieray, and P. M. Gold, *J. Org. Chem.*, 1981, **46**, 3555. (b) B. Choi, I.K. Youn and C.S. Pak, *Synthesis*, 1988, 792.
6. M.J. Gaunt, H.F. Sneddon, P.R. Hewitt, P. Orsini, D.F. Hook and S.V. Ley, *Org. Biomol. Chem.*, 2003, **1**, 15.
7. F. Figueras, *Topics Catal.* 2004, **29**, 189.
8. B.C. Ranu, S.Bhar and R. Chakraborti, *J. Org. Chem.*, 1992, **57**, 7349.
9. A. Gervasini, A. Auroux, *J. Catal.*, 1991, **131**, 190.
10. H. Sneddon, A. Heuvel, A. Hirsch, R. Booth, D. Shaw, M. Gaunt and S. V. Ley, *J. Org. Chem.*, 2006, **71**, 2715.
11. E. Diez, A. Lopez, C. Pareja, E. Martin, R. Fernandez and J. Lassaletta, *Tetrahedron Lett.*, 1998, **39**, 7955.
12. W. Woessner and R. Ellison, *Tetrahedron Lett.*, 1972, 3735.
13. E. Taylor and J. LaMattina, *J. Org. Chem.*, 1978, **43**, 1200.
14. M. Zahouily, A. Mezdar, J. Rakik, A. Elmakssoudi, A. Rayadh and S. Sebti, *J. Mol. Catal. A: Chem.*, 2005, **233**, 43.
15. H. Yu, Q. Liu, Y. Yin, Q. Fang, J. Zhang and D. Dong, *Synlett*, 2004, 999.

16. K. Cheung, S. Coles, M. Hursthouse, N. Johnson, P. Shoolingin-Jordan, *Angew. Chem. Int. Ed. Engl.*, 2002, **41**, 1198.

17. I. Stahl, R. Manske and J. Gosselck, *Chemische Berichte*, 1980, **113**, 800.

Chapter 6

Transesterification of vegetable oil to biodiesel with MgO as catalyst

6.1 Introduction

Since traditional fossil fuel resources are limited and greenhouse gas emissions are becoming a greater concern, research is now being directed towards the use of alternative renewable fuels that are capable of fulfilling an increasing energy demand.[1] Vegetable oils are a renewable and potentially inexhaustible source of energy with an energetic content close to diesel fuel. The use of vegetable oils as alternative fuels has been around for 100 years when Rudolph Diesel, the inventor of the diesel engine, first tested peanut oil in his compression ignition engine.[2] However, due to cheap petroleum products, such non-conventional fuels never took off. With recent increases in petroleum prices and uncertainties concerning petroleum availability, there is renewed interest in vegetable oil fuels for diesel engines. The use of vegetable oils as an alternative renewable fuel competing with petroleum was proposed in the beginning of 1980s.[3]

Although vegetable oils occupy a prominent position in the development of alternative fuels, there have been many problems associated with using it directly in a diesel engine. Two of the problems are the high viscosity (about 11-17 times higher than diesel fuel) and lower volatilities of vegetable oils, which causes the formation of deposits in engines due to incomplete combustion and incorrect vaporization

characteristics. Different ways have been considered to reduce the high viscosity of vegetable oils:

- Dilution of 25 parts of vegetable oil with 75 parts of diesel fuel,
- Microemulsions with short chain alcohols such as ethanol or methanol,
- Thermal decomposition, which produces alkanes, alkenes, carboxylic acids and aromatic compounds,
- Catalytic cracking, which produces alkanes, cycloalkanes and alkylbenzenes, and
- Transesterification with methanol or ethanol.

Among the many ways and procedures to convert vegetable oil into a diesel-like fuel, transesterification process was found to be the most viable oil modification process.[4] This is an attractive alternative (or extender) to petrodiesel fuel due to well-known advantages:[5] (i) lower dependence on foreign crude oil, (ii) renewable resource, (iii) limitation on greenhouse gas emissions because of the closed CO_2 cycle, (iv) lower combustion emission profile (especially SOx),[6] (v) potential improvement of rural economies, (vi) biodegradability, (vii) use without engine modifications, (viii) good engine performance, (ix) improved combustion because of its oxygen content, (x) low toxicity, and finally (xi) ability to be blended in any proportion with regular petroleum-based diesel fuel.

Vegetable oils and animal fats are comprised of complex mixtures of triglycerides and other minor components, such as free fatty acids (FFAs), gums, waxes, etc. Triglycerides are esters of glycerol with three chains of aliphatic or olefinic FFAs of variable length (12-24 carbons). Triglycerides must be converted to simple esters to achieve desirable flow properties and combustion characteristics for use in diesel

engines.[7] Biodiesel has been produced by transesterification of triglyceride (VOs) to methyl esters with methanol in the presence of catalysts as illustrated by reaction scheme 6.1. In transesterification, the triglyceride in vegetable oil reacts with an alcohol to form a mixture of glycerol and fatty acid esters, called biodiesel. Complete conversion of the triglyceride involves three consecutive reactions with monoglyceride and diglyceride intermediates (Scheme 6.2). There are different processes that can be applied to synthesize biodiesel: (i) base-catalyzed transesterification,[8] (ii) acid-catalyzed transesterification,[9] (iii) integrated acid-catalyzed pre-esterification of FFAs and base-catalyzed transterification,[10] (iv) enzyme-catalyzed transesterification,[11] (v) pyrolysis,[3] and (vi) supercritical alcohol transesterification.[12] At present, the most common way to produce biodiesel is to transesterify triglyceride in vegetable oil or animal fats with an alcohol in the presence of an alkali or acid catalyst.[13]

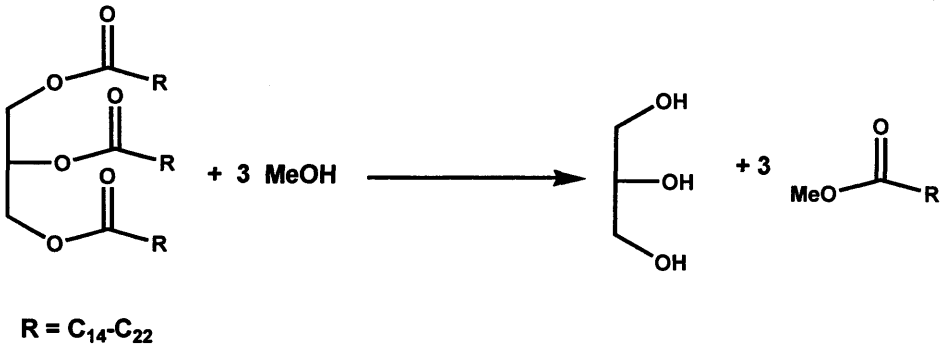

Scheme 6.1

Triglyceride + MeOH $\rightleftharpoons$ Diglyceride + MeOOR

Diglyceride + MeOH $\rightleftharpoons$ Monoglyceride + MeOOR

Monoglyceride + MeOH $\rightleftharpoons$ Glycerol + MeOOR

Scheme 6.2

Conventional synthesis techniques rely on homogeneous catalysts. Base catalysis is preferred to acid catalysed routes using sulphuric or sulfonic acids, which are more corrosive with lower activities.[14] Potassium hydroxide, sodium hydroxide, and their carbonates, as well as sodium alkoxides such as $NaOCH_3$, are usually used as homogeneous basic catalysts for this reaction.[15-17] However removal of these catalysts is technically difficult and brings extra cost to the final product. The production of diesel from vegetable oil calls for an efficient solid catalyst to make the process fully ecologically friendly.

Commercial homogeneous base-catalyzed transesterification of vegetable oil with methanol was conducted at 60 °C and ambient pressure with a molar ratio of methanol to triglyceride of 6:1 (this corresponds to two alcohols per ester group). Peterson *et al.* has made attempts to use heterogeneous catalysts for the transesterification reactions, which were conducted under the same reaction conditions to the homogeneous catalysed system.[18] In most of the experiments, the reaction proceeded at a relatively slow rate. Due to the presence of heterogeneous catalysts, the reaction mixture constitutes a three-phase system, oil-methanol-catalyst, which for diffusion reasons inhibits the reaction. Nevertheless, the use of heterogeneous catalysts simplifies greatly the technological process by facilitating the separation of the catalyst from the post reaction mixture.

Efforts have been made to try and improve the mutual oil-methanol solubility for the synthesis of biodiesel. Co-solvents, such as THF as well as hexane, can increase the mutual oil-methanol solubility, and hence, the activity of the catalyst.[19-20] Methanol-oil ratio and reaction temperature are two variables that affect the activity of heterogeneous

basic catalysts. Suppes *et al.* achieved conversion of 78% at 240 °C and >95% at 260 °C using calcium carbonate as a catalyst.[21] At a high methanol to oil ratio of 275 and 22h of reaction time at methanol reflux, the cesium-exchanged NaX faujasites gave a conversion of 70%, whereas 34% conversion was obtained by using hydrotalcite.[22] In addition to the above catalysts, several other heterogeneous base catalysts have been developed to catalyze the tranesterification of vegetable oils to prepare biodiesel, including alkali earth metal catalysts such as MgO,[22-24] $Ba(OH)_2$,[19] CaO[19,25] as well as $Ca(OH)_2$,[19] zeolites,[22,26] a zinc aluminium mixed oxide,[27] Na/NaOH/γ-Al_2O_3[20] and KF/ZnO.[28]

Magnesium oxide (MgO) is a typical basic oxide (Hammett constant, $H_- = +26.0$)[29] and is inexpensive and easily obtained. In view of this, we consider that MgO has the potential to be a reusable catalyst, and can be readily applied in large scale manufacture. In this chapter, the effect of preparation and reaction conditions, including: the methanol to oil ratio, the reaction temperature and the amount of catalyst, on the activity of MgO was studied for the transesterification of vegetable oil. The reuse of MgO was also studied. The results show that MgO made in a simple way can be an active catalyst (Table 6.1, entry 11).

6.2 Experimental

6.2.1 Catalyst preparation

The catalysts prepared in Cardiff were obtained via the calcination of the commercially available precursors $(MgCO_3)_4 \cdot Mg(OH)_2$, $Mg(OH)_2$ (Fluka) and hydrotalcite in static air

at different temperatures for 2 hours (see Chapter 2 for further details). The heating ramp used in all cases was 10 °C/min.

The catalysts prepared by Johnson Matthey were obtained via the calcination of the commercially available precursor $(MgCO_3)_4 \cdot Mg(OH)_2$ (Alfa Aesar) in a flow of N_2 at different temperatures for 2 hours. The heating ramp used in all cases was 4°C/min.

6.2.2 Transesterification reaction

6.2.2.1 Reaction performed at 60 °C

The reactions are carried out in a standard round bottomed glass flask equipped with a vertical condenser at 60 °C under vigorous stirring. Typical reactions were performed with 1ml of vegetable oil (100% rapeseed oil; Fluka or Lidl) and 10ml of methanol (molar ratio of methanol to vegetable oil of 250:1) using 0.06 g of catalyst (Calcination temperature 450 °C) at 60 °C for the specified time.

The reaction products were analysed using the following procedure. The samples are separated from catalyst by syringe filters and the methanol removed using a vacuum pump. The obtained product is added to deuterated chloroform for ^{1}H-NMR[30] since the by-product glycerol is immiscible with chloroform and does not interfere with the detection of biodiesel.

6.2.2.2 Reaction performed at 200 °C at Johnson Matthey

The autoclave is loaded with 220 g (0.250 moles) of rapeseed oil (ex-Cargill) and 49 g (1.5 moles) of dry methanol. To this is added 10 g catalyst. The autoclave is then sealed and purged three times with nitrogen gas, after this the vessel is left with a 10 bar pressure and the stirrer set to approximately 300 rpm.

The temperature is set to 200 °C and the time taken as zero when the temperature reaches 200 °C. The heating rate is 5 °C/min. In total the reaction run for 15 minutes after which time the heat is turned off. The reactor is cooled down to room temperature by a water bath. It takes about 20 min to make the reactor temperature below 100 °C, and 1h to room temperature.

The resulting product consisted of two layers that are separated in a separating funnel and the lower (glycerol) layer discarded. The biodiesel product layer is diluted to exactly 500 ml in a volumetric flask with HPLC grade THF and then 10 ml of this solution was pipetted and then diluted to 100ml in a second volumetric flask.

Three filtered and undiluted samples from this second flask were analysed by HPLC.

6.2.2.3 Reaction performed at 200 °C in Cardiff University

The autoclave is loaded with 27.3 g (0.03 moles) of rape seed oil and 7.3 ml (0.18 moles) of methanol. To this is added 1.33 g catalyst. The autoclave is then sealed and purged three times with Helium gas, after this the vessel is left with a 10 bar or 50 bar internal pressure and the stirrer set to approximately 1000 rpm.

The temperature is set to 200 °C and time is taken as zero once the temperature reached 200 °C. The heating rate is 5 °C/min. In total the reaction ran for 15 minutes after which time the heating is turned off and the autoclave quickly cools in an ice water bath.

The reaction products are analysed using the following procedure. The samples are separated from catalyst and glycerol by centrifuge. The glycerol could be separated because it is insoluble in the esters and has a much higher density. Then methanol is removed using a vacuum pump and the obtained product added to deuterated chloroform for ^{1}H-NMR to determine the yield to methyl ester. The degree of transesterification achieved is calculated by comparison with reference samples.[33]

6.2.3 Analytical monitoring of biodiesel production

Various analytical methods have been developed for analyzing mixtures containing fatty acid esters and mono-, di-, and tri-glycerides obtained by the transesterification of vegetable oils, such as TLC,[34] GC,[35] HPLC,[36] GPC,[37] ^{1}H NMR[33] and NIR[38]. In this study, ^{1}H NMR and HPLC have been used to analyse the transesterification reactions. HPLC is calibrated by referral to standard samples and provides more accurate results than NMR.

6.2.3.1 ^{1}H NMR analysis[33]

The signal due to methylene protons adjacent to the ester group in triglycerides appears at 2.3 ppm and after reaction the methoxy protons of the methyl esters appear at 3.7 ppm (Figure 6.1, 6.2, 6.3 and 6.4). Gelbard *et al.* have reported a method using the

areas of the signals of methylene and methoxy protons to monitor the yield of transesterification.

A simple equation is given by the authors:

$$\text{Yield} = \left(\frac{2A_{ME}}{3A_{CH_2}}\right) \times 100\%$$

Where A_{ME}, is the area of the signal corresponding to the protons of the methyl esters (the strong singlet); and A_{CH_2}, is the area of the signal corresponding to the protons of the methylene protons. The factors 2 and 3 are derived from the fact that the methylene carbon possesses two protons and the alcohol (methanol derived) carbon has three attached protons.

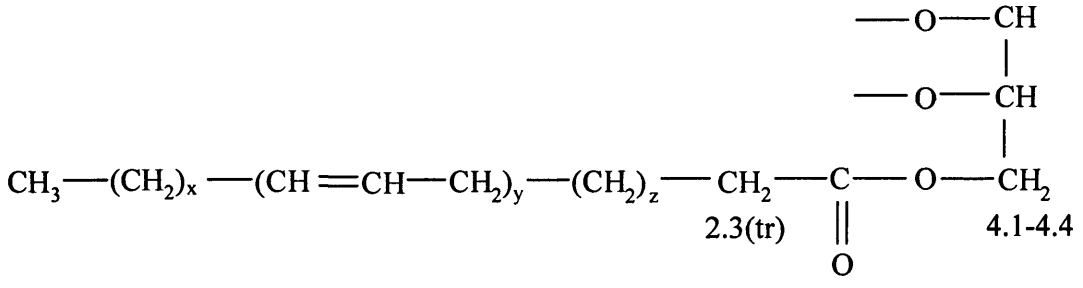

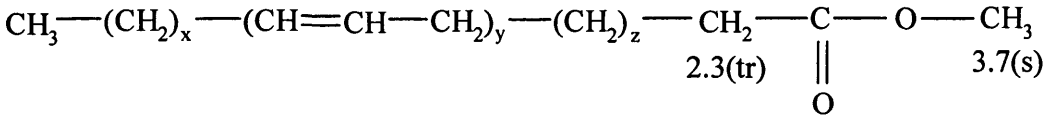

Figure 6.1 Assignment of chemical shifts of protons in transesterification reactions.

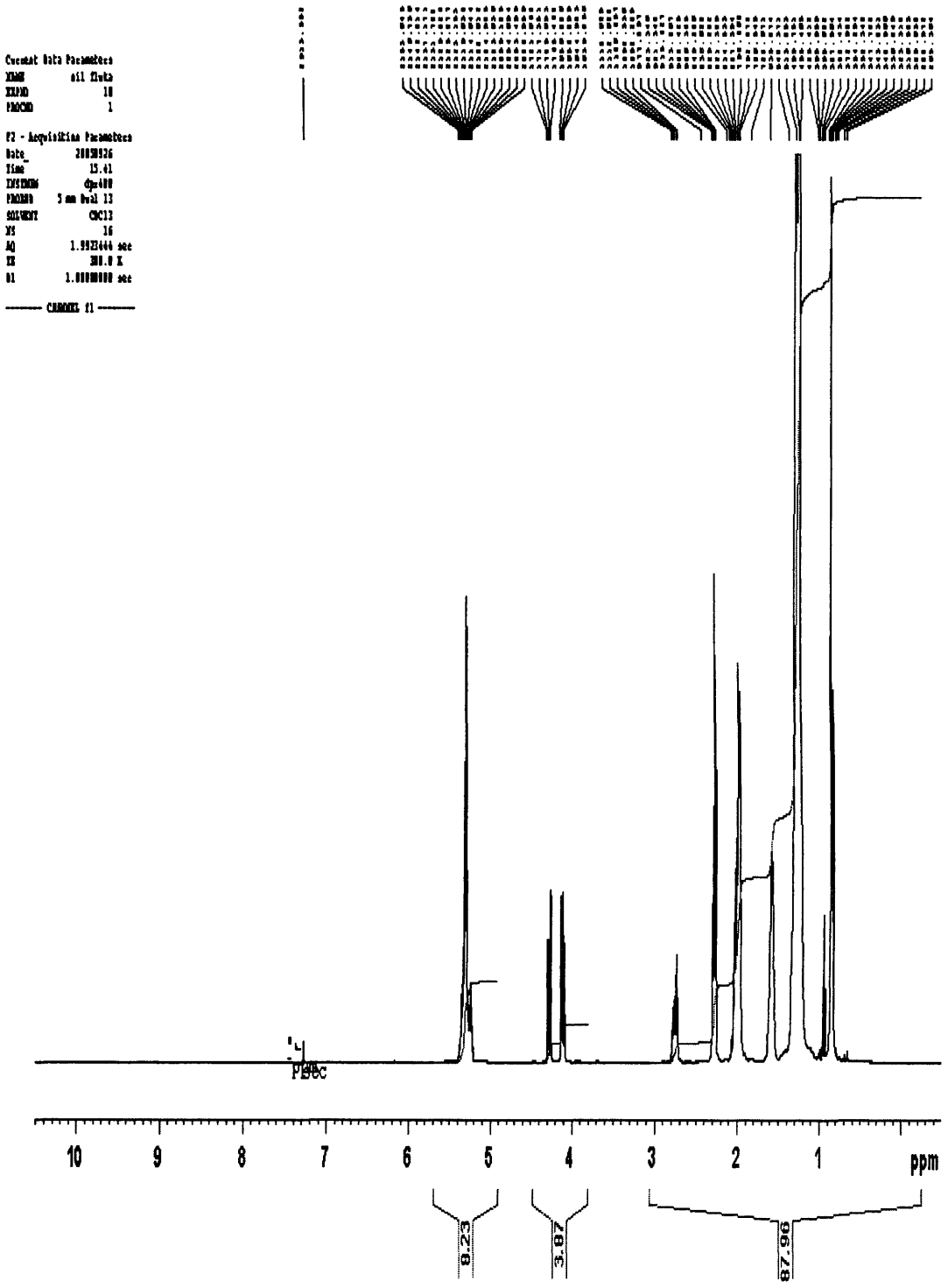

Figure 6.2 ^{1}H NMR of pure vegetable oil (tri-glyceride).

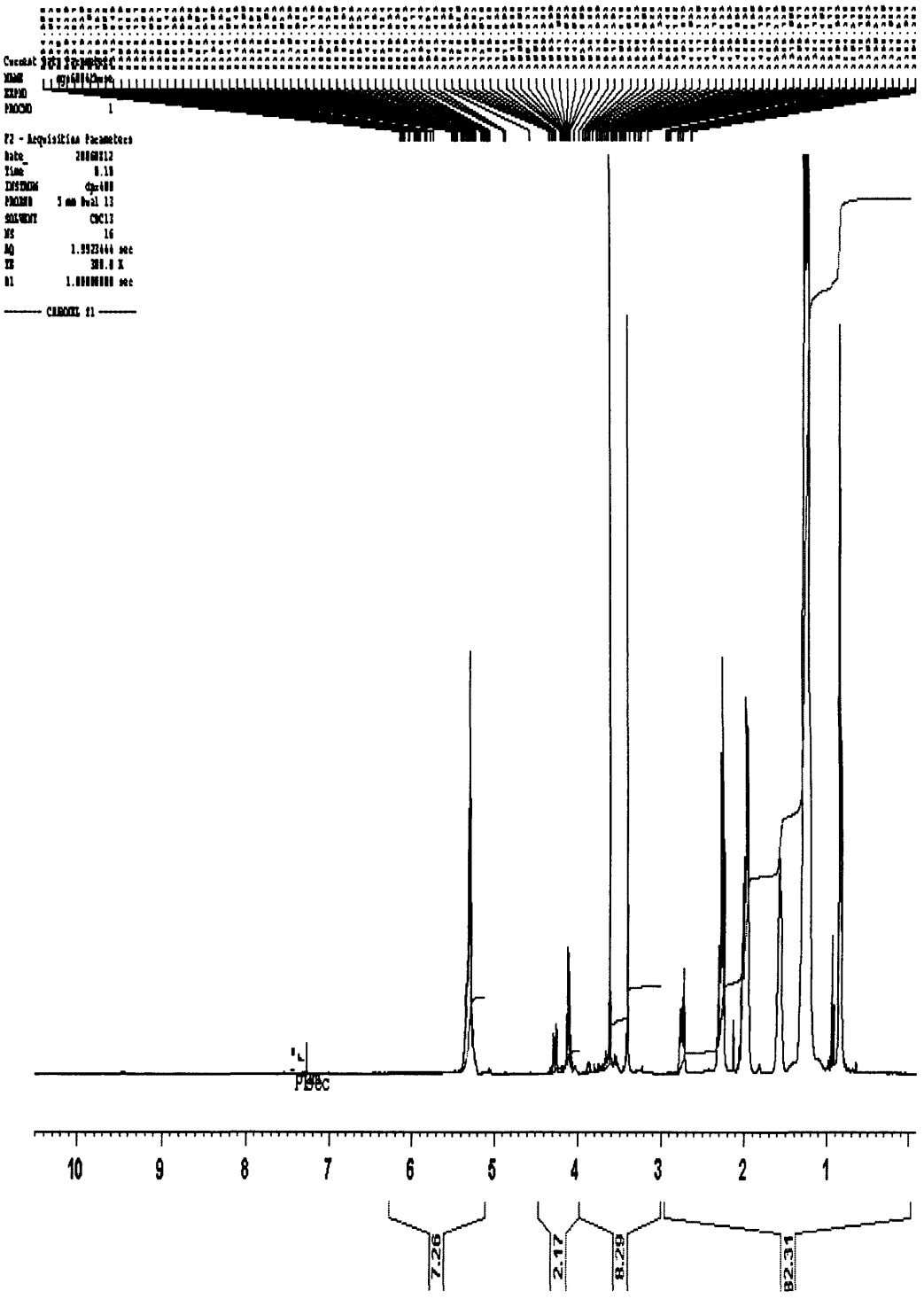

Figure 6.3 ^{1}H NMR of mixture of fatty acid esters and mono-, di-, and tri-glycerides.

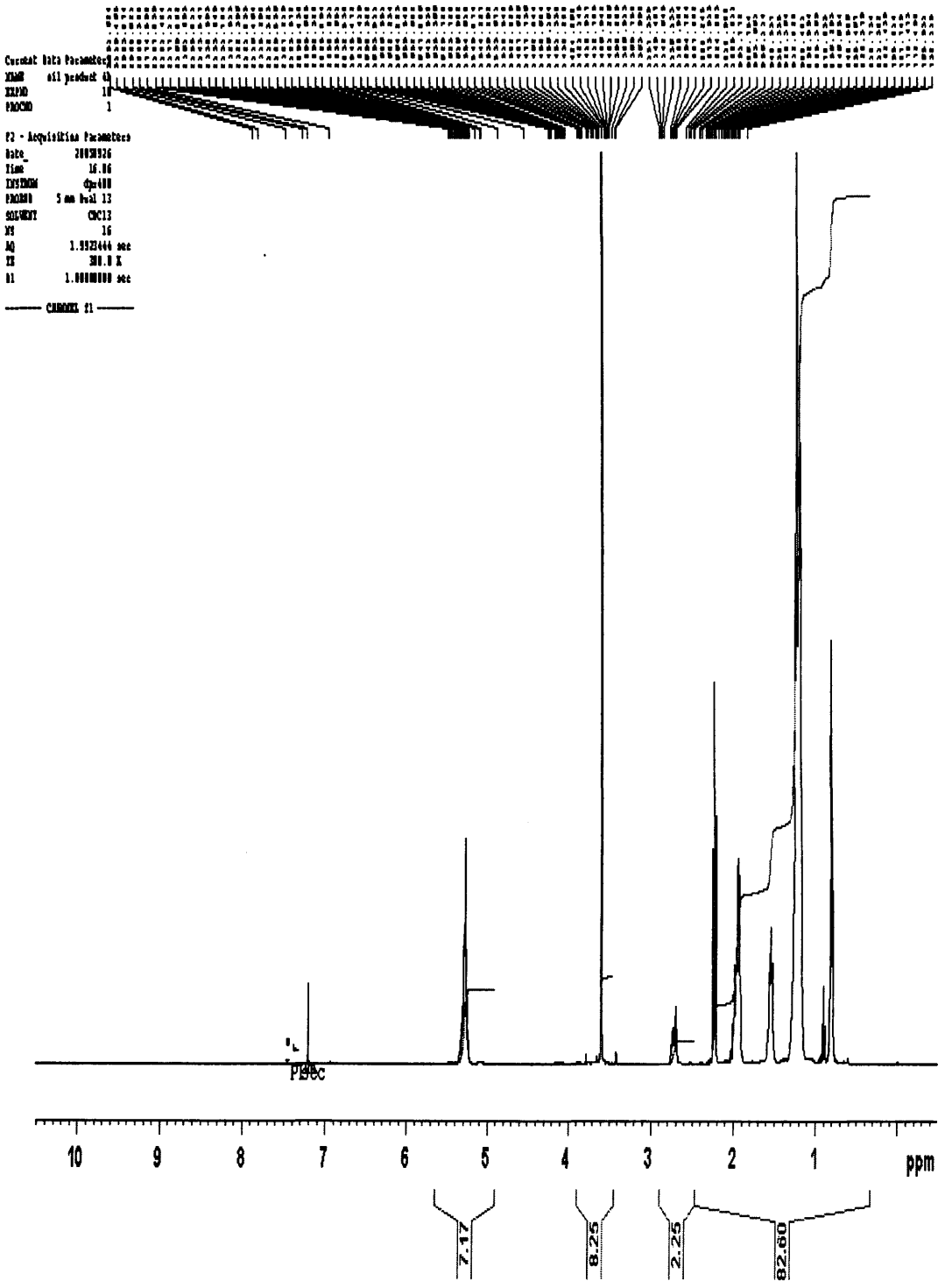

Figure 6.4 ^{1}H NMR of fatty acid esters.

6.2.3.2 High performance liquid chromatography analysis

HPLC can determine the content of each compound in the mixture of fatty acid esters and mono-, di-, and tri-glycerides. This means that the conversion and selectivity of the reaction can be obtained by this method, which is an improvement on ^{1}H NMR that can only determine the yield the reaction. As shown in Figure 6.5, the larger the molecular weight of the chemicals, the longer the retention time of the compounds. The retention time of fatty acid esters and mono-, di-, and tri-glycerides are found to be 31.70 min., 30.65 min., 28.71 min., and 27.65 min, respectively.

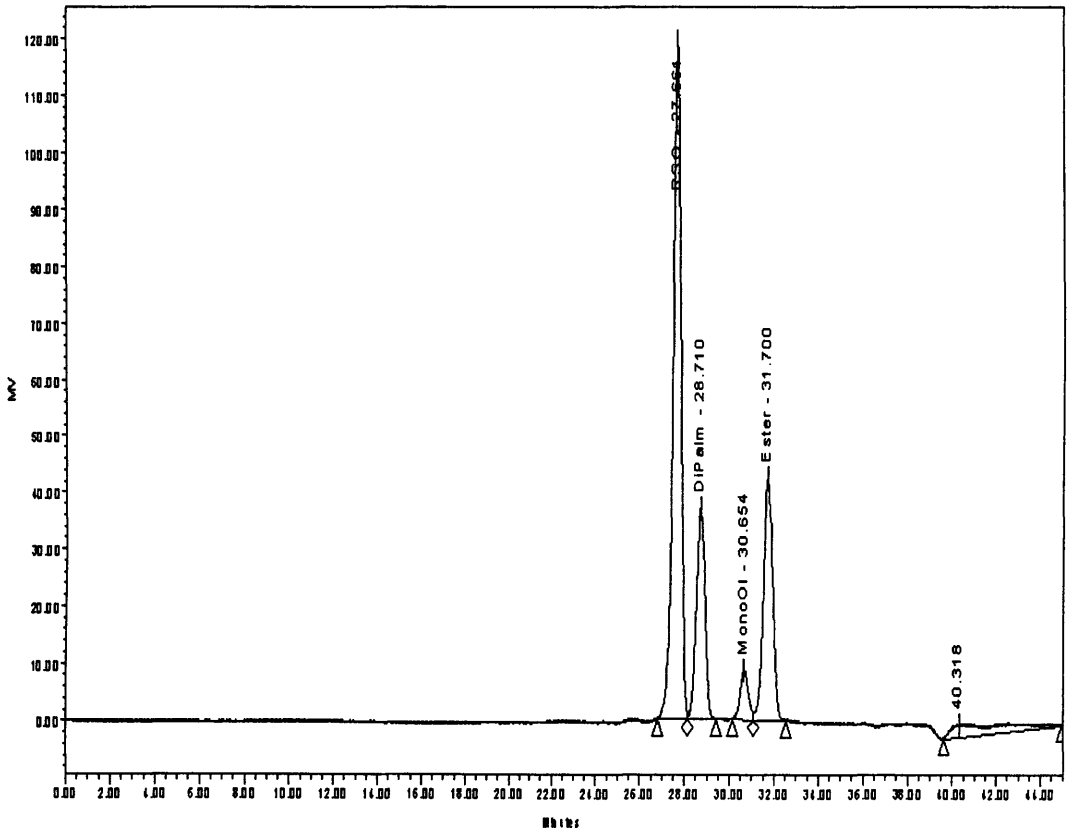

Figure 6.5 HPLC result example.

6.3 Results and Discussion

6.3.1 Reaction performed at 60 °C

When a small amount of catalyst was used the maximum product yield could not be reached. However, increasing the amount of catalyst lead to the slurry (mixture of catalyst and reactants) becoming too viscous, giving rise to a problem of mixing and a demand of higher power consumption for adequate stirring. To avoid this kind of problem, an optimum amount of catalyst loading is determined. As shown in Figure 6.6, the yield increase with increasing the catalyst loading weight up to 0.06 g. However, the yield does not increase when the catalyst loading weight is above 0.06 g. Getting the reactants to and from the catalyst becomes the rate determining step (mass transport limitation) which is why adding more catalyst doesn't have an effect. Therefore, the optimum catalyst loading amount is found to be 0.06 g in this system.

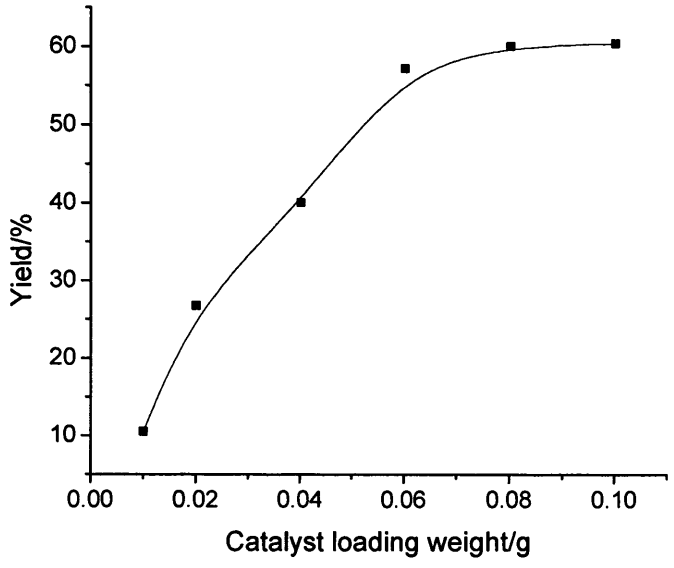

Figure 6.6 Effect of the amount of catalyst on the biodiesel production conversion Reaction condition: methanol/VO molar ration 250:1, reaction temperature 60 °C, reaction time 1h.

The experimental results detailing the influence of the methanol:oil molar ratio on oil conversion are reported in Figure 6.7. It is shown that the reaction cannot operate in the presence of MgO when the methanol:oil ratio is too low. When the methanol:oil molar ratio is 6:1, almost no conversion is obtained as methanol and vegetable oil are immiscible.[22] The conversion increases with increasing methanol:oil molar ratio, and reaches a maximum when the ratio is above 200. This phenomenon is not only due to the weaker solubilization of the oil in methanol. By contrast, glycerol could act as a poison since, once formed, it precipitates readily, whereas it is soluble in methanol/oil ratios over 30.

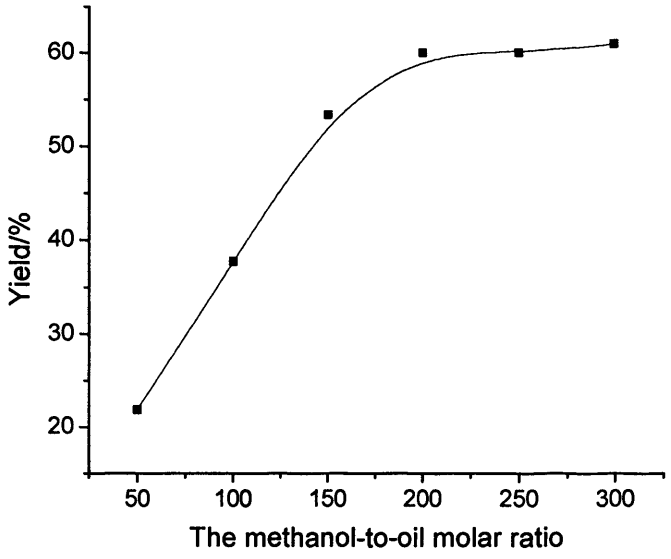

Figure 6.7 Effect of methanol:oil ratio. Reaction condition: reaction temperature 60 °C, reaction time 1h.

To overcome the mixing problem, an appropriate co-solvent n-hexane (hexane:oil ratio 5:1) is introduced to the reaction running at 60 °C with 6:1 methanol:oil molar ratio in the presence of MgO. For both of these two reactions, yield < 1% is obtained after running 3h. Therefore, co-solvent n-hexane does not improve the yield for reaction running at 60 °C.

The 100% rapeseed oil from Fluka (£20 per litre) is far more expensive than the 100% rapeseed oil from a supermarket (£0.60 pre litre), for example Lidl or Tesco. In order to know the effect of vegetable oil from different manufacturers, the activity of oil from Fluka and supermarket is tested (Figure 6.8). As shown in Figure 6.8, the oil conversion increases with time, 94% is reached after running for 4h. The oil from Lidl and Fluka shows similar activity. This means that biodiesel can be synthesised with the ordinary vegetable oil from supermarket using MgO as catalyst.

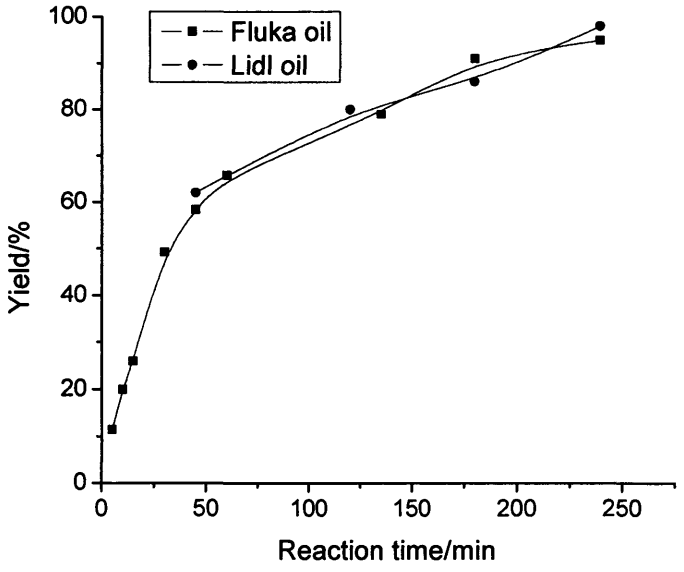

Figure 6.8 Effects of the reaction time on the conversion to methyl esters. Reaction condition: methanol/VO molar ration 250:1, reaction temperature 60 °C.

The influence of reaction temperature has been investigated (Figure 6.9). The temperature was actually the flask temperature. The conversion increases with temperature up to 60 °C (oil bath temperature). Above 60 °C, there is no apparent increase of conversion. Since the boiling point is 64 °C, the bath oil temperature > 60°C, at which methanol refluxes, does not affect the actual reaction temperature. It explains why the yield does not change when the bath oil temperature is above 60 °C.

Calcined commercially available (Aldrich) and laboratory made hydrotalcite (Mg^{2+}:Al^{3+}=3:1) is studied for the synthesis of biodiesel (Figure 6.10). Calcined laboratory made hydrotalcite show similar activity to MgO (Figure 6.8). Both of those result in 90% under the running condition. However, < 5% yield is obtained when calcined commercially available hydrotalcite is used as catalyst. The difference of activity between the commercially available and laboratory made hydrotalcite may be ascribed to the difference of their structure. Further work is needed to investigate the structure difference between commercially available and laboratory made hydrotalcite.

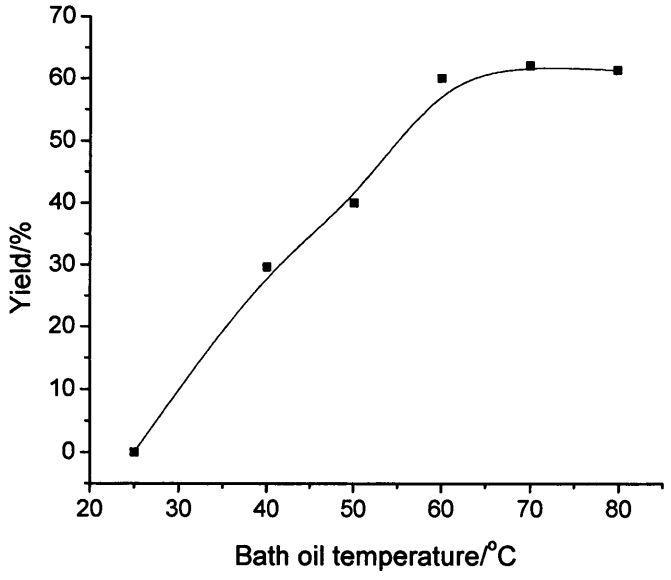

Figure 6.9 Effects of reaction temperature on the conversion to methyl esters.

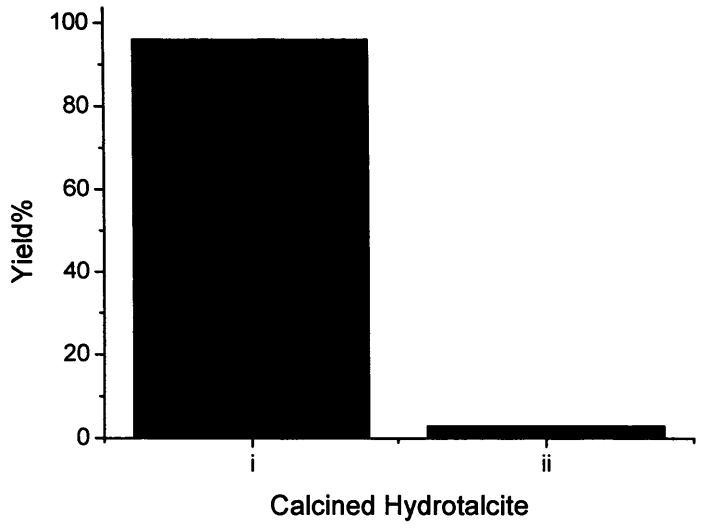

Figure 6.10 Activity of calcined hydrotalcite (Calcination temperature 450 °C). Reaction condition: methanol/VO molar ration 250:1, reaction temperature 60 °C, reaction time 3h. (i) Calcined laboratory made hydrotalcite, (ii) Calcined commercially available hydrotalcite

Because vegetable oils and alcohols usually contain water, the influence of the presence of water on MgO has been investigated. In order to investigate the effect of H_2O, wet methanol (80% methanol/20% H_2O by volume) has been used to make biodiesel with vegetable oil in the presence of MgO. Compared to the 90% conversion obtained with pure methanol, almost no conversion is found after 3h reaction with the wet methanol. The low conversion could result from the fact that the presence of a large amount H_2O could deactivate MgO for the reaction running at 60 °C. Serio *et al.* has tested the effect of water in the biodiesel synthesis under 200 °C. They reported that the activity of MgO was not affected by the presence of an excess of water (water concentration 10 000ppm).[23] However, the activity of the catalyst used in IFP technology is strongly reduced by the presence of water and a water concentration of < 1000 – 1500 ppm must be used.[42]

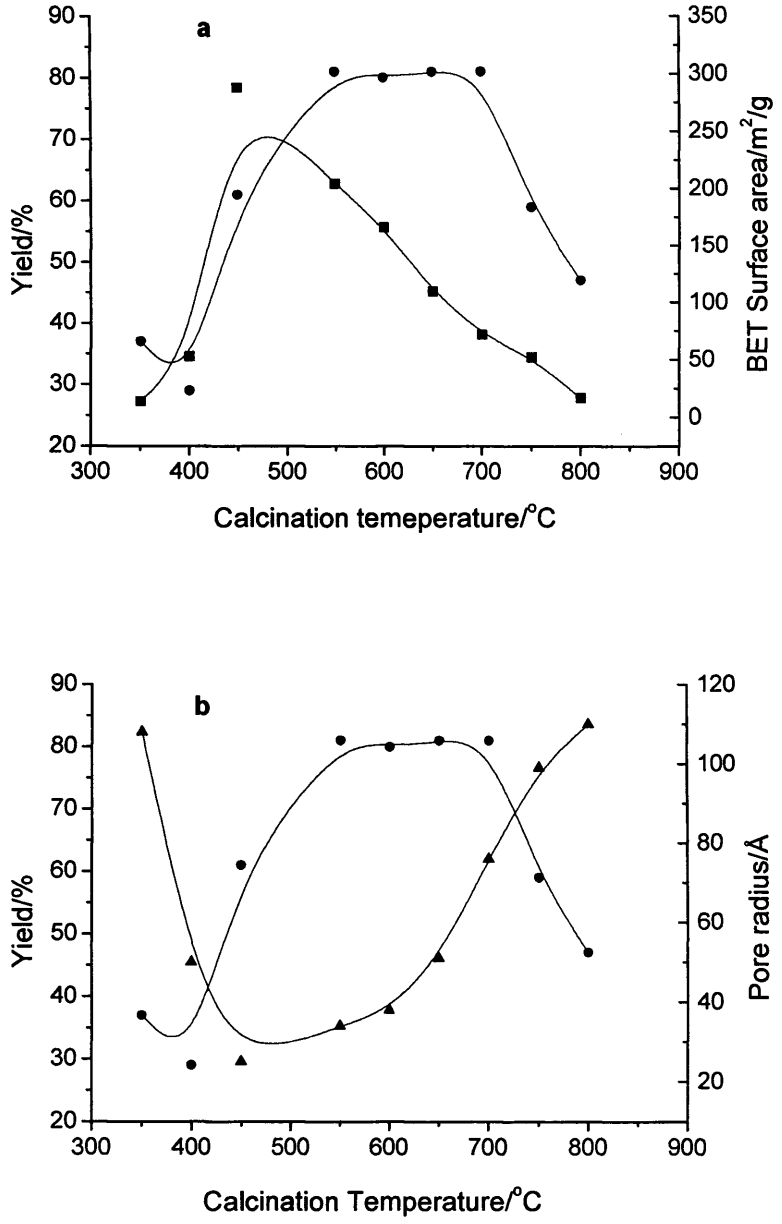

Figure 6.11 Influence of calcination temperature, surface area and pore size distribution: (a) Yield and surface area versus calcination temperature, (b) Yield and pore radius versus calcination temperature. Reaction conditions: 200 °C for 15min in the presence of catalyst. (●) Yield, (■) BET surface area, (▲) Mean pore radius.

Table 6.1 Textual structure of MgO-CBC obtained from $(MgCO_3)_4 \cdot Mg(OH)_2$ (Fluka)[a]

Calcination T (°C)	Surface Area (m^2g^{-1})	Va [0.7ads] (cm^3g^{-1}) [b]	Va [0.98des] (cm^3g^{-1}) [b]	r_p (Å)[c]
350	13	0.01	0.06	108
400	53	0.04	0.11	50
450	292	0.21	0.32	25
550	213	0.21	0.33	34
600	166	0.19	0.30	38
650	110	0.13	0.27	51
700	72	0.11	0.26	76
750	51	0.05	0.24	99
800	17	0.01	0.08	110

[a] Perpormed at a Micromeritics ASAP 2400 from Johnson Matthey
[b] Pore Volume
[c] Average Pore Radius

6.3.2 Reaction performed at 200 °C

Since MgO showed low activity for reaction running at 60 °C and low methanol oil ratio, the activity of MgO was tested at 200 °C and a low methanol:oil ratio (6:1 or 12:1). The reaction has been running at Cardiff University and Johnson Matthey concurrently. The difference in the running conditions used was; catalysts were calcined in static air at Cardiff University and in N_2 at Johnson Matthey; the product was analysed using NMR at Cardiff University and HPLC at Johnson Matthey.

6.3.2.1 Results obtained at Cardiff University

Figure 6.11 presents the variation of the yield of transesterification of vegetable oil to biodiesel after 15 minutes of reaction, as a function of the calcination temperature. Calcination of the catalyst below 400 °C, leads to low yield, whereas for calcination temperatures between 550 and 700 °C, the conversion reaches maximum values. When

catalyst is calcined above 750 °C, activity of MgO decreases with increasing calcination temperatures.

The results are not consistent with changes observed in the surface area of the catalyst, which varies with calcination temperature (Figure 6.11, a; table 6.1). From the BET surface area results, the largest surface area is found when the calcination temperature is 450 °C. The surface area decreases with increasing the calcination temperature. However, the highest ester yield is found when the calcination temperature is between 550 °C to 700 °C. The low activity of MgO calcined at 350 °C, 400 °C, 750 °C and 800 °C may be ascribed to its low surface area. However, the activity of MgO calcined at 450 °C is lower than that calcined at 550 °C, which can not be explained by the lower surface area since the surface area of MgO calcined at 450 °C (292 m^2g^{-1}) is higher than that at 550 °C (213 m^2g^{-1}). It implies that for the biodiesel reaction the yield does not only depend on the surface area of the catalysts. This phenomenon was different from the reactions, using smaller reactants, such as Michael addition (Figure 4.1) and MPV reduction (Figure 3.1), for which the activity of MgO is consistent with changes in the surface area.

In contrast to the pore radius r_p and pore volume Va of each material calcined at different temperatures, we find that the pore size and pore volume changes as the calcination temperature increases until 800 °C where, the pores collapsed (Figure 6.12, b; table 6.1). At calcination temperature 350 °C, the pore radius r_p is 108 Å. The pore radius r_p decreases to 25 Å with calcination temperature increasing to 450 °C. Above 450 °C, the pore radius r_p increases to 108 Å with increasing the calcination temperature. The pore radius r_p at calcination temperature 350 °C mainly comes from the pores among the particles of the precursor $(MgCO_3)_4 \cdot Mg(OH)_2$. Above 400 °C, a

large amount of pores with lower radius are formed, caused by the removal of CO_2 and H_2O from the precursor. Above 550 °C, rearrangement of surface and bulk atoms also occurs in addition to desorption of CO_2 and H_2O, which is evidenced by a decrease in the surface area and pore volume, and an increase in the pore radius.

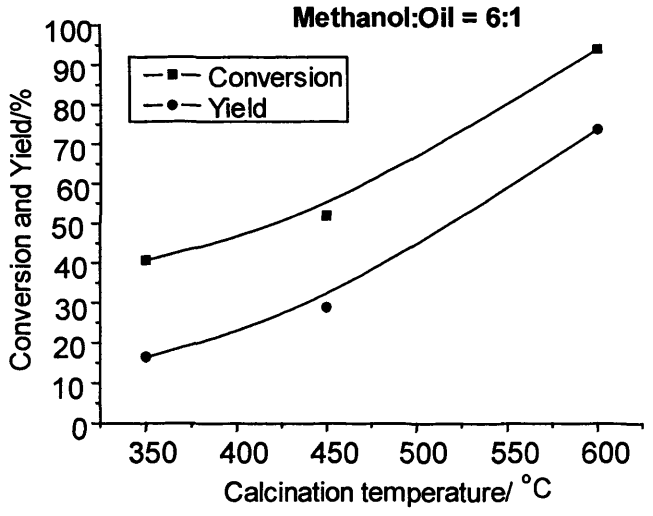

a

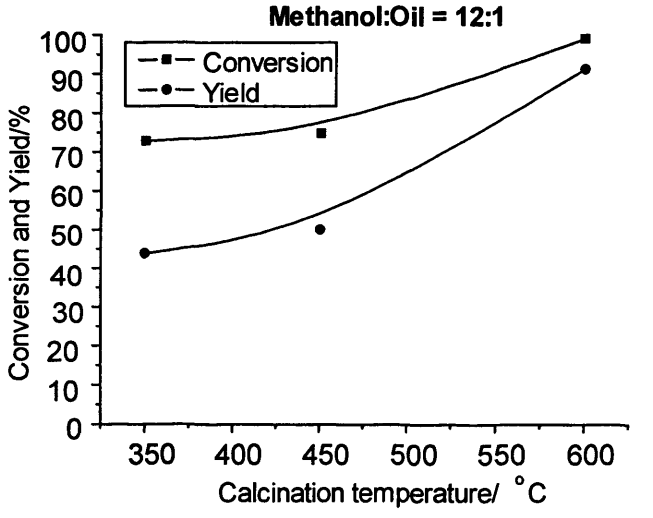

b

Figure 6.12 Yield of triglyceride to methyl esters versus calcination temperature for two methanol oil ratios: (a) 6:1, (b) 12:1. Reaction condition: 200 °C for 15min in the presence of catalyst (Johnson Matthey).

The pore radius r_p of MgO calcined at 550 °C is 34 Å, which is higher than that calcined at 450 °C (25 Å). The lower pore radius r_p can explain the low activity of MgO calcined at 450 °C. However, this is not true, since MgO calcined at 750 °C and 800 °C, which show lower activity than calcined at 550 °C, have higher pore radius r_p.

Since the texual structure in the surface area, pore radius and pore volume can not explain the activity of MgO, which change with calcination temperature, other structural factors may affect the activity of MgO. Amoung them are the number and basic strength of basic sites. As the calcination temperature increases, the molecules covering the surfaces are successively desorbed according to the strength of the interaction with the surface sites. The molecules weakly interacting with the surfaces are desorbed at lower calcination temperatures, and those strongly interacting desorb at higher temperatures. The sites that appeared on the surface by calcination at low temperatures are suggested to be different from those that appeared at high temperatures. If simple desorption of molecules occurs during pretreatment, the basic sites that appeared at high temperatures should be strong. However, rearrangement of surface and bulk atoms also occurs during calcination in addition to the desorption of the molecules, which results in a decrease of the of number of basic sites.[39]

Coluccia and Tench proposed a surface model for MgO.[40] There exist several Mg-O ion pairs of different coordination numbers. Ion pairs of low co-ordination numbers exist at corners, edges, or high Miller index surfaces of the (100) plane. Different basic sites generated by increasing the calcination temperature appear to correspond to the ion pairs of different coordination numbers. However, the correspondence between the catalytically active sites for different reaction types and the co-ordination number of the

ion pairs is not definite yet. Among the ion pairs of different co-ordination numbers, the ion pair of 3-fold Mg^{2+} - 3 fold O^{2-} is the most reactive and adsorbs carbon dioxide most strongly. To reveal the ion pair $Mg^{2+}_{3c} - O^{2-}_{3c}$, the highest calcination temperature is required. At the same time, the ion pair $Mg^{2+}_{3c} - O^{2-}_{3c}$ is the most unstable. The Mg^{2+}_{3c} and O^{2-}_{3c} tend to rearrange easily at high temperature. The appearance of such highly unsaturated sites by the removal of carbon dioxide and the elimination by the surface atom rearrangement compete. Such competition results in the activity maxima as the pre-treatment temperature is increased.

Therefore, for the synthesis of biodiesel, number and basic strength of basic sites decide the activity of MgO. Below calcination temperature 400 °C , the number and basic strength of basic sites is low, which lead to the low activity. At 450 °C, the number of basic sites may be high because of the high surface area, but the basic strength is low. Between 550 °C and 700 °C, the number and basic strength of basic sites is high enough to result in high activity. Above 750 °C, the number of basic sites is low, which result in low activity. Accordingly the yields of the reactions increased until the calcination temperature reached 550 °C and dropped dramatically when the calcination temperature is above 750 °C.

6.3.2.2 Results obtained at Johnson Matthey

The activity of materials obtained by calcining the commercially available $(MgCO_3)_4{\cdot}Mg(OH)_2$ (Alfa Aesar) in a flow of N_2 at 350, 450 and 600 °C for 2h has been tested under at 200 °C with a methanol:oil ratio (6:1 and 12:1) for 15min. The mass balance and yield of biodiesel and intermediates are shown in appendix two (Table A6.1 to A6.8).

The surface area, pore volume and pore radius results are shown in table 6.2. The surface area changes with calcination temperature which was measured at 21 m^2g^{-1} at 350 °C, 142 m^2g^{-1} at 450 °C, and 117 m^2g^{-1} at 600 °C. The pore volume and pore radius also change with calcination temperature. Pore radius is 80 Å at 350 °C, 36 Å at 450 °C, and 61 Å at 600 °C. The trend of surface area and pore radius with calcination temperature are similar to MgO calcined in static air (Table 6.2). However, the absolute value of the surface area is lower than that prepared in static air. The surface area is 142 m^2g^{-1} calcined at 450 °C in flowing N_2, but 292 m^2g^{-1} in static air. The difference of surface area result from the ramp, 4 °C/min in flowing N_2 and 10 °C/min in static air. Ramp 4 °C/min will result in longer time reaching to the calcination temperature than Ramp 10 °C/min. The longer time will decrease the surface area and increase the pore radius. The reason for this has been explained in section 6.3.2.1.

Table 6.2 Textual structure of MgO-CBC obtained from $(MgCO_3)_4 \cdot Mg(OH)_2$ (Alfa Aesar)[a]

Calcination T (°C)	**Surface Area (m^2g^{-1})**	**Va [0.7ads] (cm^3g^{-1}) [b]**	**Va [0.98des] (cm^3g^{-1}) [b]**	**r_p (Å)[c]**
350	21	0.02	0.08	80
450	142	0.13	0.25	36
600	117	0.12	0.35	61

[a] Perpormed at a Micromeritics ASAP 2400 from Johnson Matthey
[b] Pore Volume
[c] Average Pore Radius

Figure 6.12 presents the variation of the conversion and yield of transesterification of vegetable oil to biodiesel after 15 minutes of reaction, as a function of the calcination temperature and methanol:oil ratio. It was found that the relationship between calcination temperature and activity are similar for materials calcined in N_2 and air (Figure 6.11, a). For example, the MgO prepared at 600 °C both under N_2 and air resulted in 80% yield. Furthermore, the conversion and yield increased with increasing calcination temperature, reaching a maximum at 600 °C (Figure 6.12).

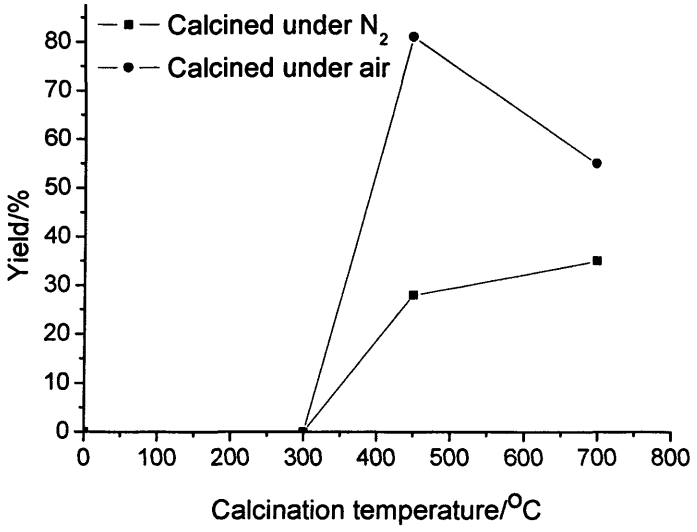

Figure 6.13 Activity of materials obtained by calcining MgC_2O_4 under N_2 and air for the transesterification of vegetable oil to biodiesel. [41]

The activity of MgO is affected not only by the preparation condition but also the precursors. Wang *et al.* have studied the activity of MgO produced from MgC_2O_4 (Figure 6.13).[41] They found that the activity of MgO was affected by the calcination temperature and the calcination atmosphere. The yields of the reaction catalysed by the samples calcined under N_2 are much lower than the ones calcined under air, which indicates that the two types of samples calcined under air and N_2 are not the same

materials. Activity of MgO prepared from commercially available $Mg(OH)_2$ is also studied (Figure 6.14). The activity of MgO calcined at 600 °C is higher than 450 °C. The trend is similar to that of MgO from commercially available $(MgCO_3)_4 \cdot Mg(OH)_2$.

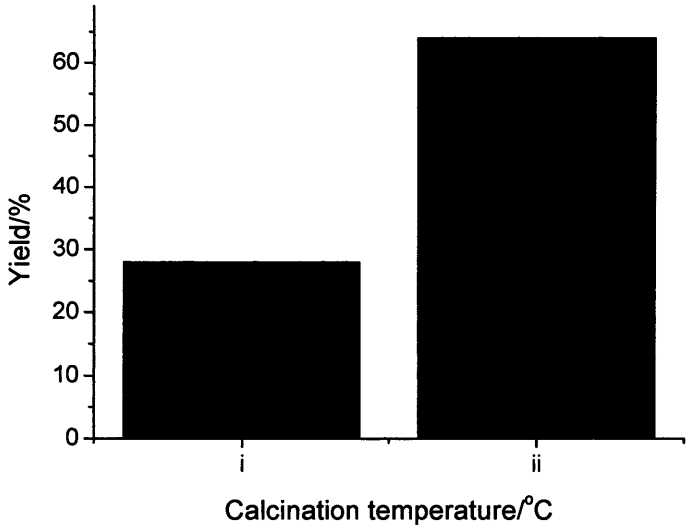

Figure 6.14 Activity of materials obtained by calcining commercially available $Mg(OH)_2$: (i) 450 °C and (ii) 600 °C

The methanol:oil ratio of 12:1 resulted in a higher yield and conversation than 6:1 (Figure 6.12). For example, an 82% yield is obtained for a methanol:oil ratio of 12:1 (Figure 6.12, b), while a 68% yield is obtained with a methanol:oil ratio of 6:1 under the same reaction conditions (Figure 6.12, a). This can be explained by the fact that glycerol could act as a poison since, once formed, it precipitates readily at a methanol:oil ratio of 6:1, whereas it is more soluble when the methanol:oil ratio was 12:1.

Table 6.3 Comparison of activity between MgO and other reported heterogeneous basic catalysts.

Entry	Catalyst	Reaction T	Methanol :oil	Co-solvent	Conversion	Selectivity	Yield	Ref
1	A variety of catalysts	60 °C	6:1		low			18
2	Zeolites and metal catalysts	60 ~150 °C	6:1		40~100%, 24h	24~96%,		26
3	Na/NaOH on alumina	60 °C	9:1	*n*-hexane			90%, 2h	20
4	Cs-exchanged NaX faujasites; commercial hydratalcite; MgO	Methanol reflux	275:1		70%, 22h; 34%, hydrotalcite; [a] MgO, 65%.	96%, 22h; 98%, MgO.		22
5	KNO_3/Al_2O_3	Methanol reflux	15:1		87%, 7h	Not available		14
6	Calcined Hydrotalcite	Methanol reflux	15:1		67%, 9h	Not available		30
7	KF/ZnO	Methanol reflux	10:1		87%, 9h	Not available		28
8	Calcium carbonate rock	240 °C	10:1		78%, 18min	Not available		21
9	None	280 °C	24:1	Super-critical MeOH and CO_2			98%, 10min	31
10	None	350 °C	42:1	Super-critical MeOH			96%, 400 s	32
11	MgO	60 °C 200 °C	250:1 12:1		 99%,15min		90%, 3h 80%	

[a] Selectivity data was not available

MgO show high activity with 99% conversion and an 82% yield obtained within 15 minutes (Appendix two, table A6.8). Without a catalyst, the conversion (15%) and yield (2%) is very low (Appendix two, table A6.5). Compared with references (Table 6.3), MgO show high activity. Furthermore, MgO was prepared in a simple way. Although no catalyst was needed under supercritical condition, the special alloy such as Hastelloy was required for the reaction vessel (Table 6.3, entry 9 and 10). Additionally, the biodiesel produced was thermally deteriorated. Therefore, MgO is an efficient catalyst for the synthesis of biodiesel.

6.4 Reuse of MgO

In industry, heterogeneous catalysts are expected to be used for a long time without leaching in a continuous reactor, i.e. fixed bed. The following experiments are an investigation and simple simulation of the industrial process of catalyst recycling.

The recycling reactions were carried out under the same conditions as mentioned before, with reaction temperatures of 60 °C and 200 °C.

For the reaction run at 60 °C, MgO recycling was studied in the following way. The reactions were performed with 1 ml of vegetable oil and 10 ml of methanol (molar ratio of methanol to vegetable oil 250:1) using 0.06 g of catalyst at 60 °C. After running for 3h, the MgO was separated from solution using a centrifuge. The recovered MgO was washed using methanol (5 ml), chloroform (5 ml) and methanol (5 ml) respectively three times. The reason that methanol and chloroform were used for washing is that the glycerol is miscible with methanol but not chloroform; the oil and product is miscible with chloroform not methanol. It was found that chloroform would deactivate the MgO, so methanol was used for washing again after chloroform. After the MgO was washed,

the same amount of oil and methanol was added and the reaction was run under the same conditions as the first run. It was found that the conversion of oil decreased from 90% (1st run) to 1% (2nd run). The loss could result from the presence of glycerol or chloroform.

For the reaction run at 200 °C, the reaction conditions were as follows. The autoclave was loaded with 27.3 g (0.03 moles) of rapeseed oil and 14.6 ml (0.36 moles) of methanol. To this was added 1.33 g catalyst and the reaction run for 15 min at 200 °C. MgO recycling was studied in two ways. After running, the solution was separated from the catalyst. As the products are very viscous and the catalyst cannot be separated by being left to stand for a few hours or even over night, the catalyst was separated from the product by filtration. The remaining catalyst was washed by THF (5 ml) and MeOH (5 ml) for three times.

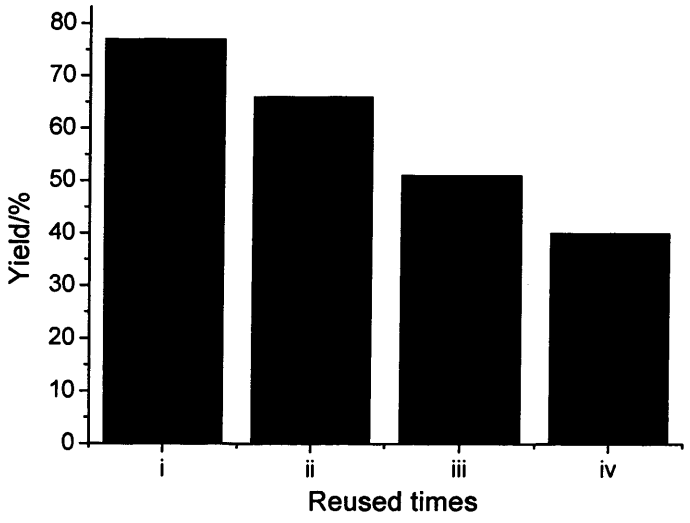

Figure 6.15 Reuse of MgO: (i) 1st use, (ii) 2nd use, (iii) 3rd use and (iv) 4th use.

After that, the same amount of rapeseed oil and methanol was added. Then the reaction was conducted under the same conditions as the first run. It was found that the yield of biodiesel decreased from 76% (1st run) to 50% (2nd run).

In order remove errors associated with the loss of MgO between runs caused by filtering and washing, a second method was used. The exact yield (1st run) was obtained under the above reaction conditions. Then a second run was conducted under the above conditions except that a larger amount of MgO was used. The catalyst from this run was filtered and washed, but the yield was discarded. After that, the solid was dried in an oven overnight and re-calcined under the same conditions as the original catalysts using exactly the same amount of catalyst. The catalyst was reused in the way for four times (Figure 6.15). It was found that the yield decreased with increasing number of reuses. The deactivation of the catalyst can be ascribed to structural changes in the catalyst because the calcination time increased with increasing number of reuses, and the surface area of MgO decrease with increasing calcination time (Chapter 3). The problem of deactivation can be solved by re-hydration of MgO (chapter 4). In this way, the surface area and structure of MgO can be reformed; hence the activity of MgO will not decrease.

6.5 Conclusions

The reaction temperature used affected the activity of MgO, a higher yield was obtained at 200 °C when compared to 60 °C. The methanol:oil ratio was found to be an important variable influencing the yield. A methanol:oil ratio of 250:1 resulted in high yield for the reaction temperature at 60 °C, but high yield can be obtained when methanol oil ratio was 6:1 or 12:1 at 200 °C.

The preparation method and calcination temperature are found to have a strong influence on the catalytic activity of MgO as catalysts for the transesterification of

vegetable oil to biodiesel. A calcination temperature of 550 - 700 °C resulted in MgO with high basic strength and basic sites, and hence, highest catalytic activity. Calcination atmosphere has no strong effect on the activity of MgO prepared from $(MgCO_3)_4 \cdot Mg(OH)_2$, but affect the activity of MgO from MgC_2O_4.

The reuse of MgO has been studied. Further work is needed to study the method regenerating MgO.

Finally, MgO catalysts are more affected by the presence of water for reaction running at 60 °C than 200 °C.

References

1. F. Ma and M. Hanna, *Biores. Technol.*, 1999, **70**, 1.
2. E. Shay, *Biomass Bioenergy*, 1993, **4**, 227.
3. A. Demirbas, *Energy Convers. Manage*, 2003, **44**, 2093.
4. B. Bala, *Energy Edu. Sci. Technol.*, 2005, **15**, 1.
5. G. Vicente, M. Martinez and J. Aracil, *Biores. Technol.*, 2004, **92**, 297.
6. M. Dorado, E. Ballesteros, J. Arnal, J. Gómez and F. López, *Fuel*, 2003, **82**, 1311.
7. D. López, J. Goowin Jr., D. Bruce and E. Lotero, ***Appl. Catal., A**: General*, 2005, **295**, 97.
8. M. Dorado, E. Ballesteros, J. Almeida, C. Schellert, H. Lohrlein and R. Krause, *Trans. ASAE*, 2002, **45**, 525.
9. E. Lotero, Y. liu, D. López, K. Suwannakarn, D. Bruce and J. Goowin Jr., *Ind. Eng. Chem. Res.*, 2005, **44**, 5353.

10. M. Canakci and J. Gerpen, *Trans. ASAE*, 2001, **44**, 1429.

11. W. Du, Y. Xu, D. Liu and J. Zeng, *J. Mol. Catal. B: Enzyme*, 2004, **30**, 125.

12. S. Saka and D. Kusdiana, *Fuel*, 2001, **80**, 225.

13. A. Demirbas, *Prog. Energ. Combust. Sci.*, 2005, **31**, 466.

14. W. Xie, H. Peng and L. Chen, ***Appl. Catal., A**: General*, 2006, **300**, 67.

15. G. Antolín, F. Tinaut, Y. Briceño and V. Castanñ, *Biores. Technol.*, 2002, **83**, 111.

16. J. Encinar, J. González and J. Rodríguez, *Energ. Fuel*, 2002, **16**, 443.

17. S. Dmytryshyn, A. Dalai and S. Chaudhari, *Biores. Technol.*, 2004, **92**, 55.

18. G. Peterson and W. Scarrach, *J. Am. Oil Chem. Soc.*, 1984, **61**, 1593.

19. S. Gryglewicz, *Biores. Technol.*, 1999, **70**, 249.

20. H. Kim, B. Kang, M. Kim, Y. Park, D. Kim, J. Lee and K. Lee, ***Catal. Today***, 2004, **93-95**, 315.

21. G. Suppes, K. Bockwinkel, S. Lucas, J. Mason and J. Heppert, *J. Am. Oil Chem. Soc.*, 2001, **78**, 139.

22. E. Leclercq, A. Finiels and C. Moreau, *J. Am. Oil Chem. Soc.*, 2001, **78**, 1161.

23. M. Serio, M. Ledda, M. Cozzolino, G. Minutillo, R. Tesser and E. Santacesaria, ***Ind. Eng. Chem. Res.***, 2006, **45**, 3009.

24. T. Dossin, M. Reyniers and G. Marin, *Appli. Catal. B: Environmental*, 2006, **61**, 35.

25. M. Kouzu, M. Umemoto, T. Kasuno, M. Tajika, Y. Aihara, Y. Sugimoto and J. Hidaka, *Journal of the Japan Institute of Energy*, 2006, **85**, 135.

26. G. Suppes, M. Dasari, E. Doskocil, P. Mankidy and M. Goff, *Appli. Catal. A: General*, 2004, **257**, 213.

27. L. Bournay, D. Casanave, B. Delfort, G. Hillion and J. Chodorge, *Catal. Today*, 2005, **106**, 190.

28. W. Xie and X. Huang, *Catal. Today*, 2006, **107**, 53.

29. A. Gervasini and A. Auroux, *J. Catal.*, 1991, **131**, 190.

30. W. Xie, H. Peng and L. Chen, *J. Mol. Catal. A: Chem.*, 2006, **246**, 24.

31. H. Han, W. Cao and J. Zhang, *Process Biochem.*, 2005, **40**, 3148.

32. K. Bunyakiat, S. Makmee, R. Sawangkeawa and S. Ngamprasertsith, *Energ. Fuel*, 2006, **20**, 812.

33. G. Gelbard, O. Bres, R. Vargas, F. Vielfaure and U. Schuchardt, *J. Am. Oil Chem. Soc.*, 1995, **72**, 1239.

34. B. Freedman, E. Pryde and W. Kwolek, *J. Am. Oil Chem. Soc.*, 1984, **61**, 1215.

35. M. Mittelbach, *Chromatographia*, 1993, **37**, 623.

36. M. Holčapek, P. Jandera, J. Fischer and b. Prokeš, ***J. Chromatogr.***, 1999, **858**, 13.

37. R. Fillieres, B. Mlayah and M. Delmas, *J. Am. Oil Chem. Soc.*, 1995, **72**, 427.

38. G. Knothe, *J. Am. Oil Chem. Soc.*, 2000, **77**, 489.

39. H. Hattori, *Chem. Rev.*, 1995, **95**, 537.

40. S. Coluccia and A. J. Tench, *Proceeding of the 7th international congress on catatalysis* Tokyo, Japan, 1980; p 1160.

41. S. Wang and M. Lunn, *Internal Report, Johnson Matthey*, 2006.

42. L. bournay and G. Hillion, Process for the production of alkyl esters from vegetable or animal oil and an aliphatic monohydric alcohol, European Paten No. 1352893 A1, 2003.

Chapter 7

Conclusions and future work

We systematically studied the preparation method of magnesium oxide as cheap heterogeneous basic catalysts, and find a very simple method to obtain MgO with high surface area and high catalytic activity. Furthermore, the structure of MgO has been characterized using many techniques, such as BET, TGA, XRD and SEM. In order to investigate in detail the catalytic activity of the prepared MgO, four different liquid phase reactions were chosen as model reactions. These were Meerwein-Pondorf-Verley reaction, Michael addition, Knoevenagel condensation, transesterification of vegetable oil to biodiesel and synthesis of β-Keto 1,3-dithianes. The reaction mechanism in the presence of MgO, and the relationship between structure and activity of MgO has been studied. It was found that the activity and structure of MgO can be affected by precursors, preparation method and reaction conditions.

7.1 Structure of MgO

TGA shows the temperatures at which the MgO precursors decompose when heated in a controlled environment. Water is removed from the precursors between 250 ~ 400 °C, whereas carbon dioxide is lost between 325 ~ 550 °C. Thermal pre-treatment results in a change in the XRD pattern, which is caused by the removal of CO_2 and H_2O from starting materials. The diffraction patterns of the samples heated at temperatures < 375 °C are different from that of MgO, while samples calcined at temperatures > 400 °C display diffraction reflections characteristic of MgO, which became, as expected, more crystalline with increasing calcination temperature.

The surface area of MgO is affected by the temperature and duration of calcination and different precursors. Below 400 °C, the surface area is low. Above 400 °C until 500 °C, high surface area is obtained. Surface area decreases with increasing calcination temperature. Surface area also decreases with increasing calcination duration. For example, surface area of MgO-CBC calcined at 600 °C decreases from 126 m^2g^{-1} to 79 m^2g^{-1} when duration increases from 2 h to 12 h. Another factor, which affects the specific surface area, is the precursor. Specific surface area of MgO-COH (58 m^2g^{-1}) is far lower than that of MgO (229~312 m^2g^{-1}) prepared from other precursors.

The pore radius r_p and pore volume V_a of each material calcined at different temperatures changes as the calcination temperature increases until 800 °C, at which point the pores collapsed. At a calcination temperature of 350 °C, the pore radius r_p is 108 Å. The pore radius r_p decreased to 25 Å with calcination temperature increasing to 450 °C. Above 450 °C, the pore radius r_p increases to 108 Å with increasing calcination temperature. The pore radius r_p at a calcination temperature of 350 °C mainly comes from the pores among the particles of the precursor $(MgCO_3)_4 \cdot Mg(OH)_2$. Above 400 °C, a large amount of pores with lower radius are formed, caused by the removal of CO_2 and H_2O from the precursor. Above 550 °C, rearrangement of surface and bulk atoms also occurs in addition to desorption of CO_2 and H_2O, which is evidenced by a decrease in the surface area and pore volume, and an increase in the pore radius.

SEM images of MgO materials and precursors have been obtained. They reveal that the size and morphology of the catalysts produced are very strongly influenced by the morphology of the catalyst precursor, which is retained during the calcination procedure.

The number and basic strength of basic sites are affected by the calcination temperature. As the calcination temperature increases, the molecules covering the surfaces are successively desorbed according to the strength of the interaction with the surface sites. The molecules weakly interacting with the surfaces are desorbed at lower calcination temperature, and those strongly interacting desorbed at higher temperatures. The sites that appear on the surface by calcination at low temperatures are suggested to be different from those that appeared at high temperatures. If simple desorption of molecules occurs during pretreatment, the basic sites that appeared at high temperatures should be strong. However, rearrangement of surface and bulk atoms also occurs during calcination in addition to the desorption of the molecules, which result in a decrease in the number of basic sites.

7.2 Model reactions

7.2.1 MPV reactions

Magnesium oxide with high surface area (229~312 $m^2 g^{-1}$) was prepared by the thermal decomposition of various precursors including $(MgCO_3)_4Mg(OH)_2$, $Mg(OH)_2$, $MgCO_3$ and MgC_2O_4. The high area MgO displayed exceptionally high catalytic activity for the liquid phase Meerwein-Ponndorf-Verley (MPV) reaction of benzaldehyde with different alcohols. At the optimum condition, 99% conversion and 97% selectivity are obtained within 1 h running time. The effect of calcination temperatures were studied, it was found that the optimum calcination temperature was 450 °C which led to the highest surface area material. This was the key controlling parameter for the catalytic activity of MgO for the MPV reaction.

Choice of precursor affected the activity of the MgO catalysts prepared. Besides MgO-COH, other MgO show similar activity, which is higher than that of MgO-COH. The low activity of MgO-COH is ascribed to its low surface area and preparation method. The high area MgO catalyst could be reused without loss of catalyst activity.

The affect of different alcohol reactants were studied. The activity of MgO was found to be influenced by the structure of the alcohols. For alcohols with same molecular weight, the ability to donate hydrogen and form a six-member intermediate affected the activity of MgO catalysts, which is discussed in Chapter 3.

Lithium doped magnesium oxide was also studied, but this modification resulted in lower conversion and selectivity than pure MgO. This was caused by a decrease in the surface area of the doped material and increase in the basic strength. It was found that the basic strength of the catalyst did not influence this reaction and that having a high surface area material was much more important. The addition of lithium to MgO caused a loss of surface area compared with the unmodified MgO. And the decrease of selectivity was as a result of the aldol condensation reaction being favoured and the selectivity to the MPV product decreased. Since the MPV reaction can be catalysed by solid base and acid catalyst and the increase in the basic strength will result in a decrease of selectivity to MPV product.

It was observed that MgO catalysts rapidly deactivate if they were left exposed to the atmosphere. The effect of CO_2 and H_2O on the activity of MgO was studied. The results showed that both CO_2 and H_2O deactivated the MgO and in order to achieve a good catalyst performance the MgO samples must be freshly calcined before use, or kept in a sealed environment, away from the atmospheric moisture and CO_2.

7.2.2 Michael additions and Knoevenagel condensation

A simple preparation method for MgO producing a catalyst that exhibits a high activity for base catalysed reactions is described. The experimental results showed that an optimal calcination temperature in the range 400~500 °C gave poorly crystalline, high surface area MgO that can be regenerated by washing and then reused. The catalytic activity of the MgO for both Michael additions and Knoevenagel condensation was found to compare favourably with previous studies using more complicated and expensive catalysts. Indeed, the simplicity of the preparation and the ease of reactivation after use may offer sufficient compensation to make MgO the base catalyst of choice even if slightly better yields can be obtained with alternative catalysts.

It wad found that the activity of MgO did not increase with the acidity of all the substrates, in contrast to many homogeneous systems. Enol formation and solvent (pKa, concentration and structure) affected the activity of MgO. The effect of enol formation has been systematically studied, which has led to the suggested reaction mechanism in the presence of MgO.

Calcium oxide (CaO) can be prepared in a similar way to MgO. The activity of MgO was compared with CaO with these reactions. It was found that MgO showed higher activity when compared to CaO for these reactions.

7.2.3 Synthesis of β-Keto-1,3-Dithianes

This is the first report of the synthesis of β-keto-1,3-dithianes by Michael additions through the use of heterogeneous basic catalyst such as MgO. It was proved that the

activity of MgO was higher than the previously published homogeneous catalyst NaOMe in a number of reactions. A yield of 98% was obtained within 0.5 h running time in the presence of a prepared MgO catalyst.

The effect of the substrates structure has been investigated. Ynones are more active than ynoates because ynoates have the group RO connected to C=O and Ynones do not, but have Me. Me has a slight positive inductive effect, which slightly reduces the electron withdrawing power of carbonyl. In the case of MeO, stronger resonance (+ve mesomeric) can occur, which causes a much greater reduction in electron withdrawal by the C=O. Therefore, the reaction rate is slower and there is more opportunity for the formation of the intermediate (α,β-unsaturated carbonyl **4** and dimeric side products **8).** Formation of the two intermediates was helpful to suggest a reaction mechanism in the presence of MgO catalyst.

Precursor and preparation method have been shown to affect the activity of the MgO catalyst. MgO-COH, MgO-ROH, MgO-CBC, MgO-OX and MgO-CC are more active in the reaction studied than MgO-RIB and MgO-AD. The low activity of MgO-RIB and MgO-AD was suggested to be due to their low surface area.

7.2.4 Transesterification of vegetable oil to biodiesel

The reaction temperature used affected the activity of MgO, a higher yield was obtained at 200 °C when compared to 60 °C. The methanol:oil ratio was found to be an important variable influencing the yield. A methanol:oil ratio of 250:1 resulted in a high yield for the reaction temperature at 60 °C, however, a high yield can be obtained

when methanol oil ratio is 6:1 or 12:1 at 200 °C. A yield of 80% biodiesel can be obtained at 200 °C in 15 minutes in the presence of a MgO catalyst. The activity of MgO catalyst is high and the preparation method was simple, compared with the reference catalysts (Table 6.3).

The preparation method and calcination temperature are found to have a strong influence on the catalytic activity of MgO as catalysts for the transesterification of vegetable oil to biodiesel. A calcination temperature range of 550 - 700 °C resulted in an MgO with high number of basic sites with high strength and, and hence, highest catalytic activity. The calcination atmosphere has no strong effect on the activity of MgO prepared from $(MgCO_3)_4 \cdot Mg(OH)_2$, but was found to affect the activity of MgO from MgC_2O_4. The yields of the reaction catalysed by the samples from MgC_2O_4 calcined under N_2 are much lower than the ones calcined under air. This indicated that the two resulting samples are not the same materials.

The reuse of MgO has been studied. Further work is needed to study the method regenerating MgO. MgO catalysts are more affected by the presence of water for reaction running at 60 °C than 200 °C.

7.3 Future work

Further work is needed to study the relationship between activity of MgO and calcination temperature. The activity maxima appear at different catalyst pre-treatment temperatures for different reaction types: 450 °C for MPV reaction and Michael additions; 550 - 700 °C for transesterification of vegetable oil to biodiesel. Different basic sites generated by increasing the pre-treatment temperature appear to correspond

to the ion pairs of different coordination numbers. However, the correspondence between the catalytically active sites for different reaction types and the coordination number of the ion pairs is not definite yet.

Further work is also needed to study the method regenerating MgO for transesterification of vegetable oil to biodiesel. The studied MgO catalyst activation procedure is at 600 °C, which cause the decrease of surface area. Regardless of the recycle method, the activity of fresh MgO catalyst can not be regenerated.

As vegetable oils and alcohols commonly contain water, the influence of the presence of water on MgO deserves further investigation. It was found that MgO catalysts were more affected by the presence of water for reaction running at 60 °C than 200 °C. Therefore, further work is needed to study the effect of water for the reaction, transesterification of vegetable oil to biodiesel.

Appendix One

Product analysis and characterization

A5.1 Product (2a) with 4-phenyl-3-butyn-2-one 1a as the substrate

Figure A5.1 gives the GC result with **1a** as the substrate. For the blank reaction, only the reactant peaks appear and no product was obtained. When the MgO was used as catalyst, no reactant peak appeared and only product was obtained.Figure A5.2 and Figure A5.3 showed the MS spectrum and ^{1}H-NMR pattern of product characteristic of **2a**.

A5.2 Product (2b) with diphenylpropynone (1b) as the substrate

The high boiling point of **2b** made it impossible to determine the conversion by GC. Therefore, the yield was calculated based on the ^{1}H NMR data. Figure A5.4 shows the ^{1}H-NMR pattern was characteristic of the product **2b**. As shown in Figure A5.4, pure **2b** was obtained almost no reactant left.

A5.3 Product (2c) with 2-octynal (1c) as the substrate

Figure A5.5 gives the GC result with **1c** as the substrate. For the blank reaction, only the reactant peaks appear and no product was obtained. When the MgO was used as catalyst, no reactant peak appeared and only product was observed.Figure A5.6 and Figure A5.7 show the MS spectrum and ^{1}H-NMR pattern of product characteristic of **2c**.

A5.4 Product (2d) with 4-(trimethylsilyl)-3-butyn-2-one (1d) as the substrate

Figure A5.8 gives the GC result with **1d** as the substrate. For the blank reaction, only the reactant peaks appear and no product was obtained. When the MgO was used as

catalyst, no reactant peak appeared and only product was obtained. Figure A5.9, Figure A5.10 and Figure A5.11 showed the MS spectrum and ^{1}H-NMR and ^{13}C-NMR patterns of product characteristic of **2d** respectively.

A5.5 Product (2e) with 3-butyn-2-one (1e) as the substrate

After a solution of **1e** and **2e** were injected in the GC, there was no peak corresponding to these observed. This may be ascribed to the fact that these two chemicals were unstable at high temperature, since the injection temperature and column temperature were high. Therefore, the yield was calculated based on the ^{1}H NMR data. Figure A5.12 and Figure A5.13 show ^{1}H-NMR and ^{13}C-NMR patterns of product characteristic of **2e**. As shown in Figures A5.12 and A5.13, pure **2e** was obtained and almost no reactant was left.

A5.6 Product (2f) with ethyl propiolate (1f) as the substrate

Figure A5.14 gives the GC result with **1f** as the substrate. For the blank reaction, only the reactant peaks appear and no product was obtained. When the MgO was used as catalyst, no reactant peak appeared and only product was obtained.Figure A5.15, Figure A5.16 and Figure A5.17, respectively, show the MS spectrum, ^{1}H-NMR and ^{13}C-NMR patterns of the product characteristic of **2f**.

A5.7 Product (2g) with methyl propiolate (1g) as the substrate

Figure A5.18 gives the GC result with **1g** as the substrate. For the blank reaction, only the reactant peaks appear and no product was obtained. When the MgO was used as catalyst, no reactant peak appeared and only product was obtained.Figure A5.19, Figure A5.20 and Figure A5.21 show the MS spectrum, ^{1}H-NMR and ^{13}C-NMR patterns of product characteristic of **2g**.

A5.8 Product (2h) with ethyl-2-butynoate (1h) as the substrate

Figure A5.22 gives the GC result with **1h** as the substrate. For the blank reaction, only the reactant peaks appear and no product was obtained. When the MgO was used as catalyst, no reactant peak appeared and only product was obtained. Figure A5.23, Figure A5.24 and Figure A5.25 showed the MS spectrum and ^{1}H-NMR and ^{13}C-NMR patterns of product characteristic of **2h** respectively.

A5.9 Product (2i) with methyl phenylpropiolate (1i) as the substrate

Figure A5.26 and Figure A5.27 showed the ^{1}H-NMR and ^{13}C-NMR patterns of product characteristic of **2i** respectively.

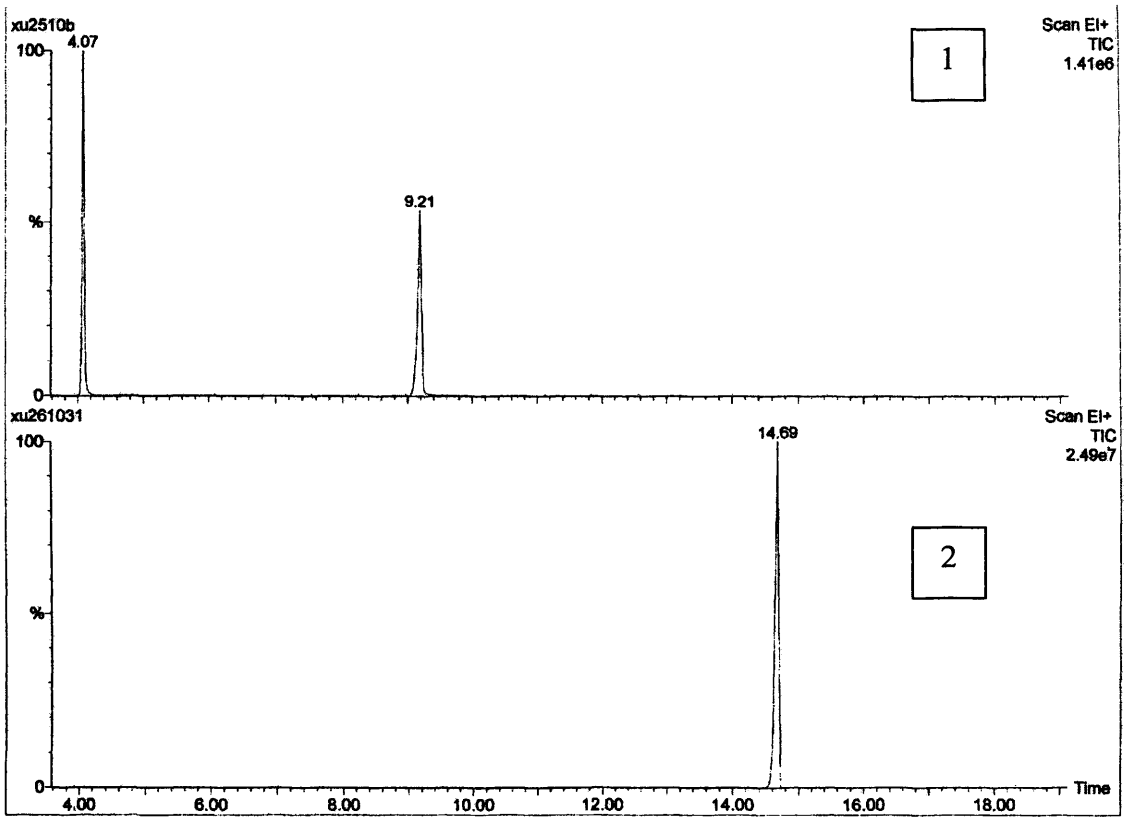

Figure A5.1 GC result with **1a** as the substrate: (1) blank; (2) with MgO-CBC catalyst. Retention time 4.07: 1,3-propanedithiol; Retention time 9.21: **1a**; Retention time 14.69: **2a**.

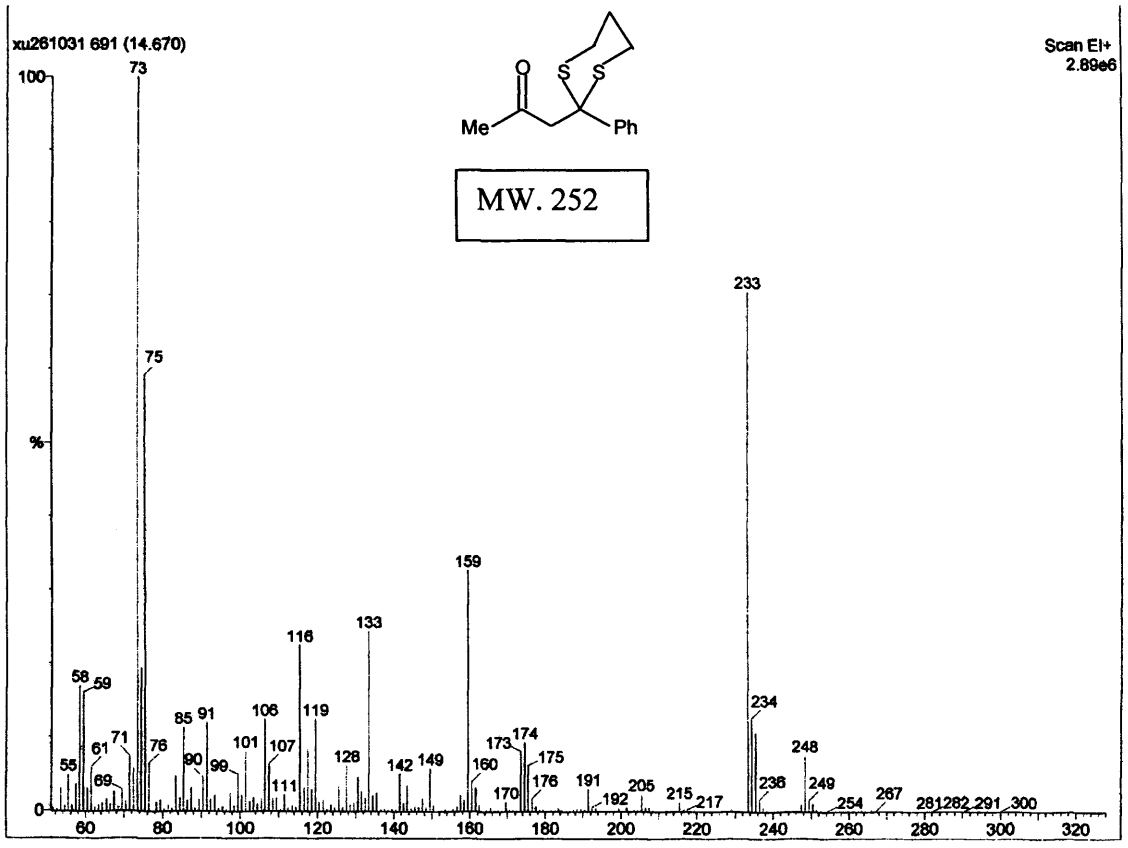

Figure A5.2 MS spectrum of **2a**

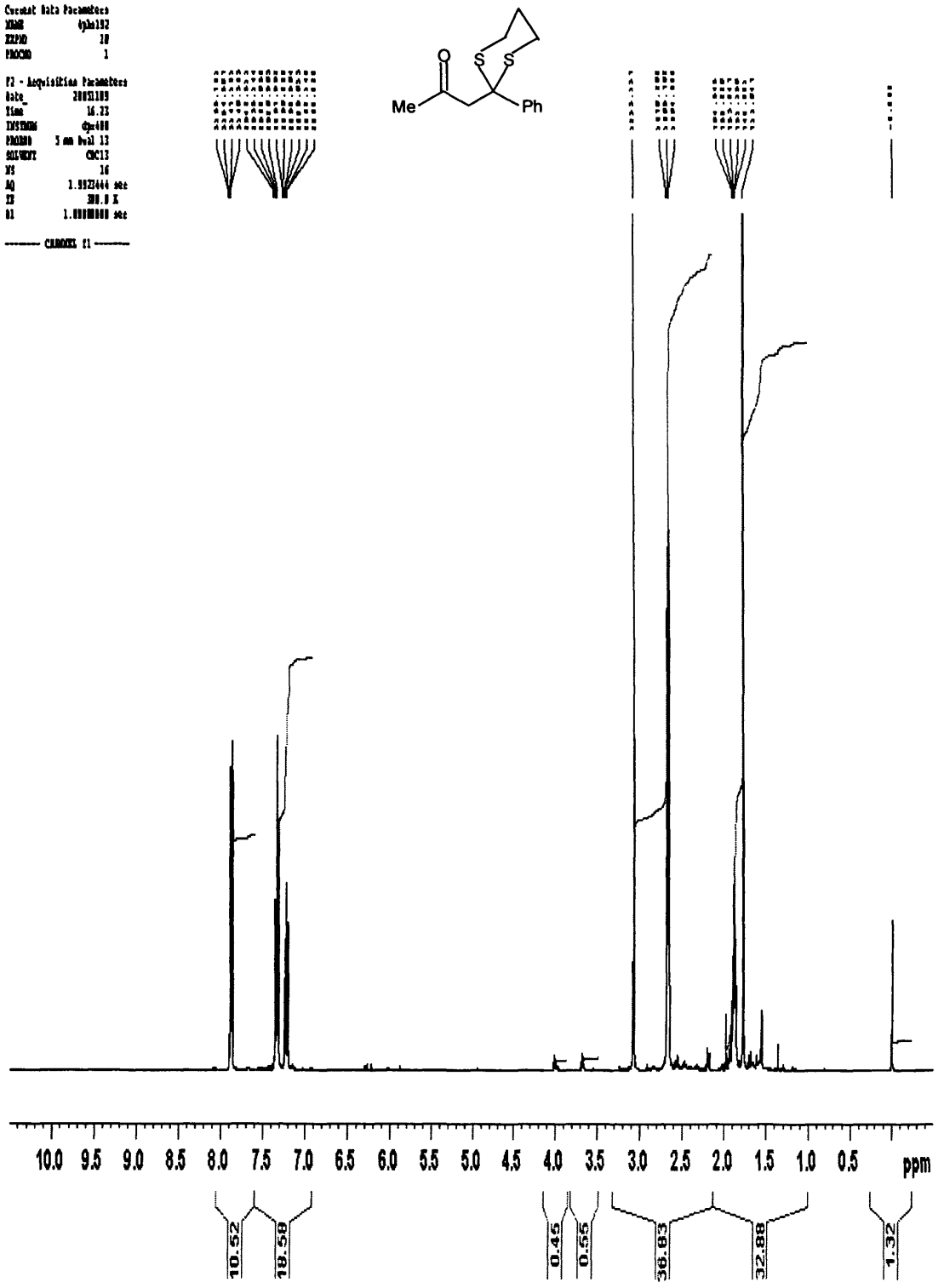

Figure A5.3 ^{1}H-NMR pattern of **2a**

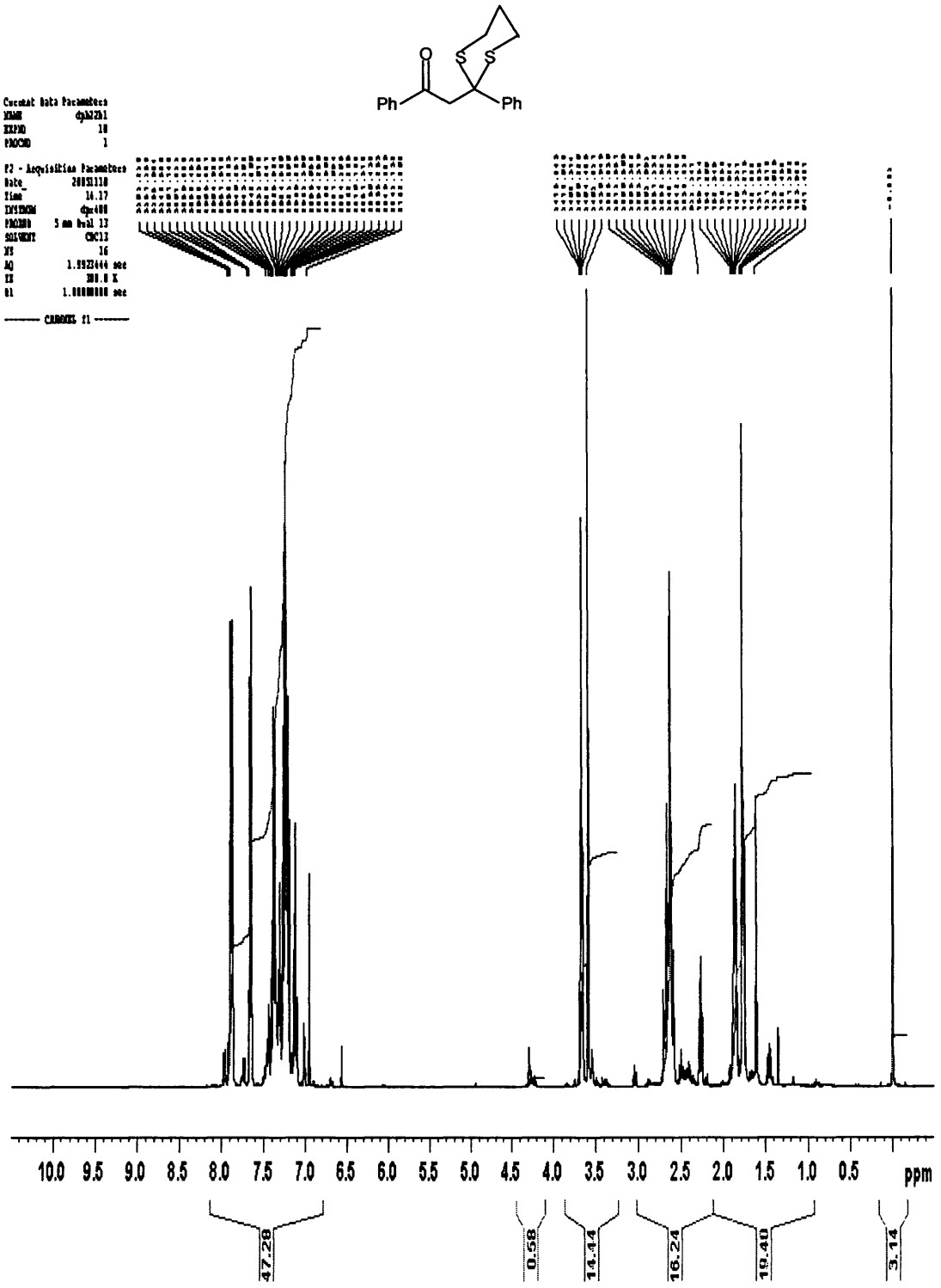

Figure A5.4 ^{1}H-NMR pattern of **2b**

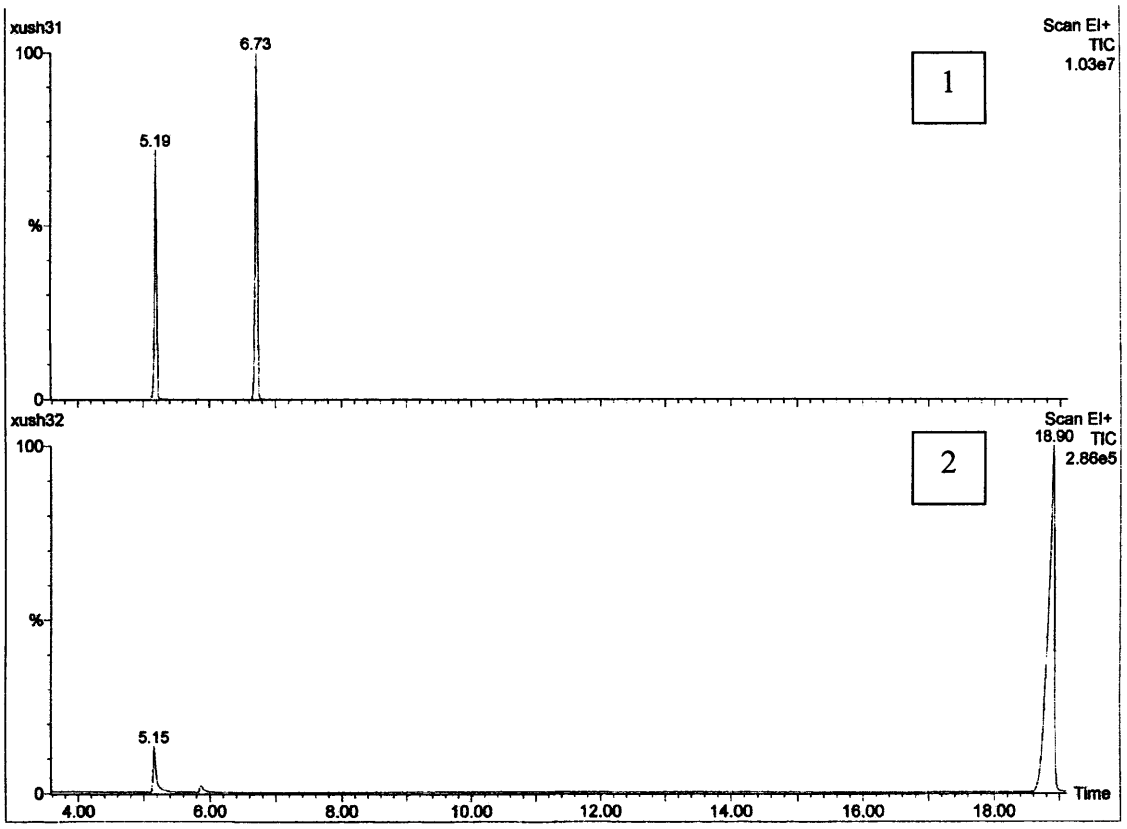

Figure A5.5 GC result with **1c** as the substrate: (1) blank; (2) with MgO-CBC catalyst. Retention time 5.19: 1,3-propanedithiol; Retention time 6.73: **1c**; Retention time 18.90: **2c**.

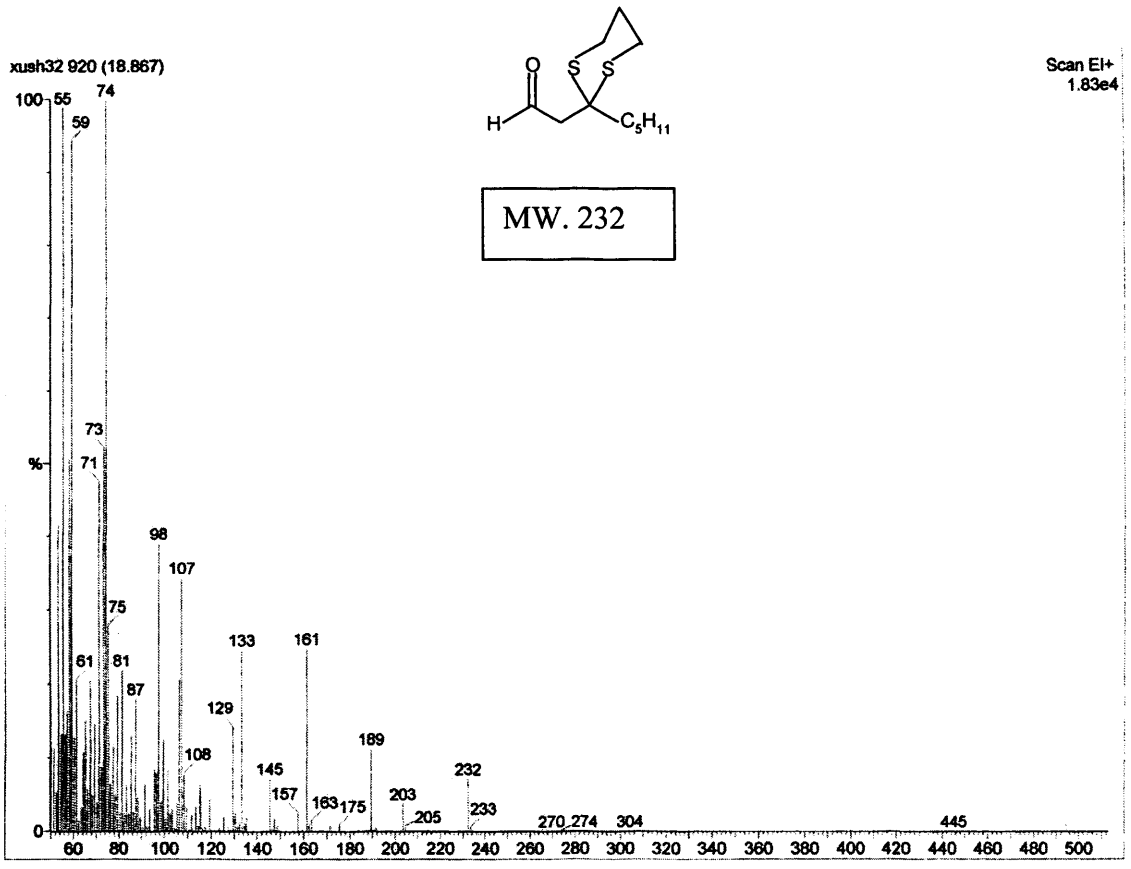

Figure A5.6 MS spectrum of **2c**.

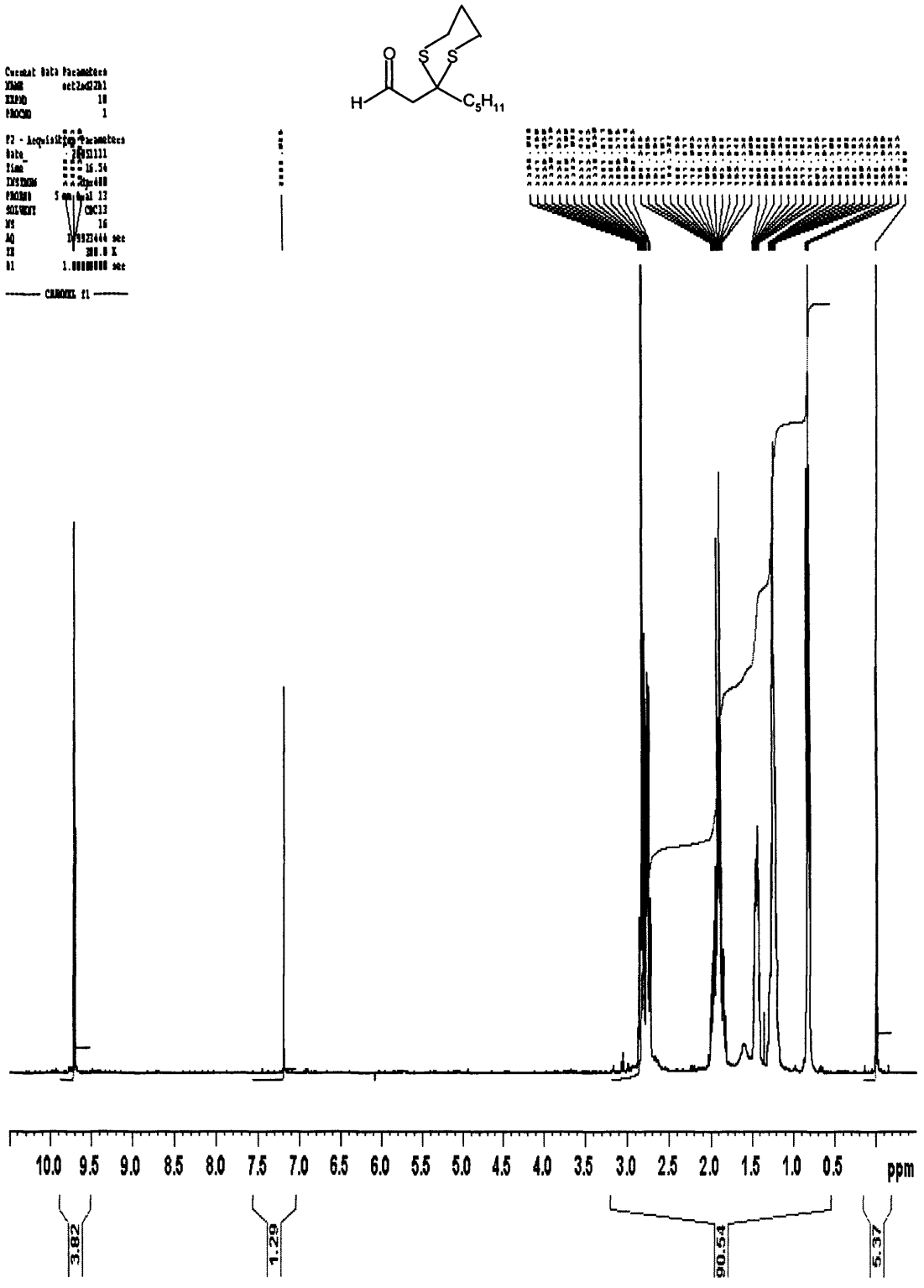

Figure A5.7 ^{1}H-NMR pattern of **2c**

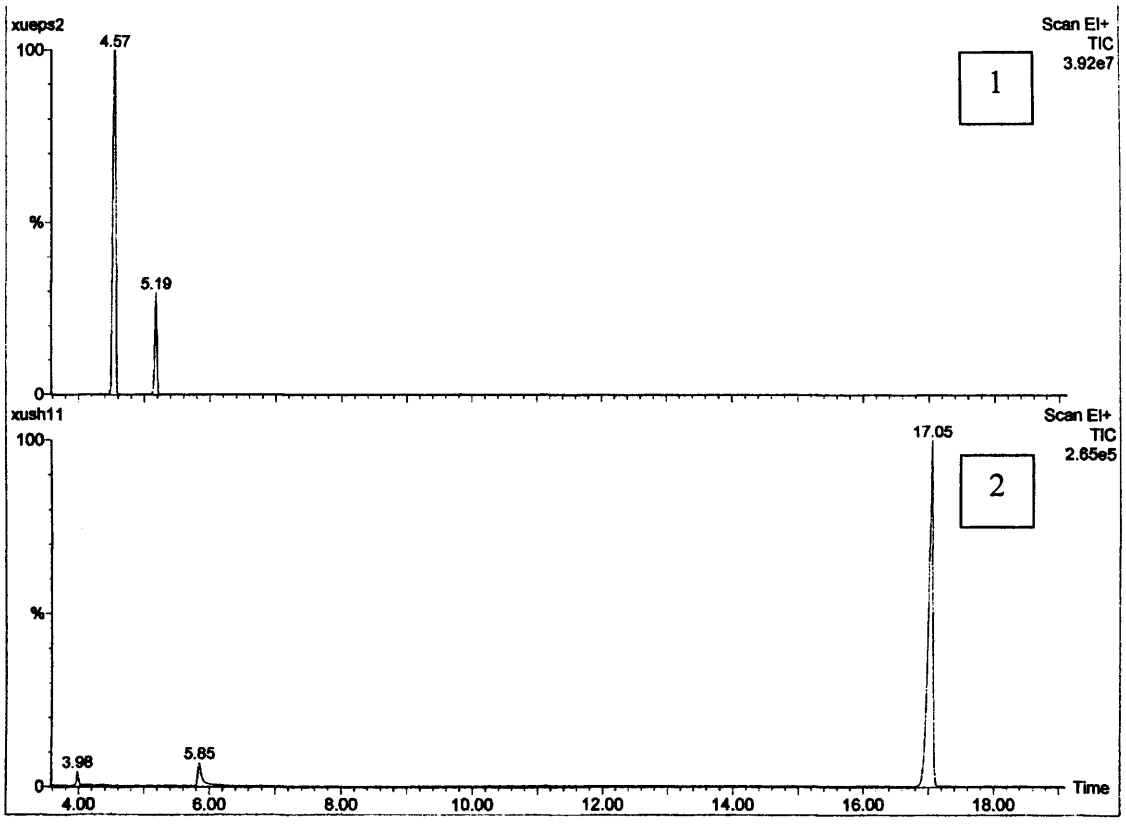

Figure A5.8 GC result with **1d** as the substrate: (1) blank; (2) with MgO-CBC catalyst. Retention time 5.19: 1,3-propanedithiol; Retention time 4.57: **1d**; Retention time 17.05: **2d**.

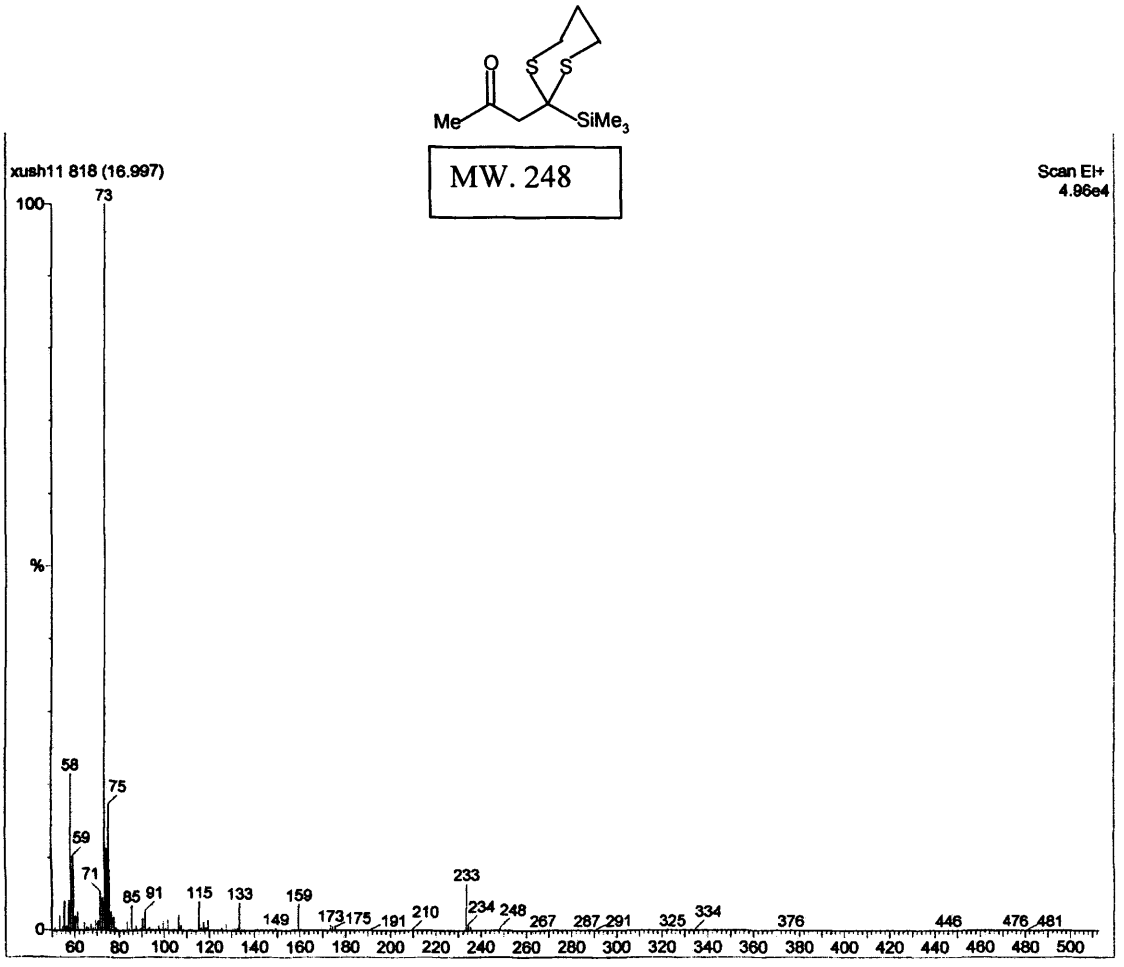

Figure A5.9 MS spectrum of **2d**

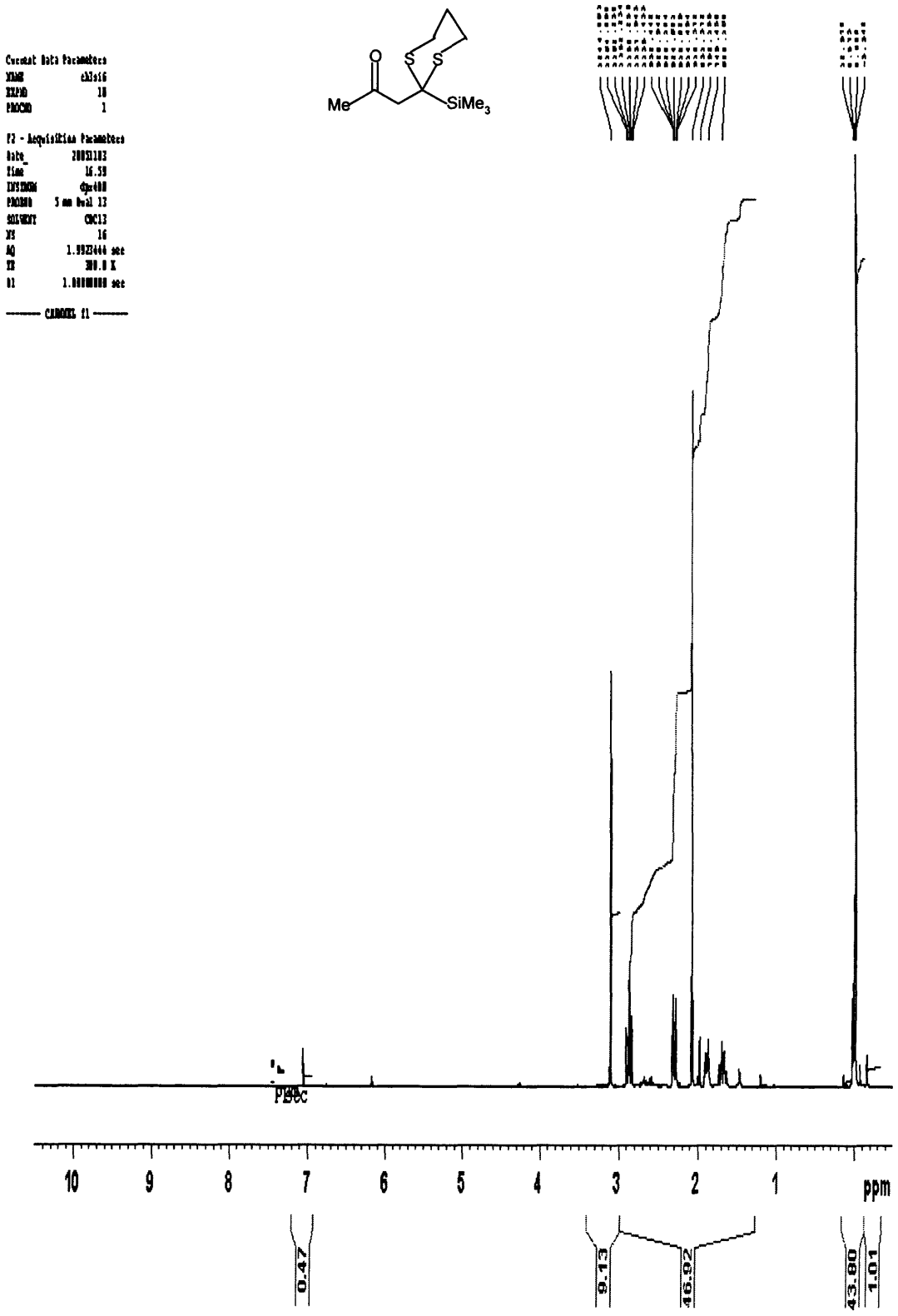

Figure A5.10 ^{1}H-NMR pattern of **2d**

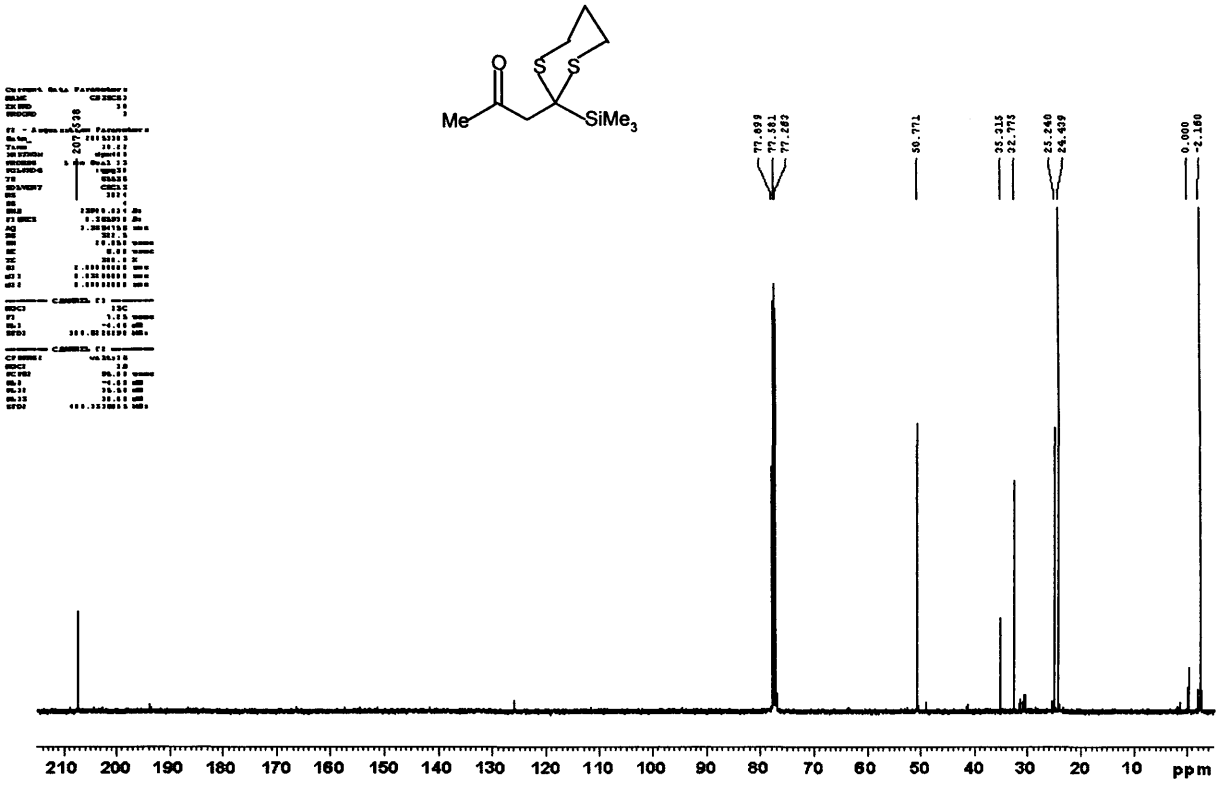


```
Current Data Parameters
NAME                  CH3SC61
EXPNO                      10
PROCNO                      1

F2 - Acquisition Parameters
Date_               20051103
Time                   18.22
INSTRUM                dpx400
PROBHD      5 mm Dual 13
PULPROG              zgpg30
TD                    65536
SOLVENT               CDCl3
NS                     1024
DS                        4
SWH                23980.814 Hz
FIDRES             0.365918 Hz
AQ                 1.3664756 sec
RG                     322.5
```

Figure A5.11 ^{13}C-NMR pattern of **2d**

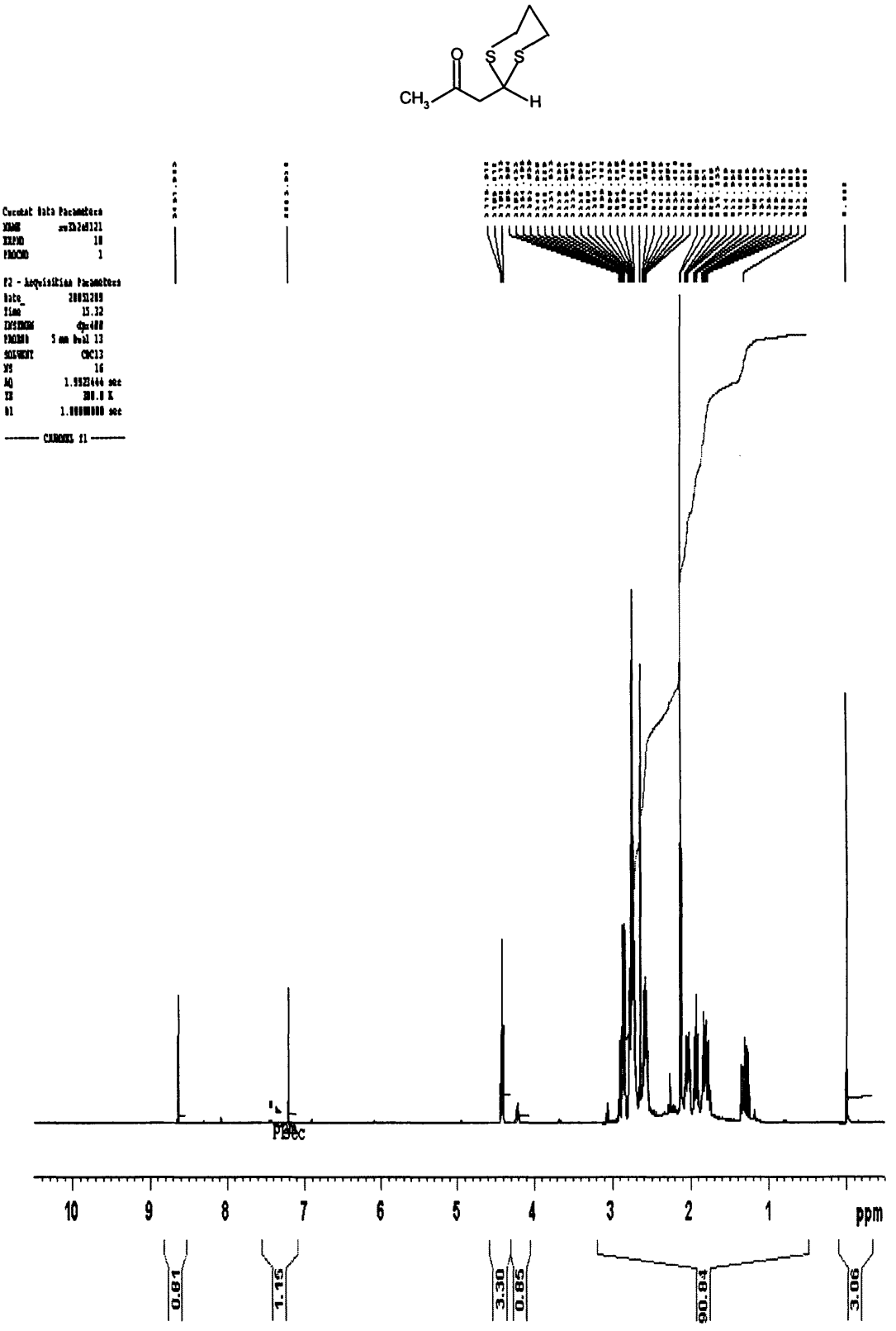

Figure A5.12 ^{1}H-NMR pattern of **2e**

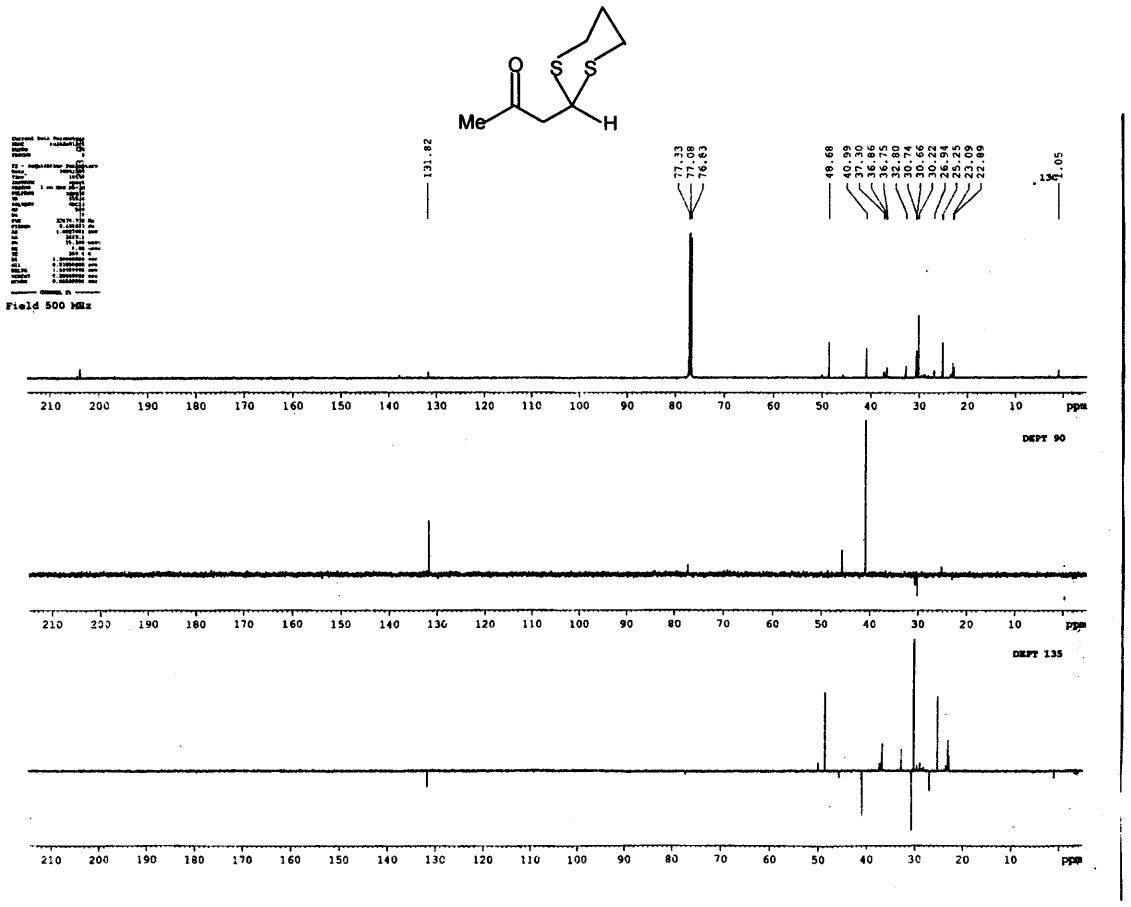

Figure A5.13 ^{13}C-NMR pattern of **2e**

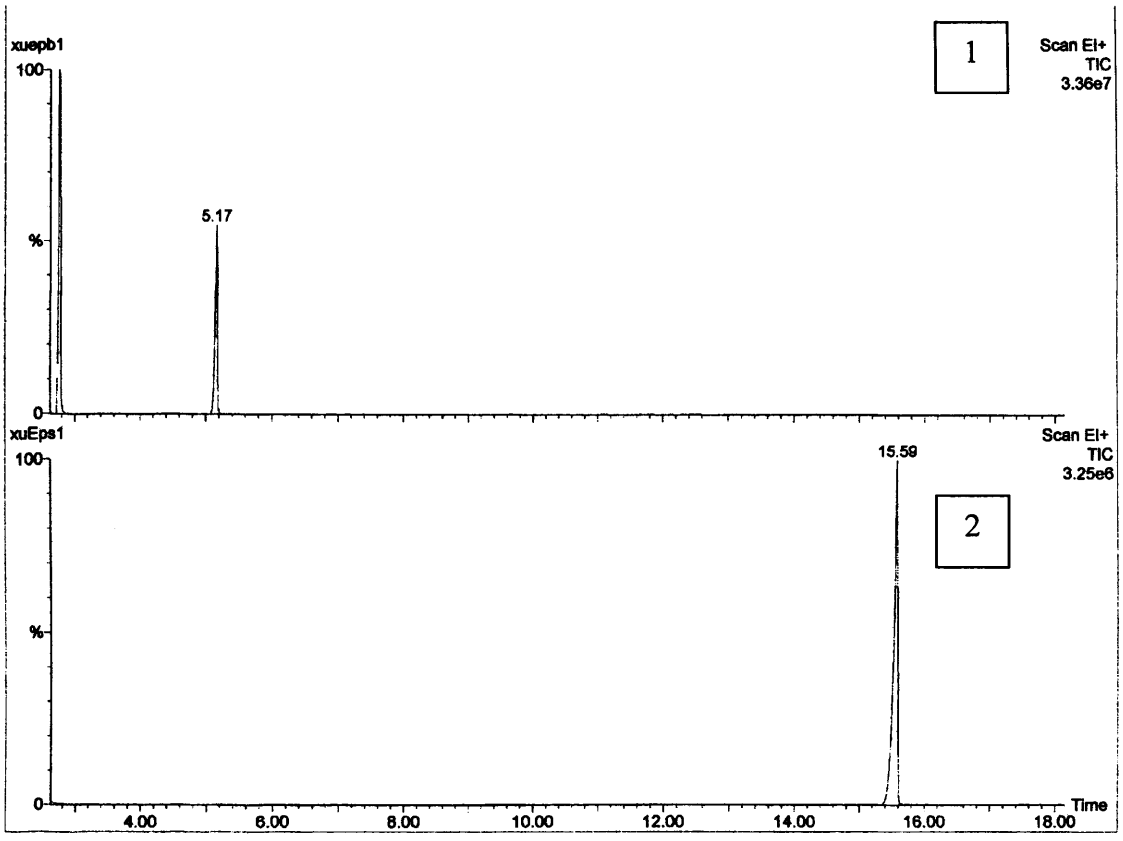

Figure A5.14 GC result with **1f** as the substrate: (1) blank; (2) with MgO-CBC catalyst.

Retention time 5.17: 1,3-propanedithiol; Retention time 15.59: **2f**.

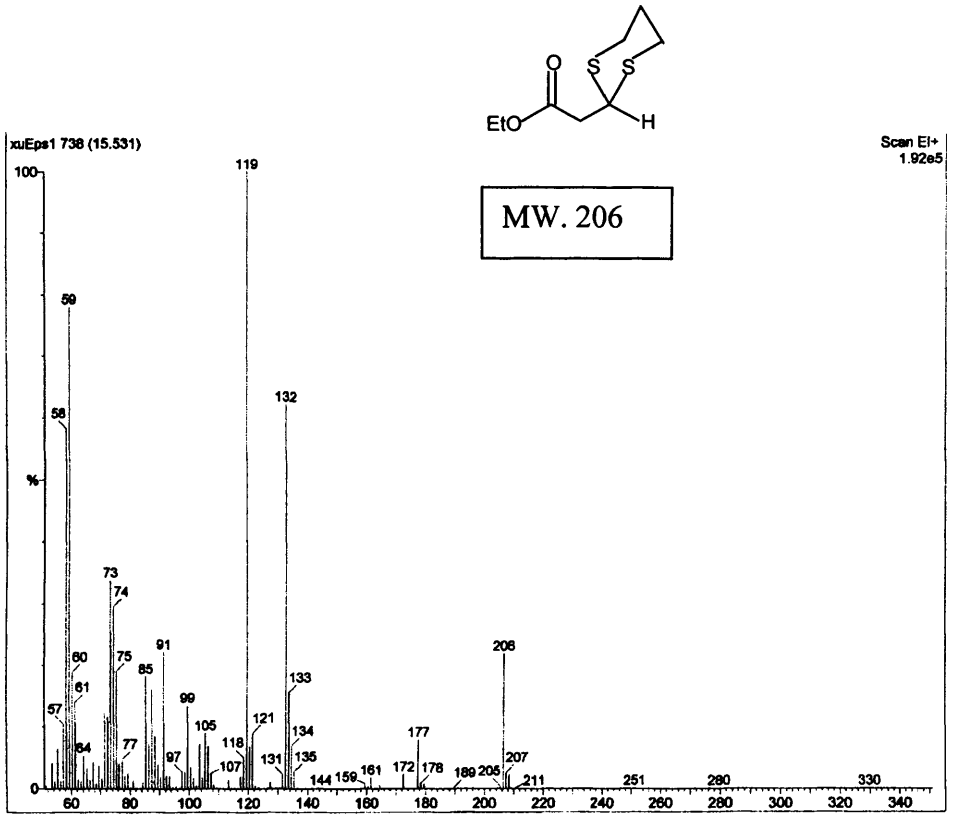

Figure A5.15 MS spectrum of **2f**.

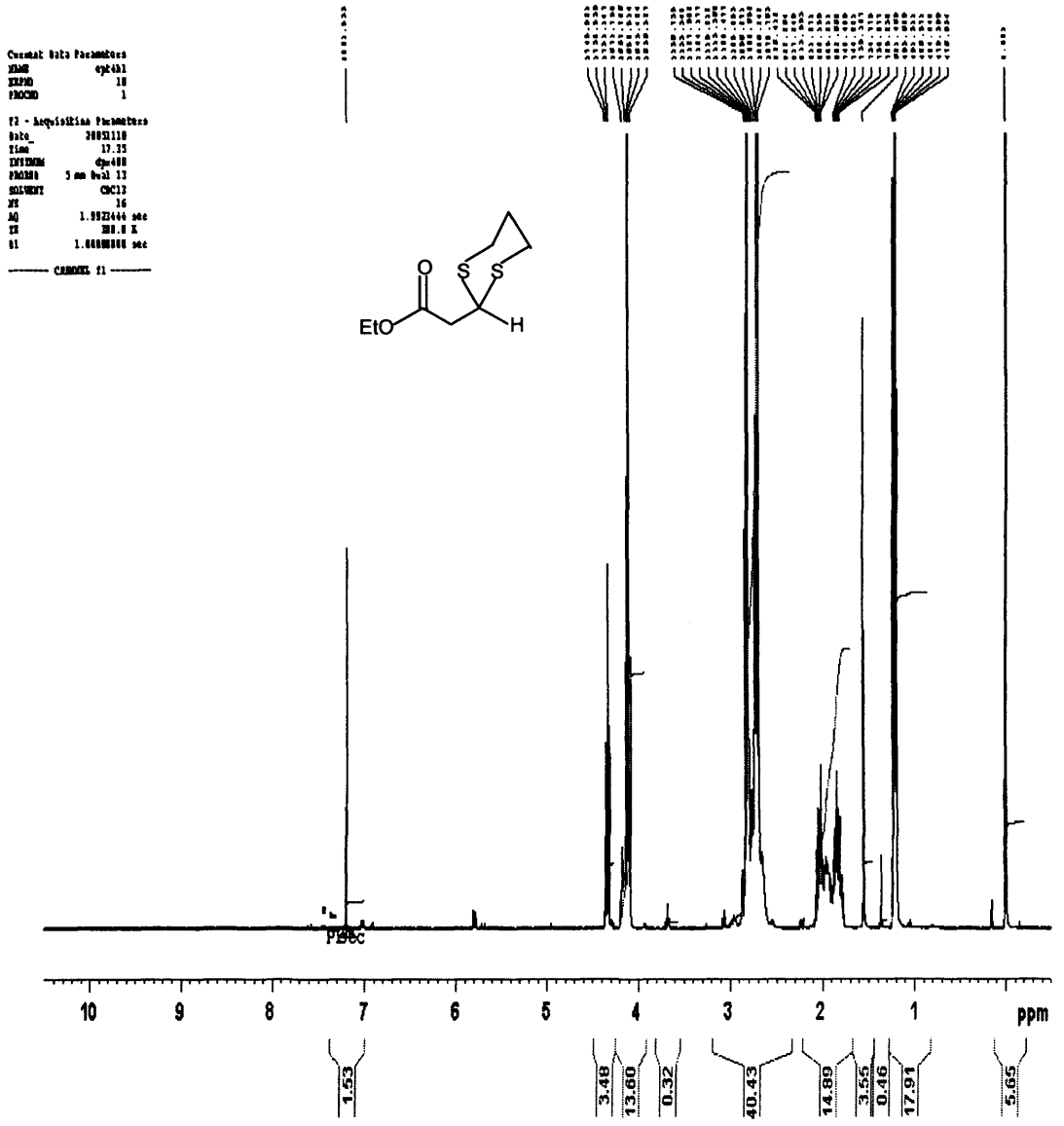

Figure A5.16 ^{1}H-NMR pattern of **2f**

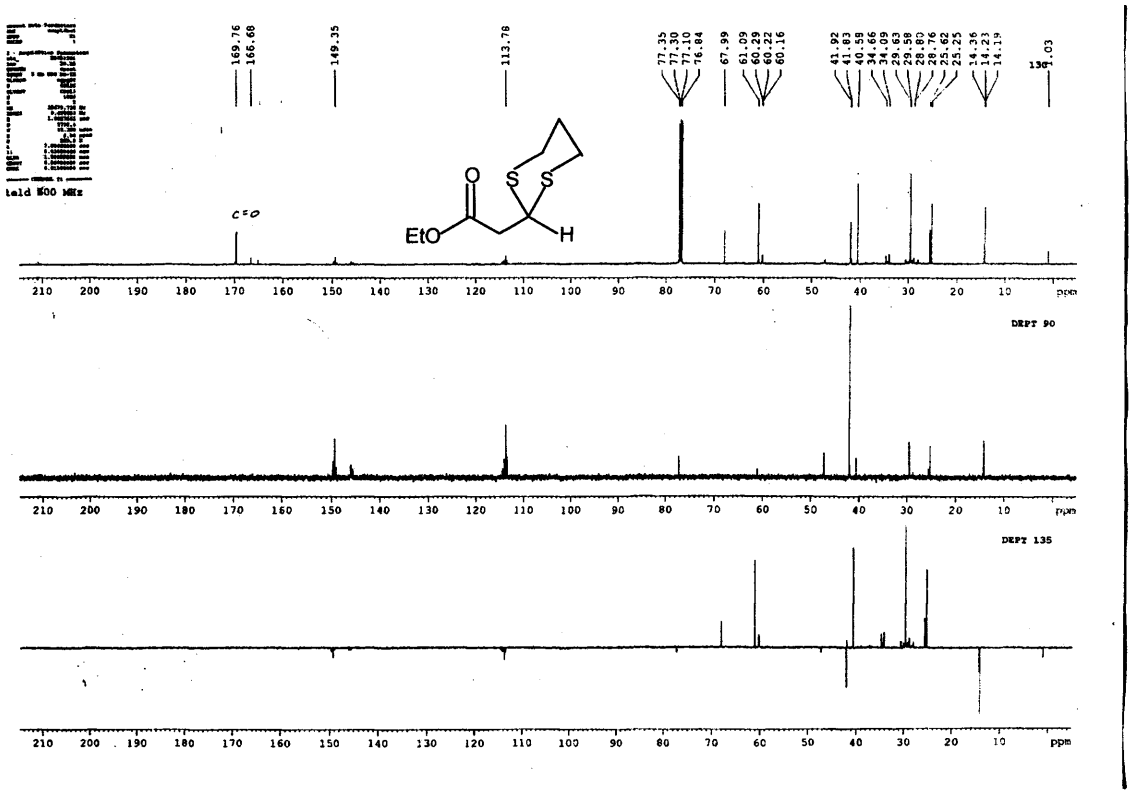

Figure A5.17 ^{13}C-NMR pattern of **2f**

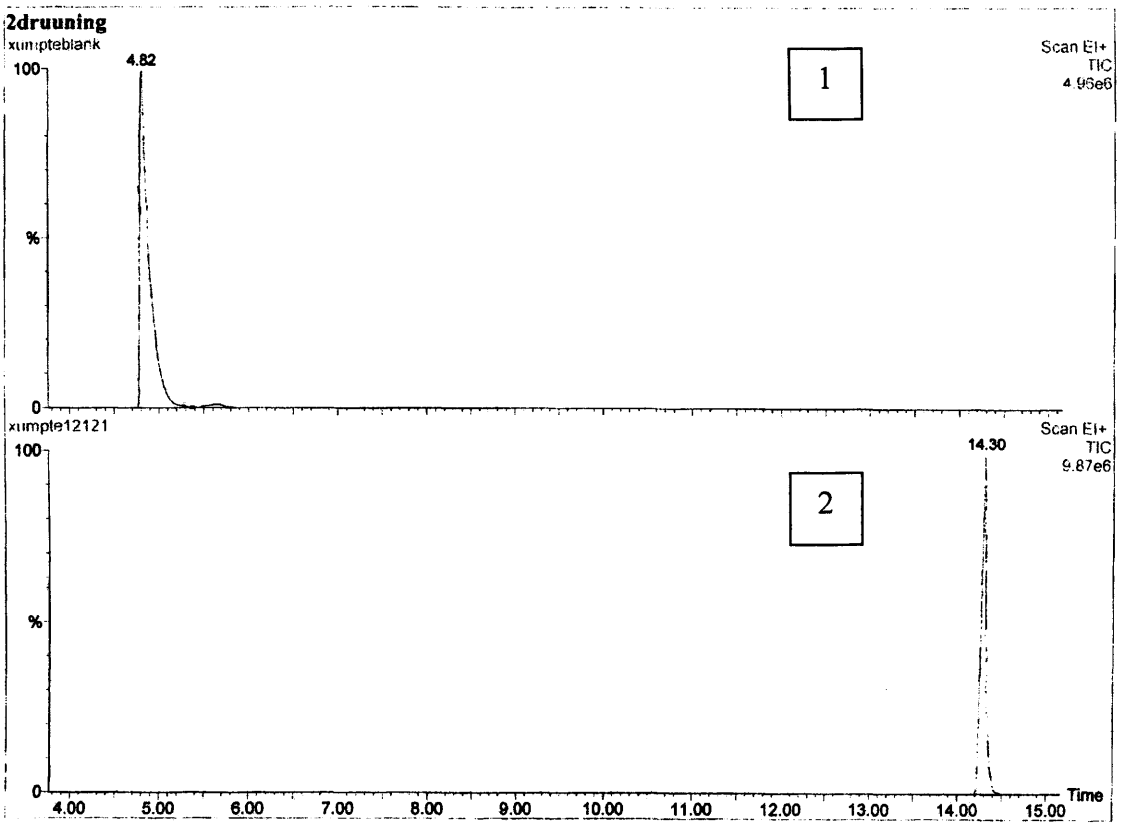

Figure A5.18 GC result with **1g** as the substrate: (1) blank; (2) with MgO-CBC catalyst. Retention time 4.82: 1,3-propanedithiol; Retention time 14.03: **2g**.

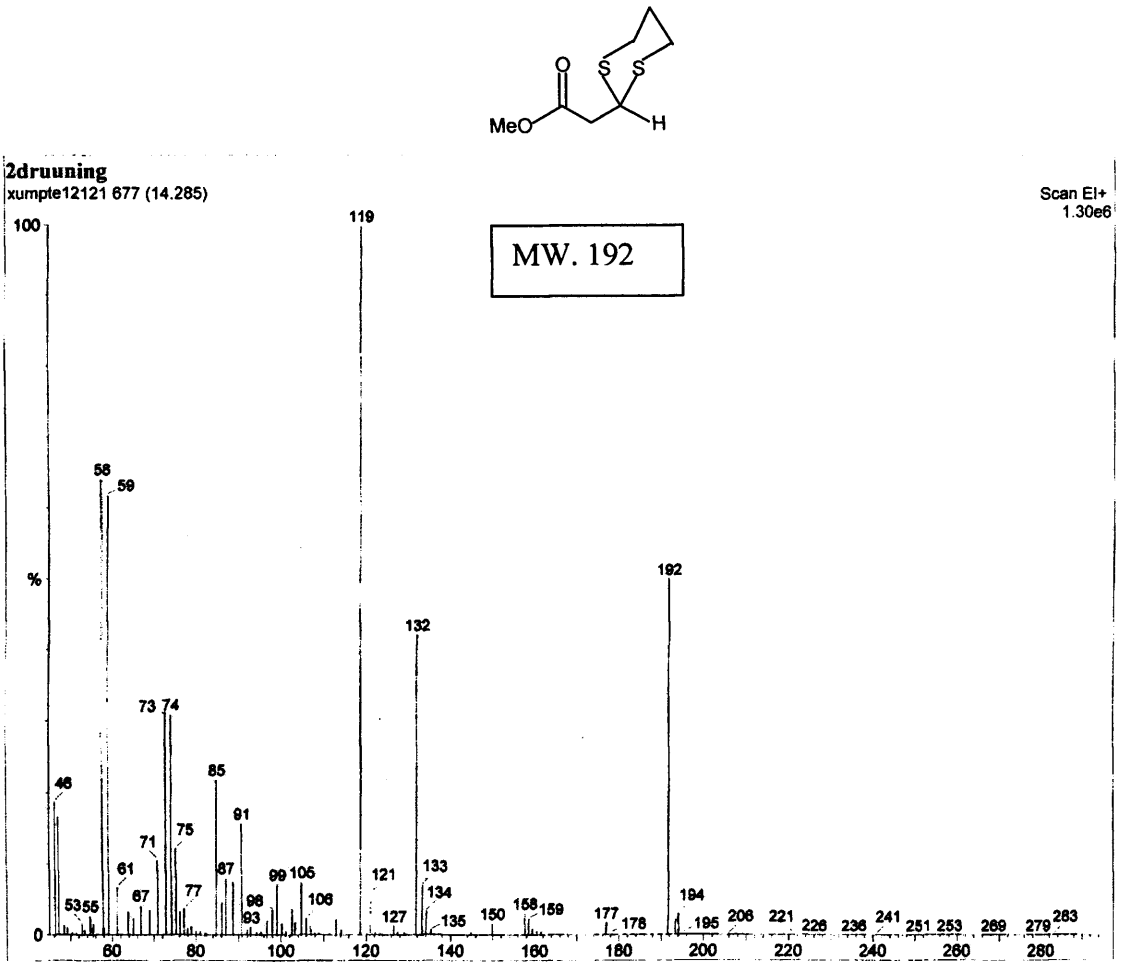

Figure A5.19 MS spectrum of **2g**

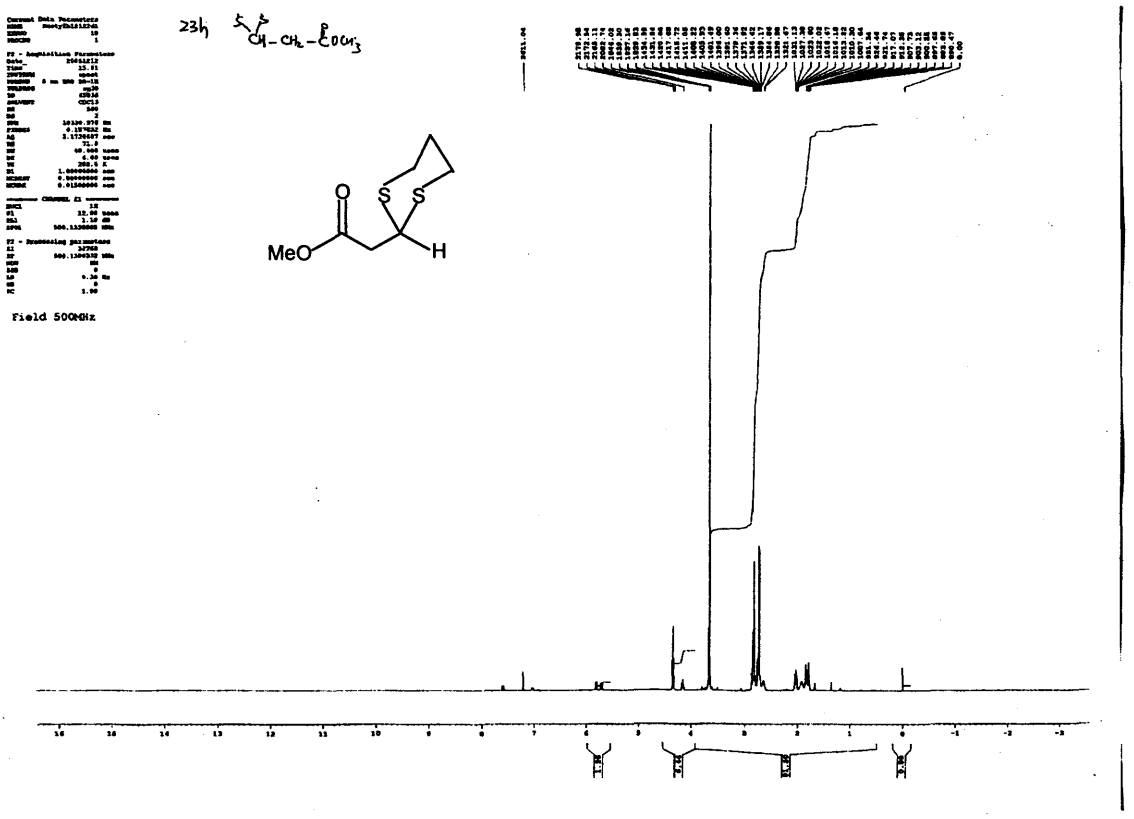

Figure A5.20 ^{1}H-NMR pattern of **2g**

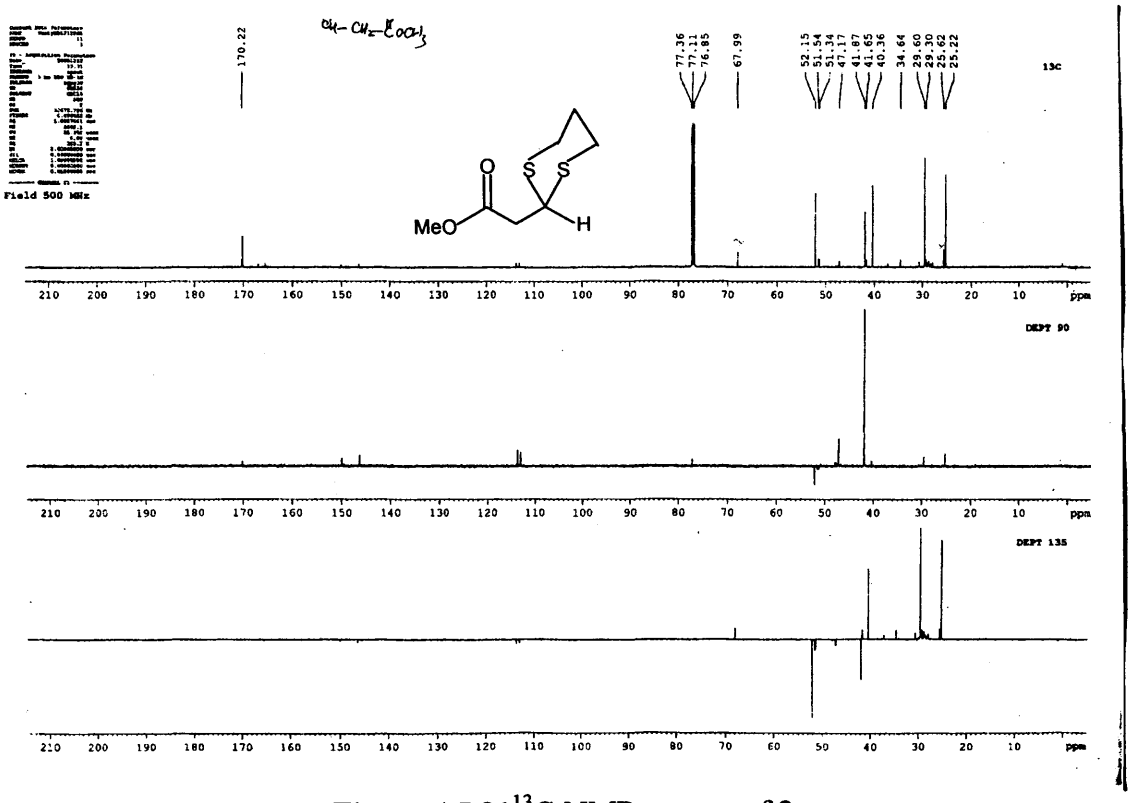

Figure A5.21 ^{13}C-NMR pattern of **2g**

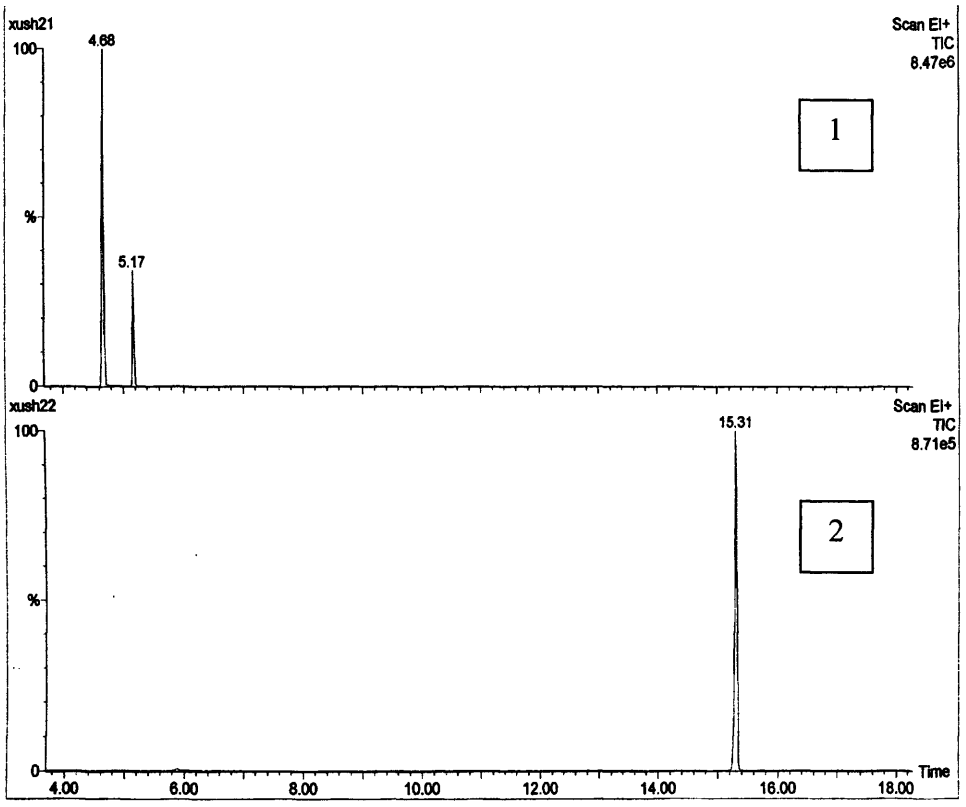

Figure A5.22 GC result with **1h** as the substrate: (1) blank; (2) with MgO-CBC catalyst. Retention time 4.68: ethyl-2-butynoate; retention time 5.17: 1,3-propanedithiol; retention time 15.31: **2h**.

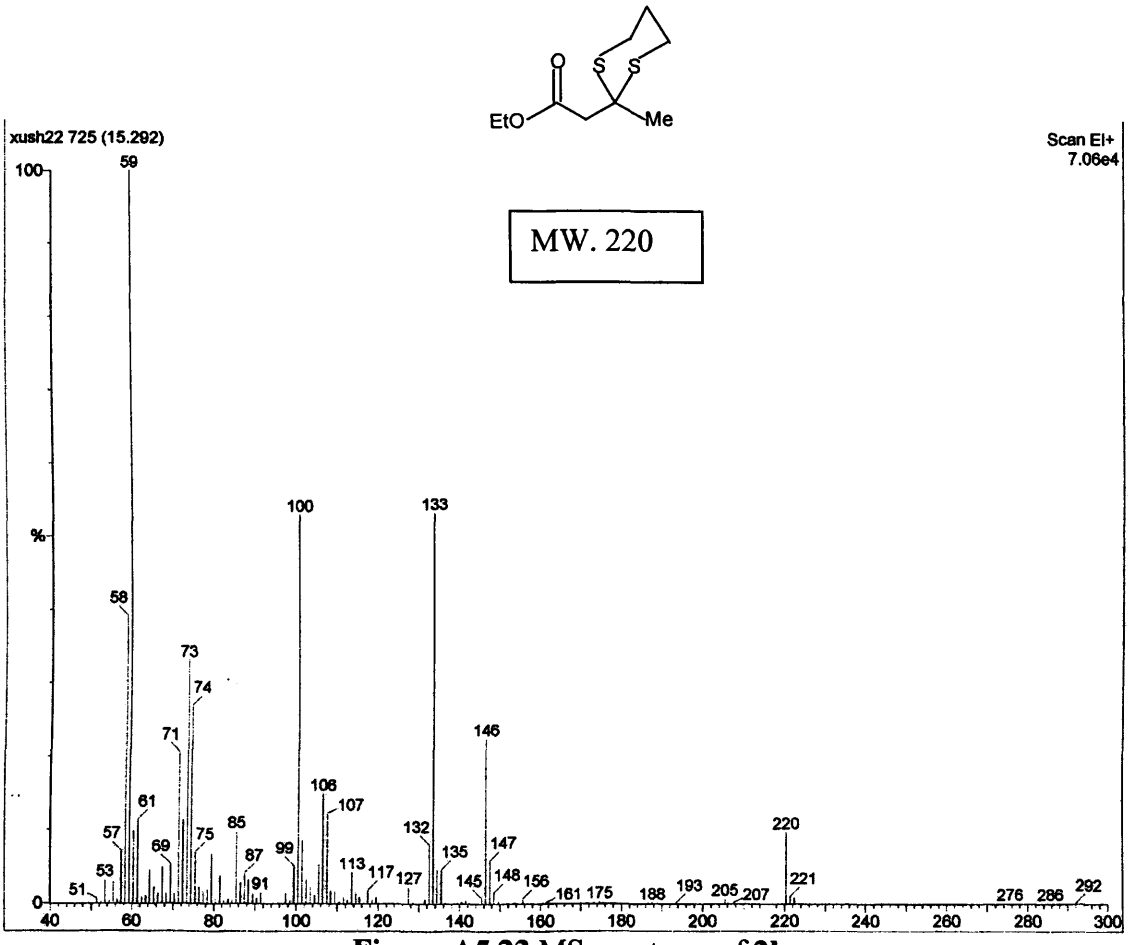

Figure A5.23 MS spectrum of **2h**

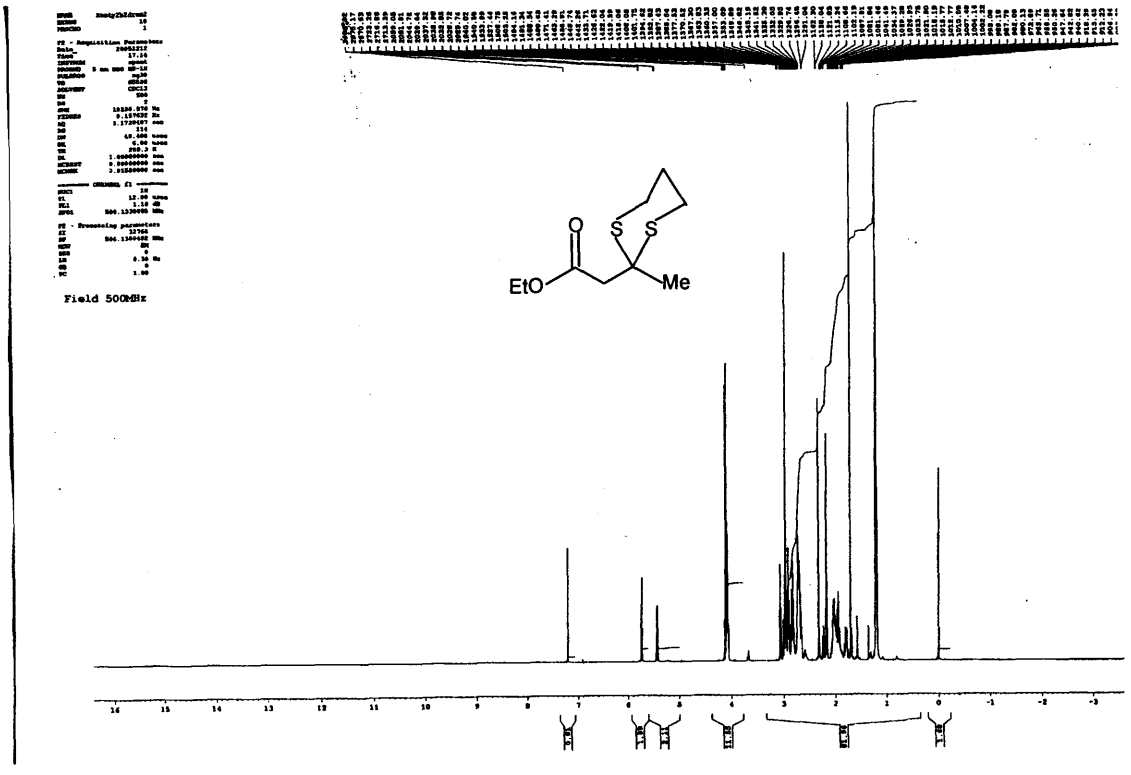

Figure A5.24 ^{1}H-NMR pattern of **2h**

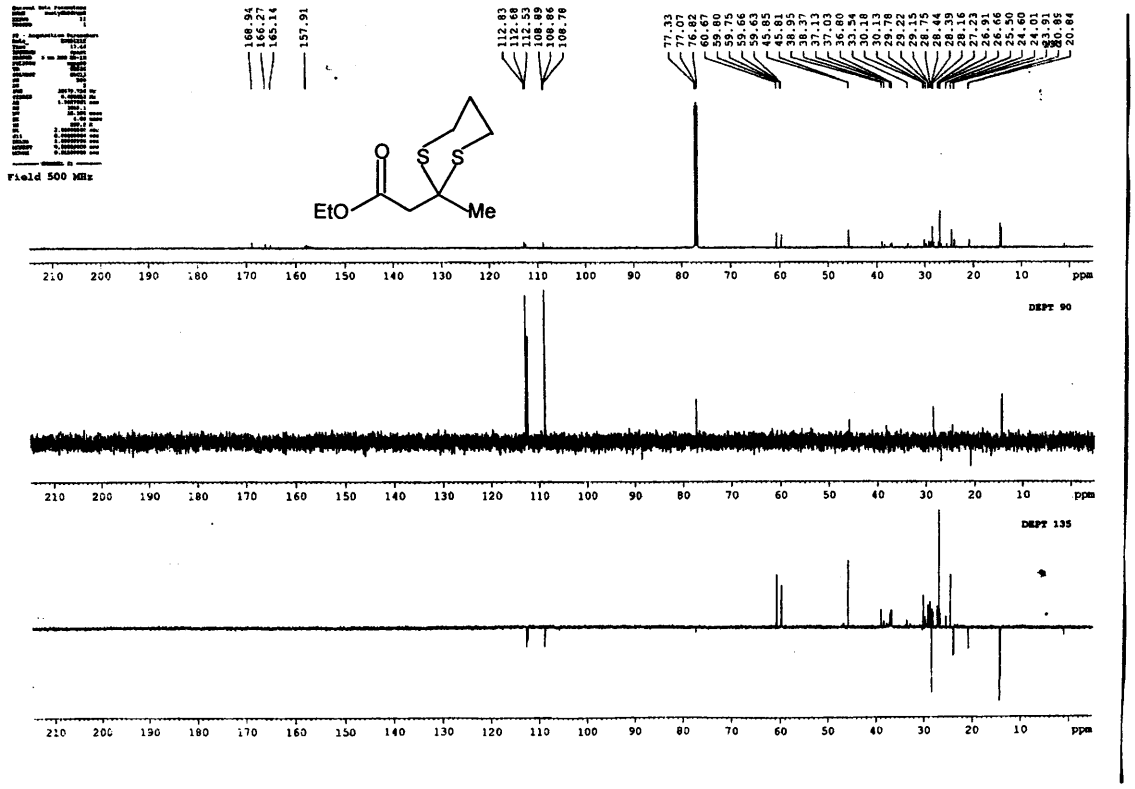

Figure A5.25 ^{13}C-NMR pattern of **2h**

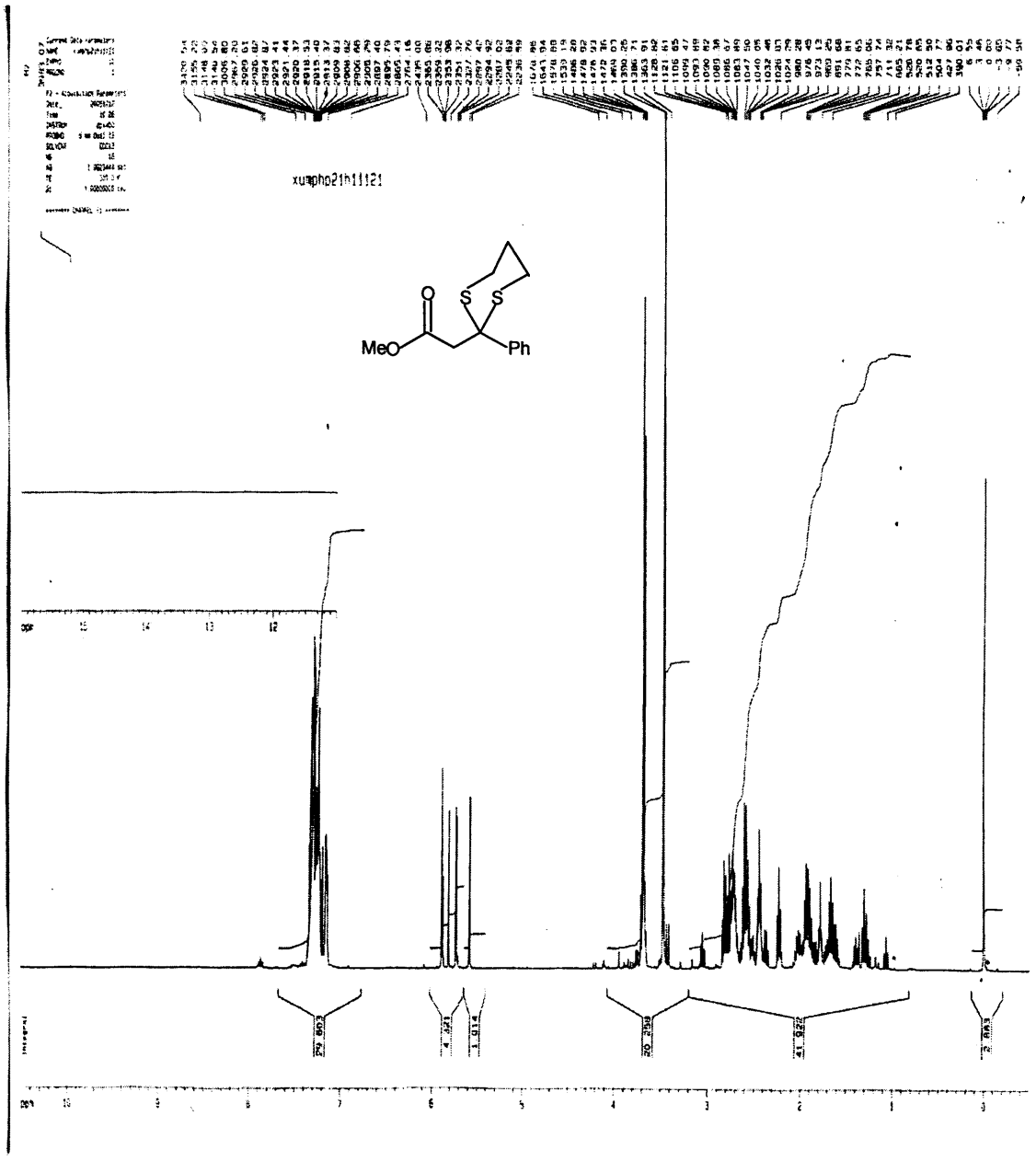

Figure A5.26 ^{1}H-NMR pattern of **2i**

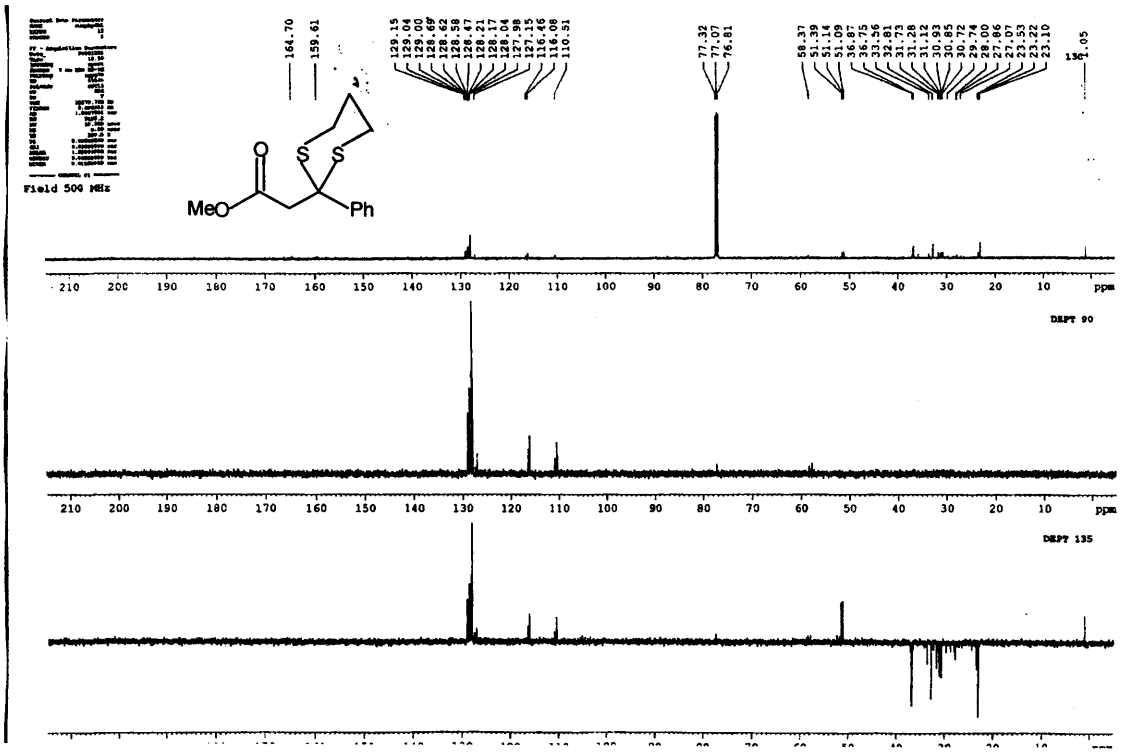

Figure A5.27 ^{13}C-NMR pattern of **2i**

Appendix Two

HPLC results for transesterification of vegetable oil to biodiesel

Table A6.1

Reaction at 200 °C for 15mins – Blank; methanol:oil ratio (6:1)

	Sample 1	Sample 2
Mass of triglyceride	172.250	173.875
Mass of diglyceride	30.925	31.250
Mass of monoglyceride	4.625	4.575
Mass of methyl ester	13.350	13.550
Moles of triglyceride	0.15972	0.19757
Moles of diglyceride	0.05009	0.05061
Moles of monoglyceride	0.01304	0.01290
Moles of methyl ester	0.04530	0.04598
Yield of triglyceride	78.24	78.98
Yield of diglyceride	13.35	13.49
Yield of monoglyceride	1.74	1.72
Yield of methyl ester	**6.04**	**6.13**
Mass balance	**99.36**	**100.31**

Table A6.2

Reaction at 200 °C for 15mins – catalyst [a]; methanol:oil ratio (6:1)

	Sample 1	Sample 2
Mass of triglyceride	120.625	121.325
Mass of diglyceride	42.475	42.250
Mass of monoglyceride	11.025	10.925
Mass of methyl ester	33.650	33.650
Moles of triglyceride	0.13706	0.13786
Moles of diglyceride	0.06880	0.06843
Moles of monoglyceride	0.03108	0.03080
Moles of methyl ester	0.11418	0.11418
Yield of triglyceride	54.78	55.10
Yield of diglyceride	18.33	18.23
Yield of monoglyceride	4.14	4.10
Yield of methyl ester	**15.21**	**15.21**
Mass balance	**92.47**	**92.65**

[a] obtained by calcination of the precursors commercially available $(MgCO_3)_4 \cdot Mg(OH)_2$ (Alfa Aesar) in flow N_2 at 350 °C for 2 hours.

Table A6.3

Reaction at 200 °C for 15mins – catalyst [a]; methanol:oil ratio (6:1)

	Sample 1	Sample 2
Mass of triglyceride	100.325	97.075
Mass of diglyceride	35.100	32.675
Mass of monoglyceride	12.750	13.500
Mass of methyl ester	63.225	64.100
Moles of triglyceride	0.114	0.1103
Moles of diglyceride	0.05685	0.05292
Moles of monoglyceride	0.03594	0.03806
Moles of methyl ester	0.2145	0.2175
Yield of triglyceride	45.55	44.08
Yield of diglyceride	15.15	14.10
Yield of monoglyceride	4.79	28.97
Yield of methyl ester	**28.58**	**28.97**
Mass balance	**94.07**	**92.22**

[a] obtained by calcination of the precursors commercially available $(MgCO_3)_4{\cdot}Mg(OH)_2$ (Alfa Aesar) in flow N_2 at 450 °C for 2 hours.

Table A6.4

Reaction at 200 °C for 15mins – catalyst [a]; methanol:oil ratio (6:1)

	Sample 1	Sample 2
Mass of triglyceride	12.550	12.375
Mass of diglyceride	16.650	18.925
Mass of monoglyceride	29.025	30.125
Mass of methyl ester	149.250	151.475
Moles of triglyceride	0.01426	0.01406
Moles of diglyceride	0.02697	0.03065
Moles of monoglyceride	0.08182	0.08492
Moles of methyl ester	0.50643	0.51398
Yield of triglyceride	5.70	5.62
Yield of diglyceride	7.19	8.17
Yield of monoglyceride	10.91	11.32
Yield of methyl ester	**67.52**	**68.53**
Mass balance	**91.33**	**93.65**

[a] obtained by calcination of the precursors commercially available $(MgCO_3)_4{\cdot}Mg(OH)_2$ (Alfa Aesar) in flow N_2 at 600 °C for 2 hours.

Table A6.5

Reaction at 200 °C for 15mins – blank; methanol:oil ratio (12:1)

	Sample 1	Sample 2
Mass of triglyceride	188.275	185.075
Mass of diglyceride	19.875	19.525
Mass of monoglyceride	0	0
Mass of methyl ester	5.350	5.400
Moles of triglyceride	0.21393	0.21029
Moles of diglyceride	0.03219	0.03162
Moles of monoglyceride	0	0
Moles of methyl ester	0.01815	0.01832
Yield of triglyceride	85.57	84.11
Yield of diglyceride	8.58	8.43
Yield of monoglyceride	0	0
Yield of methyl ester	**2.42**	**2.44**
Mass balance	**96.57**	**94.99**

Table A6.6

Reaction at 200 °C for 15mins – catalyst [a]; methanol:oil ratio (12:1)

	Sample 1	Sample 2
Mass of triglyceride	55.200	54.875
Mass of diglyceride	42.700	42.425
Mass of monoglyceride	22.525	21.750
Mass of methyl ester	89.550	88.825
Moles of triglyceride	0.06272	0.06235
Moles of diglyceride	0.06916	0.06871
Moles of monoglyceride	0.06350	0.06131
Moles of methyl ester	0.30386	0.30140
Yield of triglyceride	25.06	24.91
Yield of diglyceride	18.42	18.30
Yield of monoglyceride	8.46	8.17
Yield of methyl ester	**40.47**	**40.14**
Mass balance	**92.40**	**91.52**

[a] obtained by calcination of the precursors commercially available $(MgCO_3)_4 \cdot Mg(OH)_2$ (Alfa Aesar) in flow N_2 at 350 °C for 2 hours.

Table A6.7

Reaction at 200 °C for 15mins – catalyst [a]; methanol:oil ratio (12:1)

	Sample 1	Sample 2
Mass of triglyceride	52.150	51.275
Mass of diglyceride	37.275	35.975
Mass of monoglyceride	20.275	20.150
Mass of methyl ester	102.500	101.050
Moles of triglyceride	0.05926	0.05826
Moles of diglyceride	0.06037	0.05827
Moles of monoglyceride	0.05716	0.05680
Moles of methyl ester	0.34780	0.34288
Yield of triglyceride	23.66	23.26
Yield of diglyceride	16.07	15.51
Yield of monoglyceride	7.61	7.56
Yield of methyl ester	**46.29**	**45.63**
Mass balance	**93.63**	**91.97**

[a] obtained by calcination of the precursors commercially available $(MgCO_3)_4 \cdot Mg(OH)_2$ (Alfa Aesar) in flow N_2 at 450 °C for 2 hours.

Table A6.8

Reaction at 200 °C for 15mins – catalyst [a]; methanol:oil ratio (12:1)

	Sample 1	Sample 2
Mass of triglyceride	1.925	1.950
Mass of diglyceride	2.525	2.800
Mass of monoglyceride	15.375	15.525
Mass of methyl ester	179.700	181.700
Moles of triglyceride	0.00219	0.00222
Moles of diglyceride	0.00409	0.00454
Moles of monoglyceride	0.04334	0.04377
Moles of methyl ester	0.60975	0.61654
Yield of triglyceride	0.87	0.89
Yield of diglyceride	1.09	1.21
Yield of monoglyceride	5.78	5.83
Yield of methyl ester	**81.28**	**82.19**
Mass balance	**89.02**	**90.12**

[a] obtained by calcination of the precursors commercially available $(MgCO_3)_4 \cdot Mg(OH)_2$ (Alfa Aesar) in flow N_2 at 600 °C for 2 hours.

Appendix Three
Publication List

1. C. Xu, J. K. Bartley, D. I. Enache, D. W. Knight and G. J. Hutchings, *Synthesis,* 2005, **19**, 3468.